The Photochemistry of
$(\eta^6\text{-arene})M(CO)_3$
(M = Cr or Mo) and Related Compounds.

A thesis presented for the degree of Doctor of Philosophy

at

Dublin City University

by

Mary Pryce B.Sc.

under the supervision of Dr. Conor Long

School of Chemical Sciences

September 1994

Declaration

I hereby certify that this material, which I now submit for assessment on the programme of study leading to the award of Ph.D. is entirely my own work and has not been taken from the work of others save and to the extent that such work has been cited and acknowledged within the text of my work.

*Signed:*____________________ *Date:*____________
Mary Pryce

Acknowledgements

Firstly I would like to thank my supervisor Dr. Conor Long, for his guidance, encourgement and patience(!) throughout the course of this research, and more recently during the writing of the Thesis.

I would like to thank the technical staff of the University, Veronica, Maurice, Damien, many others who have come and gone, and especially Mick for his help with the NMR experiments

I would like to express my gratitude to Prof. Friedrich Grevels, for allowing me the opportunity to work for a brief period of time in the Max Planck Institute in Mulheim. Also, I would like to thank Dr. Graham Russell for all his help and the technical staff of the institute for all their assistance.

And not forgetting the researh group, both past - Barry, Gerry, Celia, Irene, Mick, Maureen and present - Ciara, Siobhan and Charlie for being there in moments of need! I would like to acknowledge Berties boys (and girls) who have made the days in AGO7 momentous, one way or the other.

I must thank two undergraduate students, Susan Gilligan and Nicholas Dunwoody for all their help.

A word of thanks to many postgrads. (whom I am not going to name individually) for just being there.

And to a few friends in particular, Carmel, Linda and Audrey, who always insisted that the social side of things is more important than the research side of things (but it does depend what you are researching).

And finally to my family who have always supported me, not only finanically throughout the last few(?) years.

To my parents
and the memory of Frank.

Table of Contents.

The Photochemistry of (η^6-arene)M$(CO)_3$ (M = Cr or Mo) and Related Compounds.

Mary Pryce.

Abstract.

The first chapter consists of a literature review of the known photochemistry of the compounds studied in this work along with relevant related systems.

The second chapter describes the photochemistry of a number of (η^6-arene)Cr$(CO)_3$ compounds. The rate constants for the reaction of photogenerated solvated dicarbonyl intermediate derived from these compounds with carbon monoxide were measured by UV/vis. monitored laser flash photolysis. These rate constants were found to depend on the nature and number of the substituents on the arene ligand. The associated activation parameters for these reactions were also determined. The difference in the rate constants were found to be the result of variations in the activation entropy term, which became less negative as the number of electron donating substituents on the ring increased. The activation enthalpy remained constant however. The displacement of various alkane solvents by CO was measured for the (η^6-benzene)Cr$(CO)_3$ system. Rate constants increased on increasing the alkane chain length. This increase was also the result of an increase in the entropy of activation. The enthalpies of activation were similar for all aliphatic solvents. The photochemisty of (η^6-benzene)Cr$(CO)_3$ was investigated in fluorinated solvents and this was found to differ significantly from the photochemistry in alkane solvents, Cr$(CO)_6$ being formed on irradiating (η^6-benzene)Cr$(CO)_3$ in fluorinated solvents under one atmosphere of CO.

Flash photolysis studies were carried out on the analogous molybdenum system in hydrocarbon solvents. No significant variation in rate constants, entropy or enthalpy of activation values were observed for this system irrespective of the nature of the arene or the solvent used.

The photochemistries of (η^6-allylbenzene)Cr$(CO)_3$ and (η^6-tetrahydronaphthalene)Cr$(CO)_3$ are reported in chapter three. (η^6-Allylbenzene)Cr$(CO)_3$ behaves differently to any of the previous chromium tricarbonyl systems investigated. Mass-spectrometry of the photoproduct confirmed the presence of three carbonyl ligands. A process involving a change in ring hapticity is proposed to explain these observations. This chapter also outlines the photochemistry of (η^6-tetrahydronaphthalene)Cr$(CO)_3$. This investigation included both UV/vis. monitored laser flash photolysis and Transient Infrared (TRIR) studies. The

primary photoproduct was assigned to the carbonyl loss product but a second long-lived species was also observed, the identity of which remains unknown.

In the fourth chapter the results of flash photolysis studies are reported for a number of polyaromatic chromium tricarbonyl compounds (namely naphthalene, phenanthrene and pyrene). The photolysis of these compounds in the presence of CO results in the formation of $Cr(CO)_6$ and the liberation of the aromatic ligand. Extensive matrix isolation work was carried out on the (η^6-naphthalene)$Cr(CO)_3$ compound which exhibited wavelength dependent photochemistry. On short wavelength irradiation the dicarbonyl photoproduct is observed while long wavelength irradiation a second species which is attributed to a (η^3-naphthalene)$Cr(CO)_3$-type intermediate was detected.

The fifth chapter discusses the photochemistries of both the *cis* and *trans*-isomers of (η^6-1,2-diphenylethene)$Cr(CO)_3$. Visible irradiation of the *cis*-isomer results in a efficient conversion to the *trans*-isomer as confirmed by NMR and UV/vis. spectroscopy. The molecular structure of the *trans*-isomer was also determined by single crystal X-ray diffraction.

Within the sixth chapter the photochemistry of a number of pentadienyl manganese carbonyls compounds is reported along with the photochemistry of (η^3-C_3H_4-C_6H_5)$Mn(CO)_4$ and $Mn(CO)_4$(η^3-C_3H_4-η^6-C_6H_5)$Cr(CO)_3$. The photochemistry of the dinuclear compound was intially investigated using laser flash photolysis but as the results were not conclusive it was decided to investigate a number of manganese ligands namely (η^1-pentadienyl)$Mn(CO)_5$, (η^3-pentadienyl)$Mn(CO)_4$ and (η^5-pentadienyl)$Mn(CO)_3$.

The final chapter consists of the experimental procedures used for the preparation and analysis of the compounds synthesised in this work.

A moment's insight is sometimes
worth a life's experience.

Oliver Wendell Holmes.

Chapter 1

Introduction.

1.1 Introduction.

After the steady growth of chemical knowledge through the first half of the century, the findings that 'spurred' the growth of organometallic chemistry came in the early 1950's. These were the discoveries of ferrocene[1] in 1951 and the development of the Ziegler process[2] in 1953. Wilkinson and Fischer proposed a structure for ferrocene consisting of an iron sandwiched between two planar cyclopentadienyl ligands that symmetrically bind the central metal atom.[2a,3]

As early as the beginning of the 1900's soluble metal salts were used commercially as catalysts for acetylene reactions but it was not until the 1940's that the widespread use of soluble catalysts began. A number of conditions at this time were favourable for development of new processes. Firstly, war time restrictions on raw materials led to new Cobalt-based processes for production of fuels and plastics. Secondly, and more importantly, the introduction of many new polymers between 1940 and 1960 necessitated worldwide development of new processes for production of monomers.

The impetus for new process technology came during a period of rapid development in the organic chemistry of transition metals. Fischer, Wilkinson, Ziegler and Natta were conducting the research that won them the Nobel prize in chemistry. Their research proved the basis for modern homogeneous catalysis. Industry has built on their fundamental discoveries to create processes that are catalysed by soluble transition metal complexes.

Among the most important commercial homogeneous catalytic processes in use is the hydroformylation of alkenes and the Wacker process for making acetaldehyde from ethylene. The hydroformylation (sometimes known as the oxo process) of unsaturated compounds was discovered by Otto Roles in 1938. Its main use is in the conversion of alkenes to the homologous aldehyde by addition of H_2 and CO catalysed by $RhH(CO)(PPh_3)_3$.

$$RCH=CH_2 + H_2 + CO \xrightarrow{\text{catalyst}} RCH_2CH_2CHO \qquad (1.1.1)$$

The aldehdydes produced may be further reduced to a alcohol.

$$RCH_2CH_2CHO + H_2 + \xrightarrow{\text{catalyst}} RCH_2CH_2CH_2OH \qquad (1.1.2)$$

Annually over four million tonnes of aldehydes and alcohols are made in this way.

Acetic acid and acetic anhydride are major industrial chemicals used in the manufacture of vinyl acetate, cellulose acetate, and pesticides. Acetic acid has been made by the carbonylation of methanol for over thirty years but this reaction has become more attractive with the development of a catalyst that operates under low pressure. The newer Monsanto process catalysed by a rhodium salt with a iodide cocatalyst will produce acetic acid at atmospheric pressures of CO although in practice higher pressures are used. The commercial synthesis of acetic acid with the rhodium catalyst is carried out by reacting methanol with CO at about 180°C and 30-40 atmospheres of pressure. A general scheme for the catalytic action of rhodium and iodine in acetic acid synthesis is given in Scheme 1.1.1.

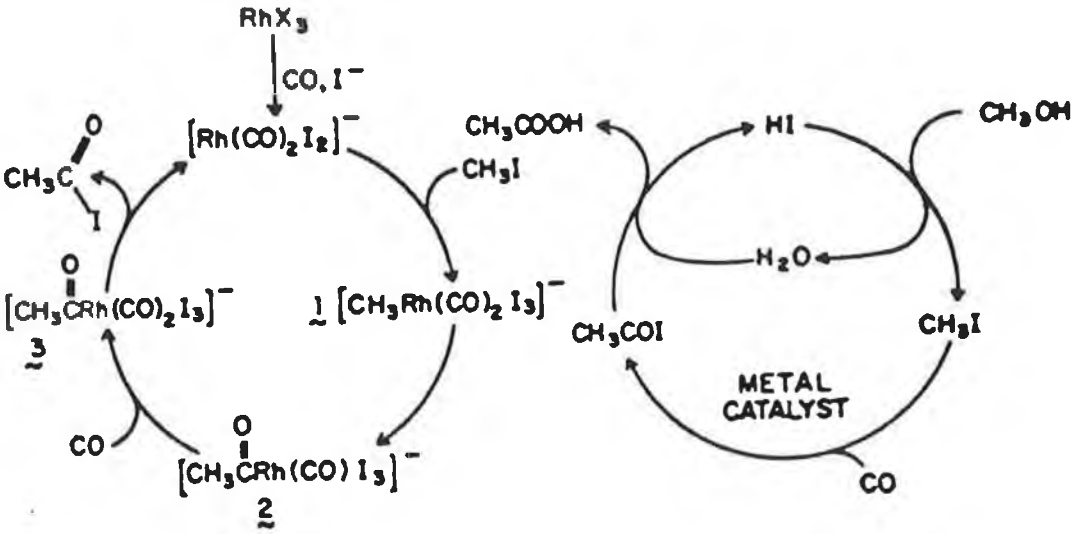

Scheme 1.1.1

Homogeneous catalysts also show potential for solving some environmental problems. Catalytic conversion of poisonous NO and CO gases to non-poisonous N_2O and CO_2 has been performed using $[RhCl_2(CO)_2]^-$ as a homogeneous catalyst in an aqueous acidic ethanol solution.

$$2NO + CO \longrightarrow N_2O + CO_2 \qquad (1.1.3)$$

Homogeneous catalysts in solution have advantages in that high activities are possible and also alteration of the electronic and steric factors through ligand substitution may allow for design of high selectivity. Homogeneous reactions can also provide a greater insight into the mechanism of catalytic reactions since they are most amenable to study by spectroscopic techniques.

1.2 Bonding in metal carbonyl compounds.

In order to discuss the bonding between a metal and a ligand, it is necessary to consider the metal and ligand orbitals involved. In bonding to ligands the metal employs its nd, (n+1)s and (n+1)p orbitals. For formation of metal carbonyl bonds the metal must have vacant d-orbitals able to accept electrons donated by the coordinated CO molecule and occupied d-orbitals able to donate electrons to the CO ligand.

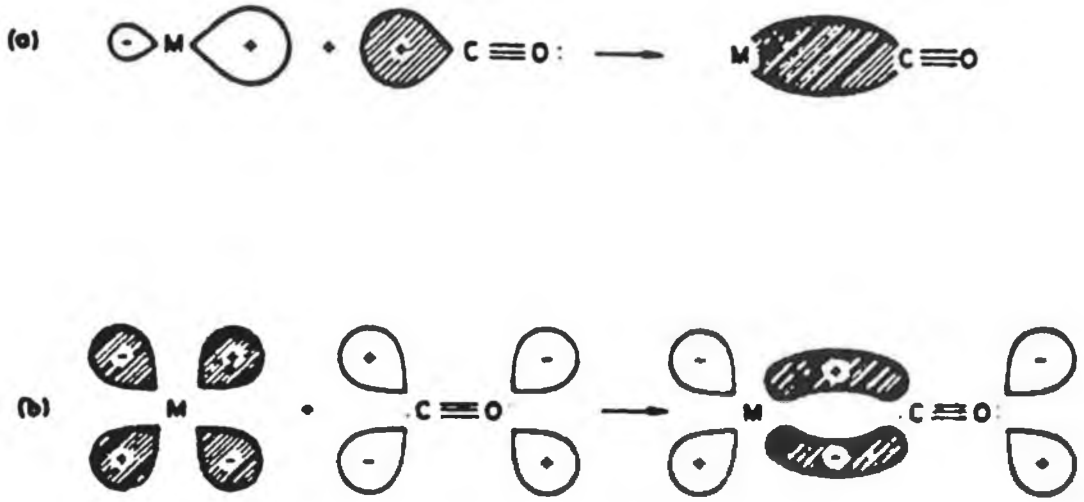

Figure 1.2.1 (a) formation of the carbon ——> metal σ bond using a lone pair on the carbon atom. (b) formation of the metal ——> carbon π bond.

The carbon monoxide has a lone pair of electrons in a molecular orbital localised at the carbon which can be donated to a vacant orbital of the metal thus forming a σ bond of the donor acceptor type. The carbon monoxide molecule has vacant antibonding molecular orbitals of correct symmetry to accept electron pairs from the occupied d-orbitals of the metal to form a π-bond. It is the σ bonding which contributes principally to the total bond energy but the π bonding has important ramifications in so far as back donation avoids the accumulation of an excess of electron density at the metal atom and strengthens the bond between the metal and the ligand. The electron donation between metal and ligand also influences the strength of the bond between carbon and oxygen in the coordinated CO molecule. Since the metal electrons are accepted into the antibonding molecular orbital of the CO molecule, the CO bond order decreases. From a direct comparison of the CO stretching frequencies in carbonyl molecules with the stretching frequency of CO itself, certain useful qualitative data can be drawn. Terminal CO groups in metal carbonyl molecules are formed in the range 2125 to 1850 cm^{-1}. When changes are made that should increase the extent of M-C backbonding the CO frequencies are shifted to even lower values.

1.3 Decarbonylation of metal carbonyl compounds.

Photodecarbonylation can be used to investigate the primary photoreaction of metal carbonyls and the reactivity of their photoproducts. The primary photoinduced photoreaction of metal carbonyls involves decarbonylation. Loss of CO can be explained by referring to the molecular orbital diagram Figure 1.3.1. The highest occupied orbital subset is the t_{2g} orbitals and the lowest unoccupied orbitals are the σ* (*i.e.* those orbitals which are strongly antibonding with respect to the σ interaction of the carbonyls). The photoinduced promotion of an electron from the t_{2g} orbital subset to the σ* orbital removes electron density from these orbitals contributing to backbonding interaction and hence populates an orbital which is strongly antibonding with respect to the carbonyl σ interaction. The result of this promotion of electrons is labilisation of a carbon monoxide ligand.

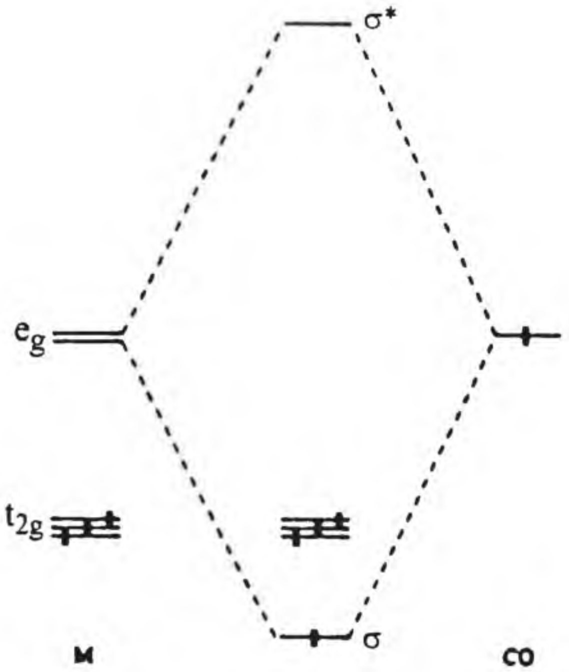

Figure 1.3.1. A molecular orbital picture of metal ligand bonding in a ML_6 complex.

1.4 Low temperature matrix isolation.

The use of inert matrices for studying reactive intermediates of metal carbonyl photofragments was originally developed by Pimental in the early 1950's.[4] Matrix isolation is a technique for trapping isolated molecules of the species of interest. This technique involves condensation of gaseous atomic or molecular species together with a large excess of an inert gas matrix or a suitable substrate at cryogenic temperatures. Irradiation of the parent compound generates photoproducts within the matrix that may then be studied by a variety of spectroscopic techniques such as UV/vis., Raman, magnetic circular dichromism or Mossbauer spectroscopy however infrared spectroscopy is the most commonly used. At sufficiently low temperature diffusion of the solute material is prevented and is hence stabilised for leisurely spectroscopic investigation. Nevertheless it is known that the photofragment may interact with the inert matrix material and known examples include $Cr(CO)_5N_2$[5], $Cr(CO)_5Ar$[6] and $Fe(CO)_4(CH_4)$.[7] Mixed matrix experiments and comparison with spectra of stable species revealed the shifts in spectra are due to specific interactions between the photofragment and the matrix species occupying the coordination site. In a solid matrix diffusion of CO away from the photofragment is unlikely due to the rigid nature of the matrix. The low temperature or some other property of the matrix ensures rigidity so that the unstable molecules cannot react with one another, while the low temperature must be sufficient to prevent self decomposition of the unstable species.

Low temperature solvent glasses have been used for spectroscopic identification of reactive metal carbonyl intermediates. A disadvantage of this method is that the infrared bands tend to be broader and hence may mask the presence of product bands. Isopentane and methyl cyclohexane are typical glasses which are maintained at 77K which is at a higher temperature than that of the inert gas matrices. Bitterwolf *et al.*[8] irradiated a number of half-sandwich compounds and group 6 metal hexacarbonyls in Nujol mulls at 77K. Annealing of the mulls resulted in CO recombination in the case of the pentacarbonyls products but formation of dinuclear complexes was proposed for the half-sandwich compounds. Matrix isolation and low temperature glasses have a number of disadvantages however: firstly very little kinetic data can be obtained by either of these methods because of the restricted temperature range employed, some photochemical pathways may be blocked because of the rigid structure of the frozen matrix and secondly neither of these methods is readily applicable to systems involving charged species.

Also included within this method of identification is the use of solvents which include liquid xenon or krypton. Low temperature solutions of liquefied noble gases have been used to examine the nature of metal dihydrogen or dinitrogen complexes.[9] The H-H stretching vibrations of coordinated dihydrogen is too weak to be observed in matrices. Liquefied noble gas allows kinetic studies and the determination of activation parameters which is a major advantage over matrix isolation.

1.5 Flash photolysis.

Conventional flash photolysis was developed in the 1950's by Norrish and Porter[10] for which they later won the Nobel prize. Because of this technique highly reactive intermediates present in many photochemical systems can be identified. The underlying principle consists of exposing a sample to a high intensity pulse of light (*e.g.* laser or discharge lamp) which generates a relatively high concentration of transient species, radicals or excited molecules. By monitoring the subsequent reactions using UV/vis. or IR detection it is possible to determine the reaction kinetics involved. The advantages of lasers consist of the monochromatic nature of the beam, its high intensity and short pulse duration.

Nasielski *et al.*[11] pioneered flash photolysis with UV/vis. detection to monitor the photofragments of $Cr(CO)_6$ produced following irradiation. Metal carbonyls are suitable for flash photolysis studies because of their production of high quantum yields and UV/vis. absorptions are intense. The basic technique involves excitation of the sample solution with a high intensity flash, while simultaneously passing a monitoring beam through the sample. Hence changes in absorbance as detected by the monitoring beam reflect the formation of intermediates or depletion of parent compound or both. Spectra are obtained as a result of point by point build up by changing the wavelength of the monochromator. A schematic diagram of a conventional flash photolysis system is given in Figure 1.5.1 The main disadvantage to UV/vis. monitored flash photolysis is very little structural information is available, however it is a useful method of obtaining kinetic data.

The measurement of IR spectra of transient species was developed by Pimentel *et al.*[12] The infrared spectrum of a metal carbonyl provides structural information as the number and intensity of the infrared bands is dependent on the molecular symmetry, also it is possible to probe the reactivities of a specific metal carbonyl intermediate in the presence of other similar species using TRIR. Generally, UV/vis. flash photolysis is combined with IR monitoring at a single IR wavelength. By repeating the measurement at a series of wavelengths within the region of interest a 'point by point' spectrum can be constructed. As with UV/vis. spectra the TRIR spectrum is a difference spectrum. With TRIR, metal carbonyl fragments can be detected at room temperature in both solution[13] and gaseous phase.[14]

As with all methods of analysis flash photolysis has inherent disadvantages. It is necessary that the solution be optically transparent for the monitoring light beam. Solvents of spectroscopic purity are required and even with this impurities prove to be a problem. Analysis of spectra may be difficult if absorption bands of several intermediates overlap.

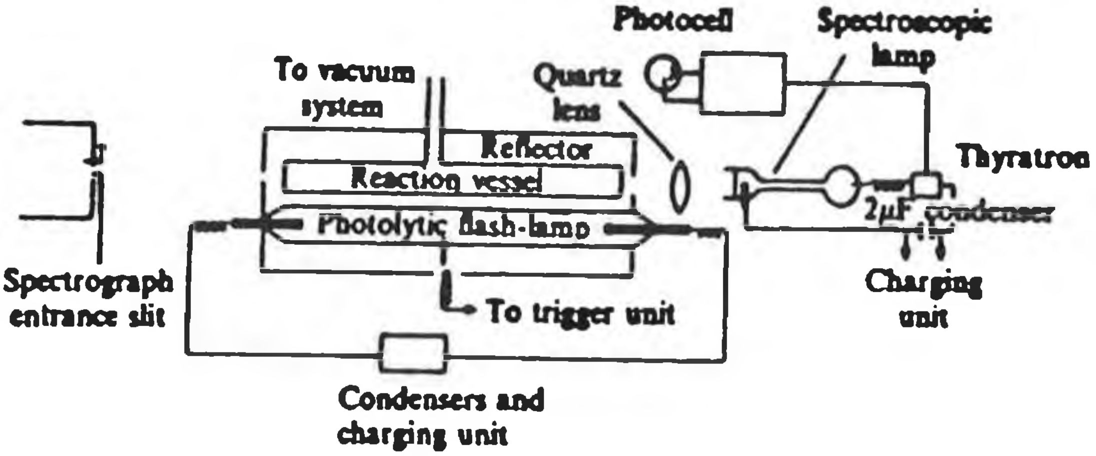

Figure 1.5.1 Schematic diagram of a conventional flash photolysis system.

1.6 Photochemistry of (η^6-benzene)Cr(CO)$_3$.

The earliest observations of the photoreactions of (η^6-benzene)Cr(CO)$_3$ were made by Strohmeier and von Hobe[15] who proposed the following reaction Scheme 1.6.1

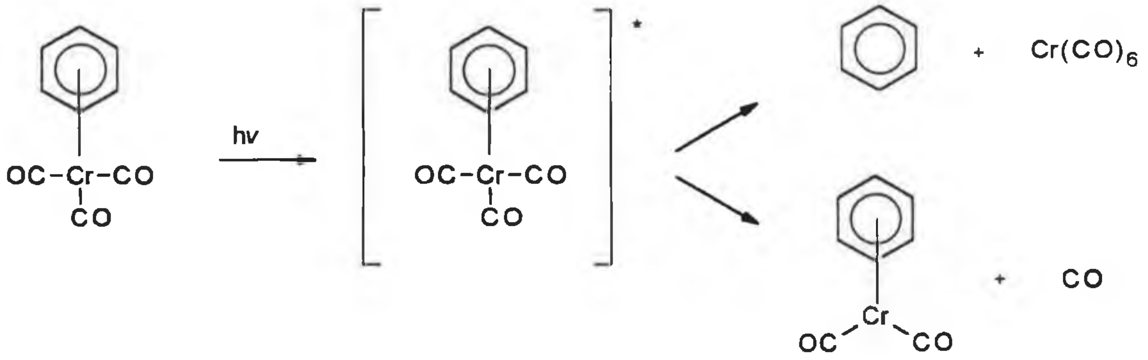

* denotes excited state

Scheme 1.6.1

These results were based on experiments in which the complexes were irradiated in the presence of ^{14}CO and ^{14}C-labelled arene; in both cases incorporation of the labelled species was observed. Exchange of the arene was believed to proceed *via* the one step dissociation of the excited molecule to give $Cr(CO)_3$ and arene.

Wrighton and Haverty[16] examined the photochemistry of (η^6-arene)$Cr(CO)_3$ according to Reaction 1.6.2 in which the arene = benzene or mesitylene and x = pyridine.

$$(\eta^6\text{-arene})Cr(CO)_3 \ + \ x \ \xrightarrow{h\nu} (\eta^6\text{-arene})Cr(CO)_2x \ + CO \qquad \Phi = 0.72 \qquad (1.6.2)$$

The chemistry observed was consistent with dissociative loss of CO as the primary photoprocess. The nearly quantitative yield of (η^6-arene)$Cr(CO)_2$(pyridine) revealed that if arene group exchange occurred at all it was only a very minor component of the photochemistry. The quantum yield for the formation of (η^6-arene)$Cr(CO)_2$(pyridine) was found to be 0.72 ± 0.07, the quantum yield was found to be independent of wavelength (λ = 313, 366, 346 nm), (solvent = iso-octane or benzene) and light intensity. They noted that irradiation of (η^6-arene)$Cr(CO)_3$ with a constant stream of CO bubbling through the solution resulted in little or no net chemical change, and in particular the lack of formation of $Cr(CO)_6$ was noted. Irradiation of (η^6-arene)$Cr(CO)_3$ in aerated iso-octane or benzene lead to decomposition of the tricarbonyl presumably by oxidation of the coordinatively unsaturated intermediate.

A quantitative study of the photosubstitution of CO in (η^6-benzene)$Cr(CO)_3$ by N-dodecylmaleimide was undertaken by Nasielski and Denisoff.[17] In benzene solution the quantum yield was calculated to be 0.9 ± 0.09 at 313 nm. No detectable mesitylene-benzene exchange was observed. In cyclohexane solution the study was hampered by the photo-instability of the reactants and products.

Gilbert *et al.*[18] studied the photoinduced CO exchange of (η^6-arene)$Cr(CO)_3$ and in accordance with the results of Haverty and Wrighton[16] obtained a similar quantum yield of 0.72. Furthermore the efficiency of arene exchange in cyclohexane was measured to be one-sixth that of CO exchange being 0.12. UV/vis. monitored flash photolysis in cyclohexane solution revealed the formation of a transient species which reacted within the first millisecond to form a second species. Both transients were found to be strongly quenched on saturating the solution with CO. The first transient species was considered to be (η^6-arene)$Cr(CO)_2$ and that exchange with benzene involves this intermediate. This conclusion was based on the observation that arene exchange is strongly suppressed in the presence of CO, whereas that of CO exchange was unaffected by the presence of benzene.

Similar conclusions concerning the photochemistry of (η^6-benzene)$Cr(CO)_3$ was reported by Bamford *et al.*[19] Scission of the chromium to CO bond was found to have been the main route of photolysis of (η^6-benzene)$Cr(CO)_3$ and (η^6-toluene)$Cr(CO)_3$ in isooctane and methylmethacrylate solutions.

The spectral changes which occurred during irradiation of (η^6-arene)$Cr(CO)_3$ in cyclohexane were reported by Trembovler *et al.*[20] and Yavorskii *et al.*[21] Uncomplexed arene and $Cr(CO)_6$ were the products of the photodecay of (η^6-arene)$Cr(CO)_3$. Substituents on the benzene ring had no effect upon the rate of decomposition of the complexes investigated, while substitution of a CO group by a PPh_3 ligand increased the rate of reaction by almost an order of magnitude. Further Trembovler *et al.*[20] determined the quantum yield of photodecomposition as a function of light intensity and proposed the simultaneous occurrence of three decay processes, with different dependencies on light intensities. However, no conclusions about the detailed photolytic reaction were drawn.

Many intermediates in metal carbonyl photochemistry have been characterised in low temperature gas matrices.[22] The first matrix experiments conducted on (η^6-benzene)$Cr(CO)_3$ were carried out by Rest *et al.*[23] who investigated the photochemistry of a number of substituted $M(CO)_3$ compounds in frozen gas matrices at 12 K. Photolysis of (η^6-benzene)$Cr(CO)_3$ in argon or methane matrices resulted in the formation of bands at 1937 and 1885 cm^{-1}, and 1925 and 1870 cm^{-1} respectively in the carbonyl stretching region. These bands were assigned to the coordinatively unsaturated dicarbonyl species as the primary photoproduct. This is in agreement with previous matrix experiments on the analogous Fe[24] and Mn[25] systems. Photolysis in a dinitrogen matrix resulted in bands at 1940 and 1896 cm^{-1} for the dicarbonyl intermediate. No evidence was obtained in this study for ejection of the arene ligand to yield a $M(CO)_3$ fragment.

Black *et al.*[26] examined the photochemistry of (η^6-benzene)$Cr(CO)_3$ in methyl-THF at 77 K. Irradiation gave rise to a four band spectrum assignable to two rotamers with the higher frequency being weaker and disappearing on warming. The bands resulted from the arrangement of solvent molecules around the photolysed molecule. This observation was not unique to the chromium metal but was also observed for $CpMn(CO)_3$ (where Cp=cyclopentadienyl).

Hill and Wrighton[27] observed oxidative addition of trisubstituted silanes to photochemically generated coordinatively unsaturated species. At low temperature (~90 K) irradiation of (η^6-benzene)$Cr(CO)_3$ in the presence of Et_3SiH led to the generation of (η^6-benzene)$Cr(CO)_2H(SiEt_3)$ without a detectable intermediate. A number of metal tricarbonyls were photolysed at low temperature (~100 K) and the reactivity toward oxidative addition of R_3SiH was reported to be

(η^6-benzene)$Cr(CO)_2$ > (η^5-pentamethylcyclopentadienyl)$Mn(CO)_2$ > (η^5-cyclopentadienyl)$Mn(CO)_2$ > (η^4-butadiene)$Fe(CO)_2$ > (η^5-cyclopentadienyl)$Re(CO)_2$.

This reactivity trend appeared to correlate with the electron density of the metal fragment as given by the stretching frequencies; the more reactive fragments have the lower average stretching frequency.

Photolysis of carbonyl compounds such as (η^6-benzene)$Cr(CO)_3$, (η^5-cyclopentadienyl)$Mn(CO)_3$ and (η^5-cyclopentadienyl)$Re(CO)_3$ as solutions or mulls in nujol at 77 K have been reported[8] to yield the carbon monoxide loss fragment. Long wavelength irradiation and annealing the matrix resulted in reversal of the carbonyl ejection photolysis. For arene and cyclopentdienyl metal tricarbonyls complexes, dinuclear complexes were formed in initial photolysis or annealing. These products were thought to result from reaction of the dicarbonyl photoproduct with unphotolysed parent material as presented in Scheme 1.6.3. Nujol mull at 77 K provides a broadly applicable technique for the study of photochemical intermediates which bridges the gap between frozen gas matrices and solution studies.

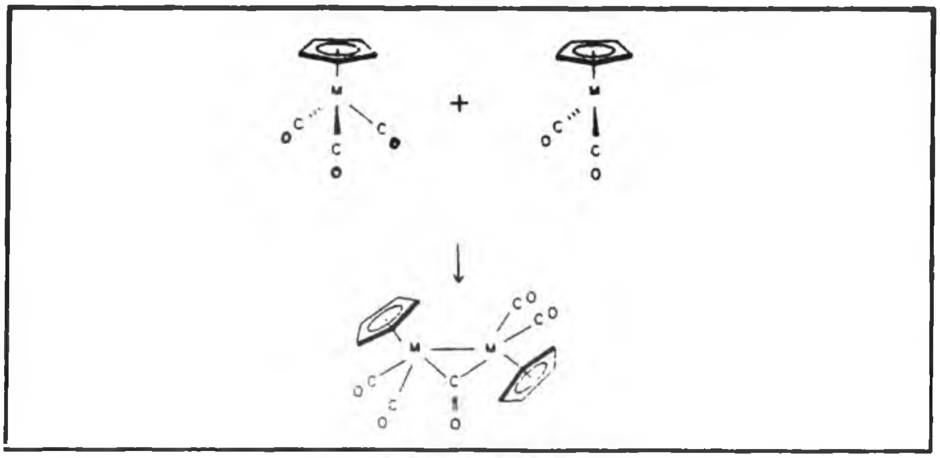

Scheme 1.6.3

More recently the photochemistry of (η^6-benzene)$Cr(CO)_3$ has been examined in the gas phase by Wang *et al.*[28] using infrared detection. The predominant photoproduct on 355 nm photolysis was identified as (η^6-benzene)$Cr(CO)_2$ while upon 266 nm both the dicarbonyl and monocarbonyl species were produced in the ratio of 2:5 respectively. Under a CO atmosphere following 355 nm flash photolysis an absorption at 1999 cm^{-1} was observed which was attributed to belonging to $Cr(CO)_6$, although this was considered to be a minor product. $Cr(CO)_6$ was assumed to form *via* the reaction of the fragment $Cr(CO)_3$ with CO, but this theory was merely speculation. Evidence for formation of a dinuclear species was also observed in the absence of CO and this they proposed to form according to Reaction 1.6.4.

$$(\eta^6\text{-benzene})Cr(CO)_3 + (\eta^6\text{-benzene})Cr(CO)_2 \longrightarrow (\eta^6\text{-benzene})_2Cr_2(CO)_5 \qquad (1.6.4)$$

Zheng *et al.*[29] studied the coordination reaction of N_2 and H_2 with photolytically generated coordinatively unsaturated (η^6-benzene)$Cr(CO)_x$ (where $x = 2$ or 1) ($\lambda = 355$ nm) in the gas phase using time resolved infrared spectroscopy. Addition of N_2 and H_2 to the dicarbonyl fragments formed the corresponding nitrogen and hydrogen complexes. The positions of the CO stretching bands of the dihydrogen and dinitrogen complexes are very close as found in the condensed phases thereby indicating that the interaction between the metal centres and the ligands are very similar for N_2 and H_2.

1.7 Thermal chemistry of (η^6-benzene)$Cr(CO)_3$.

It is generally considered that flash photolysis of (η^6-benzene)$Cr(CO)_3$ leads to formation of the solvated dicarbonyl species whereas thermal reactions carried out on the tricarbonyls result in arene exchange. Strohmeier and Starrico[30] carried out thermal reactions on (η^6-benzene)$Cr(CO)_3$ with various substituted arene ligands (benzene, toluene or naphthalene) which resulted in exchange of the arene moiety. These exchange reactions were carried out at high temperatures (140°C) in sealed NMR tubes. Addition of a donor solvent such as THF to the reaction solution catalysed the arene exchange.

Mahaffy and Pauson[31] subsequently investigated arene exchange and they proposed that it occurred through partial displacement of arene ($\eta^6 \longrightarrow \eta^4$) which was initiated by coordinating solvents. In the absence of a coordinating solvent it has been proposed that a second molecule of arene chromium complex could catalyse the reaction by coordinating through the carbonyl oxygen.

Rates of exchange of arene ligand with hexamethylbenzene according to Reaction 1.7.1 (where arene = benzene, *p*-xylene or mesitylene)

$$(\eta^6\text{-arene})Cr(CO)_3 \quad + \quad \text{hexamethylbenzene} \xrightarrow{\Delta} (\eta^6\text{-hexamethylbenzene})Cr(CO)_3 + \quad \text{arene} \qquad (1.7.1)$$

have been determined in cyclohexane solution at several temperatures in the range 80 - 140°C by Zimmerman *et al.*[32] In all three cases the reactions were first order in the complex and independent of the concentration of hexamethylbenzene. The rates of exchange decrease in the order benzene > *p*-xylene > mesitylene - in agreement with the work of Strohmeier and Starrico.[30] Activation enthalpies decrease in this order and the activation entropies become increasingly negative as the number of methyl groups on the complex increase.

More recently, Traylor *et al.*[33] carried out kinetic studies of the displacement of benzene or substituted benzenes from their chromium carbonyl complex by other substituted benzenes. The arene exchange reactions were followed by ^1H NMR with the disappearance of complex as well as the appearance of product being monitored. Reactions were carried out at 170°C in sealed NMR tubes. The general mechanistic scheme which resulted from this work involves a $\eta^6 \longrightarrow \eta^4$ hapticity change (see Scheme 1.7.2) of the arene ligand with a subsequent step-wise displacement of the arene. The catalytic η^2 (L) ligands dissociate whether they are arenes or nucloephiles and can be any two electron Lewis base including ketones, alkenes or even another arene.

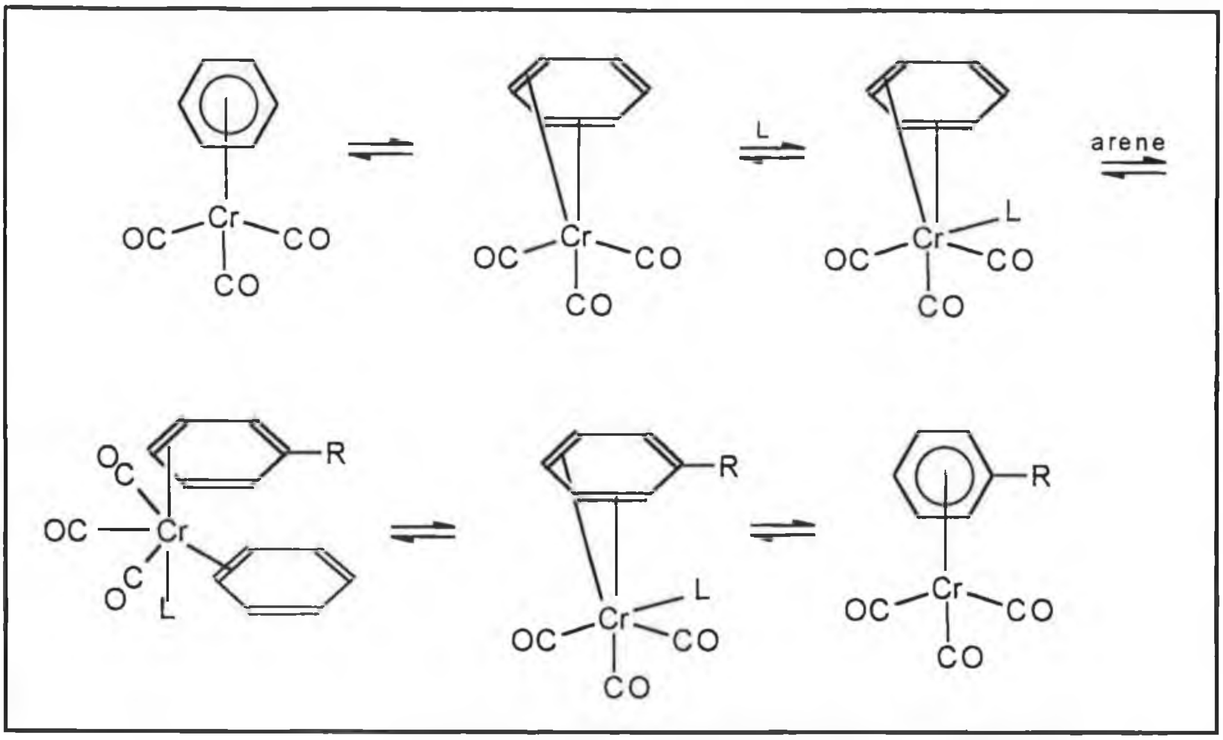

Scheme 1.7.2

It is well established that arene substitution is more rapid in complexes of polycyclic arenes,[34] and this is generally attributed[35] to the relatively favourable energies of ring slippage to generate a η^4-arene intermediate which results from the retention of aromaticity in the noncoordinated rings.

Howell *et al.*[36] examined arene exchange reactions in (η^6-naphthalene)$Cr(CO)_3$ and (η^6-pyrene)$Cr(CO)_3$ in hydrocarbon solvents. Molecular orbital calculations at the extended Huckel level were used to construct potential energy surfaces for ring slippage in the benzene, naphthalene and pyrene complexes. A $\eta^6 \longrightarrow \eta^4$ was found to be the most favourable for the naphthalene system, but a $\eta^6 \longrightarrow \eta^1$ path required the least energy in pyrene. The calculations predict arene lability to be in the order benzene << naphthalene << pyrene.

1.8 Haptotropic rearrangements in (η^6-arene)$Cr(CO)_3$.

Haptotropic rearrangement processes have been a specific focal point in current research. The migration of a metal group between fused five and six membered rings mainly in complexes containing a fluorenyl ligand[37] and between two six membered rings in naphthalene complexes[38] receiving primary attention.

Albright *et al.*[39] carried out a detailed theoretical investigation into the minimum energy pathways for shifting of the ML_n group from one ring to another in bicyclic polyenes. A number of compounds were treated in depth including (η^6-naphthalene)$Cr(CO)_3$, (η^5-indenyl)-FeCp, (η^5-fluorenyl)-FeCp and a number of other anionic and cationic tricarbonyls (Cp = cyclopentadienyl). It was established that the main contribution to the bonding in the ground state of π complexes of this type comes from the interaction of the two higher occupied molecular orbitals with the lower unoccupied molecular orbitals of the organometallic and metal carbonyl fragments. In most cases the path of least motion from ring to ring through the middle of the carbon-carbon bond, which is common for these rings, is forbidden. More preferable is metal migration over the polycyclic periphery *via* an intermediate η^3-allyl structure.

The metal migration between two non-adjacent rings in phenyl anthracenes was reported by Cunningham *et al.*[40] On heating a solution of I to its reflux temperature a colour change from yellow to purple was observed which indicated migration of the $Cr(CO)_3$ moiety from the non-adjacent (benzene ring) to a terminal phenyl (anthracene) ring.

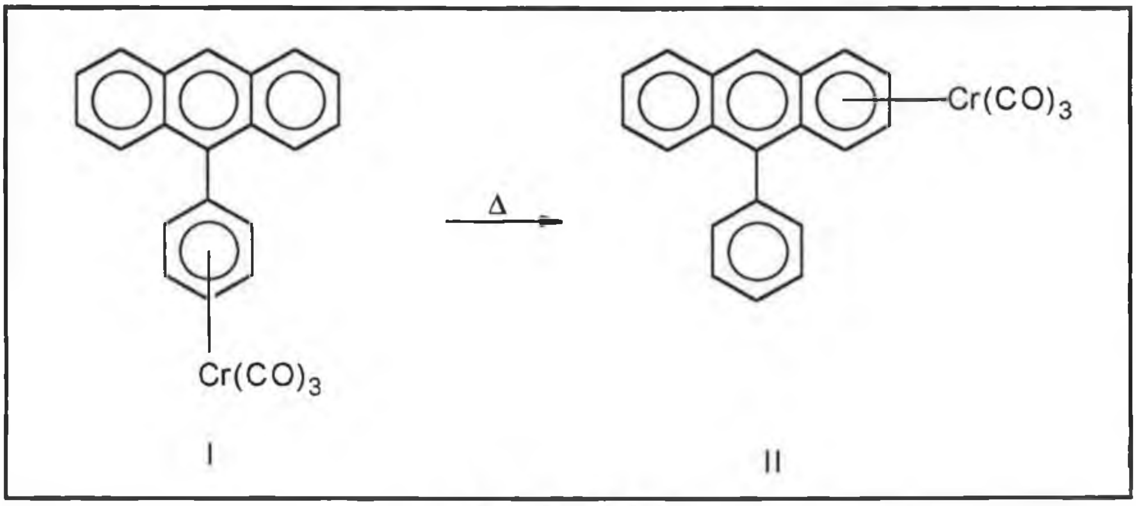

Reaction 1.8.1

This migration from I——>II as presented in Reaction 1.8.1 was confirmed by ^1H NMR spectroscopy. The purple solution reverts to a yellow colour on standing overnight.

The first experimental evidence for η^6 —> η^5 rearrangement for a manganese carbonyl system was proposed by Rerek and coworkers.[41] Activation enthalpies $\Delta H^{\neq}$ for the rearrangement of a number of η^6-fluorenyl complexes to η^5-fluorenyl complexes were reported and all $\Delta H^{\neq}$ were found to be within experimental error of 101 kJ/mol. These values were close to those predicted experimentally by Albright and coworkers of 113-122 kJ/mol.[39] The mechanism for the η^6 —> η^5 rearrangement is given in Scheme 1.8.2

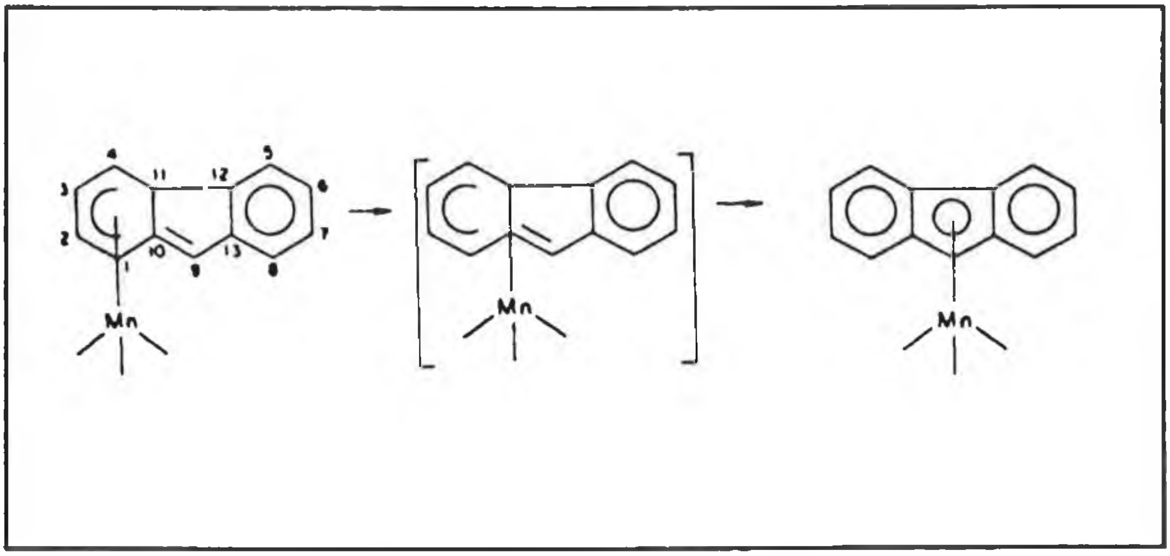

Scheme 1.8.2

These rearrangements are considered to be intramolecular, most probably going through a η^3 intermediate. Varying the concentration of compound had no effect on the rate constant and along with a negligible $\Delta S^{\neq}$ which further supports an intramolecular rearrangement occurring.

Haptotropic rearrangements were determined experimentally in naphthalene chromium tricarbonyls compounds by Kirss *et al.*[42] Kinetic data and calculated activation energies for two complexes (3-deuterio 2,7-dimethoxynaphthalene)$Cr(CO)_3$ and (3-deuterio-2,6-dimethoxynaphthalene)-$Cr(CO)_3$ were determined.

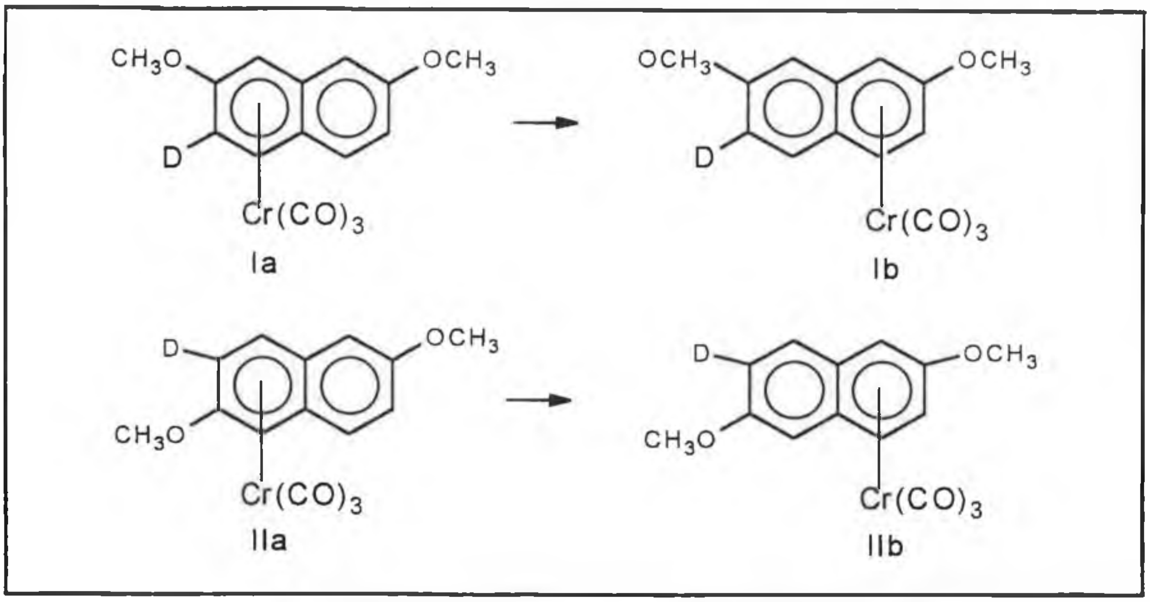

Reaction 1.8.3

When dissolved in benzene-d_6 both compounds were found to undergo a haptotropic migration of the metal tricarbonyl group to the undeuterated ring, with (1:1) at equilibrium. Arene exchange with solvent or decomposition appeared to be an insignificant factor in either of these systems. Both processes were followed by ^{1}H NMR. The rate constants values for IIa—>IIb are about 14 times less than that for Ia—>Ib. This implies that the methoxy groups play a small role in stabilisation of the transition state which translates to a higher rate of exchange of Ia—>Ib. Activation energies were also calculated and they were found to be very similar for both compounds being 113 and 118 kJ/mol for Ia—>Ib and IIa—>IIb respectively. Rerek and Basolo[41] determined activation parameters for $\eta^6 \longrightarrow \eta^5$ migrations in several fluorenyl manganese species, the values they obtained for $\Delta H^{\neq}$ compare well with those of Kiriss *et al.*[42] They also suggested that hexadienyl-arene bonding may be necessary to permit $\eta^6 \longrightarrow \eta^5$ rearrangements since Fe(η^6-$C_{13}H_9$)(η^5-C_5H_5)[43] does not undergo a $\eta^6 \longrightarrow \eta^5$ rearrangement and this compound has been shown to have a delocalised-arene-bonded-iron.

Berno *et al.*[44] reported the migration of the Cr(CO)$_3$ unit from the eight to the six member ring in benzocyclo-octatrene (Reaction 1.8.4) which was studied in decalin and n-butyl ether at temperatures between 428 - 454K.

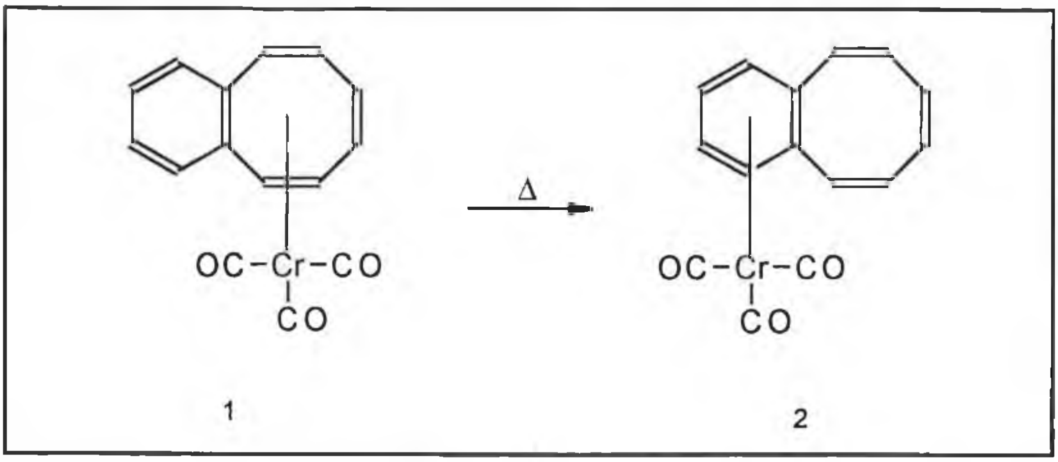

Reaction 1.8.4

The activation enthalpy at 443 K for isomerisation of 1 —> 2 was measured to be 122 kJ/mol and 130 kJ/mol in decalin and n-butyl ether respectively. The entropy value was calculated to be close to zero in decalin and n-butyl ether. The activation enthalpies in both solvents are very close to the values obtained for the haptotropic migration of the $Cr(CO)_3$ in dimethoxy and dimethyl naphthalene complexes[42] ($\Delta H^{\neq}$ = 118 and 126 kJ/mol respectively). In the theoretical investigation carried out by Albright *et al.*[39] it was proposed that in the metal group migration in naphthalene did not occur through the least motion pathway whereas in the benzocyclo-octatraene complex it is partially allowed. In contrast to the naphthalene system decomposition competes with isomerisation for benzocyclo-octatetraene compound whereas no decomposition was observed for naphthalene compounds (*vide supra*).

More recently Oprunenko and coworkers[45] have reported ricochet inter-ring haptotropic rearrangements of annulene tricarbonyl complexes of chromium. From this study they observed reversible intramolecular inter-ring rearrangements consisting of correlated metal shifts and hydrogen migrations between the metal atom endo positions of the hydroaromatic ligand.

1.9 Solvent effects on the photochemistry of metal carbonyl compounds.

Following flash photolysis of $Cr(CO)_6$ in cyclohexane solution a highly reactive species was observed by Kelly *et al.*[46] This reactive species was suggested to be $Cr(CO)_5$ which reacts readily with CO to reform $Cr(CO)_6$. Results obtained were consistent with the reactions outlined in 1.9.1 and 1.9.2

$$Cr(CO)_6 \xrightarrow{h\nu} Cr(CO)_5 + CO \qquad (1.9.1)$$

$$Cr(CO)_5 + CO \longrightarrow Cr(CO)_6 \qquad (1.9.2)$$

As a result of this study rates of reaction of $Cr(CO)_5$ with several solvents L (L = acetone, acetonitrile, benzene, ethylether, ethyl acetate and methanol have been measured.[47] It was anticipated that in the presence of L, Reactions 1.9.3 and 1.9.4 would take place after the photochemical generation of $Cr(CO)_5$, hence forming a solvated species.

$$Cr(CO)_5 + L \longrightarrow Cr(CO)_5L \qquad (1.9.3)$$

$$Cr(CO)_5L \longrightarrow Cr(CO)_5 + L \qquad (1.9.4)$$

Perutz and Turner[6] observed that the position of the maximum absorption ($\lambda_{max.}$) of the visible band of the chromium pentacarbonyl species formed from $Cr(CO)_6$ depends markedly on the matrix in which it is formed (*e.g.* $\lambda_{max.}$ = Ne:624, Ar:533 and CH_4:489 nm) and this blue shift has been interpreted in terms of an increasing interaction of the electrons of the matrix material with the vacant coordination site on the metal.

Simon *et al.*[48] utilised picosecond absorption spectroscopy to examine the primary photochemical process in the photolysis of $Cr(CO)_6$ in cyclohexane/THF mixtures. The first observable intermediate (formed in less than 25 ps) was suggested to be the solvated cyclohexane-pentacarbonyl species, in which a cyclohexane molecule occupies the vacant coordination site created by the photoelimination of CO. In addition, the rate of exchange of cyclohexane from (cyclohexane)$Cr(CO)_5$ by THF to form THF$Cr(CO)_5$ was found to be a bimolecular process and entropically controlled.

The generation of a highly reactive coordinatively unsaturated species was investigated in perfluormethylcyclohexane by Kelly and coworkers.[49] Results indicated that the pentacarbonyl species (Reaction 1.9.1) produced in this solvent was much more reactive (3.3×10^9 $dm^3mol^{-1}s^{-1}$) than the pentacarbonyl species previously observed in cyclohexane (3.0×10^6 $dm^3mol^{-1}s^{-1}$). Also observed in this study was the formation of $Cr_2(CO)_{11}$ by the reaction of $Cr(CO)_6$ with $Cr(CO)_5$.

Church *et al.*[50] investigated flash photolysis of $Cr(CO)_6$ using infrared detection. The presence of a water trace impurity in CO saturated cyclohexane solution was kinetically and spectroscopically identified. Studies in H_2O/CO saturated cyclohexane solutions show that $Cr(CO)_5C_6H_{12}$ is 13 times more reactive towards water than CO.

Picosecond absorption spectroscopy has been used to measure the formation kinetics of $Cr(CO)_5(MeOH)$ and $Cr(CO)_5$(cyclohexane) in methanol and cyclohexane solutions respectively.[51] The transient absorption characteristic of $Cr(CO)_5$(cyclohexane) was observed to rise with the instruments response (< 0.8 ps). In contrast, in alcohol solutions a 2.5 ps rise time for formation of the solvated species was observed. The longer rise time in methanol reflects solvent reorganisation resulting in the coordination of a solvent molecule to the vacant site of the reactive $Cr(CO)_5$ intermediate. Later, Simon and Xie[52] carried out time resolved studies of $Cr(CO)_6$ in pentanol. The thermodynamically most stable complex involves coordination of the hydroxyl end of the solvent molecule. Thus, if initial solvation produces intermediates where the alkyl group is coordinated to the chromium metal, rearrangement or exchange will occur to form the most stable complex. The transient spectrum in pentanol ($\lambda_{max.}$:460 nm) is identical to that previously observed in methanol. In cyclohexane solution the absorption band is at 505 nm, thereby reflecting the weaker interaction between the bound solvent molecule and the chromium metal.

Ishikawa *et al.*[53] reported formation of the complex $W(CO)_5C_2H_6$ in gas phase time resolved spectroscopy, following 308 nm laser photolysis of $W(CO)_6$ in the presence of C_2H_6. Results have been obtained for linear alkanes, from propane to hexane, for isobutane and for cyclopropane, pentane and hexane. All showed behaviour similar to that of ethane in forming $W(CO)_5$solvent complexes. The spectra of all the nonsubstitued alkane solvents are very similar, indicating that the structure and therefore the binding mechanism are the same in all cases.

More recently volumes of activation for reactions proceeding according to Scheme 1.9.5 for $Cr(CO)_6$, $Mo(CO)_6$ and $W(CO)_6$ for several solvents and incoming nucleophiles were investigated by Zhang *et al.*[54] in order to obtain an overview of the mechanistic possibilities for solvent displacement in these systems.

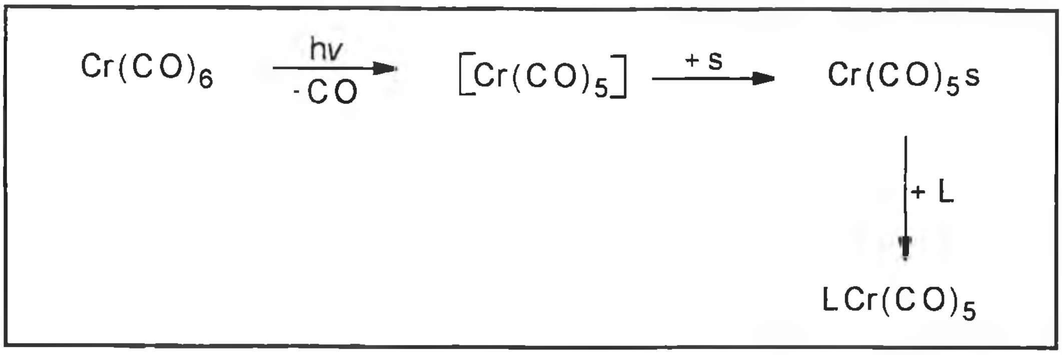

Scheme 1.9.5

The activation volume data reported favoured dissociative desolvation pathways for arene solvent (path B - Scheme1.9.6) but an interchange pathway for heptaneCr(CO)$_5$ (path A). The results further demonstrated that volumes of activation observed for solvent displacement reactions for M(CO)$_5$(s) complexes are sensitive to the identities of the incoming nucleophile and metal atom.

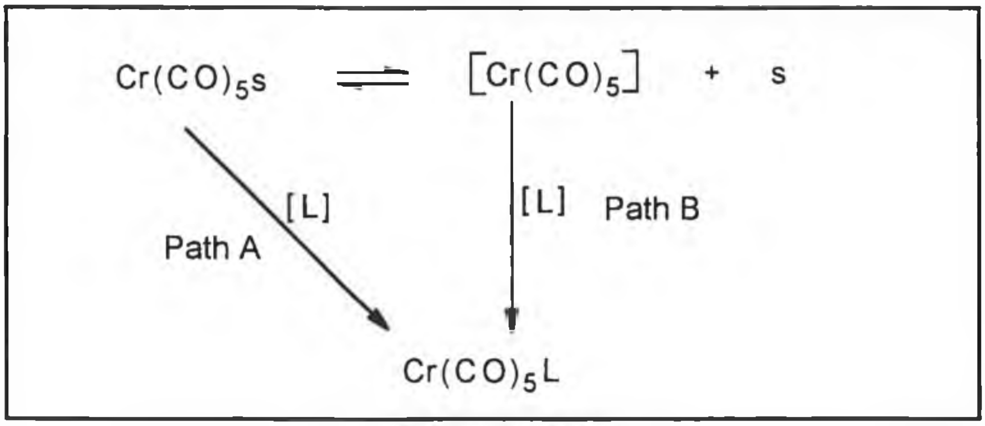

Scheme 1.9.6

Joly and Nelson[55] observed that CO dissociation appeared to be independent of the solvent, implying that the dissociating fragment feels no significant force or viscous drag from solvent neighbours. In a previous study, they determined that CO dissociation is complete within 35fs. The dynamics of solvent complexation to bare M(CO)$_5$ photofragment demonstrates that the solvent has no significant effect on which CO dissociated, and that the solvent undergoes no significant rearrangement before coordinating to the open site.

The stereospecific interaction between the metal and the alkane can formally be described as an intermolecular agostic bond.[56] Enthalpies of intermolecular agostic bonds have only recently been investigated. Morse *et al.*[57] investigated the enthalpy of CO dissociation from M(CO)$_6$ (M= Cr, Mo or W) in alkane solvent by photoacoustic calorimetry. The reaction involves the substitution of a M-CO bond by an intermolecular agostic bond - M-alkane bond. The enthalpies of CO dissociation from $Cr(CO)_6$ in pentane, heptane, isooctane and cyclohexane were found to be endothermic by 109, 113, 117 and 100 kJ/mol respectively. The differences in enthalpies for heptane and cyclohexane were considered significant and attributed to a stronger agostic bond to cyclohexane and hence it was concluded that agostic bond formation is preferential with secondary CH bonds relative to primary CH bonds. Bond strengths determined from time resolved photoacoustic calorimetry depend on the experimentally determined bond strength for CO dissociation from $Cr(CO)_6$ in the gas phase and upon quantum yields for CO dissociation upon photolysis.[58] The latter have recently been found to be sensitive to the identity of the weakly-interacting solvents as previously observed by Nayak and Burkey[59] (*vide infra*).

The relative heats of CO photo-substitution on $Cr(CO)_6$ by cyclohexane, benzene and 1,2-dichloroethane (as ligands) in perfluorocarbon solvents and in neat ligand was determined by Nayak *et al.*[59] From these results and the quantum yield of CO substitution in neat ligand (0.67, 0.67 and 0.62 respectively) the quantum yield in perfluorodecalin was found to be 0.3. The low quantum yield in perfluorodecalin can be attributed to its weaker coordination of $Cr(CO)_5$. It was considered that the more efficient recombination of CO in a fluorocarbon solvent is primarily responsible for the lower quantum yield of substitution.

1.10 Photochemistry of $(\eta^3\text{-allyl})Mn(CO)_4$.

Since it was first demonstrated in the 1950's that $(C_4H_7)Co(CO)_3$ has η^3 bonding configuration[60] there has been interest in η^3-allyl organometallic complexes.[61] Investigations by Mutteries and coworkers[62] have shown that $(\eta^3\text{-}C_3H_5)Co(PR_3)_3$ and $(\eta^3\text{-}C_3H_5)Mn(CO)_2(PR_3)_2$ act as catalysts for hydrogenation of alkenes and arenes. Originally it was proposed that catalysis involved a $\eta^3 \longrightarrow \eta^1$ allyl conversion which opens a coordination site on the metal. However, subsequent work[62d] on $(\eta^3\text{-}C_8H_{13})Co(P(OCH_3))_3$ suggest that η^1 complexes are not involved in catalysis. The allyl group is hydrogenated to give the corresponding alkane which releases the coordinatively unsaturated $Co(P(OCH_3))_3$ species which is believed to be the active catalyst. Three types of allyl complexes of transition metals have been identified: σ-allyl $(\eta^1\text{-}C_3H_5)$, π-allyl $(\eta^3\text{-}C_3H_5)$ and allyl bridged $(\mu\text{-}C_3H_5)$ complexes.[61] In general η^1-allyl bonds are thermally less stable and may decompose to give the η^3-allyl complex. A $\sigma \longrightarrow \pi$ rearrangement is an intramolecular reaction in which an organic group σ-bonded (η^1) to a metal becomes π bonded (η^n) and this process is often reversible. The σ-allyl complexes of $M(\eta^1\text{-}C_3H_5)(\eta^5\text{-}C_5H_5)(CO)_3$ (M = Mo[63] or W[64]) on irradiation undergo a σ —> π rearrangement. However on addition of CO the reverse reaction is observed as indicated in Reaction 1.10.1

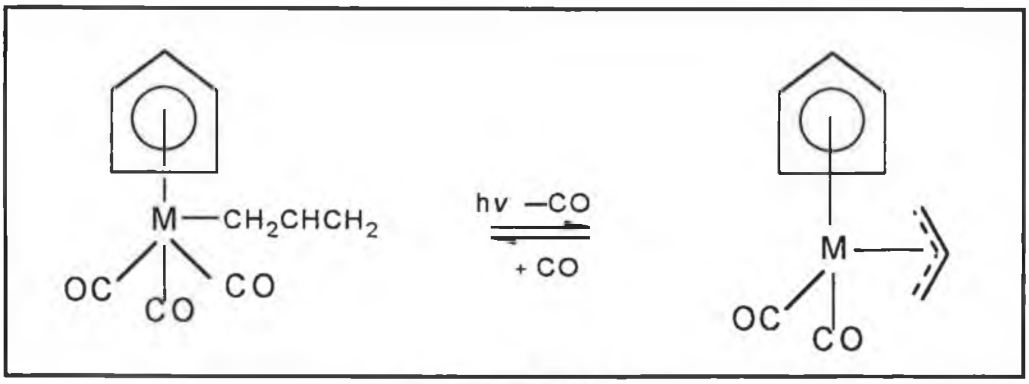

Reaction 1.10.1

Other consequences of CO dissociation from substituted allyl complexes e.g. $Fe(\eta^5\text{-}C_5H_5)(CO)_2(\eta^1\text{-}C_3H_4R)$ include *syn* and *anti* conformations of the R group after σ —> π rearrangement as shown in Reaction 1.10.2

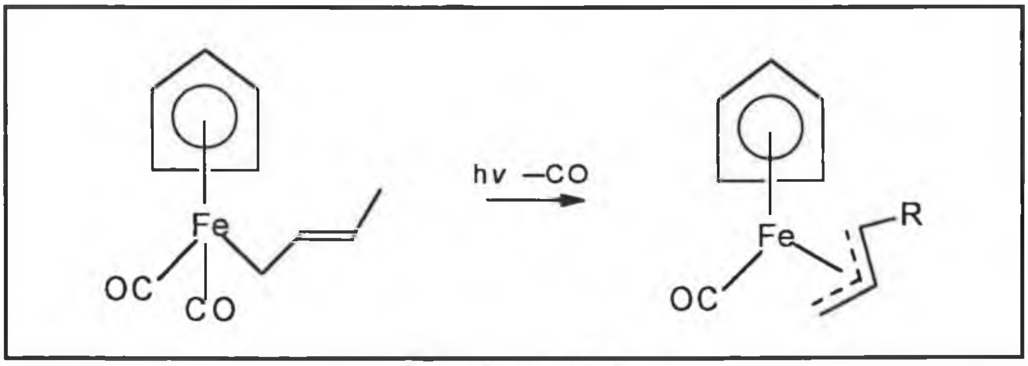

Reaction 1.10.2

In most cases the thermal σ —> π rearrangement are irreversible but in theory should be reversible

Perutz *et al.*[65] carried out addition and substitution reactions of pentadienyltricarbonylmanganese compounds with various ligands. Photolysis of $(\eta^5\text{-}C_5H_7)Mn(CO)_3$ at 20K in a CO matrix for 3 hours resulted in complete conversion to $(\eta^3\text{-}C_5H_7)Mn(CO)_4$. Photolysis of this compound in a dinitrogen matrix led to formation of bands tentatively assigned to $(\eta^3\text{-}C_5H_7)Mn(CO)_3N_2$. Irradiation of $(\eta^5\text{-}C_5H_7)Mn(CO)_3$ in hexane solution required 30 hours under a CO atmosphere to generate bands assigned to that of the tetracarbonyl species, and evidence for the presence of the pentacarbonyl species.

Palmer and Basolo[66] examined reactions for various allyl complexes of the type in Reaction 1.10.3.

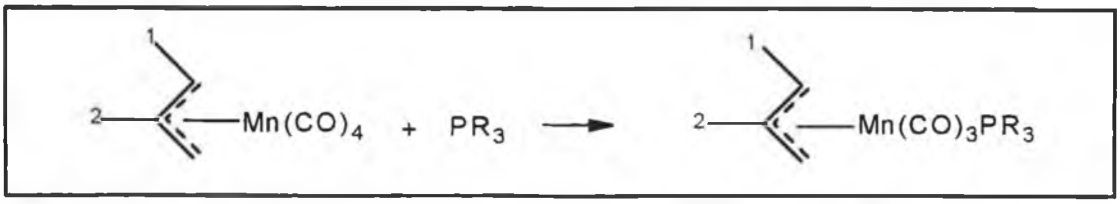

(1.10.3)

It appears that the allyl manganese complexes react by a simple S_N1 CO dissociative process. Also, the rate of CO dissociation is dependent upon the steric bulk and isomeric configuration of the substituted allyl ligands. Substituents effects for η^3-allyl manganese carbonyls on the rates of CO substitution were measured. Generally a substituent in the 2 position increases the reaction rate whereas in the 1 position decreases the reaction rate. It is possible that this is a steric effect because the rate of enhancement correlates to the size of the substituent.

The photochemistry of (η^3-allyl)Co(CO)$_3$ was investigated in frozen gas matrices.[67] Photolysis of (η^3-allyl)Co(CO)$_3$ in argon or methane matrices at 12K led to formation of the coordinatively unsaturated species (η^3-allyl)Co(CO)$_2$ which is in accord with the dissociation mechanism proposed for kinetic studies for the CO substitution reactions of (η^3-allyl)Co(CO)$_3$ in solution.[68] Photolysis in a CO matrix results in the formation of a tetracarbonyl species - (η^1-allyl)Co(CO)$_4$ which also underwent a hapticity change. The photoreactions of this system are given in Scheme 1.10.4

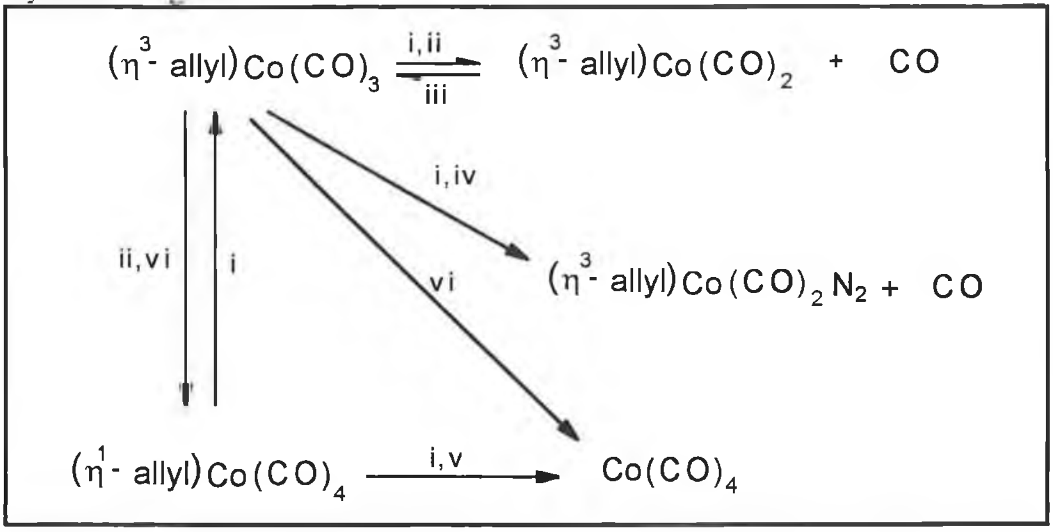

i - hν(UV), ii - Ar,CH$_4$, iii - hν(visible), iv - N$_2$, v - CO, vi - UV-vis

Scheme 1.10.4

Hitman *et al.*[69] carried out matrix isolation experiments with (η^1-C_3H_5)Mn(CO)$_5$. UV irradiation (η^1-C_3H_5)Mn(CO)$_5$ in a methane matrix resulted in a decrease of the parent bands and an increase in the bands due to (η^3-C_3H_5)Mn(CO)$_4$ along with a band at 2138 cm^{-1} which indicated further loss of CO to produce the 16 electron species (η^3-C_3H_5)Mn(CO)$_3$ which was later confirmed by ^{13}CO labelling experiments. The photochemical reaction pathway for this compound is outlined in Scheme 1.10.5

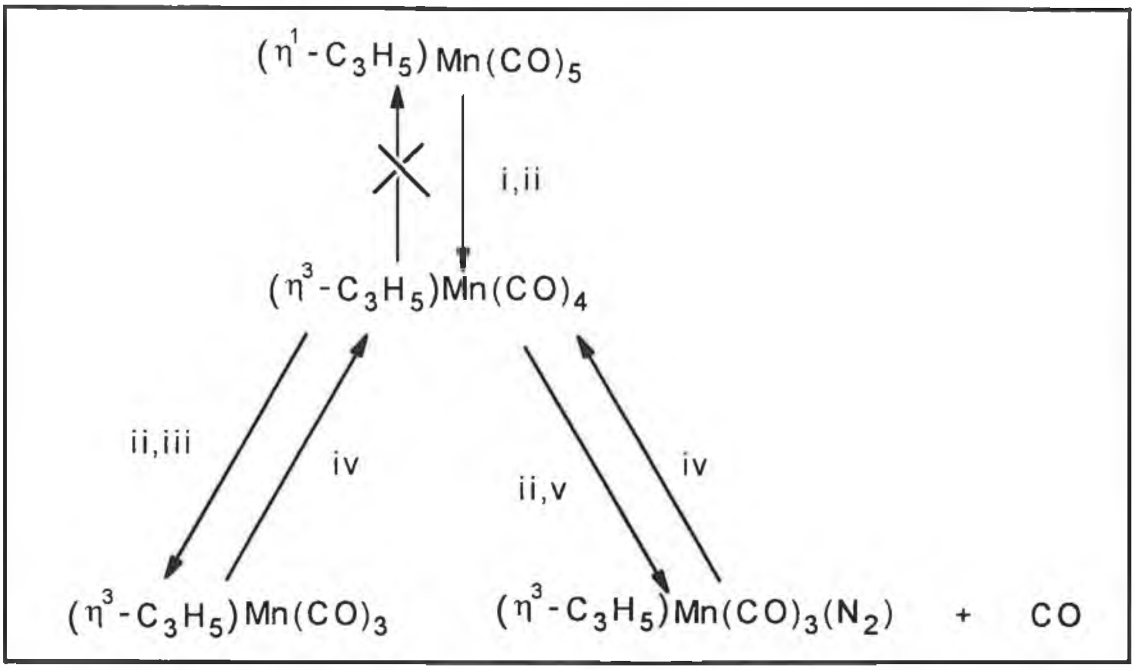

i - Ch$_4$,Ar,N$_2$ or CO, ii - hν(UV), iii - Ch$_4$,Ar, iv - hν(vis) or annealing, v - N$_2$

Scheme 1.10.5

Recombination with CO to form (η^3-C_3H_5)Mn(CO)$_4$ upon visible photolysis and annealing was also monitored for this 16 electron species. Similar chemistry was observed in an argon matrix although less efficiently. Photolysis in a dinitrogen matrix resulted in the appearance of bands in the ν_{CO} carbonyl region attributed to the (η^3-C_3H_5)Mn(CO)$_3$(N$_2$). Photolysis in a CO matrix generated bands assigned to the tetracarbonyl species - no evidence was found for the tricarbonyl intermediate however.

The observation of η^1—>η^3 conversion in all matrices suggests that this is a facile process. The conversion from η^1—>η^3 was found to be irreversible in contrast to Co and W systems which indicates that η^3-allyl manganese compounds are more stable. This reversibility for Mn is consistent with gas phase UV photoelectron[70] and x-ray photoelectron spectroscopic[71] studies.

Lee and Liu[72] reported the synthesis, characterisation and reactivity of pentacarbonyl (η^1-2,4-pentadienyl)manganese. Photolysis of a ethereal solution of (η^1-C_5H_7)Mn(CO)$_5$ at -20°C for 12 hours led to the formation of *syn* (η^3-C_5H_7)Mn(CO)$_4$. No evidence was found for the formation of the η^5 compound even on prolonged photolysis. Heating of (η^1-C_5H_7)Mn(CO)$_5$ to its reflux temperature in cyclohexane lead to formation of the (η^5-C_5H_7)Mn(CO)$_3$ together with a small amount of the η^3 compound. The overall photolytic and thermal pathway for (η^1-2,4-pentadienyl)manganese is given in Scheme 1.10.6

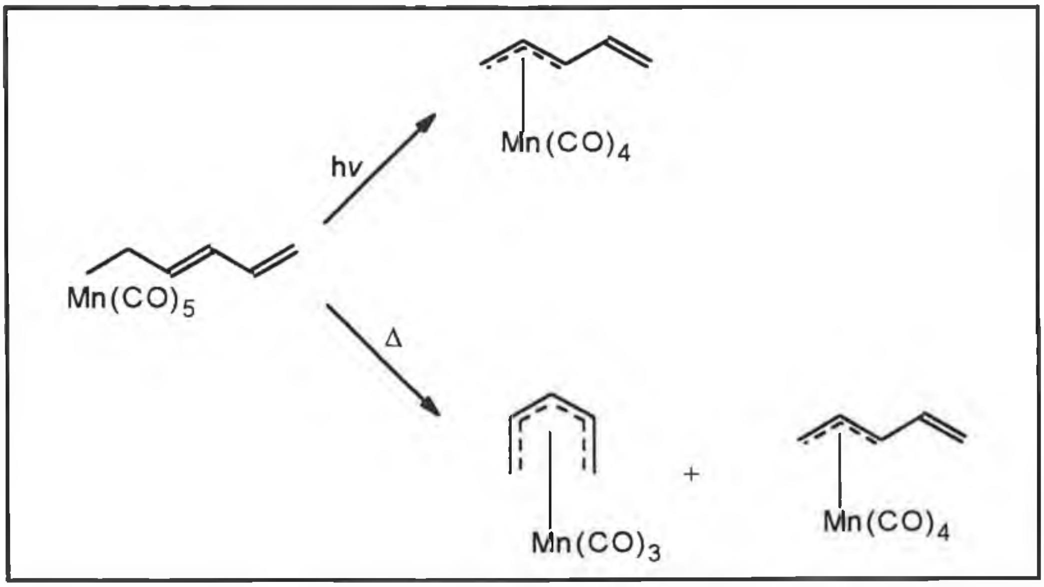

Scheme 1.10.6

More recently Young and Wrighton[73] investigated low temperature photolysis of (η^1-$C_6H_5CH_2$)Mn(CO)$_5$. Irradiation of this compound in methylcyclohexane at 95K lead to the growth of bands assigned to (η^3-$C_6H_5CH_2$)Mn(CO)$_4$. No evidence was found for the 16 electron η^1-species. Trapping experiments with CO and PPh$_3$ results in spectroscopic data consistent with formation of the η^3-tetracarbonyl photoproduct. Warm up of the glass resulted in reversal to the η^1 parent material as given in Reaction 1.10.7 and 1.10.8

$$(\eta^1\text{-}C_6H_5CH_2)Mn(CO)_5 \xrightarrow{h\nu} (\eta^3\text{-}C_6H_5CH_2)Mn(CO)_4 + CO \qquad (1.10.7)$$

$$(\eta^3\text{-}C_6H_5CH_2)Mn(CO)_4 \xrightarrow[CO]{\Delta} (\eta^1\text{-}C_6H_5CH_2)Mn(CO)_5 \qquad (1.10.8)$$

The ratio of CO loss to Mn-R bond homolysis was found to be wavelength dependent for R = $CH_2C_6H_5$ in argon purged alkane solution at 200K. From NMR data it was concluded that $(\eta^3\text{-}C_6H_5CH_2)Mn(CO)_4$ is fluxional at 200K and the two structures in Reaction 1.10.9 are rapidly interconverting. This fluxionality was not considered unexpected as the π-σ-π allyl interconversion should be facile due to the aromatic stabilisation of the phenyl ring in the 16 electron $(\eta^1\text{-}C_6H_5CH_2)Mn(CO)_4$.

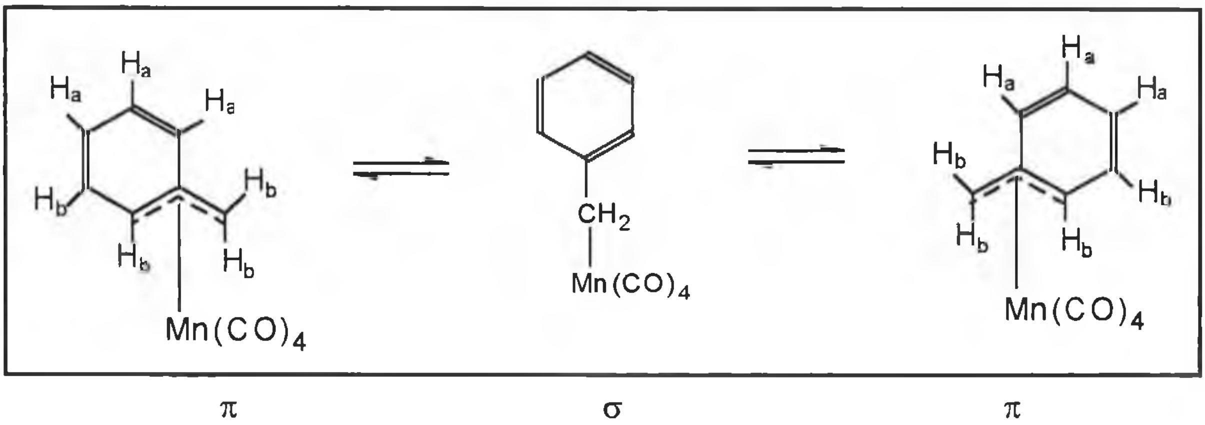

(1.10.9)

1.11 Photochemistry of dimetallic carbonyl systems.

Over the last number of years there has been an increased interest in the chemistry of compounds containing two or more metal centres. A wide variety of transition metal cluster compounds have been studied because of the presumed analogy of their chemistry to that of heterogeneous catalyst surfaces. For compounds such as $Mn_2(CO)_{10}$, $(\eta^5\text{-}C_5H_5)_2Fe_2(CO)_4$ there are two primary photochemical processes, homolysis of the metal-metal bond and CO loss.[74] The former process giving rise to 17 electron radicals may undergo a variety of reactions including atom transfer, recombination, electron transfer and substitution.[75] The chemical behaviour of dinuclear CO loss intermediates has gained importance because of the interest in the reactions of mononuclear coordinatively unsaturated species such as $(\eta^5\text{-}C_5H_5)Rh(CO)$,[76] $(\eta^5\text{-}C_5H_5)Mn(CO)_2$[77] and $Cr(CO)_5$.[78] In the dinuclear compounds the coordinatively unsaturated molecule resulting from CO loss can engage in a form of "self repair" through formation of bridging $(Cp_2Fe_2)(\mu^2\text{-}(CO)_3)$[79] or semibridging $(Mn_2(CO)_9)$[80] CO linkages.

The photochemistry of $Mn_2(CO)_{10}$ in a rigid matrix at 77K was found to be somewhat different to that observed in solution.[81] Dissociative loss of CO from photoexcited $Mn_2(CO)_{10}$ was observed which yielded a CO bridged $Mn_2(CO)_9$ species, which in the presence of 2 electron donors will react to form $Mn_2(CO)_9L$. Presumably in a rigid matrix only the CO loss product was observed because of the immediate cage recombination of the $Mn(CO)_5^{\bullet}$ radicals. In contrast, in solution the predominant reaction was found to be M-M scission along with CO loss which accounted for approximately 30% of the reaction. These results were later supported by Yesaka *et al.*[82] who proposed homolytic cleavage and CO loss as the photochemical reaction of $Mn_2(CO)_{10}$ as shown in Reaction 1.11.1

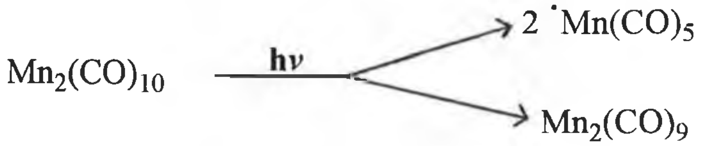

(1.11.1)

The first direct evidence for the transient species $Mn(CO)_5$ and $Mn_2(CO)_9$ in solution was proposed by Church *et al.*[83] The pentacarbonyl radical was found to recombine at nearly diffusion controlled rate to regenerate parent material. The decay of the $Mn_2(CO)_9$ species was affected by the presence of CO and the reactivity of this intermediate was found to be similar to that of $Cr(CO)_5$. The behaviour of $Mn_2(CO)_9$ was found to be solvent dependent which is similar to that of $Cr(CO)_5$ which is known to coordinate rapidly to the solvent.[84]

A number of heterodinuclear compounds have been investigated photochemically and amongst those are $MnRe(CO)_{10}$. Sonnenberger and Atwood[85] investigated the kinetics of substitution reactions of $MnRe(CO)_{10}$ with a number of entering ligands. For all ligands studied the Re substituted product $(CO)_5MnRe(CO)_4L$ was found to predominate although a very small amount of $L(CO)_4MnRe(CO)_5$ was formed early in the reaction.

Matrix isolation and time resolved infrared studies indicated the primary photoprocess of $MnRe(CO)_{10}$ to be formation of a $MnRe(CO)_9$ bridged species along with $Mn(CO)_5$ and $Re(CO)_5$.[86] Oyer and Wrighton[87] have reported that unsaturated $MnRe(CO)_9$ resulting from photolytic CO loss when in the presence of PPh_3 will yield the Mn substituted compound. These results indicate that photosubstitution occurs at the site from which CO is extruded in the primary photoprocess.

Much of the literature regarding heterodinuclear carbonyl compounds involve systems that contain metal atoms directly bonded. As none of these compounds have extended bridging systems separating the metal centres they are not useful for studying the effect of metal conjugation through a complexed ligand.

1.12 References

1 (a)Kealy,T.J.;Pauson,P.L.; *Nature*; 1951,**168**,1039.
(b)Wilkinson,G.;Rosenblum,M.;Whiting,M.C.;Woodward,R.B.; *J. Am. Chem. Soc.*; 1952,**74**,2125.

2 Ziegler,K.;Holtzkampf,E.;Breil,H.;Martin.M; *Angew. Chem.*; 1955,**67**,543.

3 Fischer,E.O.;Pfah,W.; *Z. Naturforsch*; 1952,**7B**,377.

4 Pimentel,G.C.;Whittle,E.;Dows,D.A.; *J. Phys. Chem.*; 1954,**22**,1943.

5 Burdett,J.K.;Downs,A.J.;Gaskill,G.P.;Graham,M.A.Turner,J.J.; Turner,R.F.; *Inorg. Chem.*; 1978,**17**,532.

6 Perutz,R.N.;Turner,J.J.; *J. Am. Chem. Soc.*; 1975,**97**,4791.

7 Poliakoff,M.;Turner,J.J.; *J. Chem. Soc., Dalton Trans.*; 1974,2276.

8 Bitterwolf,T.;Cott,K.A.;Rest,A.J.;Mascetti,J.; *J. Organomet. Chem.*; 1991,**419**,113.

9 Howdle,S.M.;Poliakoff,M.; *J. Chem. Soc.,Chem. Comm.;* 1989,1099.

10 Norrish,R.G.;Porter,G.; *Nature*; 1950,**164**,685.

11 Nasielski,J.;Kirsch,P.;Wilputte-Steinert,L.; *J. Organomet. Chem.*; 1971,**29**,269.

12 (a)Lefohn,A.S.; Pimentel, G.C.; *J. Phys. Chem.*; 1971,**55**,1213.
(b)Tan,L.Y.;Winter,A.M.; Pimentel, G.C.; *J. Phys. Chem.*; 1972,**57**,4028.

13 (a)Church,S.P.;Grevels,F-W.;Hermann,H.;Schnaffner,K.; *J. Chem. Soc., Chem. Comm.*; 1985,30.
(b)Church,S.P.;Grevels,F-W.;Hermann,H.;Schnaffner,K.; *Inorg. Chem.* 1984,**23**,3830.

14 (a)Fletcher,T.R.;Rosenfeld,R.N.; *J. Am. Chem. Soc.*; 1985,**107**,2203.

(b)Seder,T.A.;Church,S.P.;Ouderkirk,A.J.;Wietz,E.; *J. Am. Chem. Soc.*; 1985,**107**,1432.
(c) Zheng,Y.;Wang,W.;Lin,J.;She,Y.;Fu,K-J.; *J. Phys. Chem.*; 1992,**96**,7650.

15 Strohmeier,S.;von Hobe,D.; *Z. Naturforsch.*; 1963,**18B**,770.

16 Wrighton,M.S.;Haverty,J.L.; *Z. Naturforsch.*; 1974,**30B**,254.

17 Nasielski,J.;Denisoff,O.; *J. Organomet. Chem.*; 1975,**102**,65.

18 Gilbert,A.;Kelly,J.M.;Budzwait,M.;Koerner von Gustorf,E.; *Z. Naturforsch.*; 1976,**31B**,1091.

19 Bamford,C.H.;Al-Lamee,K.G.;Konstantantinov,C.J.; *J. Chem. Soc., Faraday Trans.* 1; 1977,**73**,1406.

20 Trembovler,V.N.;Baranetskaya,N.K.;Fok,N.V.;Zaslauskaya,G.B.; Yavorskii,B.M.;Setkina,V.N.; *J. Organomet. Chem.*; 1976,**117**,339.

21 Yavorskii,B.M.;Trembovler,V.N.;Setkina,V.N.;Baranetskaya,N.K.; Zaslavskaya,G.B.;Evdokimora,M.G.; *Russian J. Phys. Chem.*; 1974,**3**,1231.

22 (a)Turner,J.J.; *Angew. Chem. Internat. Edn.*; 1975,**14**,304.
(b)Ogden,J.S.;Turner,J.J.; *Chem. in Britain*; 1971,**7**,186.

23 Rest,A.J.;Sodeau,J.R.;Taylor,D.J.; *J. Chem. Soc., Dalton Trans.*; 1978,651.

24 Chapman,O.L.;Pacansky,L.;Wojtkowski P.W .; *J. Chem. Soc., Chem. Comm.*; 1973,681.

25 Braterman,P.S.;Black,J.D.; *J. Organomet. Chem.*; 1972,**39**,C3.

26 Black,J.D.;Boylan,M.J.;Braterman,P.S.; *J. Chem. Soc. Dalton Trans.*; 1981,673.

27 Hill,R.H.;Wrighton,M.S.; *Organometallics*; 1987,**6**,632.

28 Wang,W.;Jin,Y.;Liu,Y.S.;Fu,K-J.; *J. Phys. Chem.*; 1992,**96**,1278.

29 Zheng,Y.;Wang,W.;Lin,J.;She,Y.;Fu,K-J.; *J. Phys. Chem.*; 1992,**96**,9821.

30 Strohmeier,S.;Starrico,E.; *Z. Phyzik. Chem. Neue Folge.*; 1966,**38**,315.

31 (a)Mahaffy,C.A.L.;Pauson,P.L.; *J.Chem. Res.(S)*; 1979,126.
(b)Mahaffy,C.A.L.;Pauson,P.L.; *J.Chem. Res.(M)*; 1979,1752.

32 Zimmerman,C.L.;Shaner,J.L.;Royh,S.A.;Willeford,B.R.; *J. Chem. Res.(S)* 1980,108.

33 (a)Traylor,T.G.;Stewart,K.J.;Goldberg,M.J.; *J. Am. Chem. Soc.*; 1984,**106**,4445.
(b)Traylor,T.G.;Stewart,K.J.;Goldberg,M.J.; *Organometallics*; 1986,**5**,2062.
(c)Traylor,T.G.;Stewart,K.J.; *J. Am. Chem. Soc.*; 1986,**108**,6977.
(d)Traylor,T.G.;Goldberg,M.J.; *Organometallics*;1987,**6**,2413.
(e)Traylor,T.G.;Goldberg,M.J.; *Organometallics*;1987,**6**,2531.

34 (a)Mutteries,E.L.;Bleeke,J.R.;Sievert,A.C.; *J.Organomet.Chem.*; 1979,**178**,197.
(b)Mutteries,E.L.;Bleeke,J.R.;Wuncherer,J.;Albright,T.A.; *Chem.Rev.*; 1982,**82**,499.
(c)Yagupsky,C.;Cais,M.; *Inorg. Chim. Acta*; 1975,**12**,L27.
(d)Howell,J.A.S.;Dixon,D.T.;Kola,J.C.;Ashford,N.F.; *J. Organomet. Chem.*; 1985,**294**,C1.

35 Kunz,V.;Nowacki,W.; *Helv. Chim. Acta*; 1967,**50**,1052.

36 Howell,J.A.S.;Ashford,N.F.;Dixon,D.T.;Kola,J.C.;Albright,T.A.; Kang,S.K.; *Organometallics*; 1991,**10**,1852.

37 Florino,S.M,Nicholas,K.M.; *J. Organomet. Chem.*; 1978,**144**,321.

38 (a)Kundig,,P.;Perret,C.;Spichiger,S.;Bernadelli,G.; *J. Organomet. Chem.*; 1985,**286**,183.
(a)Oprunenko,Y.F.;Malyuginen,S.G.;Ustynyuk,Y.A.;Ustynyuk,N.A.; *Izv. Akad. Nauk. SSSR. (Engl. transl.)*; 1984,2199.

39 Albright,T.A.;Hofman,P.;Hoffmann,R.;Lillya,C.;Dobosh,P.A.; *J. Am. Chem. Soc.*; 1983,**105**,3396.

40 Cunningham,S.D.;Ofele,K.;Willeford,B.R.; *J. Am. Chem. Soc.*; 193,**108**,3725.

41 Rerek,M.E.;Baslo,F.; *Organometallics*; 1984,**3**,647.

42 Kirss,R.V.;Treichel,P.M.; *J. Am. Chem. Soc.*; 1986,**108**,853.

43 Johnson,J.W.;Treichel,P.M.; *J. Am. Chem. Soc.*; 1977,**99**,1427.

44 Berno,P.;Ceccon,A.;Dapra,F.;Gambaro,A.;Venzo,a.; *J. Chem. Soc., Chem. Comm.*; 1986,1548.

45 Oprunenko,Y.F.;Reshetova,M.D.;Malyugina,S.G.;Ustynyuk, Y.A.;Ustynyuk,N.A.;Batsanov,;A.S.;Yanorsky,A.I.;Srruchkov,Y.T.; *Organometallics*; 1994,**13,**2284.

46 Kelly,J.M.;Hermann,H.;Koerner von Gustorf,E.; *J. Chem. Soc., Chem. Comm.*; 1973,105.

47 Kelly,J.M.;Bent,D.V.;Hermann,H.;Schlute-Frohlinde,D.K.;Koerner von Gustorf,E.; *J. Organomet. Chem.*; 1974,**69**,259.

48 Simon,J.D.;Peters,K.S.; *Chem. Phy. lett.*; 1983,**98**,53.

49 Kelly,J.M.;Long,C.;Bonneau,R.; *J. Phys. Chem.*; 1983,**87**,3345.

50 Church,S.P.;Grevels,F-W.;Hermann,H;Schnafer,K.; *Inorg. Chem.*; 1985,**24**,418.

51 Simon,J.D.;Xie,X.; *J. Phys. Chem.*; 1986,**90**,6751.

52 Simon,J.D.;Xie,X.; *J. Phys. Chem.*; 1987,**91**,5538.

53 Ishikawa,Y.;Brown,C.E.;Hackett,P.A.;Raye,D.M.; *Chem. Phy. Lett.*; 1988,**150**,506.

54 Zhang,S.;Zang,V.;Bajaj,H.C.;Dobson,G.R.;van Eldik,R.; *J. Organomet. Chem.*; 1990,**397**,279.

55 Joly,A.G.;Nelson,K.A.; *J. Chem. Phy.*; 1991,**152**,69.

56 Brookhart,M.;Green,M.L.H.; *J. Organomet. Chem.*; 1983,**250**,395.

57 Morse,J.M.;Parker,G.H.;Burkey,T.J.; *Organometallics*; 1989,**8**,2471.

58 Lewis,K.E.;Golden,D.M.;Smith,G.; *J. Am. Chem. Soc.*; 1984,**106**,3905.

59 Nayak,S.K.;Burkey,T.J.; *Organometallics*; 1991,**10**,3745.

60 Jonassen,H.B.;Stearns,R.J.;Kenttama,I.; *J. Am. Chem. Soc.*; 1958,**80**,2586.

61 Green,M.LH.;Nagy,P.L.I.; *Adv. Organomet. Chem.*; 1964,**2**,325.

62 (a)Mutteries,E.L.;Hirsekorn,F.J.; *J. Am. Chem.Soc.*;1973,**95**,5419.
(b)Mutteries,E.L.;Hirsekorn,F.J.; *J. Am. Chem. Soc.*; 1974,**96**,4063.
(c)Stuhl,L.S.;Mutteries,E.L.; *Inorg. Chem.*;1978,**17**,2148.
(d)Bleeke,J.R.;Mutteries,E.L.; *J. Am. Chem. Soc.*; 1981,**103**,556.

63 Cousins,M.;Green,M.L.H.; *J. Chem. Soc.;* 1963,889.

64 Green,M.L.H.;Stear,A,N.; *J.. Organomet. Chem.*; 1964,**1**,230..

65 Paz-Sandoval,M.;Powell,P.;Drew,M.G.B.;Perutz,R.N.; *Organometallics*; 1984,**3**,1026.

66 Palmer,G.T.;Basolo,F.; *J. Am. Chem. Soc.*;1985,**107**,3122.

67 Rest,A.J.;Taylor,D.J.; *J. Chem. Soc., Dalton Trans.*; 1983,1291.

68 (a)Heck,R.F.; *J. Am. Chem. Soc.*; 1963,**85**,655.
(a)Heck,R.F.; *J. Am. Chem. Soc.*; 1964,**87**,2572.

69 Hitman,R.B.;Mahmound,K.A.;Rest,A.J.; *J. Organomet. Chem.*; 1985,**291**,321.

70 Worley,S.D.;Gibson,D.H.;Hsu,W-L.; *Inorg. Chem.*; 1981,**20**,1327.

71 Ricco,A.J.;Bakke,A.A.;Jolly,W.L.; *Organometallics*; 1982,**1**,94.

72 Lee,F.W.;Liu,R-S.; *J. Organomet. Chem.*; 1987,**320**,211.

73 Young,K.M.;Wrighton,M.S.; *J. Am Chem. Soc.*; 1990,**112**,157.

74 Meyer,T.L.;Caspar,J.V.; *Chem. Rev.*; 1985,**85**,187.

75 (a)Kochi,J.K.; *J. Organomet. Chem.*; 1986,**300**,139.
(b)Baird,M.C.; *In Organometallic Radical Processes*; Trogler,W.C. Ed. Elsevier Amsterdam 1990, 49.

76 (a)Hoyano,J.K.;Graham.W.A.G.; *J. Am. Chem. Soc.*; 1982,**104**,3723.

(b)Weiller,B.H.;Wasserman,E.P.;Bergman,R.G.;Moore,C.B.; Pimentel,G.C.; *J. Am. Chem. Soc.*;1989,**111**,3583.

77 Schubert,U.; *Adv. Organometal. Chem.*; 1990,**30**,151.

78 (a)Wrighton,M.;Schroeder,M.A.; *J. Am. Chem. Soc.*; 1973,**95**,5764.
(b)Dobson,G.R.;Zhang,S.; *J. Coord. Chem.*; 1990,**21**,155.

79 (a)Caspar,J.V.;Meyer,T.L.; *J. Am. Chem. Soc.*; 1980,**102**,7795.
(b)Hepp,A.F.;Blaha,J.P.;Lewis,C.;Wrighton,M.S.; *Organometallics*; 1984,**3**,174.

80 (a)Fox,A.;Poe,A.; *J. Am. Chem. Soc.*; 1980,**102**,2497.
(b)Seder,T.A.;Church,S.P,Weitz,E.; *J. Am. Chem. Soc.*; 1986,**108**,7518.

81 Hepp,A.F.;Wrighton,M.S.; *J. Am. Chem.*; 1983,**105**,5934.

82 Yesaka,H.;Kobayashi,T.;Yasufuku,K.;Nagakura,S.; *J. Am. Chem. Soc.*; 1983,**105**,6249.

83 Church,S.P.;Hermann,H.;Grevels,F-W.;Schaffner,K.; *J. Chem. Soc., Chem. Comm.*; 1984,785.

84 Turner,J.J.;Poliakoff,M.; *Am. Chem. Soc. Symp. Ser.*; 1983,**211**,35.

85 Sonnenberger,D.;Atwood,J.D.; *J. Am. Chem. Soc.*; 1980,**102**,3484.

86 Firth,S.;Hodges,P.M.;Poliakoff,M.;Turner,J.J.; *Inorg. Chem.*; 1986,**25**,4608.

87 Oyer,T.J.;Wrighton,M.S.; *Inorg. Chem.*; 1988,**27**,3689.

Chapter 2

An investigation into the effect of substituent and solvent on the reactivity of (η^6-arene)M(CO)$_2$(s) (where M = Cr or Mo).

2.1 Laser flash photolysis of (η^6-arene)Cr(CO)$_3$.

The photochemical carbonyl substitution of Group 6 metal carbonyls (M(CO)$_6$, M=Cr, Mo or W) is well established, with decarbonylation resulting on absorption of light.[1] The coordinatively unsaturated species so generated, M(CO)$_5$ reacts with a ligand,L, to give M(CO)$_5$L, as given in Reactions 2.1.1 and 2.2.2.

$$M(CO)_6 \xrightarrow{h\nu} M(CO)_5 + CO \qquad (2.1.1)$$

$$M(CO)_5 + L \longrightarrow M(CO)_5L \qquad (2.1.2)$$

In comparison there have been relatively few investigations into the photochemistry of (η^6-arene)Cr(CO)$_3$. Early work using conventional flash photolysis identified (η^6-benzene)Cr(CO)$_2$(s) (s = alkane solvent) as the primary photoproduct on the basis of kinetic rather than spectroscopic data (reaction 2.1.3).[2] The arene exchange process was also observed following photolysis (reaction 2.1.4), and the ability of CO to quench this process implies the intermediacy of (η^6-benzene)Cr(CO)$_2$ in this reaction.[2]

$$(\eta^6\text{-arene})Cr(CO)_3 \xrightarrow{h\nu} (\eta^6\text{-arene})Cr(CO)_2 + CO \qquad (2.1.3)$$

$$(\eta^6\text{-arene})Cr(CO)_3 + \text{arene*} \xrightarrow{h\nu} (\eta^6\text{-arene*})Cr(CO)_3 + \text{arene} \qquad (2.1.4)$$

Previously, flash photolysis studies have been carried out on a number of alkyl substituted benzene compounds in order to investigate the effect of substituents on the reactivity of the dicarbonyl species toward CO.[3] The aim of this study was to further this investigation by using other alkyl substituents but also using halogenated benzene compounds.

2.1.1 Electronic absorption spectrum of (η^6-arene)Cr(CO)$_3$.

The UV/vis. spectrum of (η^6-benzene)Cr(CO)$_3$ in cyclohexane is shown in Figure 2.1.1 (this spectrum is typical of these compounds). The absorption spectrum of these complexes is dominated by metal to ligand charge transfer (MLCT) absorptions.[4] These compounds exhibit a well defined lowest energy absorption maximum at approximately 320 nm which has been assigned to Metal

----> arene CT with some M ----> π* CO CT character. There is also a shoulder centred around 265 nm which is assigned to a M ----> π* CO CT transition. This band undergoes a blue shift as the number of electron donating substituents on the ring increases and as a result becomes less resolved from the 230 nm absorption but as we add electron withdrawing substituents a marked shift of this band towards the red region of the spectrum is noticeable as is indicated in Figure 2.1.1.2.

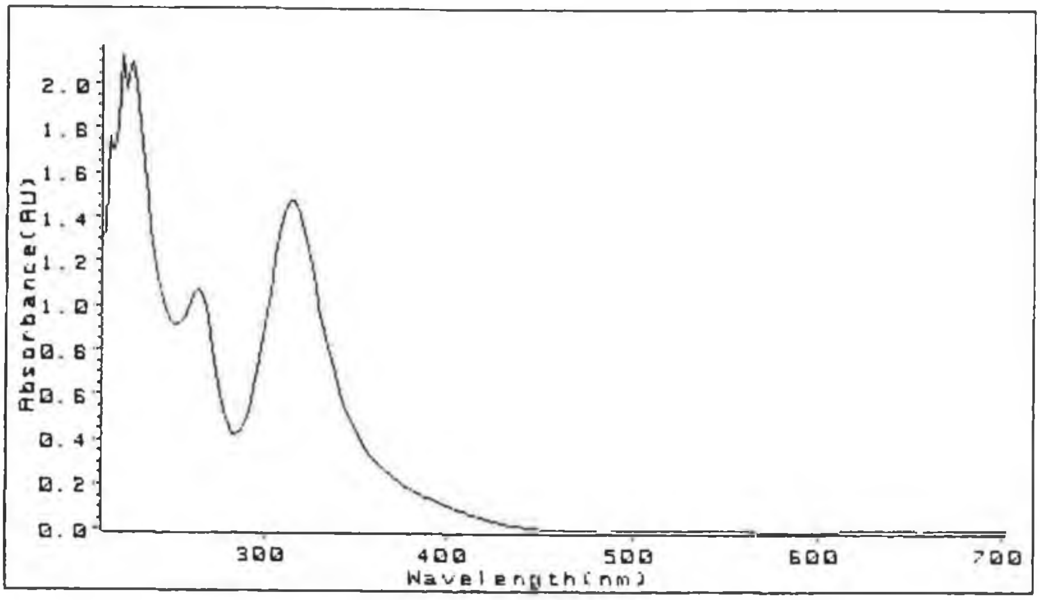

Figure 2.1.1.1 UV/vis. spectrum of (η^6-benzene)Cr(CO)$_3$ (1.7 x 10^{-4}M) in cyclohexane.

A summary of the UV/vis. extinction coefficients of the compounds used in this study at 355 nm and the ν_{CO} infrared stretching frequencies in cyclohexane for all the compounds investigated is presented in Table 2.1.1.1. The values used for calculation of the extinction coefficients are tabulated in Appendix C.

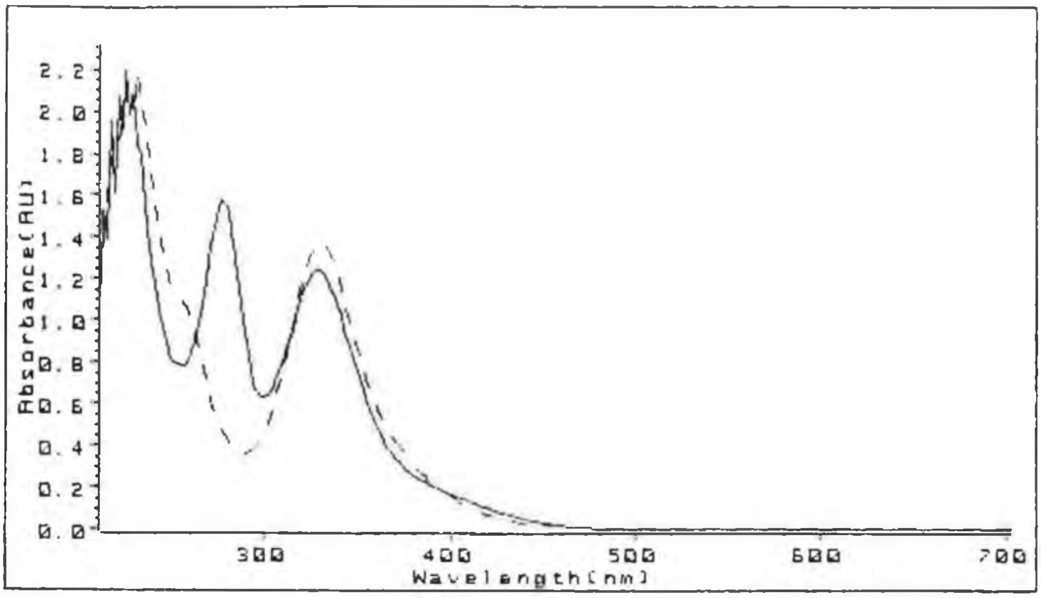

Figure 2.1.1.2 UV/vis. spectra of --- (η^6-hexaethylbenzene)$Cr(CO)_3$ (2.1 x 10^{-4}M) and — (η^6-1,2-dichlorobenzene)$Cr(CO)_3$ (1.1 x 10^{-4}M) in cyclohexane.

(η^6-arene)$Cr(CO)_3$	$\varepsilon_{355\ nm}$ $dm^3\ mol^{-1}\ cm^{-1}$ (± 2%)	ν_{CO} cm^{-1} (± 2cm^{-1})
benzene	3060 [a]	1983, 1915 [a]
ethylbenzene	3269	1979, 1910
o-xylene	4121	1973, 1905
t-butylbenzene	3227	1971, 1908
hexaethylbenzene	3354	1953, 1881
p-chlorotoluene	4005	1986, 1918
p-fluorotoluene	3195	1987, 1916
chlorobenzene	3867	1989, 1926
1,2dichlorobenzene	6079	1994, 1937, 1933

Table 2.1.1.1 A summary of the extinction coefficients and the ν_{CO} infrared stretching frequencies in cyclohexane. [a] data taken from reference 7.

2.1.2 Primary Photoproduct.

Previous work carried out on this system has demonstrated conclusively that the (η^6-arene)Cr(CO)$_2$(s) (where s = solvent) is the primary photoproduct in the photochemistry of (η^6-arene)Cr(CO)$_3$ compounds in condensed phase.[5,6] TRIR studies[7] confirmed that (η^6-benzene)Cr(CO)$_2$(s) (1927,1877 cm^{-1}) is the primary photoproduct in alkane solution at room temperature and these results correlate well with those previously observed in a methane matrix (1937,1885 cm^{-1}).[5] It is likely that the vacant coordination site in this intermediate is occupied by a molecule of solvent(s) as a "token ligand"[8] as in the case of Cr(CO)$_5$ where these highly reactive 16 electron species are known to coordinate weakly to matrices, even these consisting of inert nobel gases.[9] The coordinatively unsaturated isoelectronic M(CO)$_5$ (M = Cr, Mo,W) complexes are now recognised as coordinating to solvent molecules following photolysis in solution at room temperature.[10]

On photolysis of (η^6-arene)Cr(CO)$_3$ (λ=355 nm) compounds in cyclohexane the first transient species observed was (η^6-arene)Cr(CO)$_2$(cyclohexane) which is probably formed within the duration of the flash(10 ns) as in the case of group 6 pentacarbonyl species.[11] The overall process is outlined in reaction (2.1.2.1)

$$(\eta^6\text{-arene})\text{Cr(CO)}_3 \xrightarrow{h\nu} (\eta^6\text{-arene})\text{Cr(CO)}_2 + \text{CO}$$

$$\xrightarrow{+\ s} (\eta^6\text{-arene})\text{Cr(CO)}_2\text{(s)} \qquad (2.1.2.1)$$

A typical transient signal obtained following 355 nm photolysis of a (η^6-benzene)Cr(CO)$_3$ monitored at 280 nm is shown in Figure 2.1.2.1 where the decay curve represents reaction of the solvated dicarbonyl intermediate towards CO to regenerate parent tricarbonyl, see Reaction (2.1.2.2)

$$(\eta^6\text{-arene})\text{Cr(CO)}_2\text{(s)} + \text{CO} \longrightarrow (\eta^6\text{-arene})\text{Cr(CO)}_3 + \text{s} \qquad (2.1.2.2)$$

The return of the transient absorption signal to the pre-irradiated level indicates complete reversibility of the system. The effect of different concentrations of CO on the lifetime of the solvated dicarbonyl species was then investigated. As the concentration of CO increased the life-time of the dicarbonyl species decreased, thus confirming reaction of the (η^6-arene)Cr(CO)$_2$(s) transient species with CO. For instance with (η^6-chlorobenzene)Cr(CO)$_3$ the life time of the dicarbonyl species is 22.4 μs in the presence of 9.0 x 10^{-3}M CO whereas it increases to 44.5 μs in the presence of 4.5 x 10^{-3}M of CO. However, the initial yield of the transient species was found to be independent of added CO, confirming that the signal is resulting from the production of a primary photoproduct.

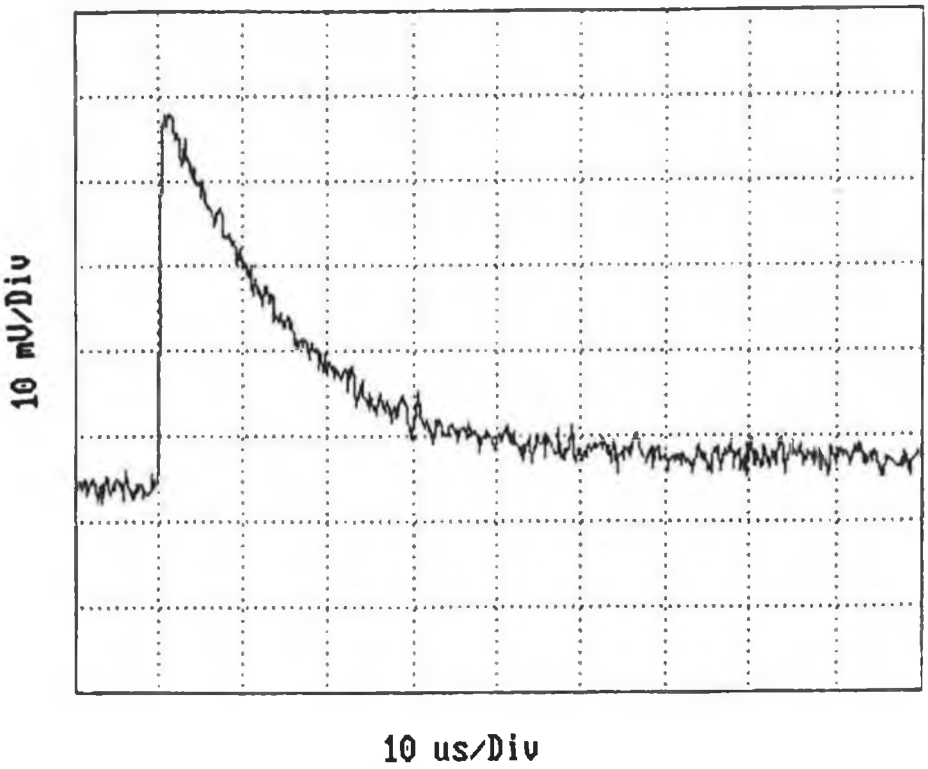

Figure 2.1.2.1 A typical transient signal obtained for the decay of (η^6-benzene)Cr(CO)$_2$(cyclohexane) at 280 nm in the presence of (9.0 x 10^{-3}M) CO.

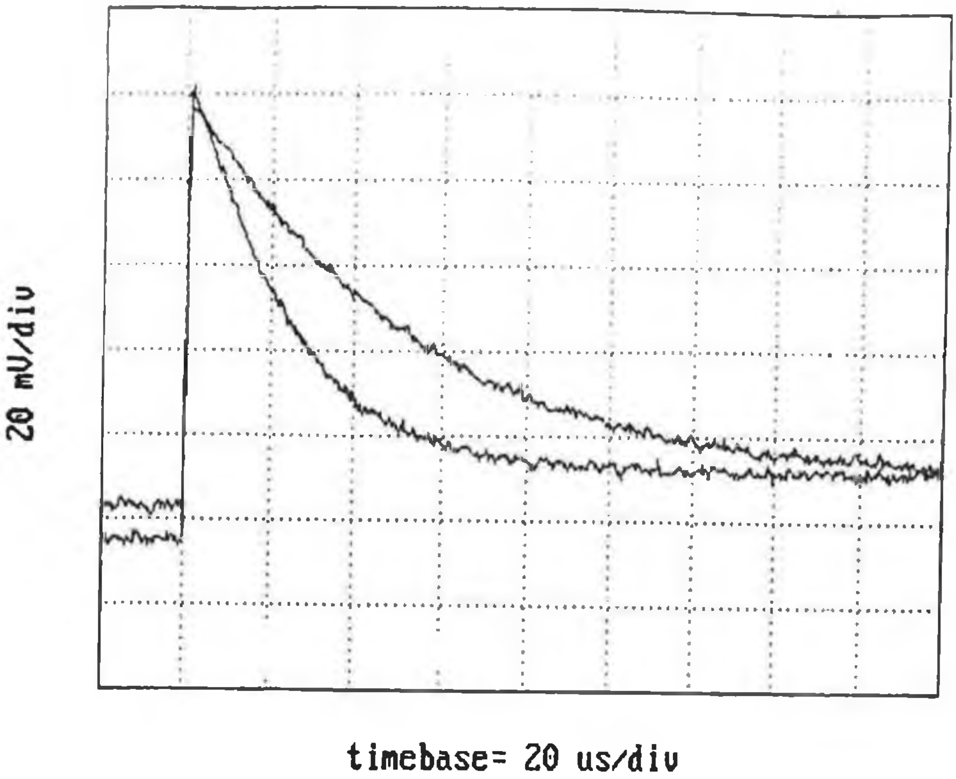

Figure 2.1.2.2 Typical transient decay curves as observed under varying concentrations of CO for (η^6-chlorobenzene)Cr(CO)$_2$(cyclohexane).

As the life-time of the solvated complex depends on the concentration of CO the second order rate for the reaction of the solvated complex with CO to regenerate parent was calculated from the slope of a plot of k_{obs} *versus* CO concentration. All data for the calculations is Tabulated in Appendix A and summarised in Table 2.1.2.1. A decay curve indicating the differences in transients under varying concentrations of CO is shown in Figure 2.1.2.2.

A typical UV/vis. difference spectrum for these compounds is given in Figure 2.1.2.3. The significant spectral features is the positive absorption band at approximately 280 nm which occurs in the valley of the absorption spectrum of the parent compound and a depletion in the region between 320 nm and 350 nm indicating depletion of tricarbonyl. $\lambda_{max.}$ for all (η^6-arene)Cr(CO)$_2$(cyclohexane) occurs around 280 nm hence indicating a similar interaction energy for all compounds, however as the number of halogen substituents on the benzene ring increases the $\lambda_{max.}$ shifts to lower energy to approximately 300 nm as in the case of (η^6-1,2-dichlorobenzene)Cr(CO)$_2$(cyclohexane). Figure 2.1.2.4 contains a difference UV/vis. spectrum under 1 atm. of CO recorded at various time intervals after the flash and further indicates reversibility of the system under these conditions.

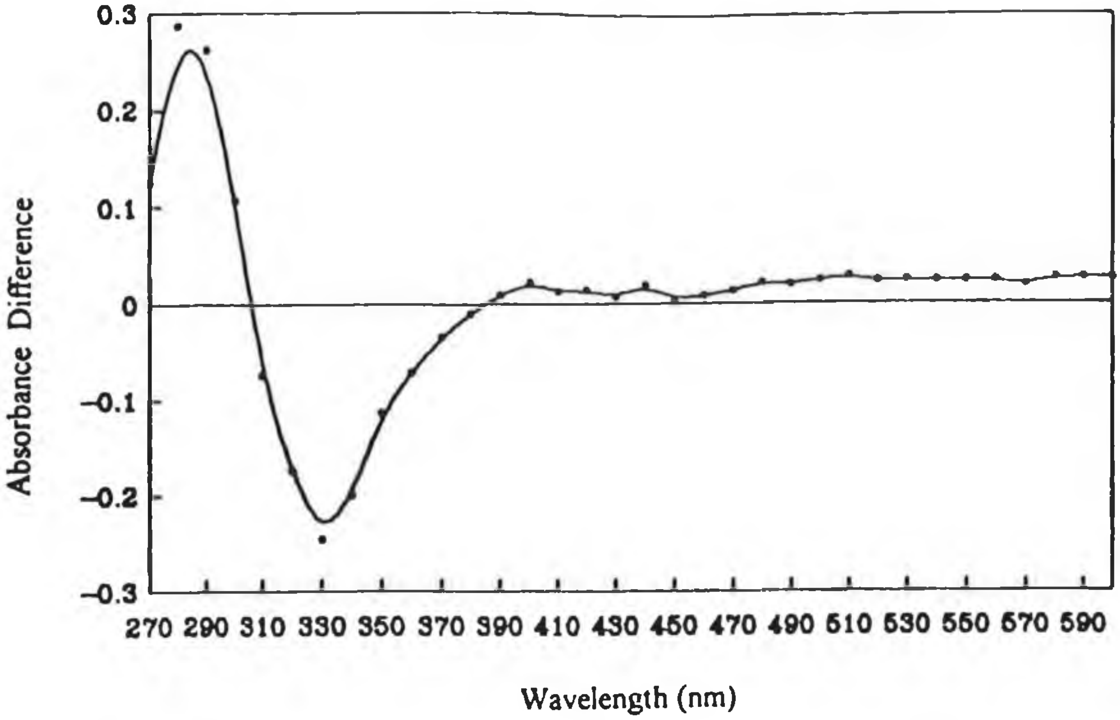

Figure 2.1.2.3 UV/vis. difference spectra after 1μs following flash photolysis of (η^6-*o*-xylene)$Cr(CO)_3$ in cyclohexane at 355nm under 1 atm CO (9.0 x 10^{-3}M) at 298K.

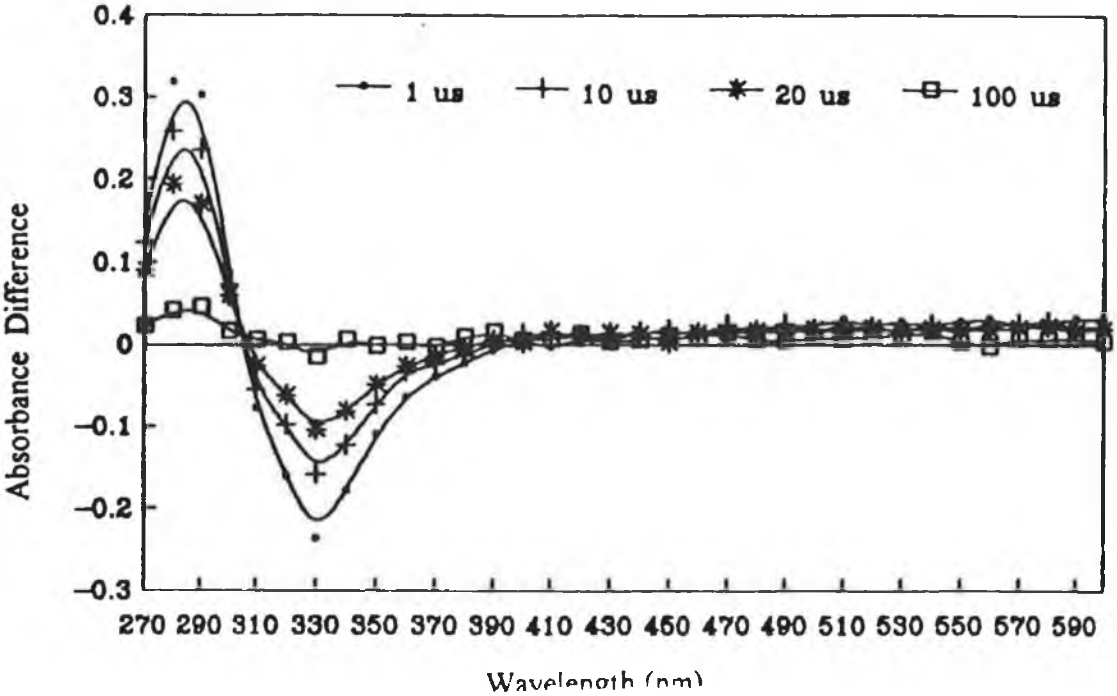

Figure 2.1.2.4 UV/vis. difference spectra at different time bases following flash photolysis of (η^6-*p*-fluorotoluene)$Cr(CO)_3$ in cyclohexane at 355nm under 1 atm CO (9.0 x 10^{-3}M) at 298K.

(a)

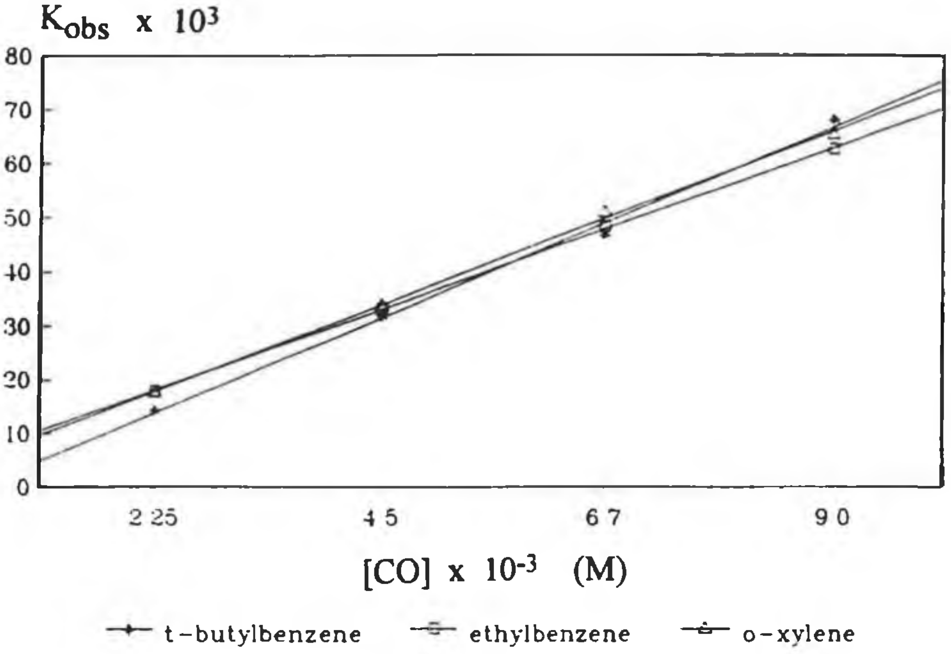

(b)

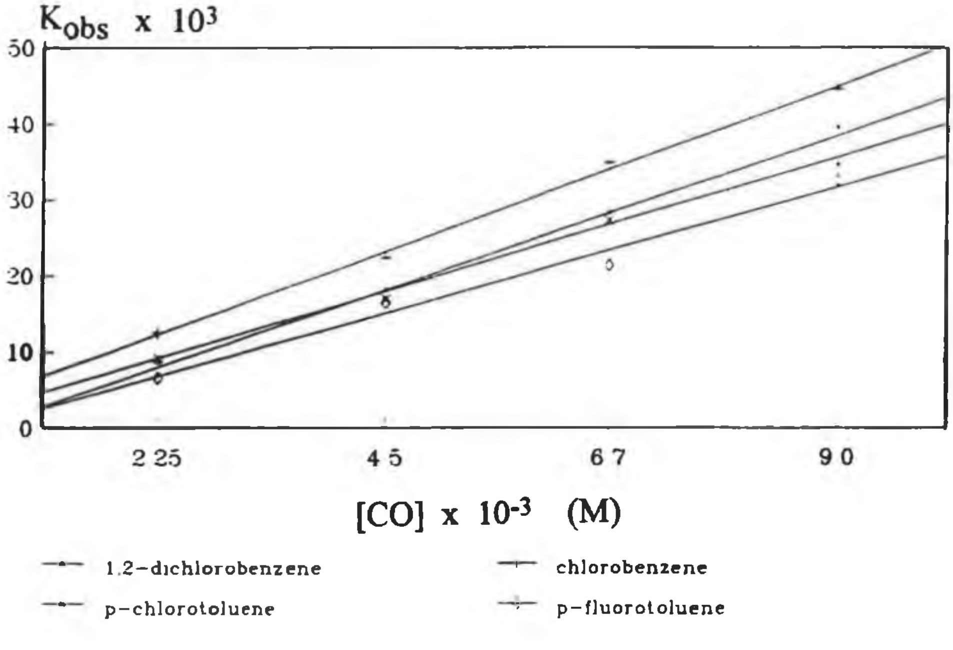

Figure 2.1.2.5 Plot of k_{obs} *versus* CO concentration (mol dm^{-3}) for the decay of (η^6-arene)$Cr(CO)_2$(cyclohexane) intermediates for all arene compounds investigated.

Arene	k_2 x (10^{-6}) mol^{-1}dm^{3}s^{-1} ± 10%
1,2 dichlorobenzene [a]	3.9
chlorobenzene [a]	4.8
p-flourotoluene [a]	3.6
p-chlorotoluene [a]	4.2
benzene [a]	9.8
toluene [b]	9.4
ethyl [a]	6.7
t-butyl [a]	7.8
o-xylene [a]	7.1
p-xylene [b]	8.3
mesitylene [b]	13
hexamethybenzene [b]	15
hexaethylbenzene [a]	60.0

Table 2.1.2.1 Second order rate constants (k_2) for reaction of (η^6-arene)$Cr(CO)_2$(cyclohexane) with CO to regenerate tricarbonyl [a] this work, [b] reference 3.

The rate constant data presented in Table 2.1.2.1 outline the variation observed in second order rate constants for Reaction 2.1.2.2 as the nature of the arene ligand is changed. As the number of electron donating substituents on the arene ring increase there is a gradual increase in the second order rate constant and *vice versa* for electron withdrawing substituents. However, it is only for the highly substituted arene complexes that significant differences in second order rate constants are observed. It was assumed that the electron donating effect of the hexaethylbenzene ligand would increase the stability of the solvated dicarbonyl and thereby decrease the reaction rate of this species towards CO by forming a more stable chromium dicarbonyl complex. The opposite effect was observed and this suggests that steric effects are important in determining the rate of reaction of the dicarbonyl fragment with CO, but these could relate to the internal freedoms associated with the intermediate. There are two processes which are influenced by steric factors, the approach of the incoming ligand (CO) and displacement of cyclohexane. Steric interactions with molecules such as CO are likely to be small and a weakening of the Cr---cyclohexane is probably the major effect. Whatever the precise nature of the steric interaction, these experiments indicate that substituents some distance from the metal centre can influence the rate of reaction of the metal.

This observation is not unique in so far as it has previously been observed for the isoelectronic (η^5-cyclopentadienyl)$Mn(CO)_3$ system where Poliakoff and coworkers[12] carried out a study of the steric effects on the kinetics of (η^5-C_5R_5)$Mn(CO)_2$(s) in *n*-heptane solution using TRIR spectroscopy as outlined in Table 2.1.2.2. For this system, the rate constant for the reaction of CO with (η^5-C_5R_5)$Mn(CO)_2$(*n*-heptane) increased significantly, as R was changed from H to Me to Et, hence indicating a similar trend to that observed in the chromium system. They proposed that the increase in rate constants was sterically controlled as C_5Me_5 and C_5Et_5 have similar electronic characters.

(η^5-C_5R_5)$Mn(CO)_3$	k_2 x (10^{-6}) $mol^{-1}dm^{-3}s^{-1}$
C_5H_5	0.81
$C_5(CH_3)_5$	1.6
$C_5(C_2H_5)_5$	5.4

Table 2.1.2.2 Second order rate constant for the reaction of substituted (η^5-C_5R_5)$Mn(CO)_2$(*n*-heptane) towards CO, data taken from reference 12.

2.1.3 Activation parameters for the reaction of (η^6-arene)$Cr(CO)_2$(s) with CO.

The activation parameters for the reaction of (η^6-arene)$Cr(CO)_2$(cyclohexane) with CO were calculated using Arrhenius and Eyring equations (Section 7.9). The second order rate constant k_2 used in the calculations was calculated as follows; $k_2 = k_{obs}/[CO]$, where $[CO] = 9.0 \times 10^{-3}$M. The activation parameters are listed in Table 2.1.3.3 and the experimental data is given in Tables B1 to B7 in Appendix B and a representative graph for the Arrhenius and Eyring plot in Figure 2.1.3.1.

(a)

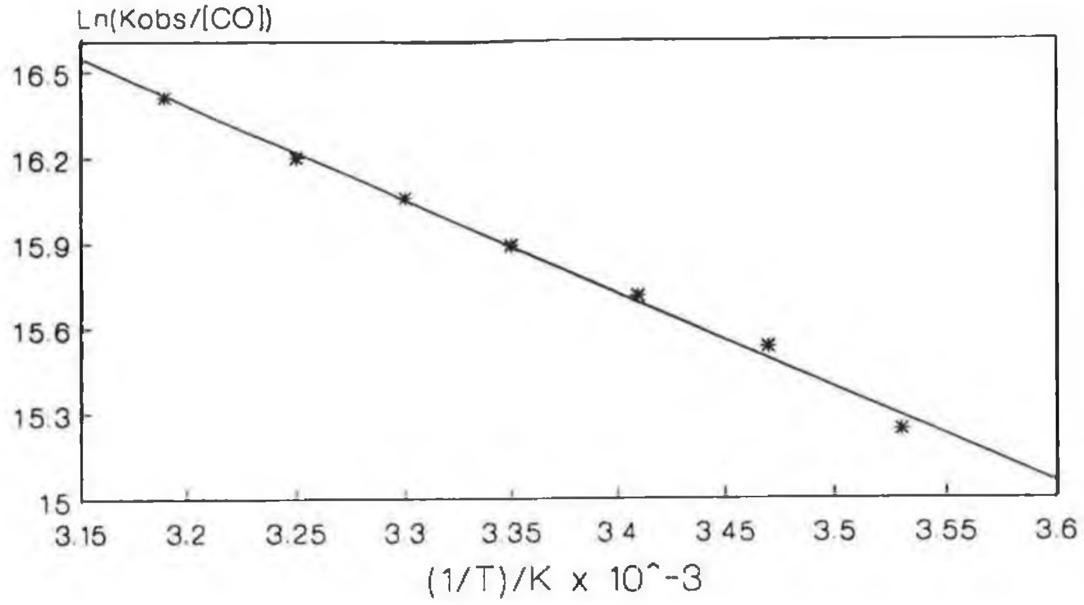

(b)

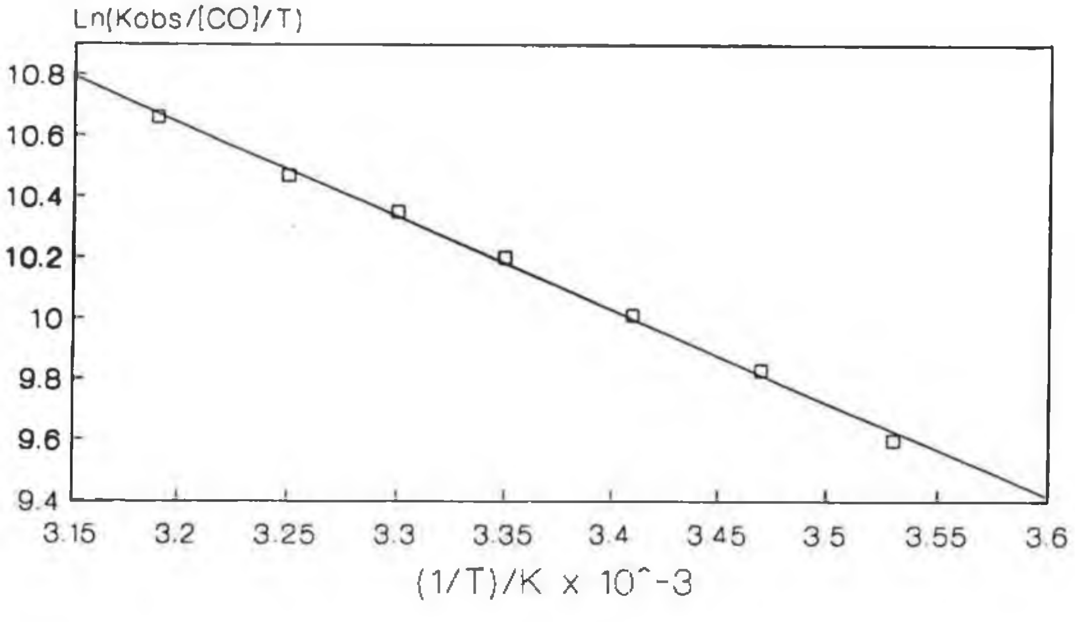

Figure 2.1.3.1 Arrhenius and Eyring plot for the reaction of (η^6-ethylbenzene)$Cr(CO)_2$(cyclohexane) with CO to regenerate parent tricarbonyl.

(η^6-arene)$Cr(CO)_3$	$\Delta H^{\neq}$ kJmol^{-1} ($\pm$ 2 kJmol^{-1})	$\Delta S^{\neq}$ Jmol^{-1}K^{-1} ($\pm$ 5 Jmol^{-1})	$\Delta G^{\neq}_{(298K)}$ kJmol^{-1} ($\pm$ 2 kJmol^{-1})
1,2dichlorobenzene [a]	22	-43	35
chlorobenzene [a]	22	-38	33
p-fluorotoluene [a]	25	-38	36
p-chlorotoluene [a]	25	-34	35
benzene [b]	22	-37	33
toluene [b]	23	-35	33
ethylbenzene [a]	25	-28	33
o-xylene [a]	25	-28	33
p-xylene [b]	24	-28	32
mesitylene [b]	24	-27	32
hexamethylbenzene [b]	25	-26	33
hexaethylbenzene [a]	22	-23	29

Table 2.1.3.3 Activation parameters for the reaction of (η^6-arene)$Cr(CO)_2$(cyclohexane) with CO. [a] denotes this work, [b] reference 3.

The enthalpy of activation $\Delta H^{\neq}$ for the carbon monoxide recombination for all the complexes is constant at 24 $\pm$ 2 kJ mol^{-1}. The reported binding energy of cyclohexane to $Cr(CO)_6$ was found to be 52 kJ mol^{-1} from photoacoustic measurements,[13] however there appears to be no literature values concerning the Cr to alkane bond in (η^6-arene)$Cr(CO)_2$ alkane intermediates. In other systems, it has been shown that reactions of the photofragment with solvent is rapid[14,15] hence $\Delta H^{\neq}$ for the loss of solvent from the solvent adduct approximates the bond energy of the metal to solvent bond. Assuming the interaction energy between $Cr(CO)_5$ and cyclohexane is similar to that of (η^6-arene)$Cr(CO)_2$ and cyclohexane and in view of the fact that these results are significantly lower than those of Burkey,[13] it is unlikely that dissociative loss of solvent is the rate determining step and that an interchange mechanism may be occurring. Thus reaction of (η^6-arene)Cr(CO)$_2$(cyclohexane) with CO involves a transition state, where the CO molecule coordinates to the metal centre concomitant with loss of cyclohexane. The activation entropies $\Delta S^{\neq}$ are negative for CO recombination studies here. This observation along with those of the $\Delta H^{\neq}$ measurements is consistent with an interchange mechanism for CO binding rather than a dissociative mechanism, in which the $\Delta S^{\neq}$ values should be closer to zero or perhaps positive. A further insight into the proposed interchange mechanism for solvent displacement was obtained by varying the nature of the alkane solvent and examining this effect on the second order rate constant. The results are discussed in Section 2.3 and are consistent with an interchange mechanism occurring.

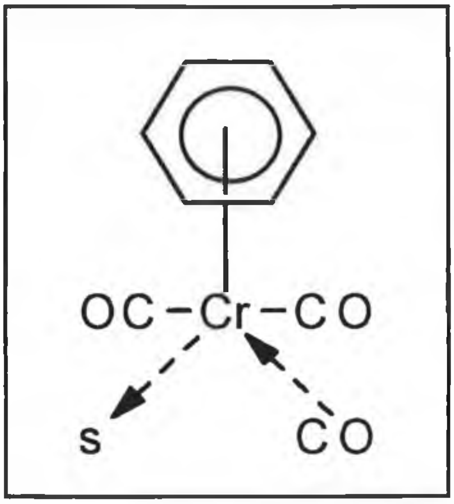

Figure 2.1.3.2 The nature of the transition state for an interchange mechanism for solvent displacement by CO in (η^6-arene)Cr(CO)$_2$(cyclohexane).

2.1.4 Secondary photoproduct.

For all the (η^6-arene)Cr(CO)$_3$ compounds investigated (those in Table 2.1.3.3) by laser flash photolysis under 1 atm. of argon only (η^6-hexaethylbenzene)Cr(CO)$_3$ was found to give rise to a secondary photoproduct. With all the other substituted arenes only one transient species was observed which was assigned to the solvated dicarbonyl intermediate. Figure 2.1.4.1 contains a typical spectrum of these systems and this spectrum appears to be no different to those under one atmosphere of CO as seen in Figure 2.1.2.3. However, with (η^6-hexaethylbenzene)Cr(CO)$_3$ a longer lived transient species was observed as seen in the UV/vis. transient spectrum in Figure 2.1.4.2 with maxima at 290 and 410 nm which is assigned to (η^6-hexaethylbenzene)$_2$Cr$_2$(CO)$_5$.

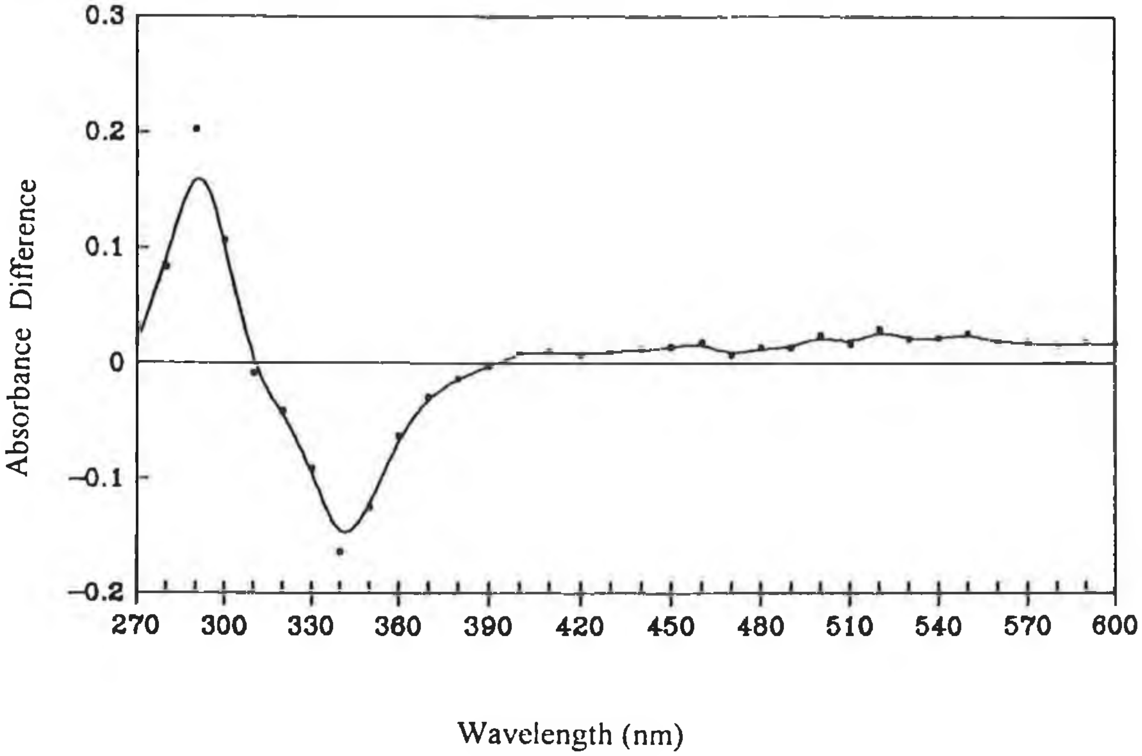

Figure 2.1.4.1. UV/vis. difference spectrum after 100 μs following flash photolysis of (η^6-*p*-chlorotoluene)Cr(CO)$_3$ in cyclohexane at 355 nm under 1 atm. of argon at 298 K.

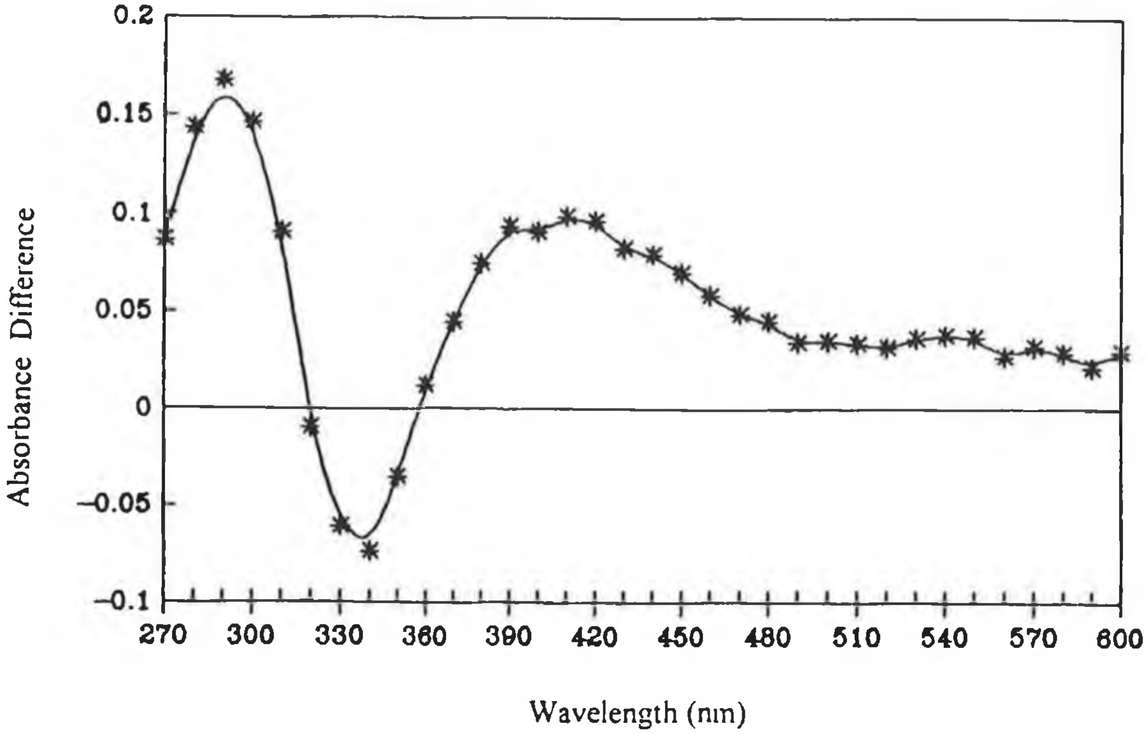

Figure 2.1.4.2 UV/vis. difference spectra after 100μs following flash photolysis of (η^6-hexaethylbenzene)$Cr(CO)_3$ under 1 atm. argon.

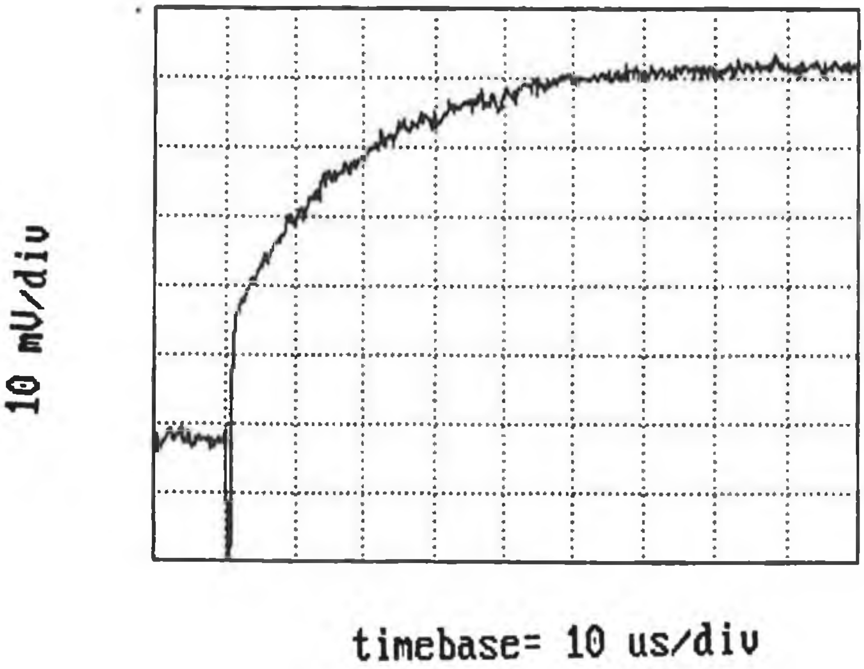

Figure 2.1.4.3 Transient signal for formation of the secondary photoproduct - at 410 nm under 1 atm. argon following flash photolysis of (η^6-hexaethylbenzene)-$Cr(CO)_3$.

The concentration of tricarbonyl was varied to investigate its effect on the observed rate constant. A linear relationship was observed and a plot of k_{obs} *versus* concentration of parent gave an estimate of the second order rate for formation of this species being 8.84 x 10^7 $mol^{-1}dm^3s^{-1}$ as illustrated in Figure 2.1.4.4.

These observations are consistent with the formation of a dinuclear species formed by the reaction of (η^6-hexaethylbenzene)$Cr(CO)_2$(cyclohexane) with the parent tricarbonyl (Reaction 2.1.4.1). Although there is no definite evidence for the structure of this dinuclear compound it is probable that the $Cr(CO)_2$ fragment is bound to the $Cr(CO)_3$ via a Cr-Cr interaction and a bridging carbonyl group. This species has previously been observed for (η^6-styrene)$Cr(CO)_3$ with a second order rate constant of formation of 3.2 x 10^7 $dm^3mol^{-1}s^{-1}$, where coordination of the unsaturated fragment to the parent occurs *via* a η^2 interaction with the vinylic group of the parent.[16] A dinuclear complex has previously been postulated for (η^6-benzene)$Cr(CO)_3$ with a second order rate constant of 4.8 x 10^7 $dm^3mol^{-1}s^{-1}$.[7]

$$(\eta^6\text{-hexaethylbenzene})Cr(CO)_2(s) + (\eta^6\text{-hexaethylbenzene})Cr(CO)_3$$

$$\longrightarrow (\eta^6\text{-hexaethylbenzene})_2Cr_2(CO)_5 + (s)$$

(2.1.4.1)

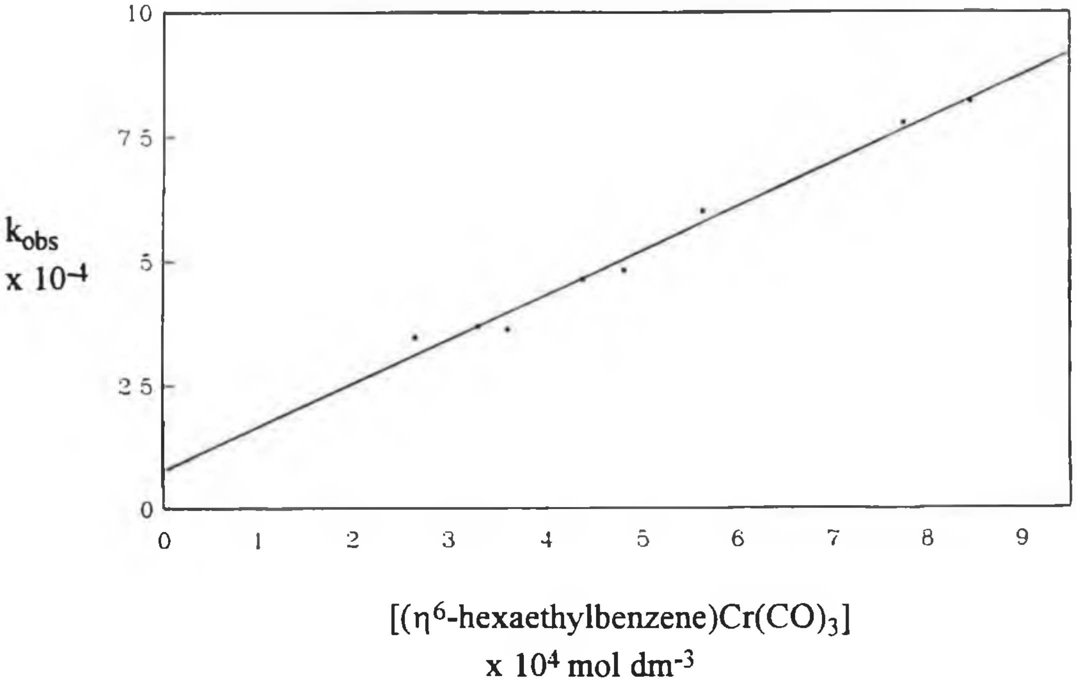

[(η^6-hexaethylbenzene)-Cr(CO)$_3$] x 10^4 mol dm^{-3}	k_{obs} x 10^{-4} (s^{-1})
2.65	3.46
3.3	3.61
3.6	3.68
4.38	4.63
4.8	4.80
5.63	5.98
7.75	7.75
8.46	8.19

Slope = 8.84 x $10^7 \pm 4.4$ x 10^6 dm^3 mol^{-1} s^{-1}
Intercept = 77.64 x $10^2 \pm 24.4$ x 10^2 s^{-1}
corr. coeff. = 0.99

Figure 2.1.4.4 A plot of k_{obs} *versus* concentration for reaction of (η^6-hexaethylbenzene)Cr(CO)$_3$ with (η^6-hexaethylbenzene)Cr(CO)$_2$(cyclohexane) at 298 K.

Using infrared detection with nujol mulls at 77 K, Rest and coworkers have recently reported formation of a dinuclear compound for (η^6-benzene)$Cr(CO)_3$, which they proposed to form by reaction of the solvated dicarbonyl species with unphotolysed material in solution.[6] Using TRIR a dinuclear species has been identified for the isoelectric (η^5-C_5H_5)$Mn(CO)_3$ compound, coordination was suggested to occur through Mn-Mn interaction with a bridging carbonyl group with a second order rate constant of formation 1.1 x 10^6 $dm^3mol^{-1}s^{-1}$.[14] From previous investigations and from the results in this study it would not be unlikely to assume that in (η^6-hexaethylbenzene)$_2Cr_2(CO)_5$ coordination occurs through Cr-Cr interaction and the presence of a bridging carbonyl group as shown in Figure 2.1.4.5.

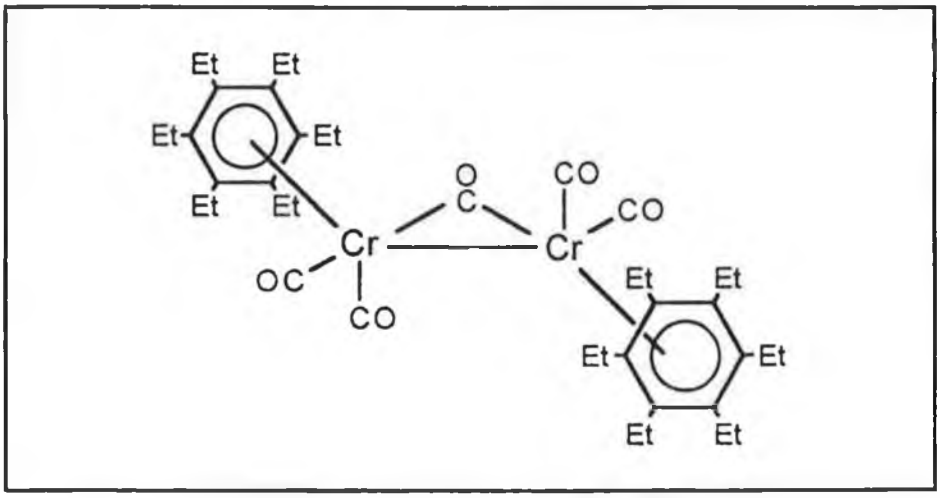

Figure 2.1.4.5 A possible structure for the dinuclear species (η^6-hexaethylbenzene)$_2Cr_2(CO)_5$.

2.2.0 Laser flash photolysis of (η^6-arene)Mo(CO)$_3$.

Surprisingly, no detailed photochemistry appears to have carried out on (η^6-arene)Mo(CO)$_3$ compounds. Hence, matrix isolation and time resolved infrared spectroscopy experiments were necessary to characterise the primary photoproduct and UV/vis. flash photolysis studies were utilised to carry out kinetic analyses on this system. The range of arenes studied include benzene, *p*-xylene, 1,3,5-mesitylene and hexamethylbenzene.

2.2.1 Electronic absorption spectrum.

The UV/vis. spectrum of (η^6-1,3,5-mesitylene)Mo(CO)$_3$ in cyclohexane is shown in figure 2.2.1.1, which is typical of the molybdenum system studied in this investigation. These compounds have a very sharp $\lambda_{max.}$ centred around 320 nm which is assigned to a Mo ----> arene charge transfer transition with some Mo ----> CO charge transfer character. There is also a shoulder around 255 nm which is assigned to a Mo ----> π* CO charge transfer.[17]

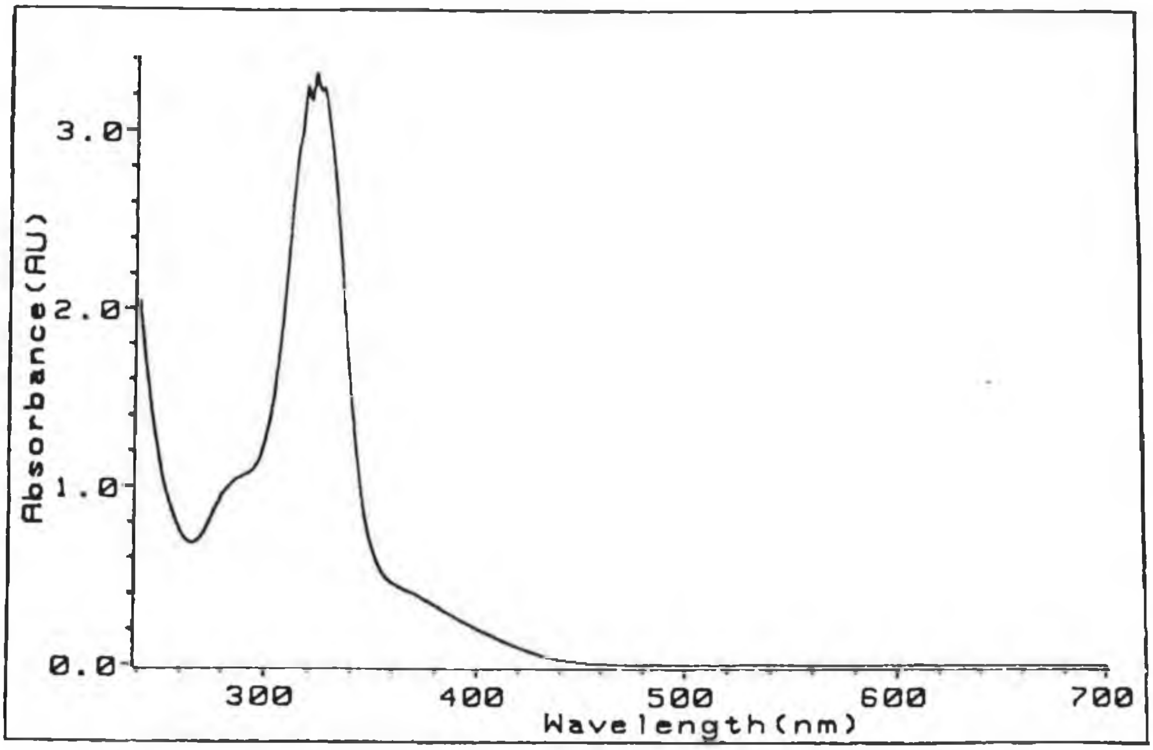

Figure 2.2.1.1 UV/vis. spectrum of (η^6-1,3,5-mesitylene)Mo(CO)$_3$ in cyclohexane (2.1 x 10^{-4}M)

A summary of the UV/vis. extinction coefficients of the compounds investigated in this study at 266 nm and the ν_{CO} infrared stretching frequencies in cyclohexane for all the compounds is presented in Table 2.2.1.1. The values used for calculation of the extinction coefficients are tabulated in Appendix C.

(η^6-arene)Mo(CO)$_3$	$\varepsilon_{266\ nm}$ dm^3 mol^{-1} cm^{-1} (± 2 %)	ν_{CO} cm^{-1} (± 2 cm^{-1})
benzene	2050	1987, 1916
p-xylene	2260	1976, 1905
1,3,5-mesitylene	2908	1973, 1901
hexamethylbenzene	3469	1959, 1884

Table 2.2.1.1 A summary of the extinction coefficients and the ν_{CO} infrared stretching frequencies in cyclohexane.

2.2.2 Primary Photoproduct.

2.2.2.1 Matrix isolation.

The technique of low temperature matrix isolation is a useful means of generating and spectroscopically characterising species that may act as intermediates in solution. The spectrum of (η^6-1,3,5-mesitylene)Mo(CO)$_3$ in a methane matrix at 12K consists of two strong bands in the terminal carbonyl stretching region at 1973 and 1898 cm^{-1}. On irradiation at 313 nm new bands were produced at 1914 and 1861 cm^{-1}, also a band assigned to free CO in the matrix is observable at 2137 cm^{-1} (albeit very weak) as seen in Figure 2.2.2.1.1.

Rest and co-workers[5] some years ago carried out matrix isolation experiments on the analogous (η^6-benzene)Cr(CO)$_3$ system. Upon photolysis new bands at 1925 and 1870 cm^{-1} were observed which they assigned to being (η^6-benzene)Cr(CO)$_2$(CH$_4$), - values are tabulated in Table 2.2.2.1.1.

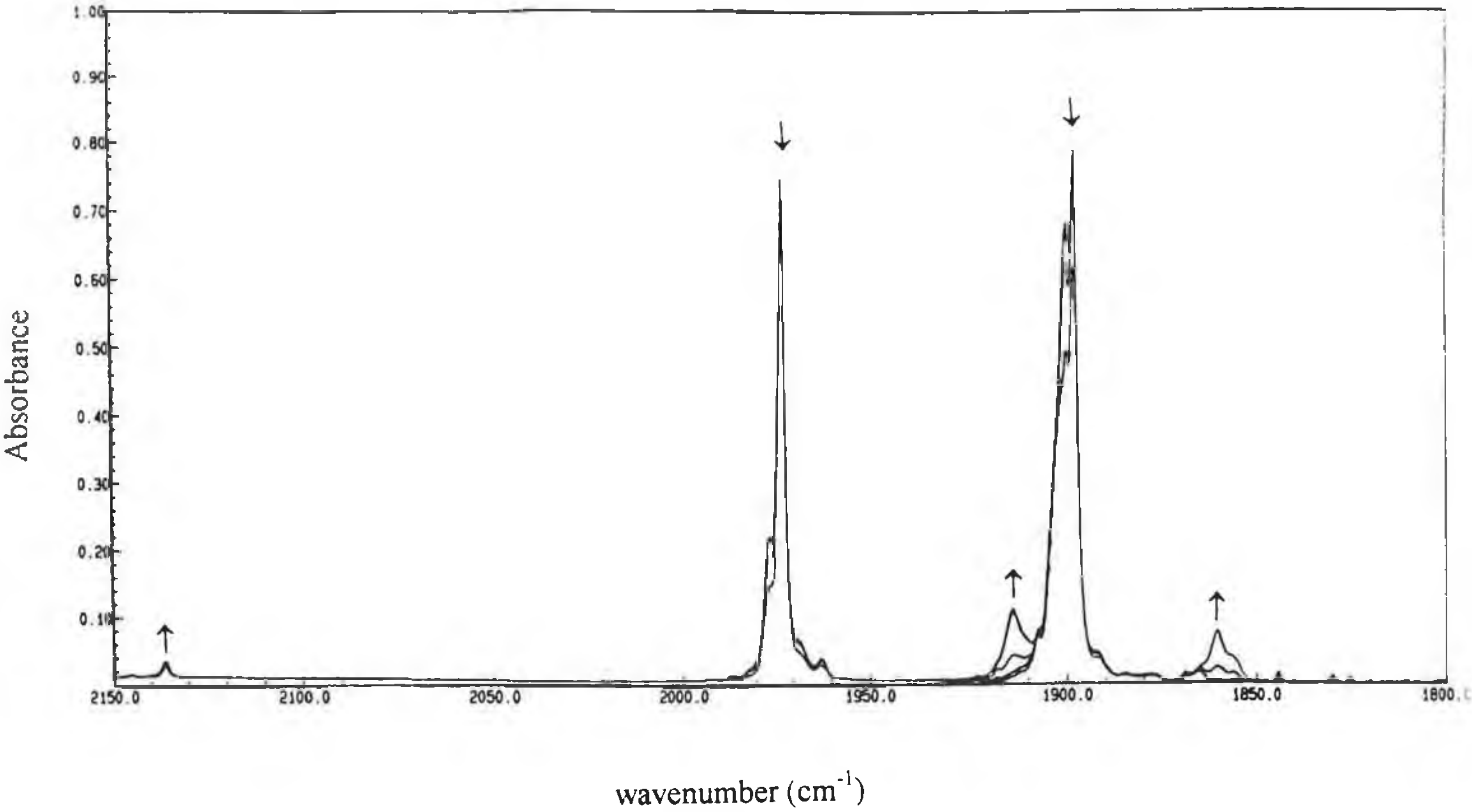

Figure 2.2.2.1.1 Spectrum of (η^6-1,3,5-mesitylene)Mo(CO)$_3$ in a CH$_4$ matrix following 313 nm irradiation at 12K.

compound	cm^{-1}
(η^6-benzene)Cr(CO)$_3$^{a}	1982, 1913
(η^6-benzene)Cr(CO)$_2$^{a}	1925, 1870
(η^6-1,3,5-mesitylene)Mo(CO)$_3$^{b}	1973, 1898
(η^6-1,3,5-mesitylene)Mo(CO)$_2$^{b}	1914, 1861

Table 2.2.2.1.1 Bands observed on photolysis of (η^6-arene)M(CO)$_3$ (M=Cr or Mo) in a methane matrix at 12 K. ^{a} data taken from reference 3 and ^{b} this work.

From a comparison of these values for both the Cr and the Mo system the most probable explanation for this new product species is (η^6-1,3,5-mesitylene)Mo(CO)$_2$(CH$_4$) with the new bands assigned to the terminal carbonyl stretching modes of a Mo(CO)$_2$(CH$_4$) fragment having local C_{2v} symmetry.

2.2.2.2 Flash photolysis with TRIR detection.

The TRIR difference spectrum obtained after 10 μs in cyclohexane in the presence of 1 atm. of CO (9.0 x 10^{-3}M) following 308 nm photolysis indicates depletion of the parent bands at 1974 and 1900 cm^{-1} along with the formation of two positive absorptions bands at 1914 and 1860 cm^{-1} which represent the production of a primary photoproduct (see Figure 2.2.2.2.1). The formation of these two new bands at decreasing carbonyl stretching frequencies have been attributed to the formation of the dicarbonyl species and their observed frequency in cyclohexane is similar to that previously observed for (η^6-benzene)Cr$(CO)_2$ in a methane matrix (*vide supra*).[5]

Previous studies have indicated that it is unlikely that a 16 electron species remains uncoordinated in solution, and hence it is most probable that this species exists as a solvated intermediate.[7,8] Thus the primary photochemical reaction of (η^6-1,3,5-mesitylene)Mo$(CO)_3$ can be summarised as follows in reactions 2.2.2.2.1 and 2.2.2.2.2;

$$(\eta^6\text{-1,3,5-mesitylene})Mo(CO)_3 \xrightarrow{h\nu} (\eta^6\text{-1,3,5-mesitylene})Mo(CO)_2 + CO \qquad (2.2.2.2.1)$$

$$(\eta^6\text{-1,3,5-mesitylene})Mo(CO)_2 \xrightarrow{s} (\eta^6\text{-1,3,5-mesitylene})Mo(CO)_2(s) \qquad (2.2.2.2.2)$$

TRIR studies have been carried out on (η^6-benzene)Cr$(CO)_3$ in *n*-heptane solution in the presence of CO (9.0 x 10^{-3}M),[7] depletion of parent was evident at 1983 and 1915 cm^{-1}, and photoproduction of a transient species at 1927 and 1877 cm^{-1} which was assigned to be (η^6-benzene)Cr$(CO)_2$(s) (where s=heptane), see Table 2.2.2.2.1. The shifts of the high and low energy bands respective to parent ν_{CO} bands are relatively comparable for both chromium and molybdenum, with a difference of 58 and 38 cm^{-1} for the high and low frequency band for the chromium system while with the molybdenum compound a difference of 60 and 42 cm^{-1} was measured for the high and low carbonyl stretching frequencies.

compound	cm^{-1}
(η^6-benzene)$Cr(CO)_3$[a]	1983,1915
(η^6-benzene)$Cr(CO)_2$[a]	1927,1877
(η^6-1,3,5-mesitylene)$Mo(CO)_3$	1974,1902
(η^6-1,3,5-mesitylene)$Mo(CO)_2$	1914,1860

Table 2.2.2.2.1 TRIR data following photolysis of (η^6-1,3,5-mesitylene)$Mo(CO)_3$ in cyclohexane and (η^6-benzene)$Cr(CO)_3$ in *n*-heptane. [a] data taken from reference 7.

The bimolecular rate constant for the reaction of (η^6-1,3,5-mesitylene)$Mo(CO)_2$(s) (s = cyclohexane) with CO using TRIR was calculated to be 1.7×10^6 $dm^3mol^{-1}s^{-1}$. This rate data can then be used to correlate the results of both TRIR and UV/vis. flash photolysis studies and is presented in Table 2.2.2.5.1 along side UV/vis. values.

Under 1atm. CO (9.0×10^{-3}M) the chromium system was found to be fully reversible but this was not so in the case of (η^6-1,3,5-mesitylene)$Mo(CO)_3$, as depletion of parent recovered to only about 50% of its initial absorbance under these conditions as observed from TRIR experiments.

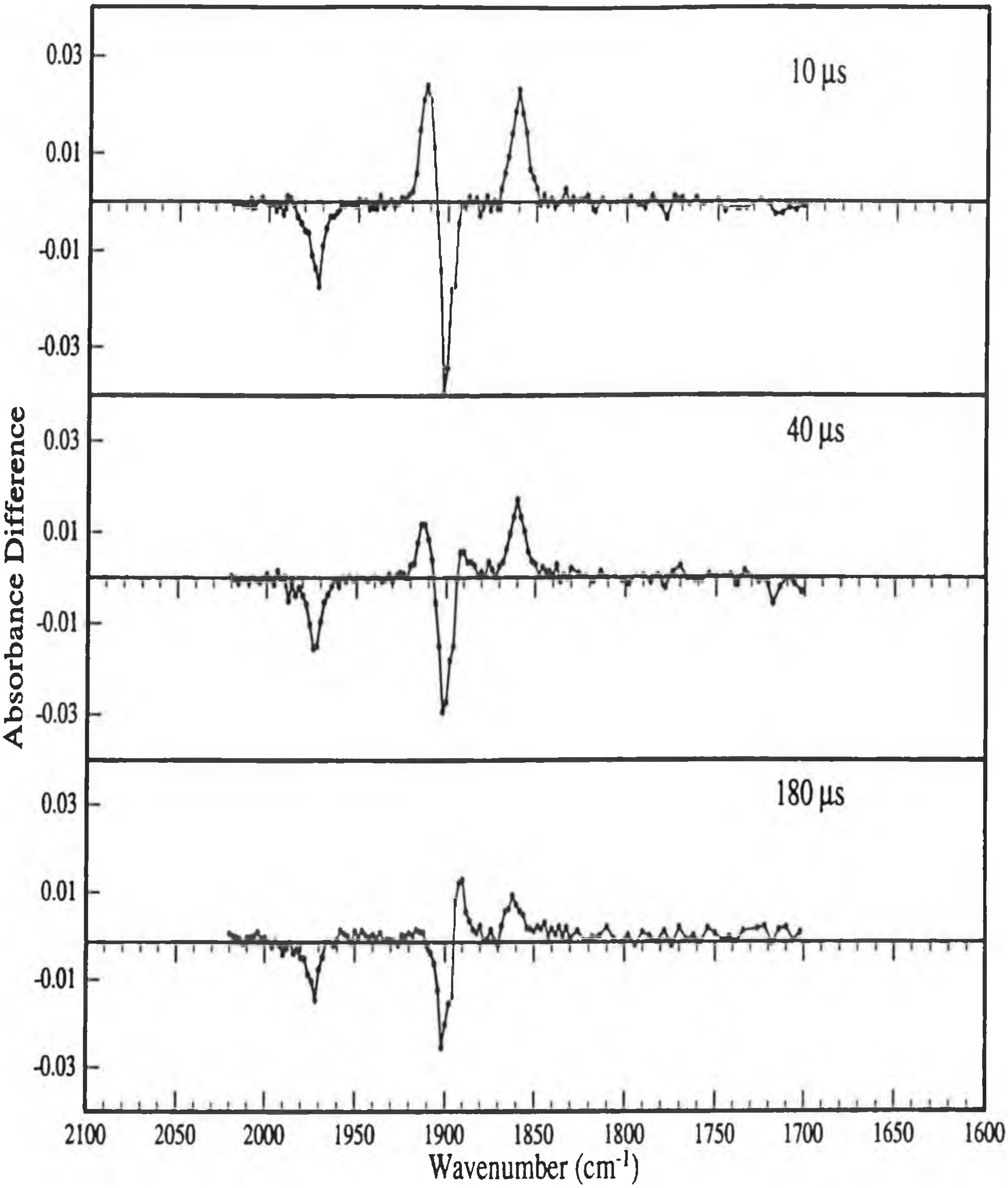

Figure 2.2.2.2.1 TRIR difference spectra of (η^6-1,3,5-mesitylene)Mo(CO)$_3$ in cyclohexane recorded 10, 40 and 180µs after the flash. 1 atm. CO (9.0 x 10^{-3}M).

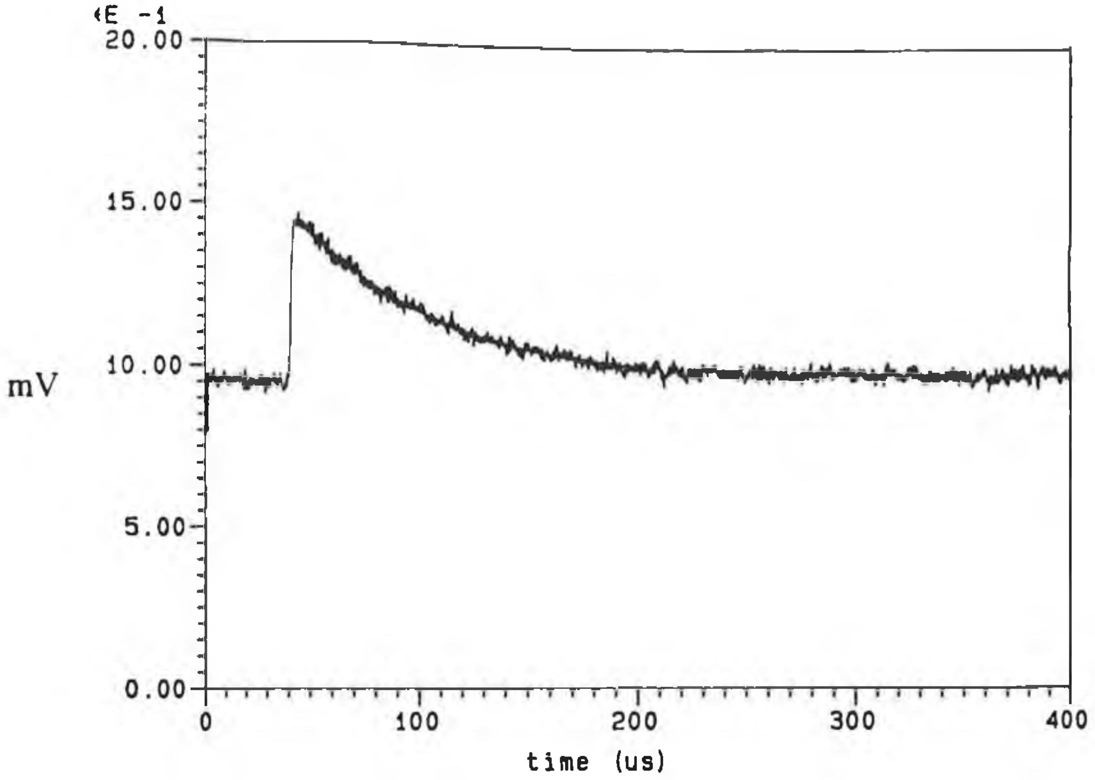

Figure 2.2.2.2.2 Transient signal at 1914 cm^{-1} following flash photolysis of (η^6-1,3,5-mesitylene)$Mo(CO)_3$ in cyclohexane, 1 atm. of CO (9.0×10^{-3}M).

2.2.2.3 Determination of the bond angle.

To a good approximation the relative intensities of different CO stretching modes can be used to calculate the angles between the carbonyls using a simple model.[18] In this model, each CO oscillator is treated as a dipole vector, and the total dipole vector for the entire vibrational mode is taken to be the vector sum of these individual vectors. Since the intensities are proportional to the square of the dipole vectors, there is a relationship between the intensities of the absorption bands and the angles between C–O bond vectors. The angle between the oscillating dipoles of these CO groups can be found from their relative absorption intensities.

For the case of two C–O groups the ratio of the intensities of the symmetric and antisymmetric bands is given by

$$\frac{I_{asym}}{I_{sym}} = \tan^2(\theta/2)$$

From Figure 2.2.2.2.1 an estimate of the OC-Mo-CO bond angle was calculated using the above equation where θ is the bond angle, I_{sym} is the intensity of the symmetric (high wave number) band, and I_{asym} is the intensity of the antisymmetric (low wave number) band. The ratio of the (I_{asym}/I_{sym}) was found to be 0.86 ± 0.1 which gives a bond angle of 85.7° ± 3.3°. This angle is in close agreement to that derived from crystallographic studies for (η^6-*p*-xylene)Mo(CO)$_2$(*cis*-cyclooctene) where the OC-Mo-CO bond angle is 84.4°.[19] and similar to that of the parent compound (η^6-1,3,5-mesitylene)Mo(CO)$_3$ (88-91 °).[20] Thus loss of CO from (η^6-1,3,5-mesitylene)Mo(CO)$_3$ does not appear to have a significant effect on the OC-Mo-CO bond angle of the (η^6-1,3,5-mesitylene)Mo(CO)$_2$ fragment possibly as a result of complexation by a solvent molecule.

2.2.2.4 Quantum yield calculations for CO loss.

The quantum yield of CO loss from (η^6-benzene)Mo(CO)$_3$ was measured to be 0.2 in cyclohexane solution using pyridine as the incoming ligand (Reaction 2.2.2.4.1). Previous workers have calculated the quantum yield for the analogous chromium system[21] to be 0.72 and this yield was found to be independent of entering ligand, its concentration and also wavelength of irradiation. The quantum yield for CO loss from chromium is some three times greater than that obtained for the molybdenum system, thereby indicating a less efficient CO loss process for the molybdenum metal centre.

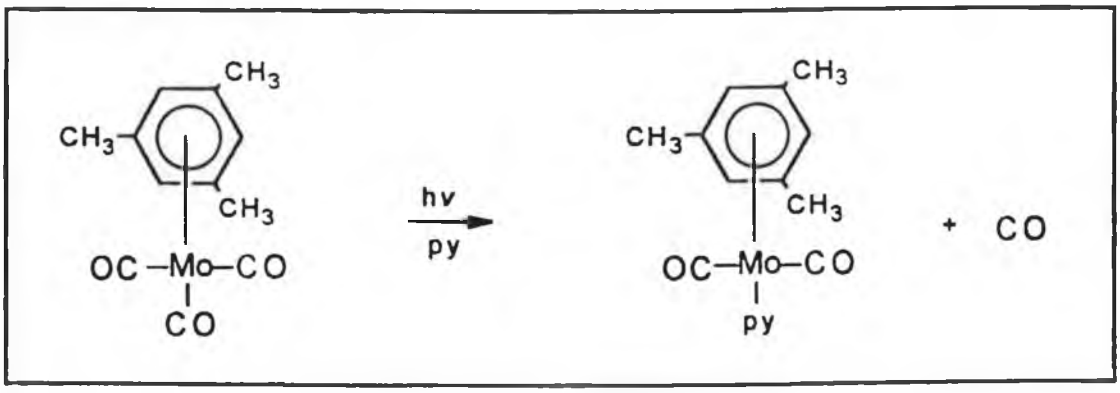

Reaction 2.2.2.4.1 Substitution of a CO molecule by pyridine following flash photolysis.

With (η^6-benzene)Cr(CO)$_3$ it is thought that the ligand field (LF) energy is below that of the metal to ligand charge transfer (MLCT) level,[4] hence the high efficiency for the CO loss process. Is it possible that in the case of the molybdenum compounds the LF level may now be at a higher energy level thereby giving very inefficient population of the LF as is outlined in Figure 2.2.2.4.1 and this theory would help to explain the differences in quantum yields between the two metals and also why a greater excitation energy is required for flash photolysis of Mo compounds.

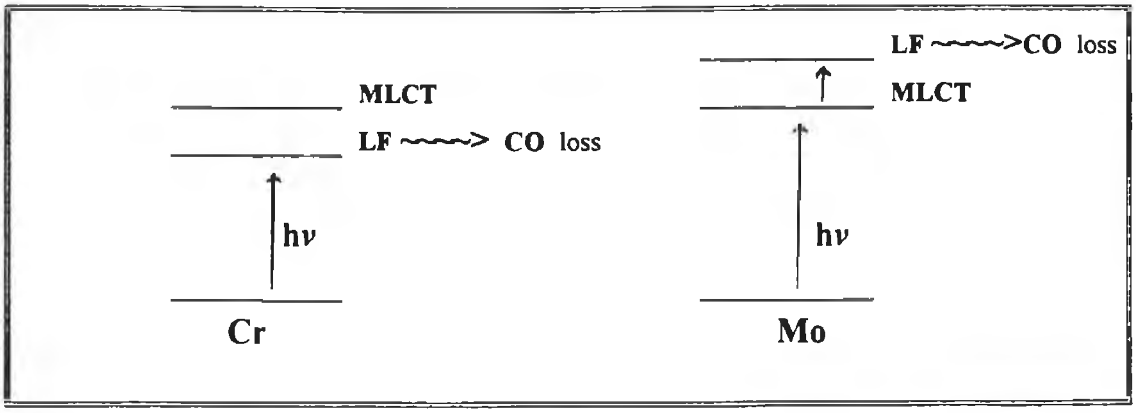

Figure 2.2.2.4.1 Possible variation in energy levels for (η^6-arene)$Cr(CO)_3$ as opposed to (η^6-arene)$Mo(CO)_3$.

There is no evidence for this postulate but this energy level diagram does help to explain the significant difference in quantum yields. To validate this theory it would be necessary to carry out resonance Raman spectroscopy measurements in order to determine whether or not the MLCT transition is below the LF level.

2.2.2.5 Flash photolysis with UV/vis. detection.

The transient signals obtained following flash photolysis of (η^6-arene)$Mo(CO)_3$ at 355 nm were extremely weak, consequently experiments were conducted using the 266 nm line in order to maximise the transient signal intensity. The energy of the laser at 266 nm is typically 70-80mJ per pulse while at 355 nm it is somewhat lower with an average laser pulse of 50mJ. The rate constant data were obtained by measuring the recovery of parent depletion rather than the rate of decay of (η^6-arene)$Mo(CO)_2$(s) absorption as the only region that the dicarbonyl absorbs more strongly than the tricarbonyl (~270 nm) is too close to the laser wavelength (266 nm) for reliable data to be obtained. A typical transient signal indicating the recovery of parent absorption is presented in Figure 2.2.2.5.1, depletion of parent occurs at 330 nm for all compounds and hence this was used as the monitoring wavelength.

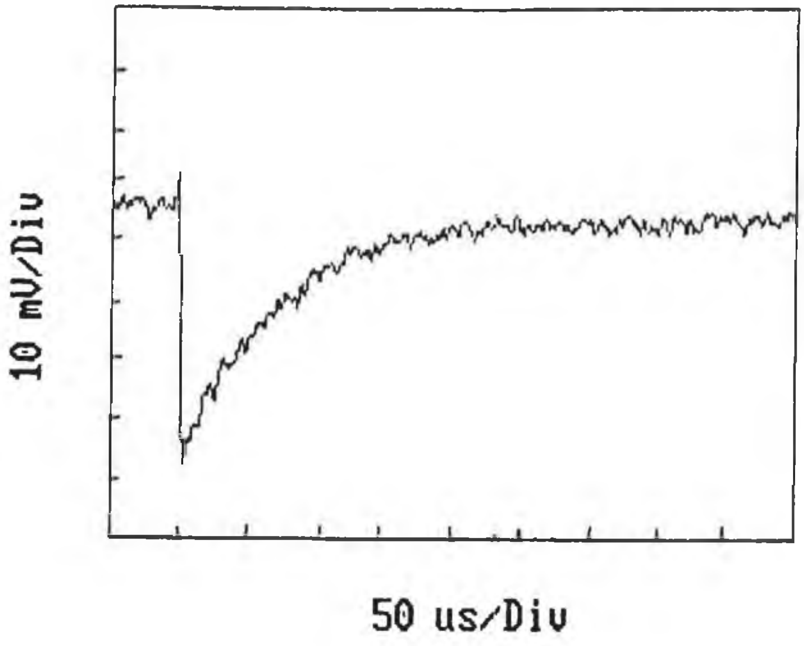

Figure 2.2.2.5.1 A typical transient signal following flash photolysis of (η^6-*p*-xylene)$Mo(CO)_3$ in cyclohexane under 1 atm. of CO (9.0×10^{-3}M) at 330 nm.

The UV/vis. difference spectrum of the first observable species recorded 20μs after the flash shows a $\lambda_{max.}$ at 270 nm and another maximum at 360 nm, also a depletion is evident at 330 nm (Figure 2.2.2.5.2) This depletion at 330 nm corresponds to $\lambda_{max.}$ of the parent tricarbonyl. The effect of different concentrations of CO on the rate of recovery of the parent tricarbonyl was investigated extensively using UV/vis. detection. This study showed that the lifetime of the primary species decreased upon addition of CO, however this addition had no effect on the degree of depletion. As the life time of the (η^6-arene)$Mo(CO)_2$(s) species depends on the concentration of CO, a plot of k_{obs}

versus CO concentration provides the second order rate constant for the reaction of this solvated species with CO to regenerate parent (data in Tables A9 to A12). The pseudo first order plots are presented in Figure 2.2.2.5.3. The concentration of CO was assumed to be 9.0 x 10^{-3}M at 1 atm.[22] The second order rate constants for the reaction for the solvated dicarbonyl intermediate are summarised in Table 2.2.2.5.1.

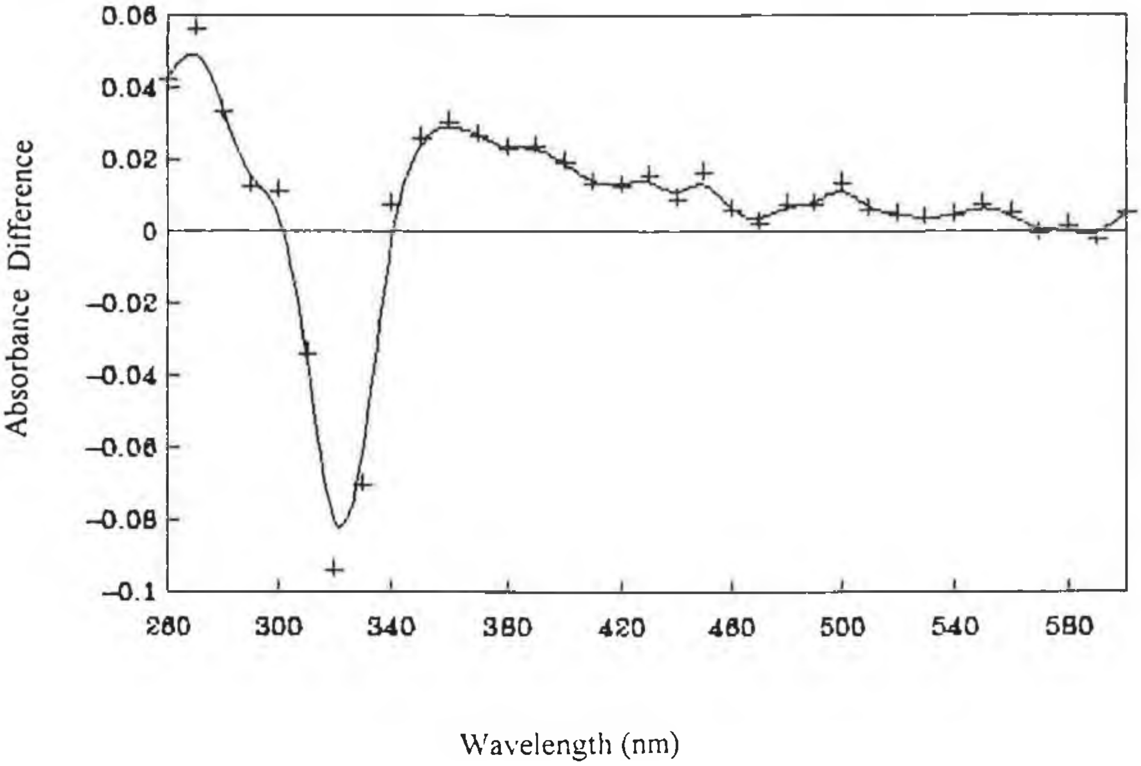

Figure 2.2.2.5.2. UV/vis. difference spectrum recorded 20μs after the flash following flash photolysis of (η^6-benzene)$Mo(CO)_3$ in cyclohexane under 1 atm CO (9.0 x 10^{-3}M)

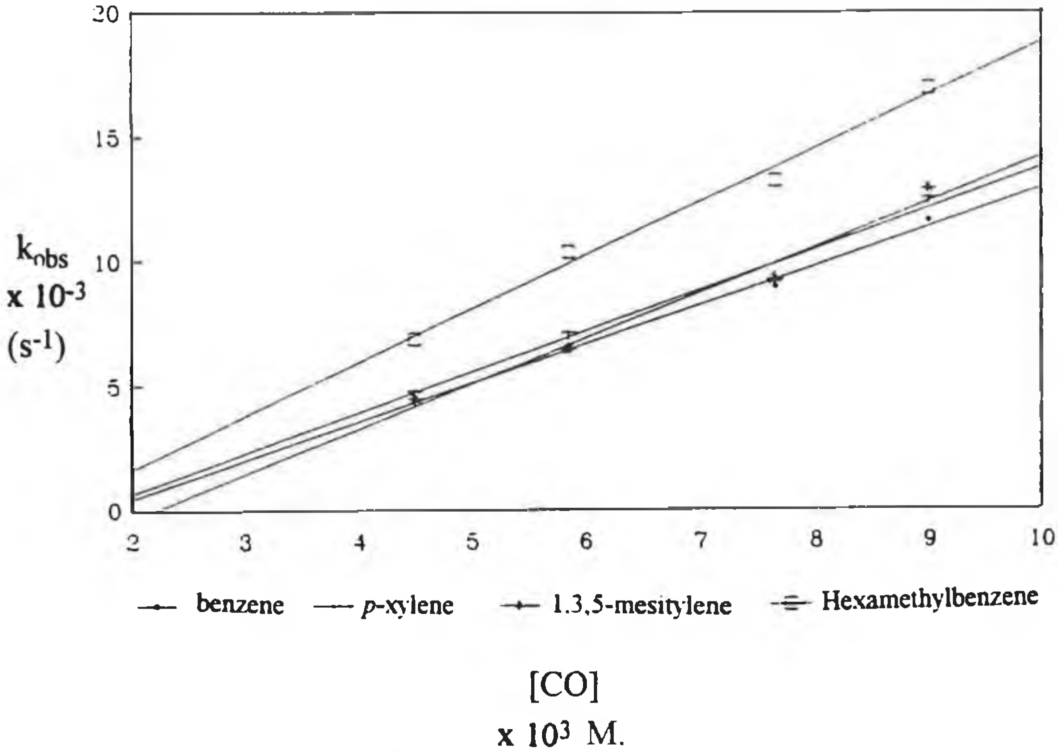

Figure 2.2.2.5.3. Plot of k_{obs} *versus* CO concentration (mol dm^{-3}) for the decay of (η^6-arene)$Mo(CO)_2$(cyclohexane).

(η^6-arene)$Mo(CO)_3$	$k_2 \times 10^{-6}$ $dm^3mol^{-1}s^{-1}$	detection
benzene	1.5	UV/vis.
p-xylene	1.6	UV/vis.
1,3,5-mesitylene	1.8	UV/vis.
1,3,5-mesitylene	1.7	TRIR
hexamethylbenzene	2.1	UV/vis.

Table 2.2.2.5.1 Second order rate constants for the reaction of the solvated dicarbonyl species towards CO to regenerate parent tricarbonyl.

The second order rate constant for the reaction of (η^6-benzene)Mo(CO)$_2$(s) towards CO is similar to that of analogous (η^6-benzene)Cr(CO)$_2$(s) compound (9.8 x 10^6 dm^{3}mol^{-1}s^{-1}),[7] and to that of Cr(CO)$_5$(s) towards CO (2.3 x 10^6 dm^{3}mol^{-1}s^{-1}).[23] Both UV/vis. and TRIR were used to measure the reactivity of the solvated dicarbonyl intermediate in the case of the mesitylene ligand and there appears to be a good correlation between these two methods of detection. The reactivity of the solvated dicarbonyl intermediate was investigated by varying the arene substituent on the benzene ring. From Table 2.2.2.5.1 it can be seen that there is little variation in second order rate constant for any of the arene compounds investigated. These results are in contrast to the results obtained for the analogous chromium system (see Section 2.1.2 and table 2.1.2.1.).

The reactivity of (η^6-1,3,5-mesitylene)Mo(CO)$_2$(s) towards pyridine was measured. The second order constant for reaction of the solvated intermediate towards pyridine (3.2 x 10^7 dm^{3}mol^{-1}s^{-1}) is more than an order of magnitude greater than that towards CO (data given in Figure 2.2.2.5.3). This difference in reactivity can be attributed to the greater σ-donating ability of pyridine, hence pyridine is a stronger nucleophile than CO. This increase in bimolecular rate constant has previously been observed for the Cr(CO)$_6$ system where a thirty fold increase in the rate of displacement of cyclohexane by pyridine compared to that of CO was calculated and the second order rate constant for formation of (η^6-benzene)Cr(CO)$_2$(pyridine) was measured to be 3.7 x 10^7 dm^{3}mol^{-1}s^{-1}.[24]

ligand	k_2 x 10^{-6} dm^{3}mol^{-1}s^{-1}
CO	1.81
pyridine	32.1

Table 2.2.2.5.2 Second order rate constants for the rate of reaction of (η^6-1,3,5-mesitylene)Mo(CO)$_2$(s) towards ligand.

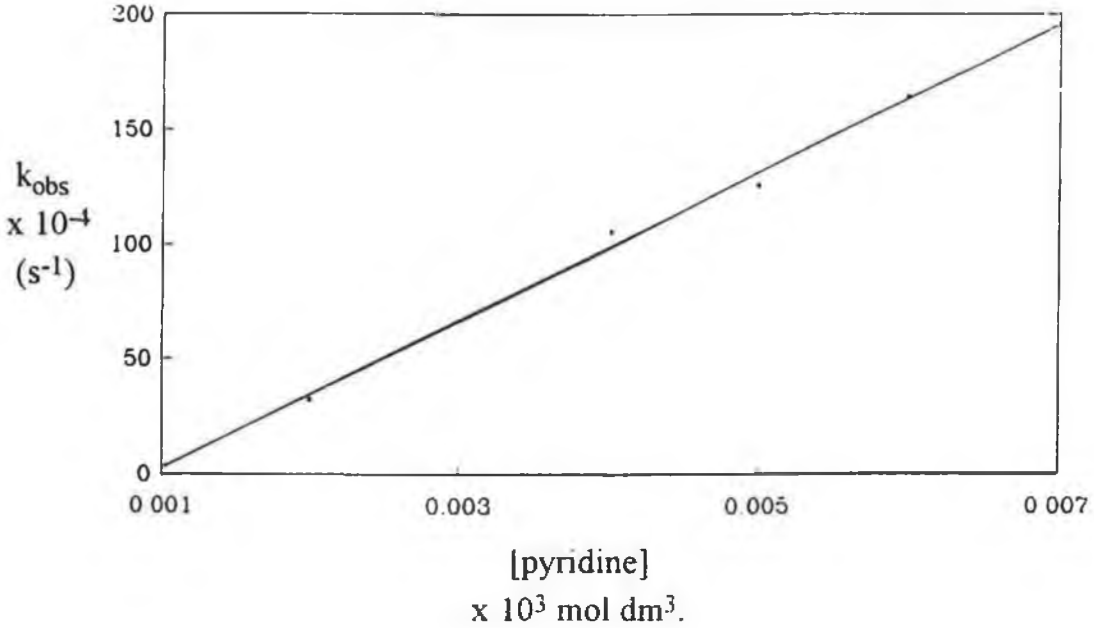

[L] x 10^3 (mol dm^{-3})	k_{obs} x 10^{-4} s^{-1}
2.0	3.25
4.0	10.61
5.0	12.54
6.0	16.45

Slope = $3.21 \times 10^7 + 2.29 \times 10^6$
Intercept = $-2.9 \times 10^4 + 6.7 + 10^3$
Corr. coeff. = 0.99

Figure 2.2.2.5.3 Second order rate constant data for formation of (η^6-1,3,5-mesitylene)$Mo(CO)_2$(pyridine) monitored at 470 nm at 298 K.

The UV/vis. Difference spectrum of the ligated pyridine dicarbonyl complex of molybdenum is contained in Figure 2.2.2.5.5. In this complex a $\lambda_{max.}$ appears at approximately 470 nm. The changes observed in the parent complex as the sample is irradiated indicate a grow in at ~470 nm. A typical grow-in at 470 nm is presented in Figure 2.2.2.5.4.

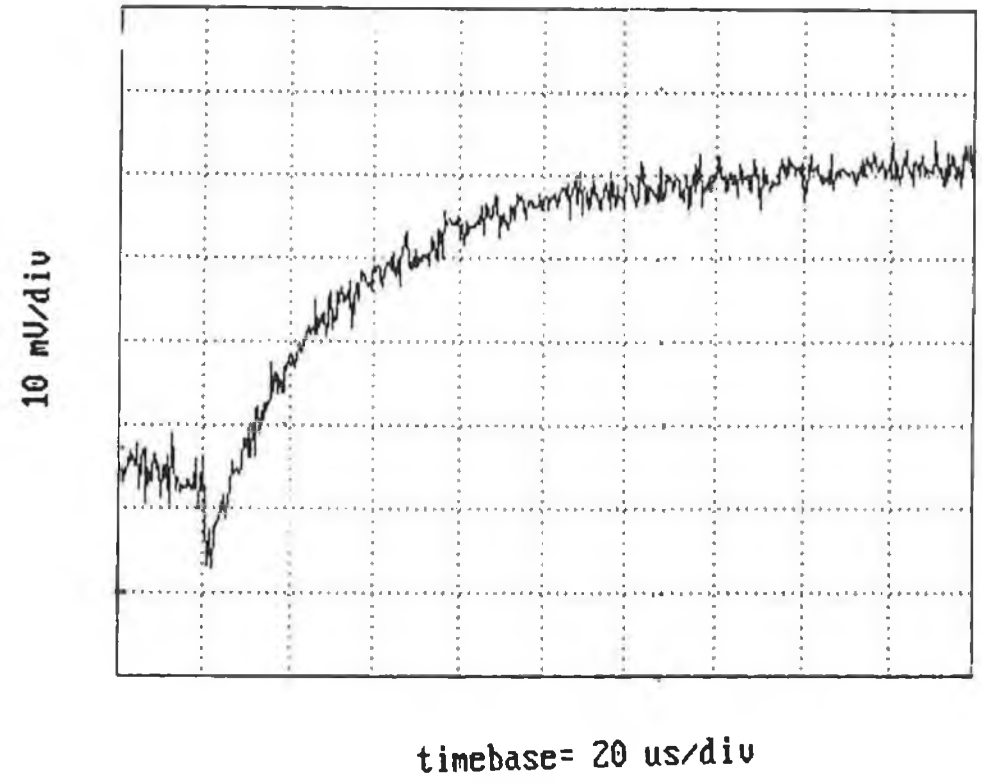

Figure 2.2.2.5.4 A grow-in transient signal for formation of the substituted (η^6-1,3,5-mesitylene)Mo$(CO)_2$(pyridine) at 470 nm.

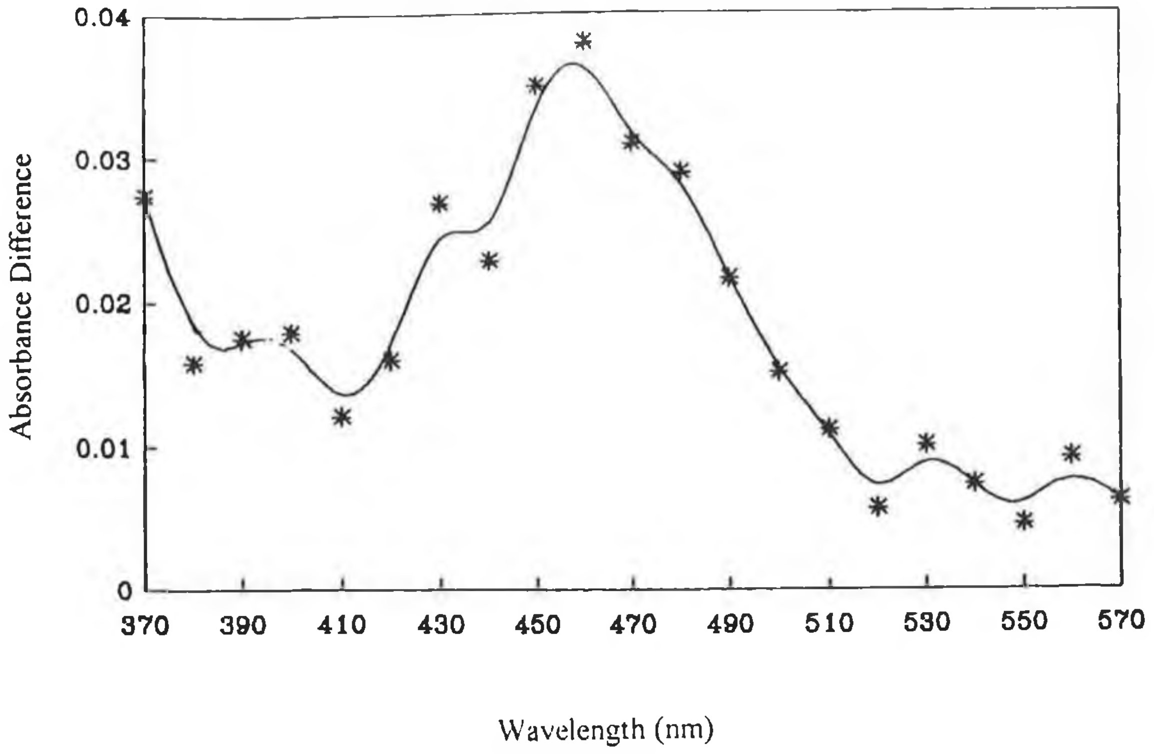

Figure 2.2.2.5.5 UV/vis. difference spectrum of the formation of (η^6-1,3,5-mesitylene)Mo(CO)$_2$(pyridine).

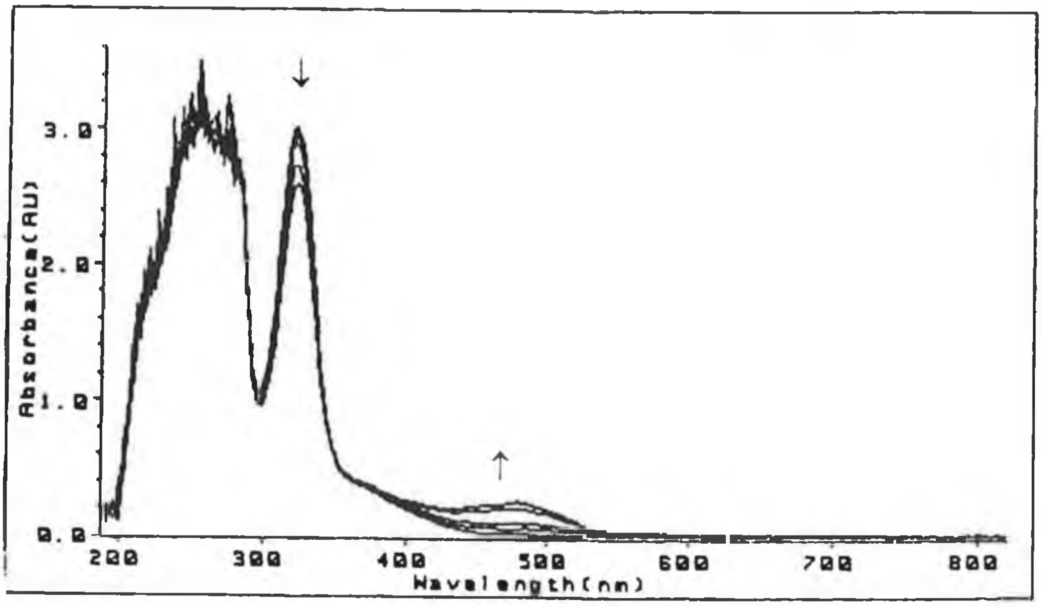

Figure 2.2.2.5.6 Differences observed in the UV/vis. absorption spectrum of (η^6-1,3,5-mesitylene)Mo(CO)$_3$ during the flash photolysis experiment in the presence of pyridine.

This substitution of a CO molecule by pyridine results in a red shift in the absorption bands of the dicarbonyl compared to that of the parent complex. This low energy absorption band is assigned to being metal to pyridine charge transfer in character. With the corresponding chromium system a grow-in ascribed to the pyridine analogue is visible at 500 nm as shown in Figure 2.2.2.5.7. This blue shift with the molybdenum system as opposed to the chromium indicates a stronger interaction of the metal towards the ligand. It is observable that for the chromium system isosbestic points are maintained at 298 and 350 nm as (η^6-benzene)Cr(CO)$_3$ is photolysed in the presence of pyridine.

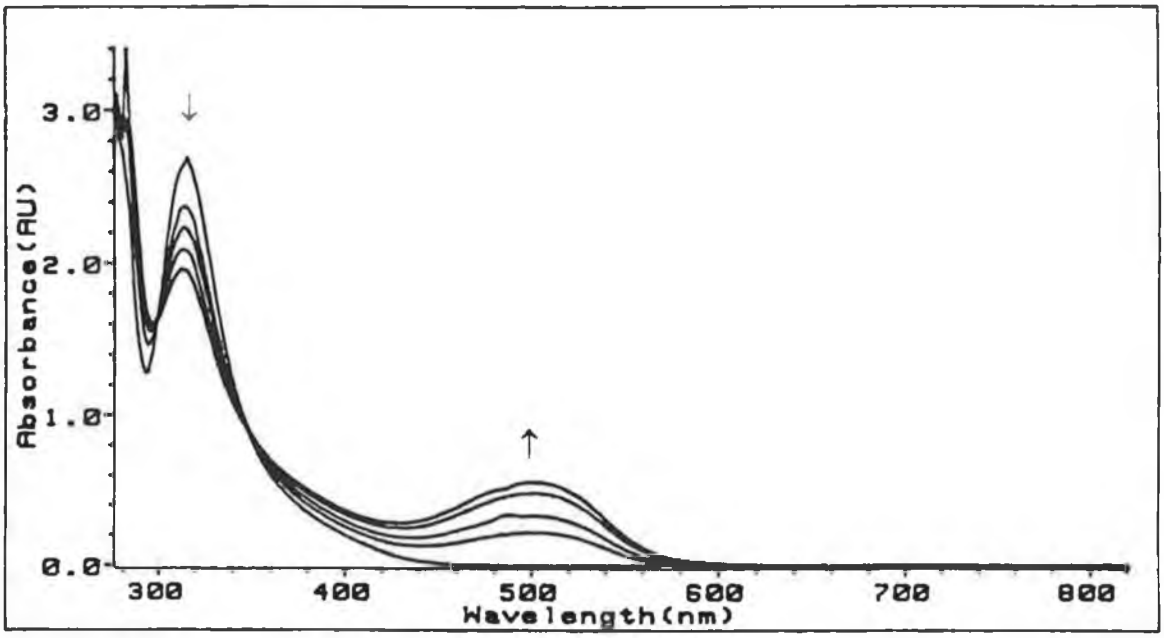

Figure 2.2.2.5.7 UV/vis. spectrum following irradiation of (η^6-benzene)Cr(CO)$_3$ in the presence of pyridine.

2.2.2.6 Activation parameters for the reaction of (η^6-arene)Mo(CO)$_2$(s) with CO.

Activation parameters were obtained using Arrhenius and Eyring plots over a temperature range of 288-320 K for Reaction 2.2.2.6.1.

$$(\eta^6\text{-arene})\mathrm{Mo(CO)_2(s)} + \mathrm{CO} \text{ -----> } (\eta^6\text{-arene})\mathrm{Mo(CO)_3} + \mathrm{s} \qquad (2.2.2.6.1)$$

Data used for Arrhenius and Eyring plots is tabulated in Appendix B -Tables B8 to B11, outlined in Table 2.2.2.6.1 and illustrated graphically in Figures 2.2.2.6.1. Activation parameters were calculated under various concentrations of CO, as formation of a secondary photoproduct is not entirely suppressed under 1 atm. of CO. k_{obs} was plotted *versus* concentration of CO at each temperature and the slope of the line gives k_2 (second order rate constant) for the reaction of the solvated intermediate with CO to regenerate tricarbonyl.

(a)

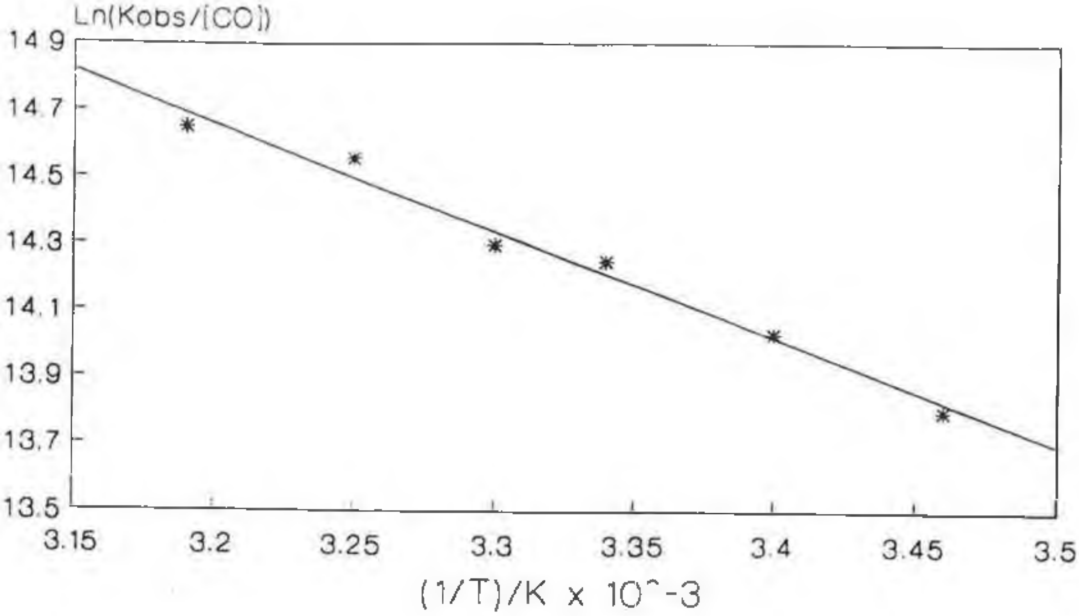

(b)

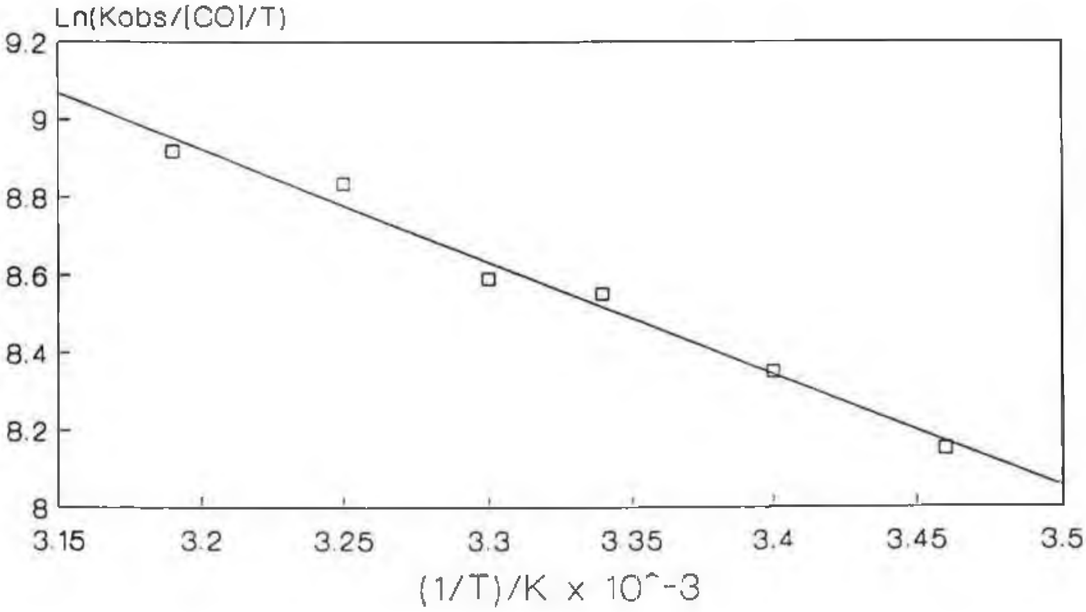

Figure 2.2.2.6.1 Arrhenius(a) and Eyring(b) plots the reaction of (η^6-benzene)Mo(CO)$_2$(cyclohexane) with CO to regenerate parent.

(η^6-arene) $Mo(CO)_3$	$\Delta H^{\neq}$ kJmol^{-1} ($\pm$ 2kJmol^{-1})	$\Delta S^{\neq}$ Jmol^{-1}K^{-1} ($\pm$ 5Jmol^{-1})	$\Delta G^{\neq}_{(298\ K)}$ kJmol^{-1} ($\pm$ 2kJmol^{-1})
benzene	24	- 46	38
p-xylene	23	- 47	37
mesitylene	23	- 46	37
hexamethylbenzene	23	- 48	37

Table 2.2.2.6.1 Activation parameters for the reaction of (η^6-arene)$Mo(CO)_2$(cyclohexane) with CO.

Enthalpy of activation $\Delta H^{\neq}$ for CO recombination for all the complexes is constant at 23 $\pm$ 1 kJmol^{-1}. The activation entropy $\Delta S^{\neq}$ is relatively negative at -47 $\pm$ 1 Jmol^{-1}K^{-1} for the recombination reaction for each arene. These values indicate a more associative mechanism than that for the chromium system, where CO recombination is proposed to occur through an interchange mechanism, and the transition state for the chromium appears to be sensitive to the nature of the arene ligand. This does not appear to be the case for the molybdenum system as kinetic data for all arene ligands are very similar and there is no variation in enthalpy ($\Delta H^{\neq}$) or entropy ($\Delta S^{\neq}$) values for reaction (2.2.2.6.1) regardless of the alkyl substituent. Here it is proposed that CO recombination proceeds *via* the formation of an intermediate with an increased coordination number resulting in an associative mechanism for solvent loss. Presumably this is a result of the increased atomic radius of molybdenum (1.29 Å) over chromium (1.17 Å). It is possible that second and third row transition metals can exist with a coordination number of seven, which is unlikely for first row metals.[25]

2.2.7 Secondary photoproduct.

2.2.7.1 Flash photolysis with TRIR detection.

In conditions of low CO concentration (*i.e.* experiments conducted under 1atm. argon) and high parent concentration formation of a long lived species other than that of the primary photoproduct was observed. The TRIR spectrum of the second transient species shows three carbonyls stretching frequencies which are shown in Figure 2.2.7.1.1. The bands at 1890 and 1860 cm^{-1} are assignable to terminal carbonyl stretching frequencies and that at a much lower frequency could possibly be a bridging carbonyl. However absorption of this band is very weak and is only obvious when viewing individual transients, (see Figure 2.2.7.1.2).

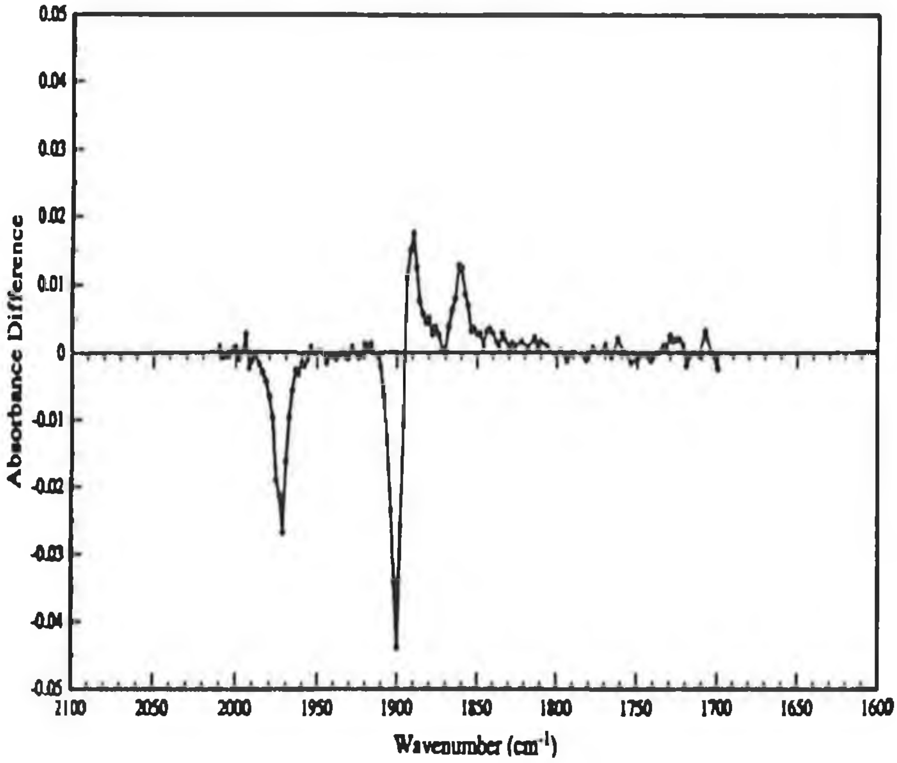

Figure 2.2.7.1.1 TRIR difference spectrum of (η^6-1,3,5-mesitylene)Mo(CO)$_3$ in cyclohexane after 360 μs following flash photolysis at 308 nm under 1 atm. of argon.

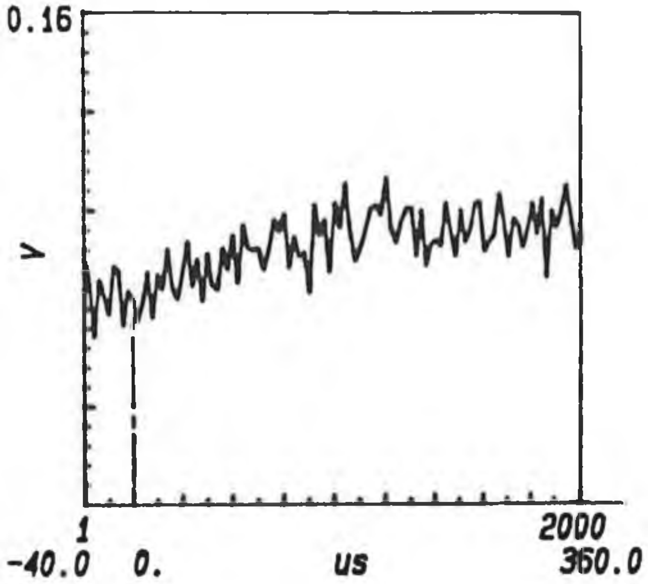

Figure 2.2.7.1.2 TRIR signal at 1726 cm^{-1} following flash photolysis of (η^6-1,3,5-mesitylene)$Mo(CO)_3$ in cyclohexane under 1 atm. of argon.

As observable from Figure 2.2.7.1.5 the rate of decay of the dicarbonyl species (η^6-1,3,5-mesitylene)$Mo(CO)_2(s)$ at 1914 cm^{-1} is the same as the rate of grow-in of the second species at 1890 cm^{-1}. Analysis of this rate data show all reactions obey first order kinetics. On examining an individual trace for depletion of the parent compound we see further depletion (see Figure 2.2.7.1.3), this observation together with that outlined above indicates that the likely explanation for this secondary photoproduct is that the dicarbonyl species is reacting with a species in solution whose concentration is much greater, and hence the reaction appears first order. Figure 2.2.7.1.4 presents a possible structure of this dinuclear complex.

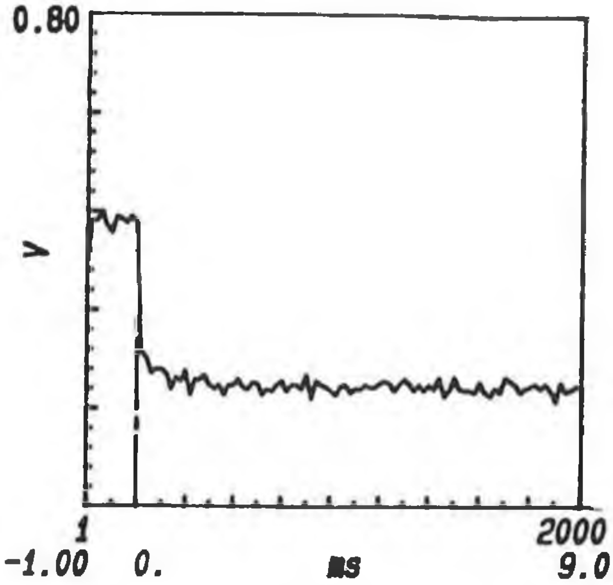

Figure 2.2.7.1.3 Further depletion of parent transient at 1976 cm^{-1}.

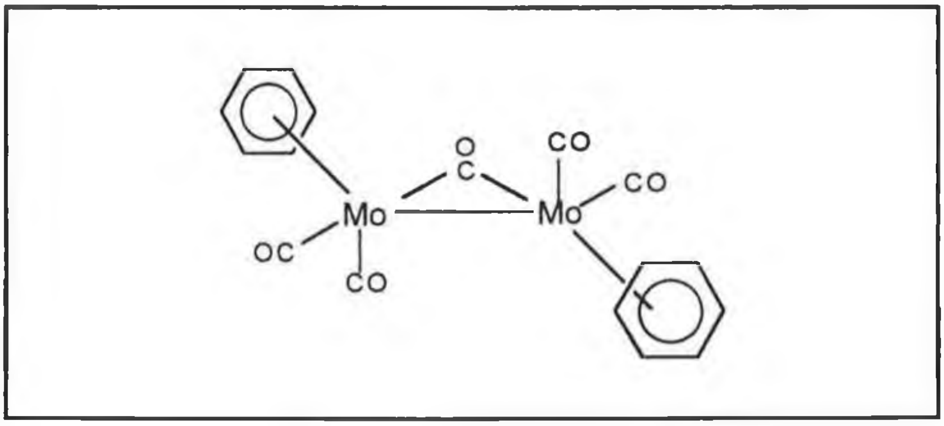

Figure 2.2.7.1.4 Possible structure for molybdenum dinuclear species.

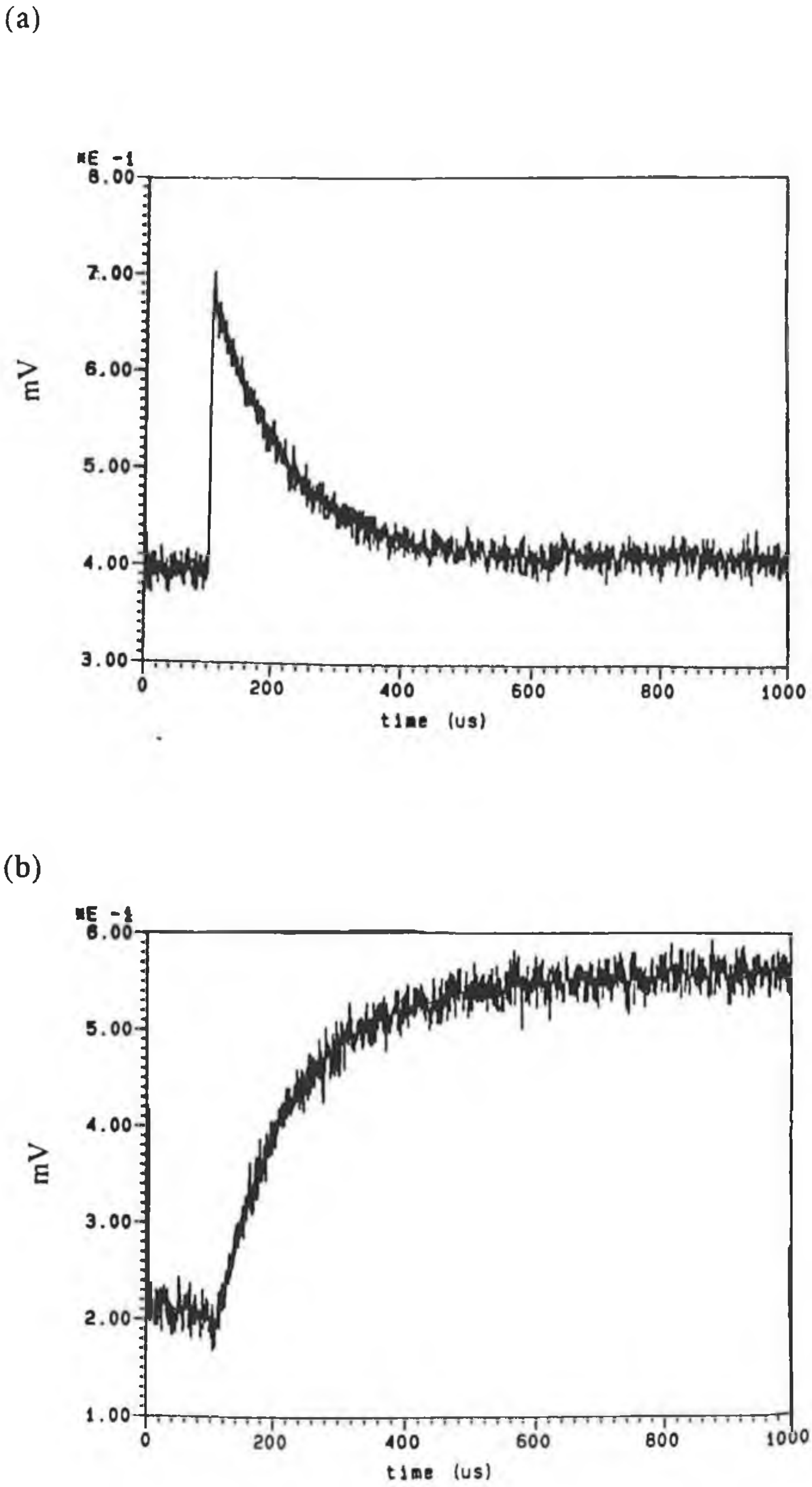

Figure 2.2.7.1.5 Decay of the transient species at 1914 cm^{-1}(a) together with the grow-in of the second species at 1890 cm^{-1}(b) following flash photolysis of (η^6-1,3,5-mesitylene)$Mo(CO)_3$ in cyclohexane under 1 atm. of argon.

The second order rate constant for formation of the secondary photoproduct for (η^6-1,3,5-mesitylene)Mo(CO)$_3$ was measured to be 1.1 x 10^7 dm^{3}mol^{-1}s^{-1} as obtained by TRIR. This dinuclear species is predominantly found under conditions of low CO concentrations but it is not entirely suppressed under conditions of high concentrations (9.0 x 10^{-3}M) of CO. It was decided to conduct an experiment with a high concentration of trapping ligand to see if it were possible to totally suppress formation of the dinuclear species. The trapping ligand chosen was *cis*-cyclooctene (5 x 10^{-2}M) in addition to CO (9.0 x 10^{-3}M) at a parent concentration of (1.0 x 10^{-3}M). In these experiments the depleted parent bands provided no evidence for recovery and the two bands previously assigned to the solvated dicarbonyl species only exhibited marginal reduction in their absorbances. However the lack of any obvious decay back of the bands at 1914 and 1860 cm^{-1} was disappointing and suggest that (η^6-1,3,5-mesitylene)-Mo(CO)$_2$(s) and (η^6-1,3,5-mesitylene)Mo(CO)$_2$(*cis*-cyclooctene) exhibit ν_{CO} at identical wavenumbers. No evidence for the bands ascribed to the dinuclear species was evident thereby indicating total suppression because of the excess of trapping ligand. It is unfortunate that the bands for the (η^6-1,3,5-mesitylene)Mo(CO)$_2$(*cis*-cyclooctene) occur at a similar frequency to those of the solvated dicarbonyl intermediate, nevertheless the (η^6-*p*-xylene)Mo(CO)$_2$(*cis*-cyclooctene) compound has previously been isolated and fully characterised, and the infrared stretching frequencies for this compound occur at 1914 and 1862 cm^{-1}.[19] These values compare well with those of the TRIR experiment following photolysis of (η^6-1,3,5-mesitylene)Mo(CO)$_3$ in an excess of *cis*-cyclooctene (*vide supra*). The over all reaction for the formation of the *cis*-cyclooctene adduct is proposed to occur through the following reactions 2.2.7.1.1 and 2.2.7.1.2;

$$(\eta^6\text{-1,3,5-mesitylene})\text{Mo(CO)}_3 \xrightarrow[s]{h\nu} (\eta^6\text{-1,3,5-mesitylene})\text{Mo(CO)}_2\text{(s)} + \text{CO} \qquad (2.2.7.1.1)$$

$$(\eta^6\text{-1,3,5-mesitylene})\text{Mo(CO)}_2\text{(s)} + \textit{cis}\text{-cyclooctene} \longrightarrow (\eta^6\text{-1,3,5-mesitylene})\text{Mo(CO)}_2(\textit{cis}\text{-cyclooctene}) + \text{s} \qquad (2.2.7.1.2)$$

These experiments identify the secondary photoproduct at 1890, 1860 and ~1726 cm^{-1} as being a dinuclear compound.

2.2.7.2 Flash photolysis with UV/vis detection.

Following laser flash photolysis at 266 nm under 1 atm of argon a transient species is observed to form at 370 nm. Figure 2.2.7.2.1. shows a typical 'grow-in' for formation of this species.

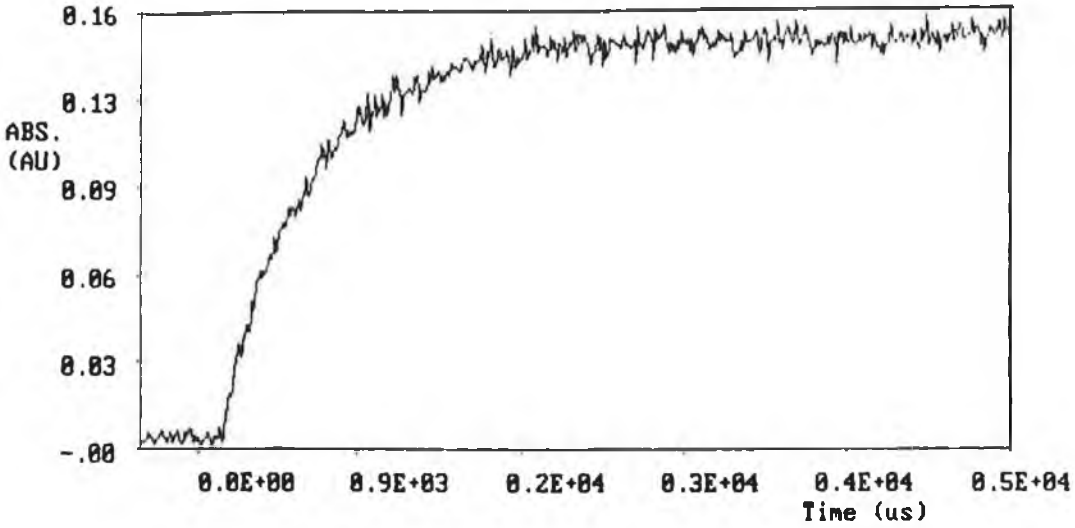

Figure 2.2.7.2.1 A transient absorbance curve showing the grow-in of the species observed at 370 nm under following flash photolysis of (η^6-1,3,5-mesitylene)$Mo(CO)_3$ under 1 atm. of argon.

The UV/vis. difference spectrum following flash photolysis of (η^6-benzene)$Mo(CO)_3$ in cyclohexane at 800 μs after the flash is shown in Figure 2.2.7.2.2 with a $\lambda_{max.}$ at 370 nm This spectrum is quite similar to that of $[(\eta^5$-cyclopentadienyl)$Mo(CO)_3]_2$ where the sharp, intense near UV-absorption seen in a spectrum of this compound is associated with a σ ---- > σ* transition.[26] The $\lambda_{max.}$ in this system is thought to arise from a similar transition hence the intense absorption at 370 nm is assigned to a σ ----> σ* transition which is a consequence of metal to metal interaction. The over all yield of the dinuclear species was found to be greatly suppressed on addition of CO as seen in Figure 2.2.7.2.3 together with a large increase in rate constant. The increase in rate of formation of the dinuclear species as CO is added, is because of competition with the reaction with CO; *i.e.* reaction of the solvated dicarbonyl with CO to regenerate parent competes with the reaction of the solvated intermediate with unphotolysed parent to generate a dinuclear species.

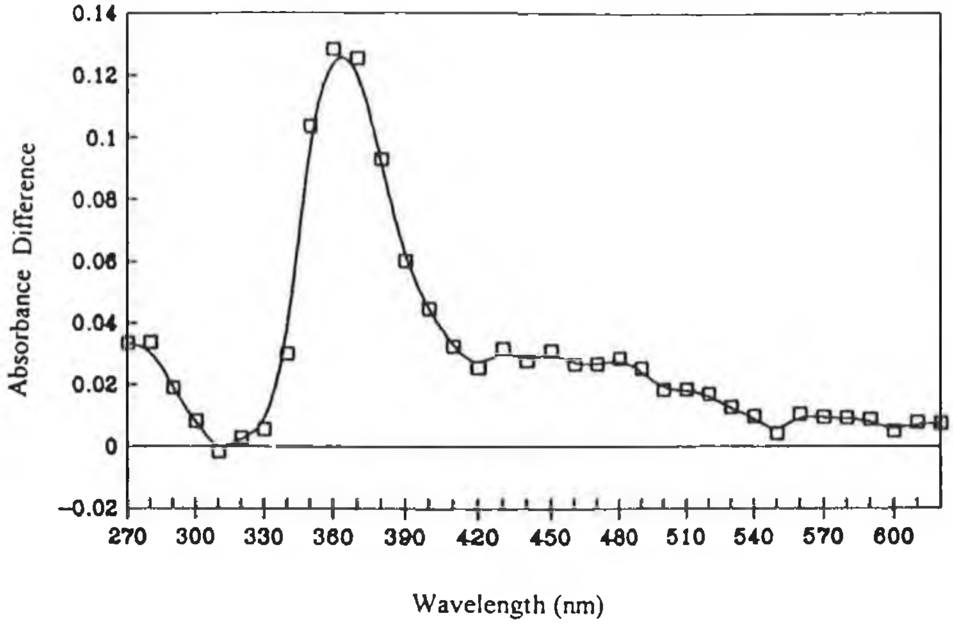

Figure 2.2.7.2.2. UV/vis. difference spectrum of (η^6-benzene)Mo(CO)$_3$ following flash photolysis at 266nm under 1atm. argon.

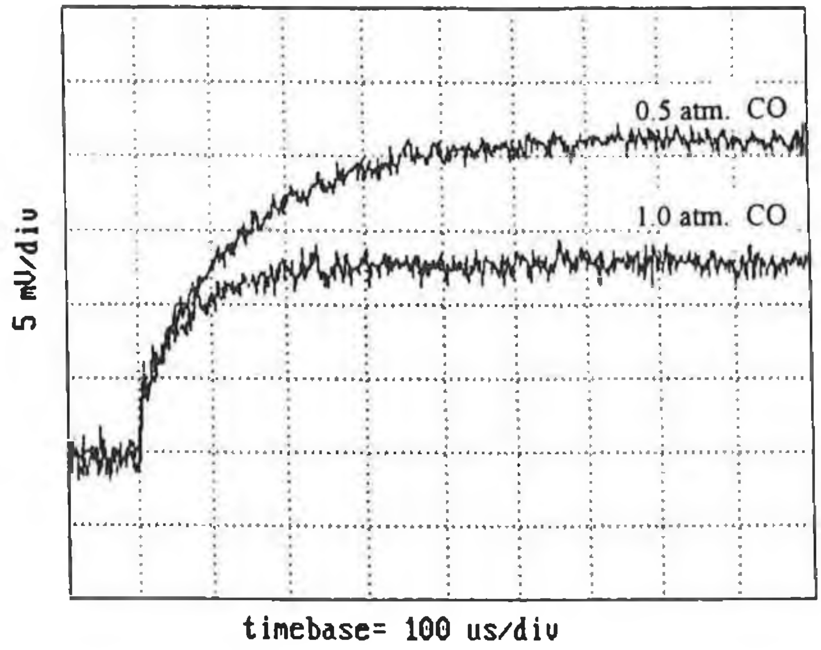

Figure 2.2.7.2.3 Differences observed in transient signals at 370 nm as various concentrations of CO is added to the cell and this effect on rate and yield of dinuclear species for (η^6-1,3,5-mesitylene)Mo(CO)$_3$.

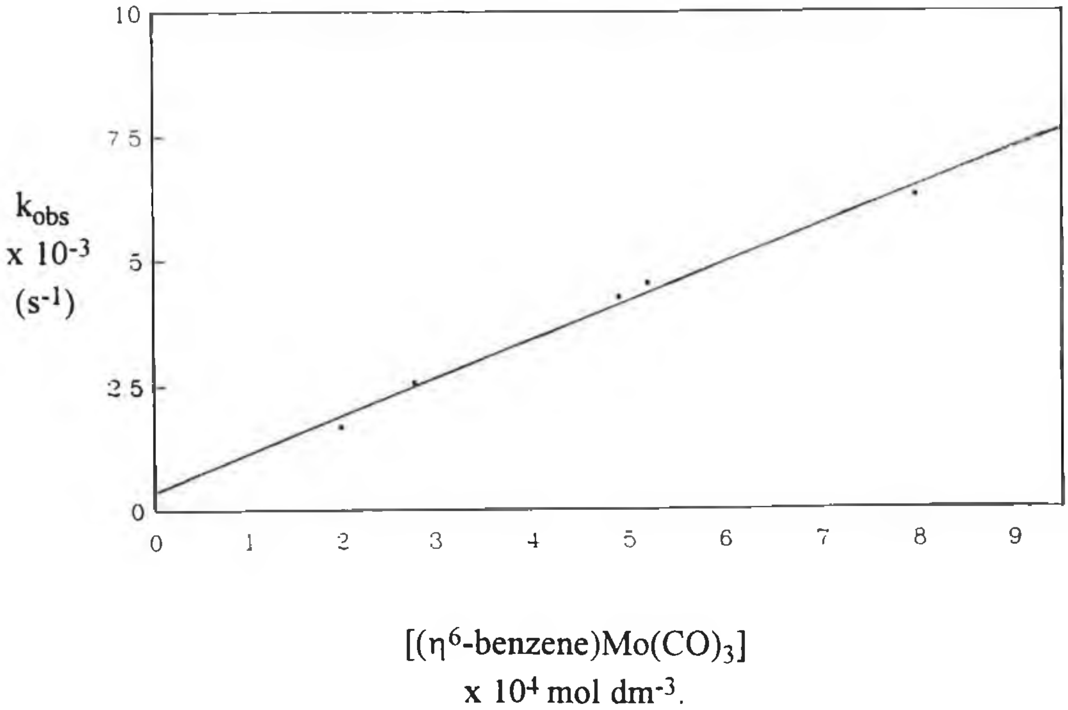

[(η^6-benzene)Mo(CO)$_3$] x 10^4 mol dm^{-3}	k_{obs} x 10^{-3} (s^{-1})
1.98	1.66
2.78	2.56
4.9	4.25
5.2	4.52
7.97	6.27

Slope = $7.61 \times 10^6 \pm 4.66 \times 10^5$ dm^3 mol^{-1} s^{-1}
Intercept = 379.1 ± 218.5 s^{-1}
corr. coeff. = 0.99

Figure 2.2.7.2.4 A plot concentration of (η^6-benzene)Mo(CO)$_3$ against the observed rate constant for the reaction of (η^6-benzene)Mo(CO)$_2$(cyclohexane) with (η^6-benzene)Mo(CO)$_3$ under 1 atm. of argon.

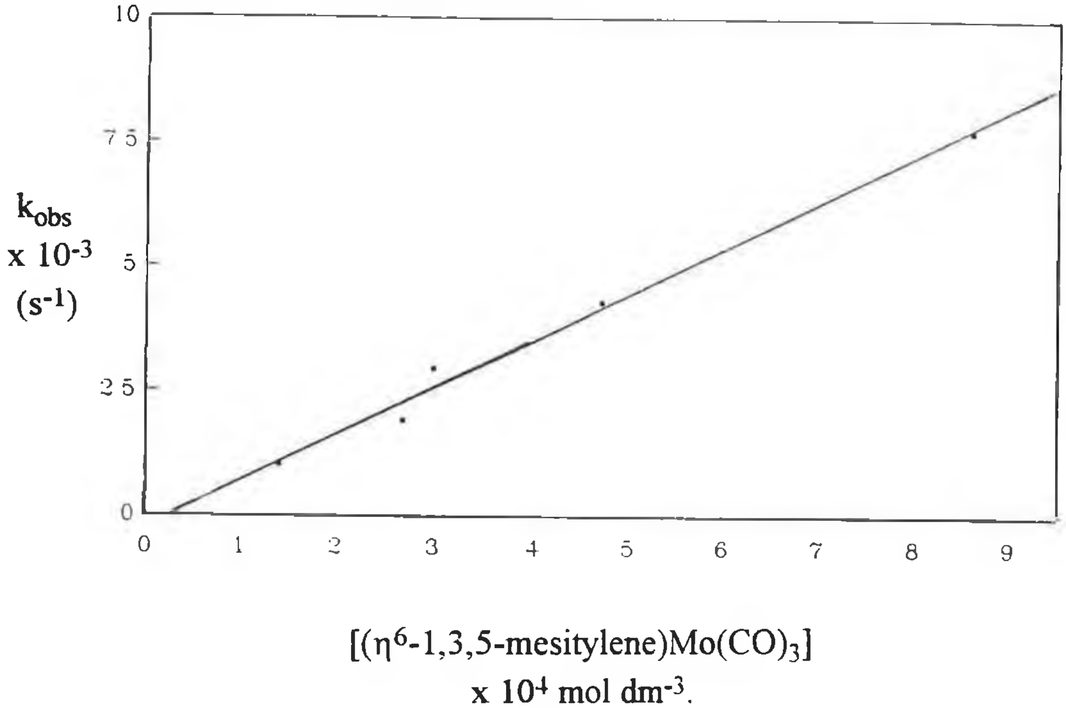

[(η^6-1,3,5-mesitylene)Mo(CO)$_3$] x 10^4 mol dm^{-3}	k_{obs} x 10^{-3} (s^{-1})
1.4	1.02
2.68	1.91
2.99	2.95
4.71	4.28
8.59	7.73

Slope = 8.86 x 10^6 $\pm$ 4.95 x 10^6 dm^3 mol^{-1} s^{-1}
Intercept = -54.7 $\pm$ x 10 s^{-1}
corr. coeff. = 0.99

Figure 2.2.7.2.5 A plot concentration of (η^6-1,3,5-mesitylene)Mo(CO)$_3$ against the observed rate constant for the reaction of (η^6-1,3,5-mesitylene)Mo(CO)$_2$(cyclohexane) with (η^6-1,3,5-mesitylene)Mo(CO)$_3$ under 1 atm. of argon.

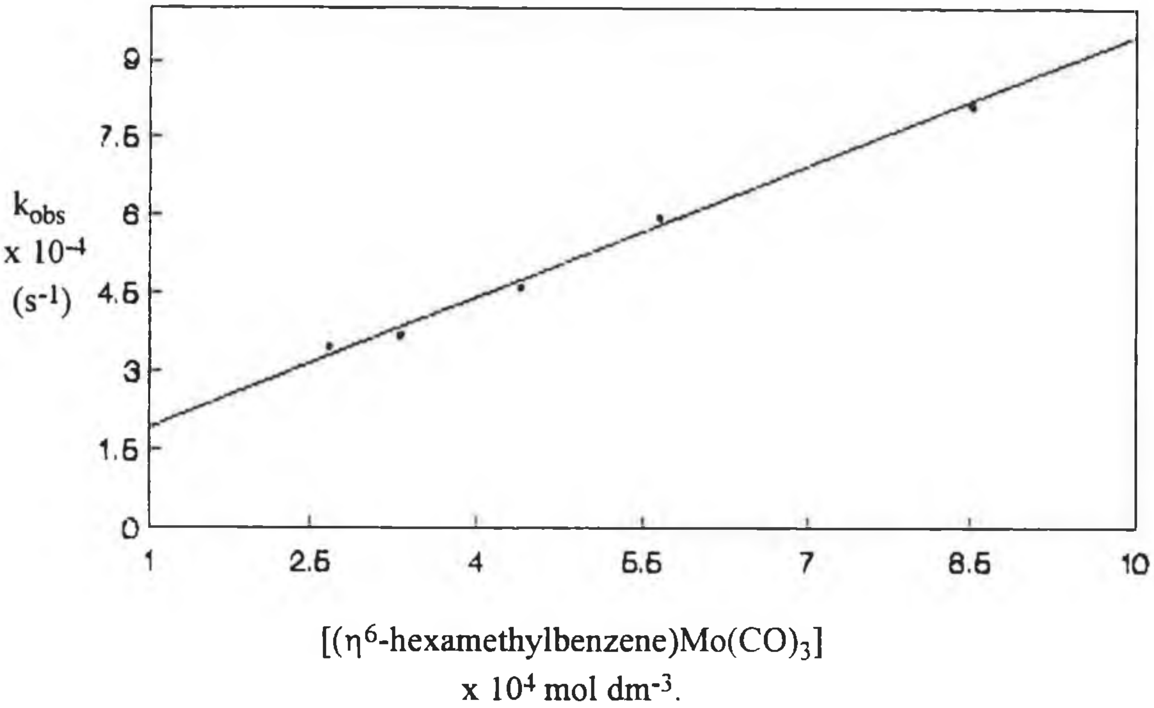

[(η^6-hexamethylbenzene)Mo(CO)$_3$] x 10^4 mol dm^{-3}	k_{obs} x 10^{-4} (s^{-1})
3.46	2.65
3.68	3.3
4.63	4.38
5.98	5.63
8.16	8.46

Slope = $8.41 \times 10^7 \pm 3.97 \times 10^6$ dm^3 mol^{-1} s^{-1}
Intercept = $1.07 \times 10^4 \pm 1.8 \times 10^3$ s^{-1}
corr. coeff. = 0.99

Figure 2.2.7.2.6 A plot concentration of (η^6-hexamethylbenzene)Mo(CO)$_3$ against the observed rate constant for the reaction of (η^6-hexamethylbenzene)Mo(CO)$_2$(cyclohexane) with (η^6-hexamethylbenzene)-Mo(CO)$_3$ under 1 atm. of argon.

(η^6-arene)Mo(CO)$_3$	x 10^{-6} dm^{3}s^{-1}mol^{-1}
benzene	7.6
mesitylene	8.9
hexamethylbenzene	84.1

Table 2.2.7.2.1. Second order rate constant for formation of the dinuclear species.

Rate of formation of this dinuclear species was calculated by plotting k_{obs} *versus* concentration of parent as shown in Figures 2.2.7.2.4. to 2.2.7.2.6. The second order rate constant for formation of the dinuclear species for all arene substituents is outlined in Table 2.2.7.2.1. The second order rate constants for formation of this secondary photoproduct increases as the number of methyl substituents increase with almost a 10 fold increase for the highly substituted hexamethyl derivative. Formation of dinuclear compounds have previously been reported upon photolysis of $Cr(CO)_6$,[23] (η^5-C_5H_5)Mn(CO)$_3$,[12] (η^4-C_4H_4)Fe(CO)$_3$[27] and a number of other systems. Rate of formation of the dinuclear species is approximately 6 times faster than that of reaction of the solvated $Cr(CO)_5$ towards CO,[23] and this increase in rate is common to the molybdenum compounds investigated in this study.

The dinuclear species is long lived, and no decay was observed on a time scale of less than 200 ms. On longer time scales any decay observed can be attributed to diffusion of the photoproduct away from the detection zone. The photochemical system appeared to be reversible for certain ligands (namely; benzene and mesitylene) as the UV/vis. spectrum of the parent monitored throughout the experiment showed no significant changes thereby indicating eventual regeneration of parent tricarbonyl. But this regeneration of parent was not so for the hexamethylbenzene derivative, where a number of hours are required for the parent to fully regenerate. It can be seen that for this system formation of the dinuclear species is accompanied by characteristic, clean isosbestic points and very significant spectral changes in the UV/vis. spectrum, with bands growing in at 375, 455 and 485 nm concomitant with a decay of $\lambda_{max.}$ at 330 nm (see Figure 2.2.7.2.7).

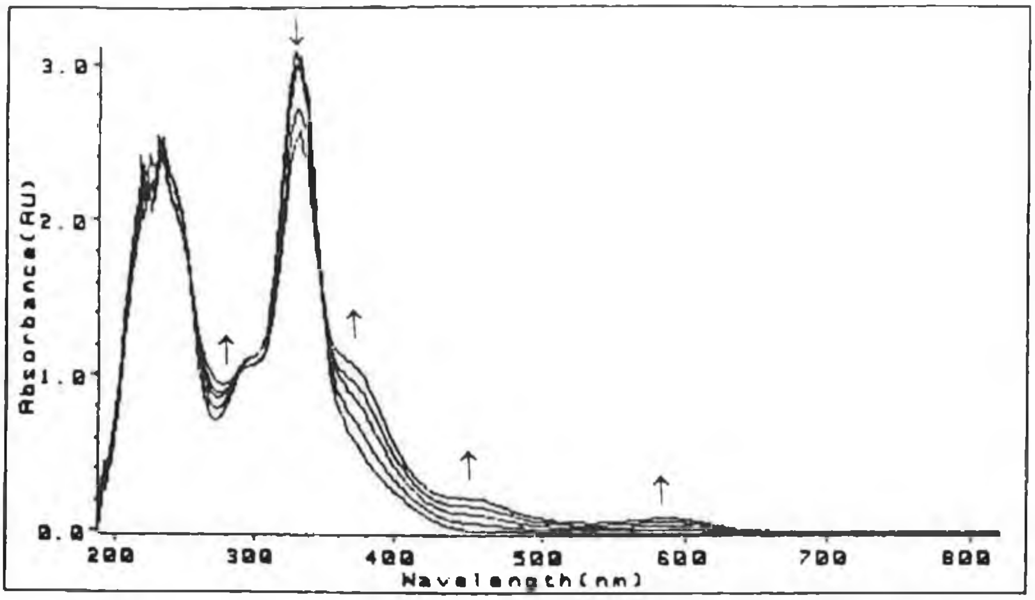

Figure 2.2.7.2.7. Spectral changes observed following irradiation of (η^6-hexamethylbenzene)$Mo(CO)_3$ (1.9 x 10^{-4}M) under 1 atm. argon.

(η^6-arene)$Mo(CO)_3$	s^{-1}
benzene	4103
1,3,5-mesitylene	934

Table 2.2.7.2.2 Second order rate constant data for decay of the dinuclear species under CO.

Rate of decay of the dinuclear species under various concentrations of CO was measured for (η^6-benzene)$Mo(CO)_3$ and (η^6-mesitylene)$Mo(CO)_3$ (Figure 2.2.7.2.8 and 2.2.7.2.9). From Table 2.2.7.2.2 it is evident that as the number of methyl substituents on the benzene ring increases the life time of this proposed dinuclear species also increases. (η^6-Hexamethylbenzene)$Cr(CO)_3$ gives rise to the more stable dinuclear compound, as determined from changes in the UV/vis. spectrum. Because of this apparent stability for the dinuclear compound of (η^6-hexamethylbenzene)$Mo(CO)_3$ attempts were made to isolate the dinuclear compound (Chapter 7). Casey and coworkers have previously synthesised and isolated a bridging carbonyl rhenium compound similar to that proposed to form in these studies.[28]

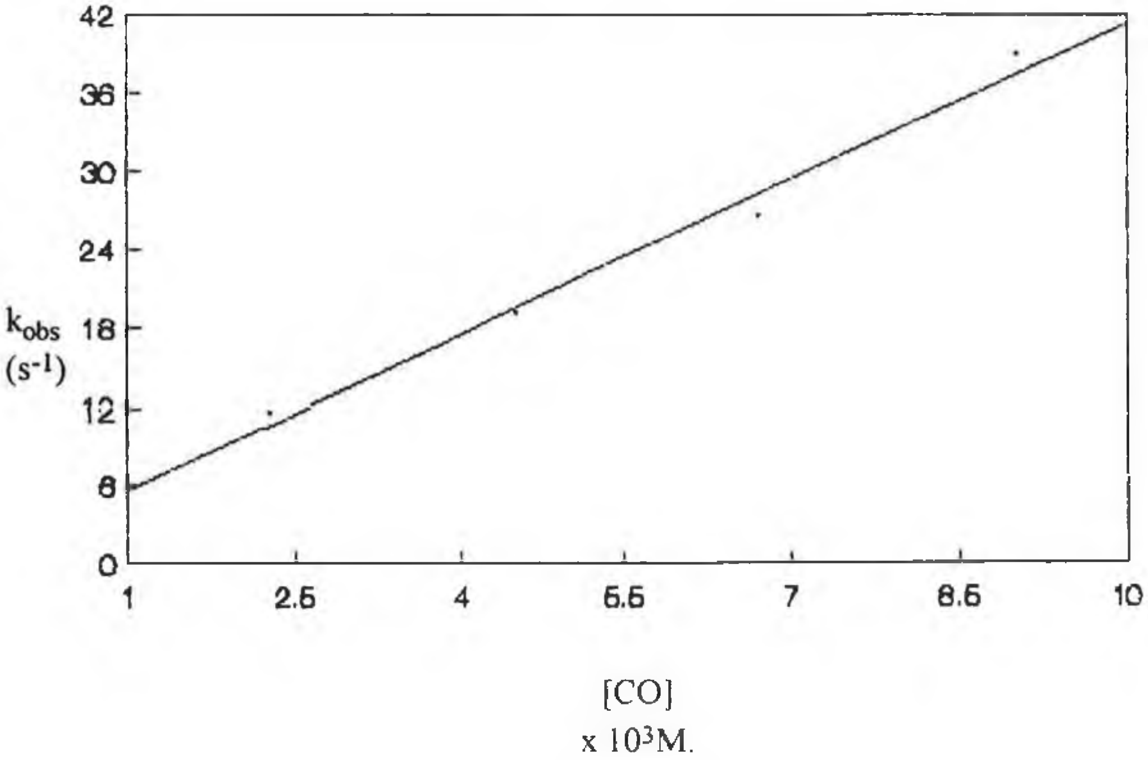

[CO] x 10^3 mol dm^{-3}	k_{obs} (s^{-1})
2.25	11.7
4.5	19.11
6.75	26.5
9.0	39.0

Slope = 4105 ± 3798 $dm^3\ mol^{-1}\ s^{-1}$
Intercept = 0.69 ± 1.84 s^{-1}
corr. coeff. = 0.99

Figure 2.2.7.2.8 Plot of concentration CO (mol dm^{-3}) against the observed rate constant for the decay of the dinuclear (η^6-benzene)$_2$Mo$_2$(CO)$_5$ complex at 298K

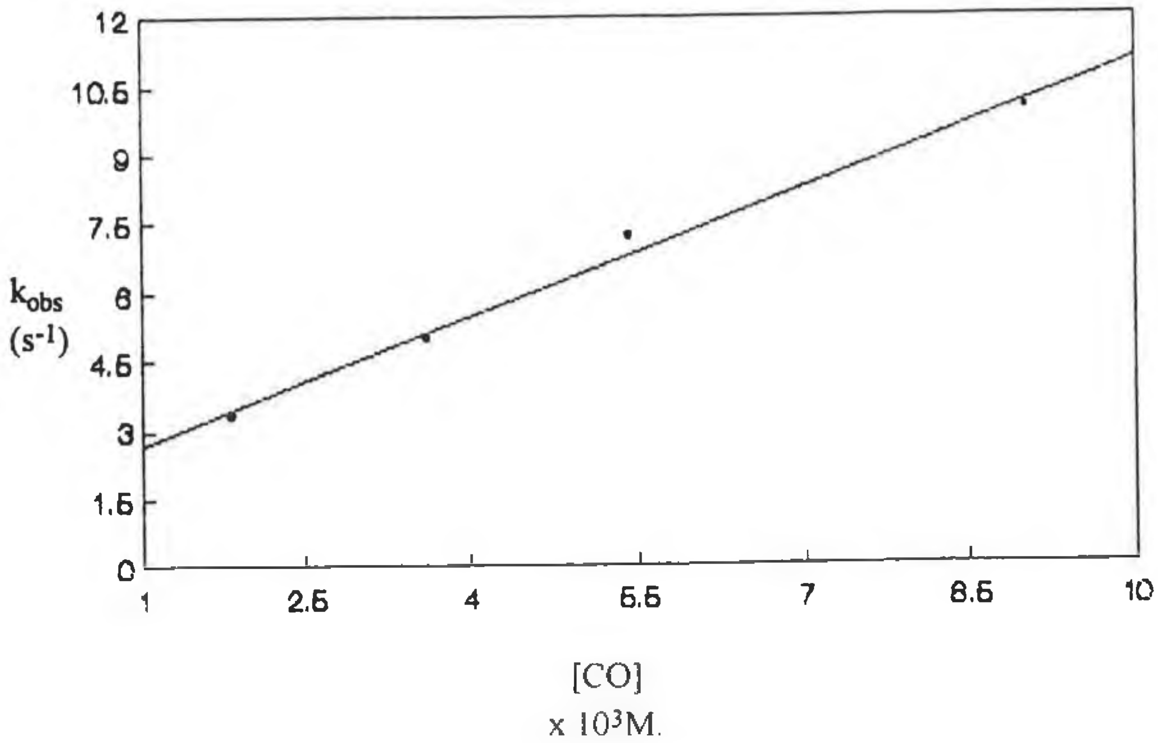

[CO] x 10^3 mol dm^{-3}	k_{obs} (s^{-1})
1.8	3.34
3.6	4.99
5.4	4.7
9.0	10

Slope = 934 ± 63 dm^3 mol^{-1} s^{-1}
Intercept = 1.77 ± 0.33 s^{-1}
corr. coeff. = 0.99

Figure 2.2.7.2.9 Plot of concentration CO (mol dm^{-3}) against the observed rate constant for the decay of the dinuclear (η^6-1,3,5-mesitylene)$_2$Mo$_2$(CO)$_5$ complex at 298 K

2.2.8 A study of the activation parameters for the formation of (η^6-arene)$Mo_2(CO)_5$.

The activation parameters for the formation of the dinuclear species were determined from Arrhenius and Eyring plots. The second order rate constant (k_2) for reaction 2.2.8.1 was calculated by dividing k_{obs} by the concentration of (η^6-arene)$Mo(CO)_3$. The data is given in Appendix B and illustrated graphically in Figure 2.2.8.1 and 2.2.8.2.

$$(\eta^6\text{-arene})Mo(CO)_3 + (\eta^6\text{-arene})Mo(CO)_2(s) \dashrightarrow (\eta^6\text{-arene})Mo_2(CO)_5 + s \qquad (2.2.8.1)$$

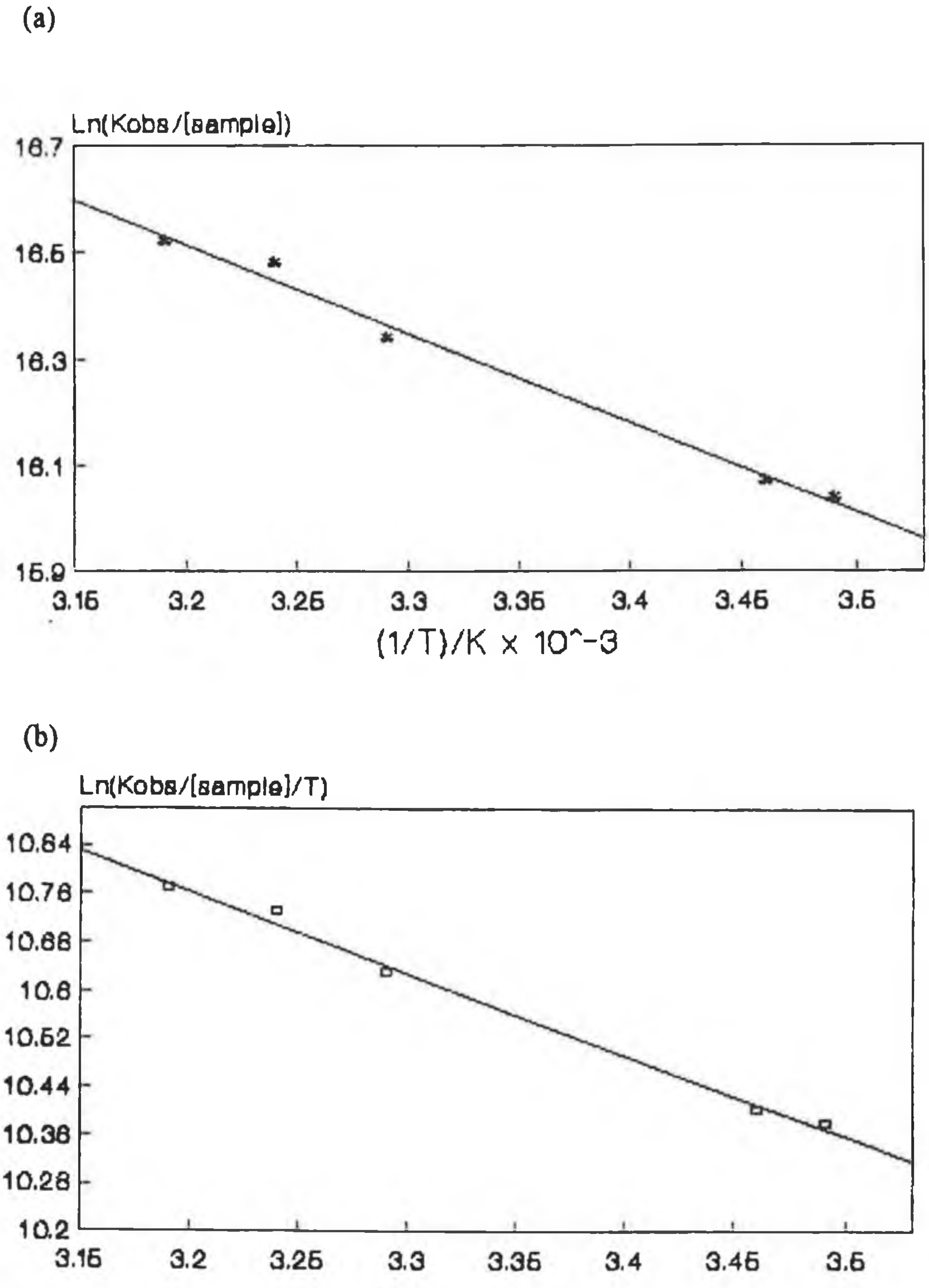

Figure 2.2.8.1 Arrhenius(a) and Eyring(b) plots for the reaction of (η^6-benzene)Mo(CO)$_2$(cyclohexane) with parent compound.

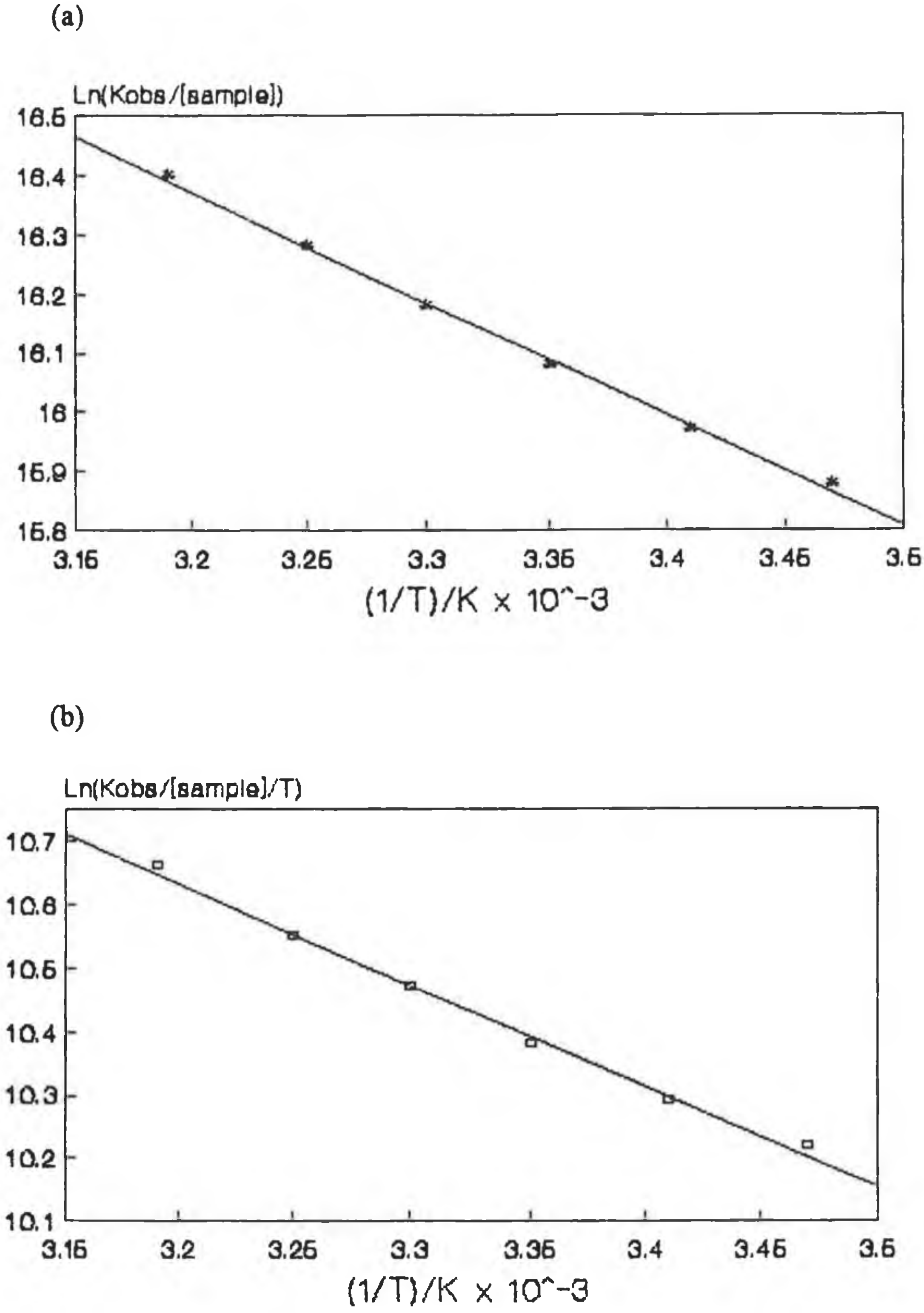

Figure 2.2.8.1 Arrhenius(a) and Eyring(b) plots for the reaction of (η^6-1,3,5-mesitylene)Mo(CO)$_2$(cyclohexane) with parent compound.

(η^6-arene)Mo $(CO)_3$	$\Delta H^{\neq}$ kJmol^{-1} ($\pm$ 2kJmol^{-1})	$\Delta S^{\neq}$ Jmol^{-1}K^{-1} ($\pm$ 2Jmol^{-1})	$\Delta G^{\neq}_{(298K)}$ kJmol^{-1} ($\pm$ 2kJmol^{-1})
benzene	11	- 71	32
mesitylene	13	- 67	33
hexamethylbenzene	*		

Table 2.2.8.1 Activation data for formation of dinuclear species under 1 atm. of argon following flash photolysis of (η^6-arene)Mo$(CO)_3$. * Activation parameters could not be calculated for this compound as the secondary product formed under argon is stable and hence no reproducible results could be obtained.

Outlined in Table 2.2.8.1 is activation data for formation of the dinuclear species for the arene compounds of molybdenum that were investigated in this study. The enthalpy of activation $\Delta H^{\neq}$ remains fairly constant at 12 $\pm$ 1 kJmol^{-1}, and a Gibbs free energy $\Delta G^{\neq}$ of 32 $\pm$ 1 kJmol^{-1}. Presumably it is owing to this energetic feasibility that formation of the dinuclear species is not fully suppressed under high concentrations of CO (9.0 x 10^{-3}M). The Gibbs free energy for formation of the dinuclear species for these compounds is lower at $\Delta G^{\neq} = 32 \pm 1$ than that of the corresponding reaction of the solvated dicarbonyl with CO to regenerate parent (37 $\pm$ 1 kJmol^{-1}). $\Delta S^{\neq}$ values are notably more negative indicating an associative type reaction and this is as expected for formation of the dinuclear species and agrees with reaction 2.2.8.1.

2.3 Laser flash photolysis of (η^6-arene)M(CO)$_3$ compounds (where M = Cr or Mo) in various hydrocarbon solvents.

Understanding the interactions between solvent molecules and the reacting systems has been an active area of research for several years.[29] With the availability of picosecond and subpicosecond techniques, time resolved studies of the reaction dynamics on the same time scale as solvent motion can be probed. Such experiments clearly indicate that the role of solvent cannot be completely described in terms of bulk properties. A complete description of the role of solvent in chemical reactions must contain a molecular picture of the solvent medium. $Cr(CO)_6$ has served as an explemar for studies of solvation in coordinatively unsaturated intermediates. It has been found that upon Cr–CO bond fission in $Cr(CO)_6$, the [$Cr(CO)_5$] produced reacts rapidly with solvent to afford $Cr(CO)_5$(solvent) species.[30] Mixed matrix[31] and mixed solvents studies have indicated that the maximum absorption of the primary intermediate "$M(CO)_5(s)$" is very sensitive to the matrix or solvent.[32] In this study the second order rate constant and activation parameters for the reaction of the photoproducts of (η^6-arene)M(CO)$_3$ (M = Cr or Mo), in various hydrocarbon solvents was investigated with the hope that a further insight into the mechanisms of these systems could be explained.

2.3.1 Electronic absorption spectra.

The UV/vis. spectra for (η^6-benzene)Cr(CO)$_3$ and (η^6-mesitylene)Mo(CO)$_3$ is contained in Figure 2.3.1.1. These spectra have previously been described in sections 2.1.1 and 2.2.1. From Figure 2.3.1.1 it is obvious that the UV/vis. spectra of the Cr and Mo systems differ enormously. The $\lambda_{max.}$ for the Mo system has a very sharp band at approximately 320 nm in comparison to the Cr analogue which has a much broader absorption band. With the Mo system a band is visible at 330 nm and a shoulder at approximately 370 nm which is not as intense with the Cr system. It is speculated that the LF band is lower in energy than the MLCT band for the Cr system and hence a relatively efficient CO loss process occurs.[4] When the quantum yield was measured for the Mo system it was found to be far less efficient being only one third that for the Cr system. So is it possible that the LF band is now greater in energy and that the band absorption at 270 nm may be attributed to a LF absorption or at least partially so. Extinction coefficients for these systems are in Table 2.3.1.1 and 2.3.1.2, 355 nm was used exclusively for the Cr experiments and 266 nm for flash photolysis of the Mo system. The data used for calculation of extinction coefficient is in Appendix C.

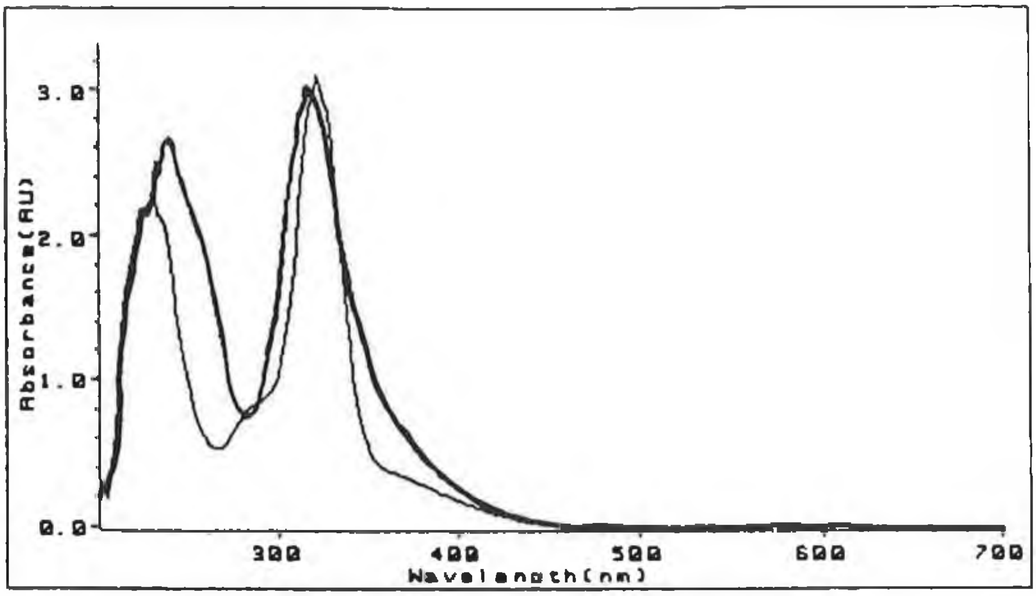

Figure 2.3.1.1 UV/vis. spectra of (η^6-benzene)Cr(CO)$_3$ (4.5 x 10^{-4}M) and (η^6-1,3,5-mesitylene)Mo(CO)$_3$ (2.4 x 10^{-4}M) in cyclohexane.

solvent (s)	molar extinction coefficient ε (dm^3 mol^{-1} cm^{-1}) ($\pm$ 2%)
cyclohexane[a]	3060
cyclooctane	5175
n-pentane	3261
n-heptane	2467
n-decane	4053
n-dodecane	3481

Table 2.3.1.1. Extinction coefficient of (η^6-benzene)Cr(CO)$_3$ in various hydrocarbon solvents (s) at 355 nm. [a] reference 7.

solvent (s)	molar extinction coefficient ε ($dm^3\ mol^{-1}\ cm^{-1}$) ($\pm$ 2%)
cyclohexane	2908
n-heptane	3439
n-decane	6387

Table 2.3.1.2. Extinction coefficient of (η^6-1,3,5-mesitylene)$Mo(CO)_3$ in various hydrocarbon solvents (s) at 266 nm.

2.3.2 Primary photoproduct.

All the data available indicate that the primary photoproduct following flash photolysis of either chromium or molybdenum tricarbonyl results in the production of the 16 electron coordinatively unsaturated dicarbonyl intermediate as outlined in reaction 2.3.2.1. However it has been reported,[8] that generally in the presence of solvent, these 16 electron intermediates do not remain uncoordinated and the vacant site becomes occupied by a solvent molecule which previously been referred to as a 'token ligand' as indicated in reaction 2.3.2.2. and 2.3.2.2.

$$(\eta^6\text{-arene})M(CO)_3 \xrightarrow{h\nu} (\eta^6\text{-arene})M(CO)_2 + CO \qquad (2.3.2.1)$$

$$(\eta^6\text{-arene})M(CO)_2 + s \longrightarrow (\eta^6\text{-arene})M(CO)_2(s) \qquad (2.3.2.2)$$

No measurements on the rate of solvent recombination with the coordinatively unsaturated arene dicarbonyl have been reported. Studies have been carried out with $Cr(CO)_6$ where the recombination of the 16 electron intermediate with cyclohexane occurs in less than 1 ps.[11] Presumably the systems being investigated here under go solvent recombination on a similar time scale. A typical transient signal for recombination of the solvated chromium dicarbonyl intermediate with CO is shown in Fig 2.3.2.1. The transient is composed of two parts, firstly the rise time during which the solvent interaction to the metal centre occurs. This rate cannot be measured with the experimental set-up used in these experiments as only a nanosecond time base is available.

The second part of the transient corresponds to the displacement of solvent by a CO ligand, hence rate of this decay provides the second order rate constant for reaction of the solvated intermediate with CO to regenerate parent. In the case of the Mo system the rate of recovery of parent depletion was used to provide rate data and a typical transient for this reaction is given in Figure 2.2.2.2.

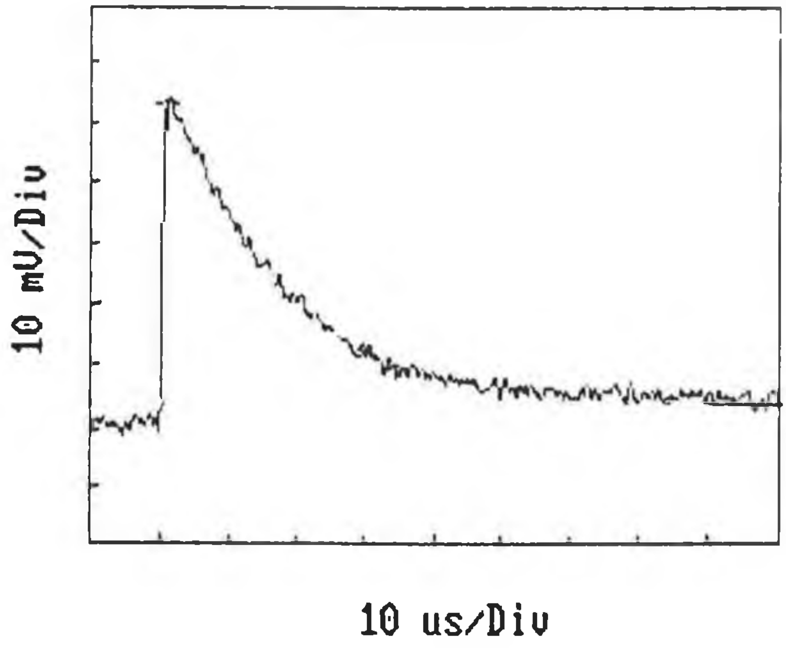

Figure 2.3.2.1 A typical transient spectrum of the rate of decay of (η^6-benzene)$Cr(CO)_2$(s).

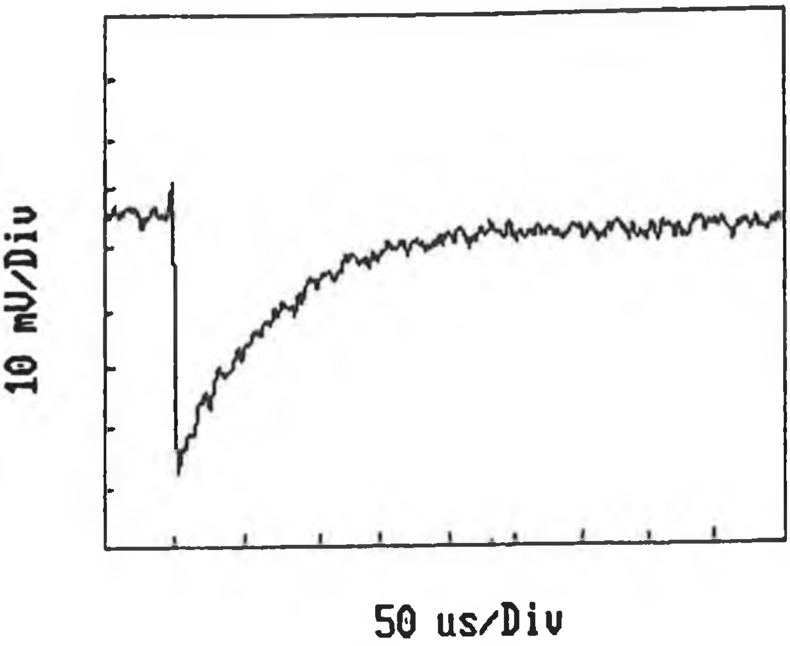

Figure 2.3.2.2 A typical transient spectrum for the recovery of (η^6-1,3,5-mesitylene)$Mo(CO)_3$.

UV/vis. difference spectra were constructed 'point by point' following flash photolysis in each solvent for (η^6-benzene)Cr(CO)$_3$. With all straight chain hydrocarbon solvents a $\lambda_{max.}$ was found at 280 ± 5 nm and hence this was used as the monitoring wavelength for all solvents. Because $\lambda_{max.}$ for this system is similar in all solvents it is indicative of a similar interaction energy for the solvated transition state. With cyclooctane the rate of recovery of tricarbonyl was measured as opposed to the decay of the transient species as the solvent absorbs up to approximately 280 nm. Again the yield of the photoproduct is unaffected by CO concentration thereby indicating presence of a primary photoproduct. As regards the molybdenum system the rate of recovery of parent was measured, because the decay of the transient dicarbonyl species occurs at 270 nm and this wavelength is too close to the laser line to yield reliable data, hence the monitoring wavelength used was 330 nm for all arene molybdenum compounds.

In this study the reaction rate of the solvated dicarbonyl intermediate towards CO was measured from pseudo first order plots of the observed rate constant *versus* the concentration of CO. The data obtained is tabulated in Appendix A (Tables A13 to A20) and illustrated graphically in Figure 2.3.2.3. Second order rate constants for each solvent are presented in Tables 2.3.2.1, 2.3.2.2 and 2.3.2.3 along with the solubility of CO at 298 K in each solvent. The rate of decay of the solvated species can be considered as a measure of the ease of displacement of the solvent molecule and hence consequently a measure of the metal to solvent interaction.

solvent (s)	k_2 x 10^{-6} $dm^3mol^{-1}s^{-1}$ (± 10%)	solubility of CO at 1 atm (x 10^2 M) (± 5%)
cyclohexane [a]	9.8	0.9
cyclo-octane	64.3	0.63
n-pentane	13	1.6
n-heptane	23	1.2
n-decane	28	0.85
n-dodecane	34	0.68

Table 2.3.2.1 Second order rate constants for the reaction of (η^6-benzene)$Cr(CO)_2$(s)with CO to regenerate tricarbonyl, data taken from reference 7.

solvent (s)	k_2 x 10^{-6} $dm^3mol^{-1}s^{-1}$ (± 10%)	solubility of CO at 1 atm (x 10^2 M) (± 5%)
cyclohexane	59	0.9
n-heptane	110	1.2

Table 2.3.2.2 Second order rate constants for the reaction of (η^6-hexaethylbenzene)$Cr(CO)_2$(s) with CO to regenerate tricarbonyl.

solvent (s)	k_2 x 10^{-6} $dm^3mol^{-1}s^{-1}$ (± 10%)	solubility of CO at 1 atm (x 10^2 M) (± 5%)
cyclohexane	1.56	0.9
n-heptane	1.96	1.2
n-decane	2.50	0.85

Table 2.3.2.3 Second order rate constants for the rate of reaction of (η^6-1,3,5-mesitylene)$Mo(CO)_2$(s) with CO to regenerate tricarbonyl.

From results outlined in Table 2.3.2.1 it is noticeable that as the carbon chain length of the solvent increases, an increase in second order rate constant is also observable, thus indicating that n-dodecane is displaced at a greater rate than *n*-pentane by the incoming ligand CO. The second order rate constants for the recombination of (η^6-benzene)$Cr(CO)_2(s)$ with CO in *n*-heptane and *n*-dodecane are approximately 2 and 3 times that respectively in cyclohexane. Just as in the case of $Cr(CO)_5(s)$[33] and $CpMn(CO)_2(s)$[14] second order rate constants are greater in n-heptane than in cyclohexane, suggesting that n-heptane may coordinate more weakly to the metal centres. The rate constant for the reaction of (η^6-hexaethylbenzene)$Cr(CO)_2(s)$ with CO in n-heptane is more than four times greater than that for the corresponding reaction of the benzene derivative (see Table 2.3.2.2). This is consistent with the results obtained for the (η^5-C_5H_5)$Mn(CO)_2(s)$and (η^5-C_5Et_5)$Mn(CO)_2(s)$ system.[12]

Possible explanations for this variation in second order rate constants have been suggested for the $Cr(CO)_5$ system.[13] The exact binding of solvent may differ from cyclohexane to the straight chain hydrocarbons. With cyclohexane there are only methylene hydrogens available for binding to the vacant site at the metal unlike the straight chain hydrocarbons which have both methyl and methylene hydrogens. Incidently these hydrocarbons are proposed to bind through agostic bonds with the metal centre. Agostic interactions are composed of 2 electron three centred bonds.[34] It has been suggested that methylene hydrogens may be more electron rich than methyl CH bonding hydrogens.

The reactivity of (η^6-1,3,5-mesitylene)$Mo(CO)_2(s)$ towards CO was examined in;- cyclohexane, *n*-heptane and *n*-decane (see Table 2.3.2.3). In comparison to the Cr system the results obtained for the equivalent reaction for the Mo compound were quite different, however this solvent study was not as extensive as that described above for (η^6-benzene)$Cr(CO)_3$. The second order rate constants indicate that the reaction of the solvated species towards CO does not appear to be sensitive to the nature of the solvent as there is effectively no variation in second order rate constant unlike the Cr analogue. Presently the reactivity of $Mo(CO)_5(s)$ is being investigated in a number of solvents and it appears from theses studies that there is not a significant increase in rate constant as the hydrocarbon chain length increases unlike $Cr(CO)_5(s)$ where the second order rate constant increases 5 fold on changing the solvent from n-pentane to n-dodecane.[34]

2.3.3 Activation Parameter study for the displacement of solvent in (η^6-arene)M($CO)_2$(solvent) by CO.

Activation parameters were measured with the hope of a gaining a greater understanding of the reaction mechanism involved in these two systems. Results are outlined in Tables 2.3.3.1 and 2.3.3.2 and illustrated graphically in Figures 2.3.3.1 and 2.3.3.2 (data used for these plots is tabulated in Appendix B). In the Mo system formation of dinuclear species is not fully suppressed under 1 atm. CO (9.0×10^{-3}M) as explained in the previous section, hence activation parameters were calculated by plotting k_{obs} *versus* concentration of CO at different temperatures and the slope of this line generates the second order rate constant (k_2) which was used in these calculations.

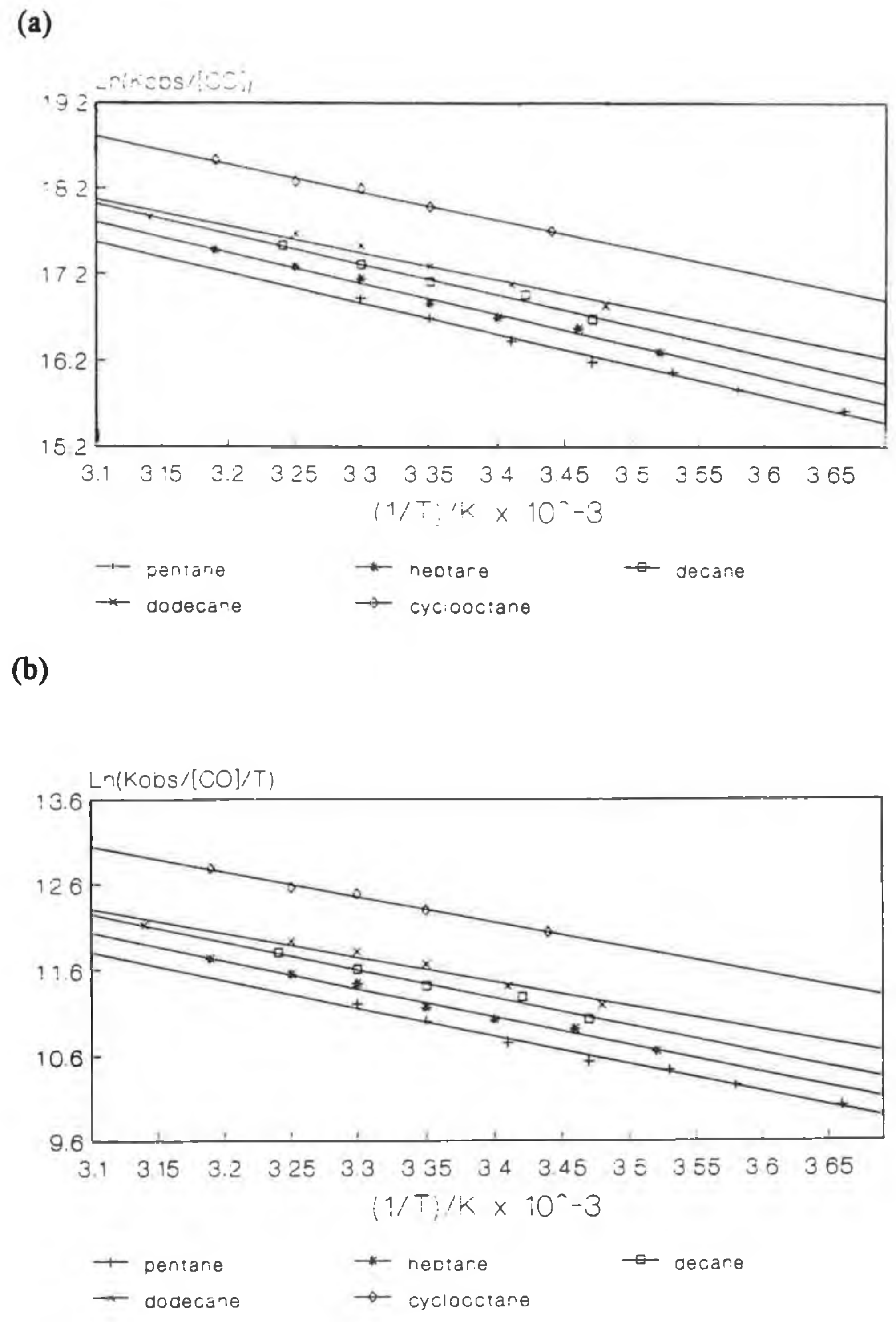

Figure 2.3.3.1. (a) Arrhenius and (b) Eyring plots for the reaction of (η^6-benzene)Cr(CO)$_2$(s) towards CO, in hydrocarbon solvents monitored at 280 nm (straight chain hydrocarbon solvents) and at 330 nm (cyclooctane) in the temperature range 288-313 K.

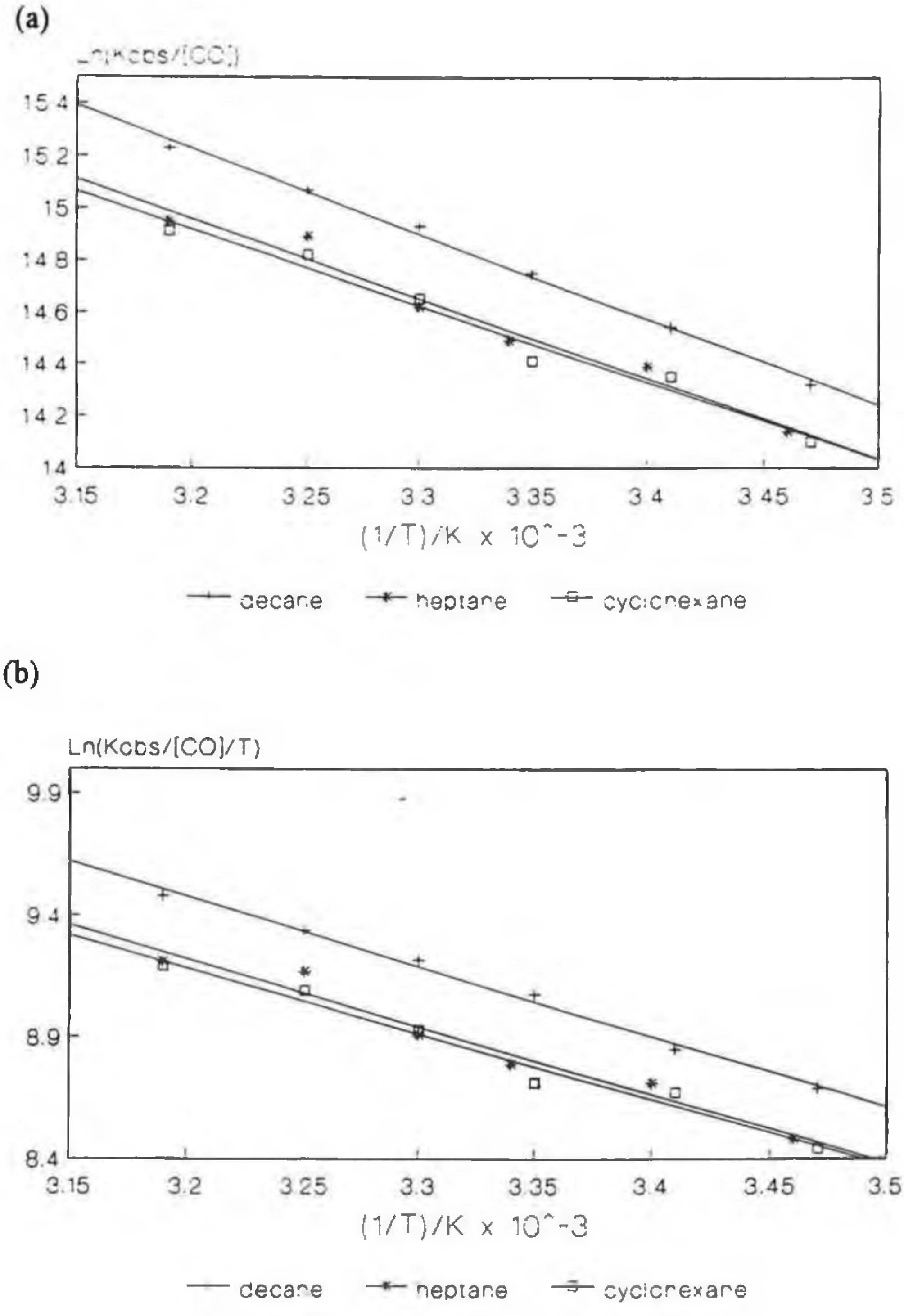

Figure 2.3.3.2 (a) Arrhenius and (b) Eyring plots for the reaction of (η^6-1,3,5-mesitylene)Mo(CO)$_2$(s) towards CO, in hydrocarbon solvents monitored at 330 nm in the temperature range 288-313 K.

solvent (s)	$\Delta H^{\neq}$ $kJmol^{-1}$ ($\pm$ 2kJmol^{-1})	$\Delta S^{\neq}$ $Jmol^{-1}K^{-1}$ ($\pm$ 5Jmol^{-1})	$\Delta G^{\neq}_{(298\ K)}$ $kJmol^{-1}$ ($\pm$ 2kJmol^{-1})
cyclohexane [a]	22	-37	33
cyclooctane	24	-13	28
n-pentane	24	-18	29
n-heptane	26	-16	31
n-decane	26	-12	29
n-dodecane	26	-10	29

Table 2.3.3.1 Activation parameters for the reaction of (η^6-benzene)Cr(CO)$_2$(s) with CO to regenerate parent. [a] data taken from reference 7.

solvent (s)	$\Delta H^{\neq}$ $kJmol^{-1}$ ($\pm$ 2kJmol^{-1})	$\Delta S^{\neq}$ $Jmol^{-1}K^{-1}$ ($\pm$ 5Jmol^{-1})	$\Delta G^{\neq}_{(298K)}$ $kJmol^{-1}$ ($\pm$ 2kJmol^{-1})
cyclohexane	23	-46	37
n-heptane	23	-46	37
n-decane	25	-39	36

Table 2.3.3.2 Activation parameters for the reaction of (η^6-1,3,5-mesitylene)Mo(CO)$_2$(s) with CO to regenerate parent.

From Table 2.3.3.1 it is noticeable that there is effectively no change in enthalpy value $\Delta H^{\neq}$ on varying the solvent medium where an average enthalpy value of 24 $\pm$ 2 kJmol^{-1} is measured for reaction of (η^6-benzene)Cr(CO)$_2$(s) towards CO. Time resolved photocalorimetric studies have shown that *n*-pentane, *n*-heptane and cyclohexane bind to the coordinatively unsaturated Cr(CO)$_5$ fragment with an interaction energy of 37, 40 and 52 kJmol^{-1} respectively.[13] This interaction energy difference was prosposed to explain the apparent difference in rate constants for cyclic as opposed to linear alkanes. The interaction enthalpies determined by Burkey *et al.*[13] are considerably greater than the activation values obtained in this study. Consequent to this, the interaction of $Cr(CO)_5$ was again investigated in a number of hydrocarbon solvents using UV/vis. flash photolysis. This time the results obtained were not in agreement with those published by Burkey and coworkers[13] as now an activation enthalpy value of 20 ± 4 $kJmol^{-1}$ was calculated for the interaction of solvent (solvents used;- cyclohexane, *n*-pentane, *n*-heptane, *n*-decane and *n*-dodecane) to the vacant coordination site.[24] This value is in closer agreement to the values measured here.

From this study it can be proposed that it is not a variation in activation enthalpy but rather a variation in the entropy term of free energy of activation that alters the rate of reaction of $(\eta^6$-benzene$)Cr(CO)_2(s)$ towards CO. In view of these results (Table 2.3.3.1) it would suggest that it is the increased freedom of the alkane fragment that dominates the entropy term. In the case of *n*-pentane there is less freedom of motion present in the transition state compared to that in *n*-dodecane. Also, there appears to be a linear relationship between the entropy term $\Delta S^{\neq}$ and the carbon chain length for linear alkanes.

The results in Table 2.3.3.2 signify that there is no variation in enthalpy value for the reaction of $(\eta^6$-1,3,5-mesitylene$)Mo(CO)_2(s)$ with CO as $\Delta H^{\neq}$ of 23 ± 1 $kJmol^{-1}$ was measured. The enthalpy value calculated here compares well with that of the of $(\eta^6$-benzene$)Cr(CO)_2(s)$. The entropy of activation for $(\eta^6$-1,3,5-mesitylene$)Mo(CO)_2(s)$ is slightly more negative with a $\Delta S^{\neq}$ of -39$Jmol^{-1}K^{-1}$ as opposed to -12 $Jmol^{-1}K^{-1}$ for the analogous reaction of $(\eta^6$-benzene$)Cr(CO)_2(s)$ in *n*-decane. With the Mo system there is effectively no variation in $\Delta S^{\neq}$ on varying the hydrocarbon solvent in contrast to Cr. Admittedly there are less solvents used in the Mo study but as there is no variation in second order rate constant it was decided not to further the number of solvent experiments. These results indicate that the transition state in Mo does not appear to be sensitive to the nature of the solvent in question and this is quite surprising in light of the experiments previously carried out with Cr. The Mo metal has a considerably greater atomic radius than Cr being 1.29 and 1.17 Å respectively, presumably this plays a significant part in the observed difference in the reactivity of these two systems. It is known that metals other than first row can exist with a formal coordination number of seven hence is it possible that this is what is occurring here.

Entropy values can be used to determine that overall mechanism for a reaction being associative, dissociative or interchange. The entropy values measured in this study for (η^6-benzene)Cr(CO)$_2$(s) would suggest that solvent displacement by ligand occurs through an interchange mechanism. For an interchange mechanism to occur, the CO ligand coordinates to the solvated dicarbonyl species as the solvent is being displaced as indicated in Figure 2.3.3.3. An interchange mechanism for solvent displacement in M(CO)$_5$(s) has previously been reported by Dobson *et al.*[35]

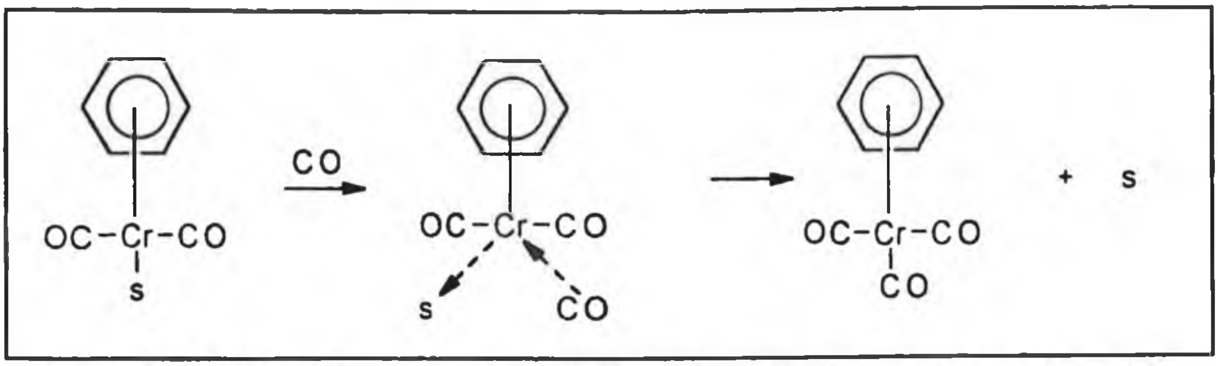

Figure 2.3.3.3 Interchange mechanism for solvent displacement by CO in (η^6-benzene)Cr(CO)$_2$(s).

The larger negative term for activation entropy ($\Delta S^{\neq}$) for (η^6-mesitylene)Mo(CO)$_2$(s) indicates a transition state with more bond making hence, it appears that the larger Mo as a metal centre has available to it an associative type pathway that the smaller Cr does not. These results give rise to the possibility of an associative mechanism being responsible for recombination of CO ligand (see figure 2.3.3.4.). Generally on going from Cr to Mo to W reactions become more ordered and from the results gathered in this study one would suggest that this is occurring.

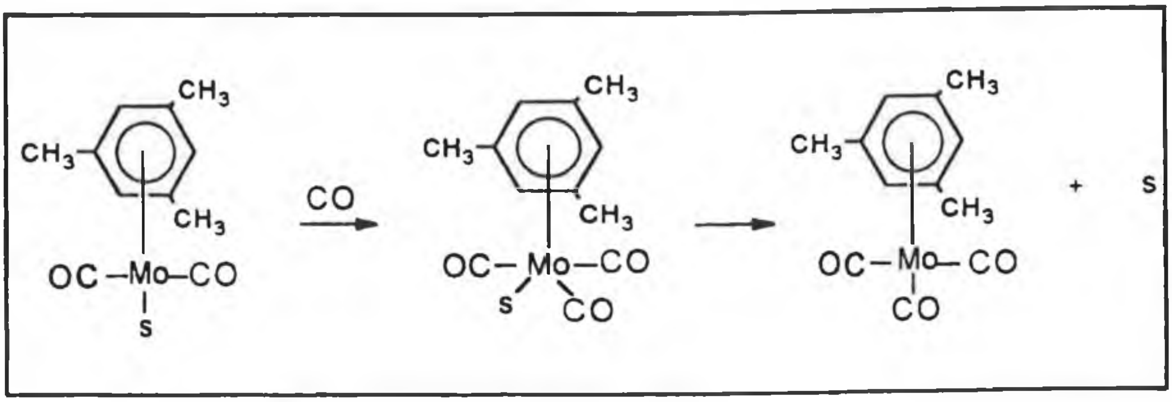

Figure 2.3.3.4 Associative mechanism for the solvent displacement by CO in (η^6-1,3,5-mesitylene)Mo(CO)$_2$(s).

2.4 Photolysis of (η^6-benzene)$Cr(CO)_3$ using fluorinated solvents.

Reports on the photochemistry of $Cr(CO)_6$ in perfluoromethylcyclohexane have indicated that the pentacarbonyl species produced following irradiation reacts with CO with a second order rate constant of 3×10^9 mol^{-1}dm^{3}s^{-1}.[23] This increased rate constant is some three orders of magnitude greater than the corresponding reaction in cyclohexane.[36] Previous to this, matrix isolation studies had indicated that interaction of the pentacarbonyl species with perfluoromethane ($\lambda_{max.}$ 547 nm) is weak in comparison to a CH_4 matrix ($\lambda_{max.}$ 489 nm).[31] As a result of the work carried out previously in hydrocarbon solvents (Section 2.3.3) it was decided to extent this 'solvent' investigation to incorporate fluorinated solvents and to compare results from this study with that already carried out on the $Cr(CO)_5$ system.

2.4.1 Electronic absorption spectrum.

The electronic absorption spectrum of (η^6-benzene)$Cr(CO)_3$ in fluorinated solvent is similar to that in alkane solvent and has previously been described in section 2.2.1.

2.4.2 Results and Discussion.

Solutions of (η^6-benzene)$Cr(CO)_3$ in perfluoromethylcyclohexane under 1 atm CO (9.0×10^{-3}M) were irradiated with $\lambda > 345$ nm, and within a short time duration (in the order of seconds) the UV/vis. spectrum of the tricarbonyl compound had significantly varied as is evident from Figure 2.4.2.1. The band at 315 nm decays away while the band at 235 and 285 nm are formed. Three isosbestic points at 256, 278 and 290 nm were maintained throughout the course of the reaction, indicating that the reaction proceeds uncomplicated by side or subsequent reactions.

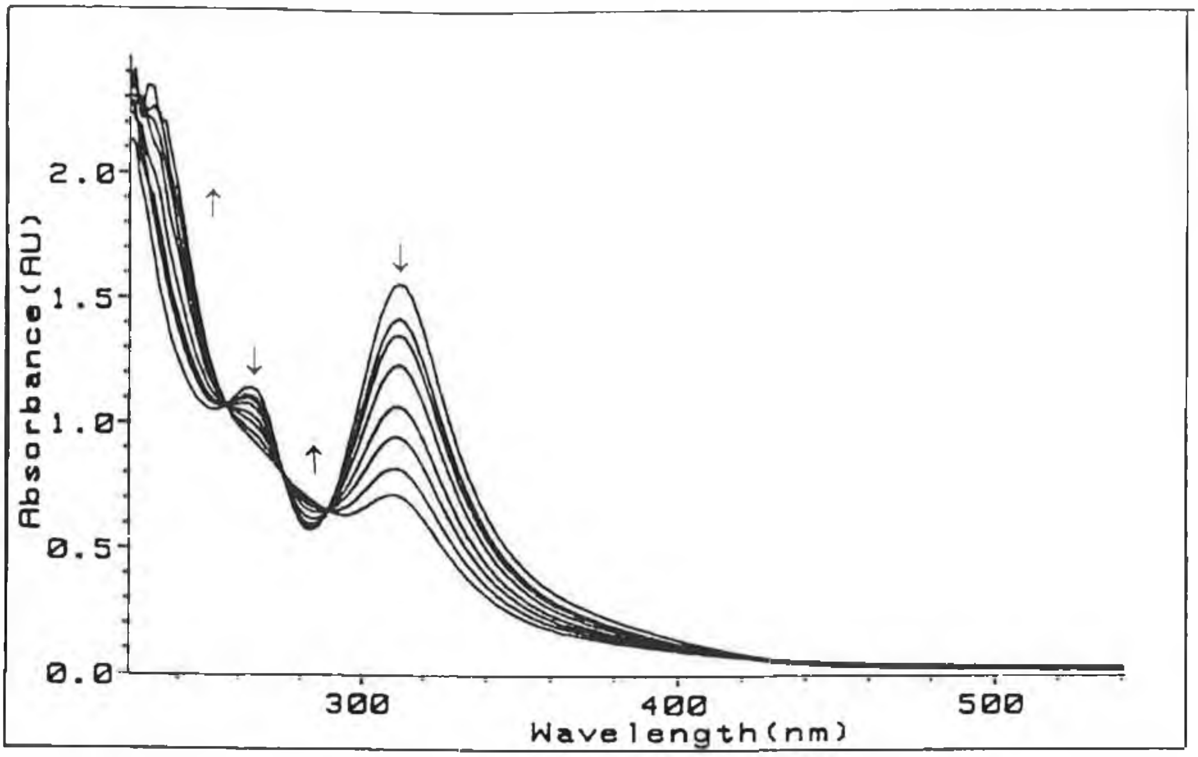

Figure 2.4.2.1. The differences observed following irradiation of (η^6-benzene)$Cr(CO)_3$ in perfluoromethylcyclohexane under 1 atm. of CO at $\lambda > 345$ nm.

At the end of the irradiation time an infrared spectrum of this sample was measured and only one band was observed at 1987 cm^{-1} which indicates formation of $Cr(CO)_6$. In the UV/vis. a band is seen to grow-in at 285 nm and presumably this indicates formation of the 280 nm band of $Cr(CO)_6$. During the irradiation time a band is also is seen to grow in at about 235 nm and $\lambda_{max.}$ for $Cr(CO)_6$ occurs in this region.

Following these results it was decided to carry a analogous experiment in another fluorinated solvent, 1,1,2 trichlorotrifluoroethane(tcfe). Similar results were observed when the sample was irradiated at λ > 345 nm as is observable from Figure 2.4.2.2. At the end of the experiment an infrared spectrum indicated the presence of $Cr(CO)_6$, see Figure 2.4.2.3. Flash photolysis studies were carried out with (η^6-benzene)$Cr(CO)_3$ under 1 atm. of CO in tcfe, the only transient species observed was that of a 'step-form' which occurred at 280 nm (Figure 2.4.2.4), and a corresponding depletion at 330 nm. An NMR experiment was conducted under 1atm CO using acetone-*d* as the external deuterated source (the sample was prepared in a similar manner to those for laser experiments). The NMR tube was irradiated at λ > 345 nm and the presence of benzene was evident within seconds with a chemical shift of 2.1 ppm for the signal of uncomplexed benzene at 6.3 ppm as opposed to the complexed benzene ligand which has a resonance at 4.2 ppm, as shown in Figure 2.4.2.3.

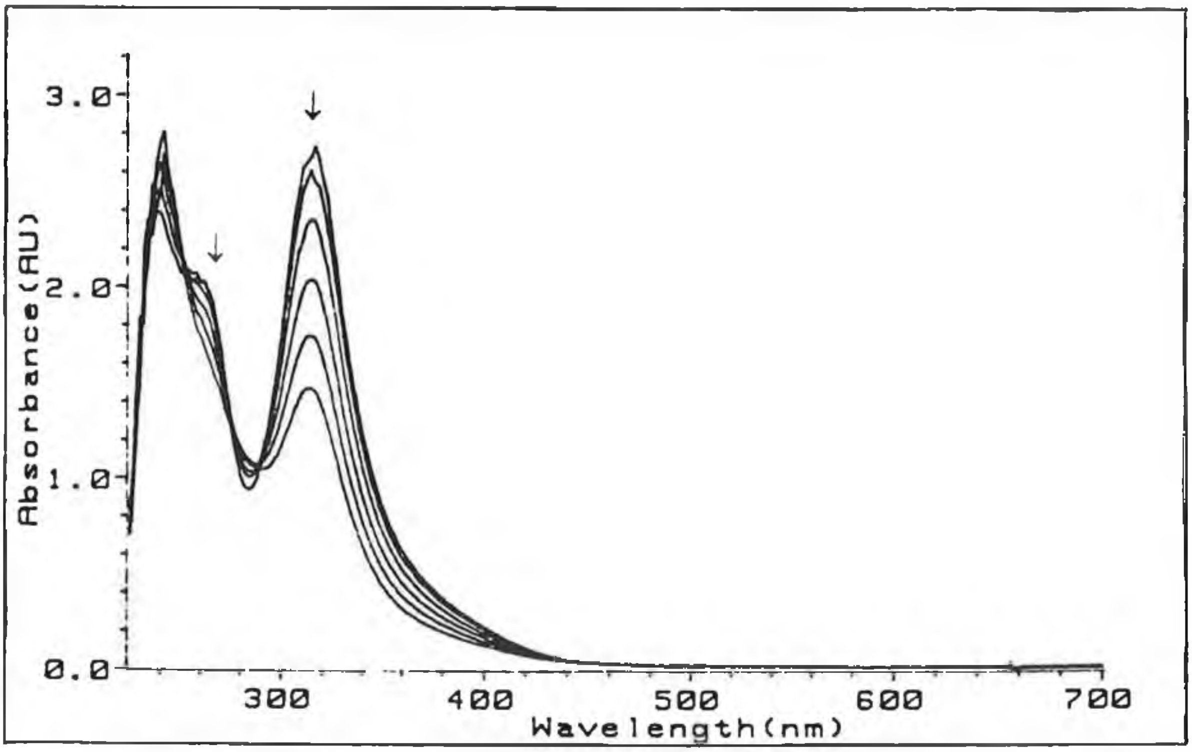

Figure 2.4.2.2 Differences in the UV/vis. spectrum of (η^6-benzene)$Cr(CO)_3$ observed upon irradiation (λ > 345 nm) in 1,1,2 trichlorotrifluoroethane under 1 atm. of CO.

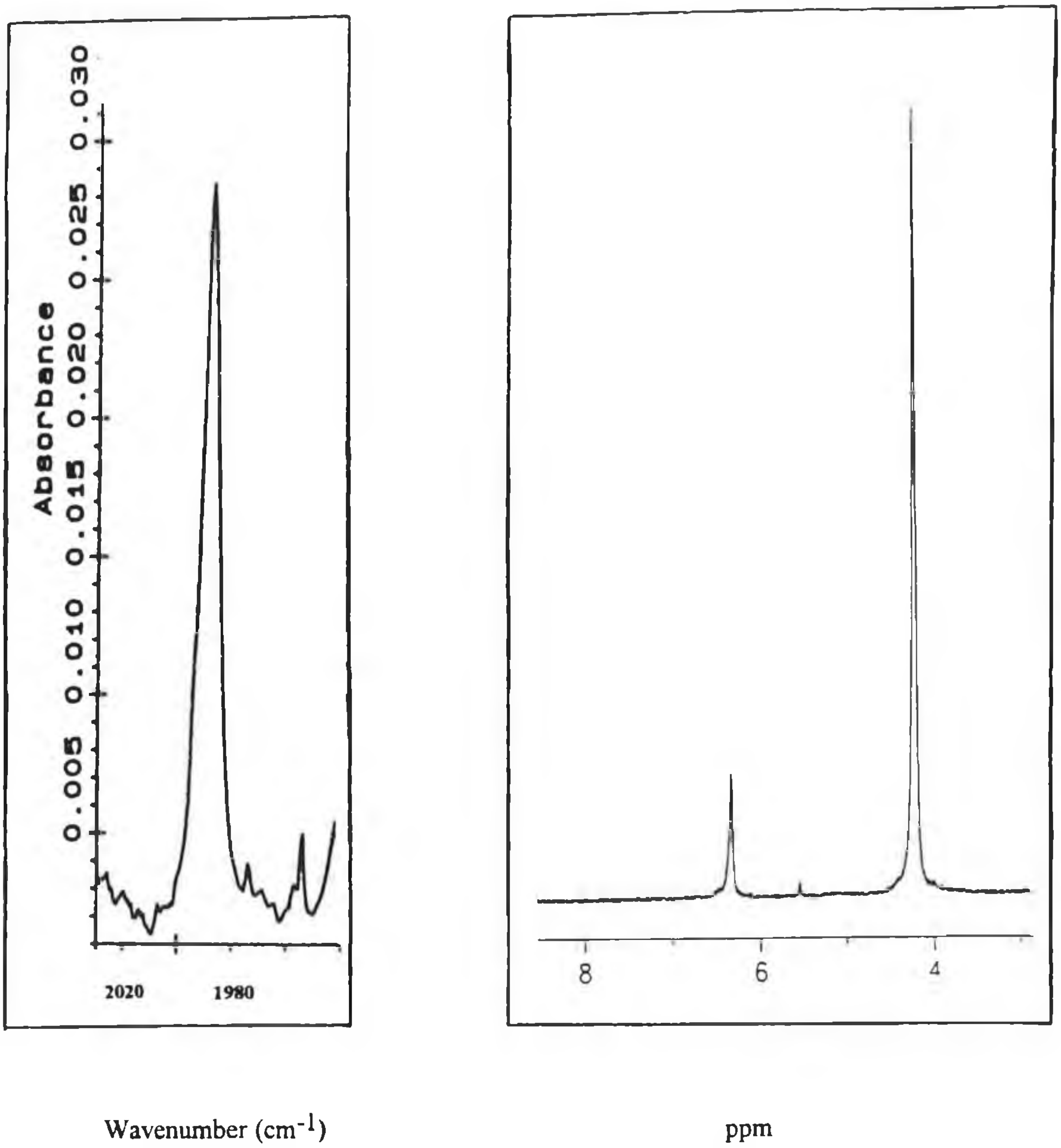

(a) (b)

Figure 2.4.2.3. The infrared(a) and ^{1}H NMR(b) spectrum following irradiation ($\lambda > 345$ nm) of (η^6-benzene)Cr(CO)$_3$ in 1,1,2 trichlorotrifluoroethane under 1 atm. of CO.

(a)

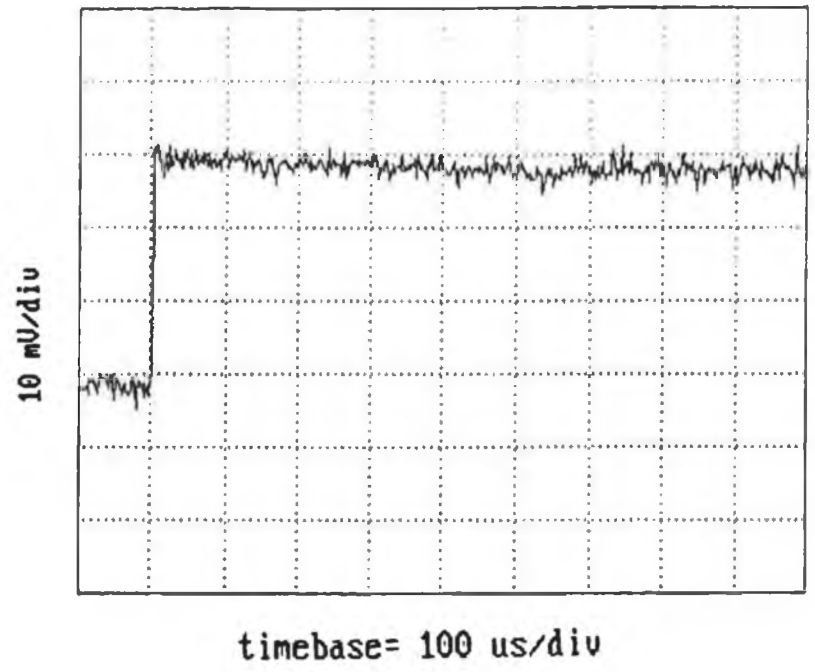

(b)

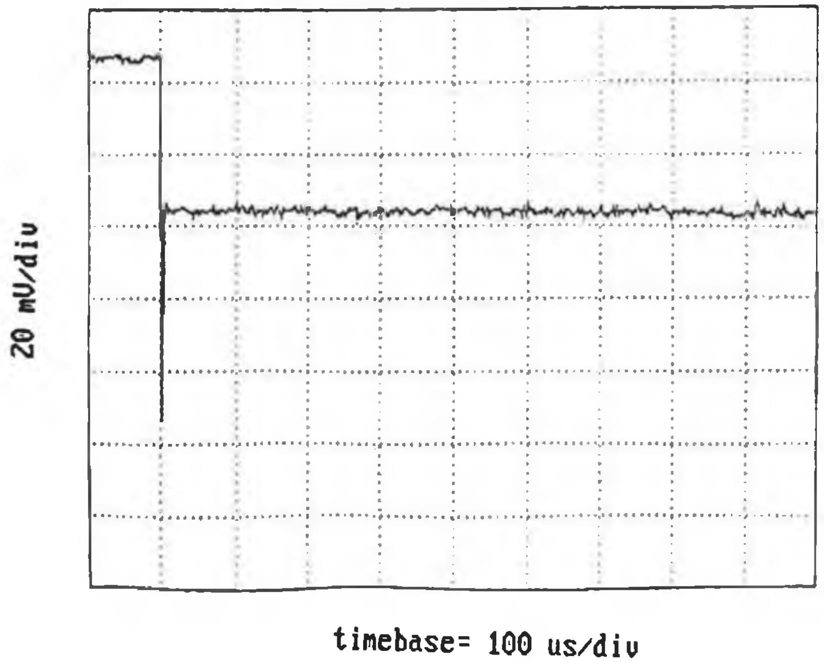

Figure 2.4.2.4. Typical transients following 355 nm flash photolysis of (η^6-benzene)Cr(CO)$_3$ in 1,1,2 trichlorotrifluoroethane at (a) 280 nm and at (b) 320 nm under 1 atm. of CO.

One explanation for this difference in photochemistry in fluorinated solvents *versus* hydrocarbon solvents may be explained by the difference in vibrational relaxation times which were investigated for M(CO)$_6$ (where M = Cr, Mo or W) in a variety of solvents by Heilwell *et al.*[37] The vibrational relaxation times differed significantly depending on the solvent, insofar as the relaxation time in carbon tetrachloride (T1 = 440 + 70 ps) is almost three times greater than that in hexane (T1 = 145 + 25ps). It is possible that the difference in relaxation times may be able to explain the differences that result on varying the solvent medium. With hydrocarbon solvents relaxation times are considered to be efficient, hence an interaction between solvent and vacant coordination site on the metal centre occurs which results in reaction of the solvated species with CO. However on moving to a fluorinated solvent (this is assuming that vibrational relaxation times are similar in fluorinated solvents to those in chlorinated solvents) there is less efficient relaxation of vibrational levels hence a further reaction is observed. Presumably this accounts for our observation of Cr(CO)$_6$ and uncomplexed benzene at the end of the experiment.

In this study it may be possible that two photolysis pathways exist , firstly - cleavage of the metal to arene bond may be occur resulting in a tricarbonyl fragment which rapidly combines with CO to yield the hexacarbonyl product. Secondly, CO loss to yield the dicarbonyl intermediate but as Cr(CO)$_6$ absorbs at 280 nm it may be masking formation of this species (see Scheme 2.4.2.1). At 330 nm where depletion of parent is observable no recovery of parent is evident. Previously, the generation of Cr(CO)$_6$ has been reported by Wang *et al.*[38] following irradiation of (η^6-benzene)Cr(CO)$_3$ in gas-phase experiments, hence, is it possible that the experiments carried out in this study in fluorinated solvents are more akin to gas phase studies than those in other solvents where an interaction with the solvent medium occurs.

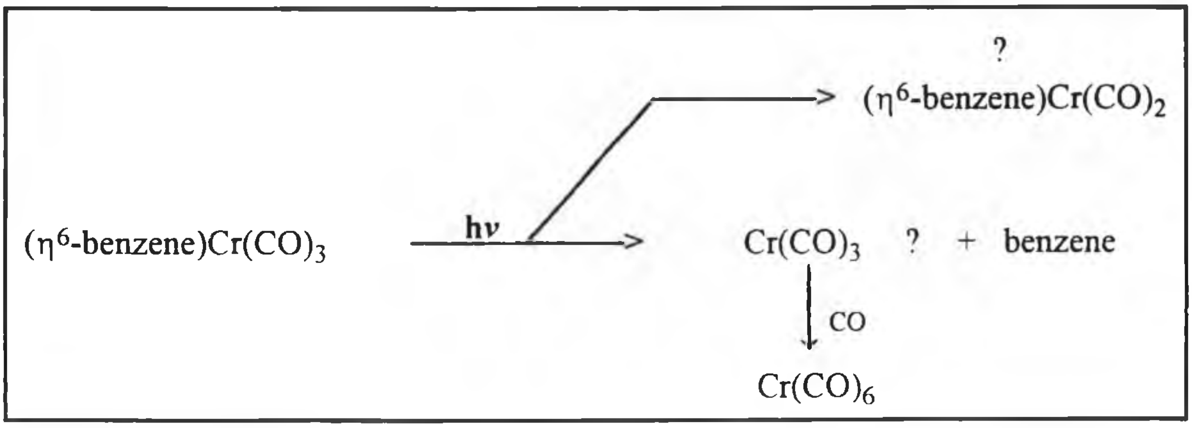

Scheme 2.4.2.1

2.5 Conclusion.

This study demonstrated that the rate of reaction of the solvated dicarbonyl intermediate in the case of chromium was affected by varying the arene ligand or the alkane solvent. As the number of electron donating substituents on the aromatic ring increased there was a corresponding increase in the second order rate constant, however it was only for the highly substituted arenes for *e.g.* hexaethylbenzene that a pronounced increase was determined. In the case of the molybdenum compounds no significant increase in the rate of reaction of the solvated dicarbonyl intermediate towards CO was measured regardless of the number of electron donating substituents on the aromatic ring or by varying the nature of the solvent.

In a recent publication by Ford *et al.*[39] flash photolysis studies were carried out on $CF_3Mn(CO)_5$ and the behaviour of this compound proved to be similar to that of the methyl complex in cyclohexane in so far as CO loss is the principal photoreaction. The one notable difference however is that backreaction of $CF_3Mn(CO)_4(s)$ with CO is about a factor of 30 less than that determined for the methyl derivative. These results are in agreement with those obtained in this study for the chromium system where the nature of the alkyl substituent was varied.

Activation parameters were determined for both systems. Activation enthalpies were very similar for all $(\eta^6\text{-arene})Cr(CO)_3$ compounds, but entropy values became less negative as the second order rate constant (k_2) increased. This observed increase in second order rate constant is thought to be entropic in origin. This difference was further explained by varying the nature of the alkane solvent. As the hydrocarbon chain length increased a corresponding increase in k_2 occurred along with an increase in activation entropy. Hence, this variation in reactivity of $(\eta^6\text{-arene})Cr(CO)_2(s)$ towards CO is explained by a change in entropy of activation and not by a variation in activation enthalpy between the coordinatively unsaturated photofragment and solvent.

On conducting experiments on the three molybdenum compounds, all k_2 values were identical within experimental error of being equivalent. Also activation enthalpies were identical regardless of the arene ligand or the hydrocarbon solvent, as were activation entropies. The one noticeable difference with this system is that activation entropies are more negative than for the corresponding chromium compounds, thereby indicating an associative path in which there is a predominance of bond making in the transition sate involving the formation of a seven coordinated activation complex. In the chromium system solvent loss is proposed to occur concomitantly to CO bond formation consequently a interchange mechanism is suggested.

Studies of ligand displacement reactions of $Cr(CO)_5(L)$ complexes have generally shown that a dissociative mechanism exists for chromium.[40] For group 6 metal complexes volumes of activation for CO displacement reactions in general are known to decrease from Cr to Mo and W. This decrease in volumes of activation was attributed to a gradual changeover from a more dissociative mechanism for smaller chromium to a more associative type mechanism for large Mo and W metal centres.[41,42] There is much evidence that volumes of activation may be a better indicator of mechanism than entropies of activation are in ligand exchange reactions involving octahedral complexes, particularly where the latter are close to zero.[43] On the basis of activation entropies measured in this study, it may be concluded that solvent displacement takes place by different mechanistic pathways for Cr *versus* Mo. This difference may result from the larger atomic radius for Mo (by ca. 0.15 Å) than for chromium.[44]

The quantum yield for $Cr(CO)_6$ with piperidine (Reaction 2.5.1) as entering ligand was determined by Wieland and van Eldik in a number of solvents ranging from *n*-pentane (0.72), *n*-dodecane (0.58) to perfluorohexane (0.47).[45]

$$M(CO)_5(s) \quad + \quad \text{piperidine} \longrightarrow M(CO)_5(\text{piperidine}) \quad + \quad s \qquad (2.5.1)$$

With increasing hydrocarbon chain length the quantum yield decreased with a more pronounced decrease in quantum yield with perfluorohexane. Quantum yields were determined for $Cr(CO)_6$(0.72), $Mo(CO)_6$ (0.93) and $W(CO)_6$ (0.79) using pyridine as entering ligand. with $Mo(CO)_6$ resulting in more efficient CO loss. The quantum yield for ligand substitution was found not to depend on the entering ligand or its concentration, but on the nature of the solvent. A direct correlation with the viscosity of the solvent was not found to exist.[46] In this study the quantum yield for (η^6-benzene)$Mo(CO)_3$ was found to be remarkably less than that for (η^6-benzene)$Cr(CO)_3$ in comparison to the hexacarbonyl system.

From the fluorinated solvent study it appears that by changing the nature of the solvent it is possible to *direct* the photochemistry. As yet further studies must be conducted in this area, but all results indicate that upon photolysis ($\lambda >$ 345 nm), uncomplexed benzene along with $Cr(CO)_6$ is produced. These results are in contrast to all other investigations conducted on (η^6-benzene)$Cr(CO)_3$, where the only reported photochemical reaction is loss if CO.

2.6 References

1 Geoffroy,G.C.;Wrighton,M.S.; *Organometallic Photochemistry*; Academic Press, New York, 1982.

2 Strohmeier,W.;von Hobe,D.; *Z. Naturforsch*; 1963,**18B**,770.

3 McGrath,I.M.; *Ph.D. Thesis*, Dublin City University; 1993.

4 Caroll,D.G.;McGlynn.S.P.; *Inorg. Chem.*;1968,**7**,1285.

5 Rest,A.J.;Sodeau,J.R.;Taylor,D.A.; *J.Chem.Soc., Dalton Trans.*; 1978,651.

6 Bitterwolf,T.E.;Lott,K.A.;Rest,A.J.;Mascetti,J.; *J. Organomet. Chem.*; 1991,**419**,113.

7 Creaven,B.S.;George,M.W.;Ginsburg,A.G.;Hughes,C.;Kelly,J.M.; Long,C.;McGrath,I.M.;Pryce,M.T.; *Organometallics*; 1993,**12**,3127.

8 Zhang,S.;Dobson.G.R.;*Organometallics*; 1992,**11**,2447.

9 Turner,J.J.; *Photoprocesses in Transition Metal Complexes, ,Biosystems and Other Molecules*; Kluwer Acamdemic Publishers, 1992.

10 Bonneau,R.;Kelly,J.M.; *J. Am. Chem. Soc.*; 1980,**102**,1220.

11 Simon,J.D.;Xie,X.; *J. Phy. Chem.*; 1986,**90**,6751.

12 Johnson,F.P.A.;George,M.W.;Bagratashvili,V.N.;Vereshchagina,L.N.; Poliakoff,M.; *J. Chem. Soc., Mendeleev Commun.*; 1991,263.

13 Morse,J.M.;Parker,G.H.;Burkey,T.J.; *Organomet*allics; 1989,**8**,2471.

14 Creaven,B.S.;Dixon,A.J.;Kelly,J.M.;Long,C.;Poliakoff,M.; *Organomet*etallics; 1987,**6**,2600.

15 Zhang,S.;Dobson,G.R.;Zang,V.;Bajaj,H.C.;van Eldik,R.; *Inorg. Chem.* 1990,**29**,3477.

16 Lyons,M.P.; *Ph.D. Thesis*, Dublin City University; 1993.

17 Lundquist,R.T.;Cais,M.; *J. Org. Chem.*; 1962,**27**,1167.

18 Braterman,P.S.; *Metal Carbonyl Spectra*: Academic Press; 1975.

19 Grevels,F.-W.;Russell,G.; Private communication.

20 Koshland,D.E.;Myers,S.E.;Chesick,J.P.; *Acta Cryst.*; 1977,**B33**,2013.

21 (a)Wrighton,M.S.;Haverty,J.L.; *Z. Naturforsch.*; 1975,**80B**,254.
(b)Gilbert,A.;Kelly,J.M.;Budzwait,M.;Koerner von Gustorf,E.; *Z. Naturforsch.*; 1976,**31B**,1091.
(c)Nasielski,J.;Denisoff,O.; *J. Organomet. Chem.*; 1975,**102**,65.

22 (a)Fog,P.G.T.;Gerrard.W.; *Solubility of Gases in Liquids*; Wiley:Chichester,U.K., 1990.
(b)Makranczy,J.;Begyery-Balog,K.;Rusz,L.;Patyi,L.; *Hung. J. Ind. Chem.*;1976,**4**,269.
(c)Gjaldbaek,J.C.; *Acta Chem. Scand.*; 1952,**6**,623.
(D)IUPAC *Solubility Data Series*; Pergamon Press: Oxford,U.K., 1990; Vol. 43.

23 Kelly,J.M.;Long,C.;Bonneau,R.; *J. Chem. Phys.*; 1983,**87**,3344.

24 Walsh,M.M.; *Ph.D. Thesis*, Dublin City University, 1993.

25 Howell,J.A.;Burkinshaw,P.M.; *Chem. Rev.*; 1983,**83**,557.

26 Meyer,T.L.;Caspar,J.V.; *Chem. Rev.* 1985,**85**,187.

27 Dixon,A.J.;Healy,M.A.;Hodges,P.M.;Moore,B.D.;Poliakoff,M.; Simpson,M.N.;Turner,J.J.;West,M.A.; *J. Chem. Soc. Faraday Trans.*; 1986,**2**,2083

28 Casey,C.P.;Sakaba,H.;Hazin,P.N.;Powell,D.R.; *J. Am. Chem. Soc.*; 1991,**113**,8165.

29 Reichart,C.;*Solvent Effects in Organic Chemistry*, Verlag Chemie: New York, 1979.

30 (a)Welch,J.A.;Peters,K.S.;Vaida,V.; *J. Phys. Chem.*; 1982,**86**,1941.
(b)Simon,J.D.;Peters,K.S.; *Chem. Phy. Lett.*; 1983,**98**,53.
(c)Simon,J.D.;Xie,X.; *J. Phys. Chem.*; 1987,**91**,5578.
(d)Wang,L.;Zhu,X.;Spears,K.G.; *J. Am. Chem. Soc.*; 1988,**110**,8695.
(e)Joly,A.G.;Nelson,K.A.; *J. Phys. Chem.*; 1989,**93**,2876.

31 Perutz,R.N.:Turner,J.J.: *J. Am. Chem.*; 1975,**97**.4791.

32 Simon,J.D.;Xie,X.; *J. Phy. Chem.*:1989,**93**.291.

33 Breheny,C.;Long,C.;Walsh,M.M.: manuscript in preparation.

34 (a)Brookhart,M.;Green,M.H.L.; *J. Organomet. Chem.*;1983,**250**,395.
(b)Brookhart,M.;Green,M.H.L.Wong,L.L.; *Prog. Inorg. Chem.*;1988,**36**,2.

35 (a)Dobson,G.R.;Zhang,S.; *J. Coord. Chem.*;1990,**21**,155.
(b)Zhang,S.;Zang,V.;Bajaj,H.C.;Dobson,G.R.;van Eldik,R.; *J. Organomet. Chem.*; 1990,**397**,279.

36 Kelly,J.M.;Bent,D.V.;Hermann.H.;Schlute-Frohlinde,D.K.;Koerner von Gustorf,E.; *J. Organomet. Chem.*; 1974,**69**,259.

37 Heilwell,E.J.;Cavanagh,R.R.;Stephenson,J.C.; *Chem. Phy. Lett.*; 1987,**134**,181.

38 Wang,W.;Jing,P.;Yanwei,L.;She,Y.;Fu,F-J.; *J. Phys.Chem.*, 1992,**96**,1278.

39 Boese,W.T.;Ford,P.C.; *Organometallics*; 1994,**13**,3525.

40 Darensbourg,D.J.; *Adv. Organomet. Chem.*;1982,**21**,113

41 Reddy,K.B.;Hoffmann,R.;Konya,G.;van Eldik,R.;Eyring,E.M.; *Organometallics*; 1992,**11**,2319.

42 Wieland,S.;van Eldik,R.; *Organometallics*; 1991,**10**,3110.

43 van Eldik,R.;Ed. *Inorganic High Pressure Chemistry: Kinetics and Mechanisms*; Elsevier: Amsterdam 1986.

44 (a)Cotton,F.A.;Darensbourg,D.J.;Ilsler,W.H.; *Inorg. Chem.*; 1981,**20**,578.
(b)Awad,H.H.;Dobson,C.B.;Dobson,G.R.;Leipoldt,J.G.;Schneider,K.;van Eldik,R.;Wood,H.E.; *Inorg. Chem.*; 1989,**28**,1654.

45 Wieland,S.;van Eldik,R.; *Coord. Chem. Rev.*; 1990,**97**,155.

46 Nasielski,J.;Colas,A.; *Inorg. Chem.*; 1978,**17**,237.

Chapter 3

Photolysis of (η^6-allylbenzene)Cr(CO)$_3$ and (η^6-tetrahydronaphthalene)Cr(CO)$_3$ with UV/visible and TRIR monitoring.

3.1 The photochemistry of (η^6-allylbenzene)$Cr(CO)_3$.

Few papers have been devoted to the formation of chelates in group 6 (η^6-arene)$Cr(CO)_3$ complexes in which the ligand is bonded to the metal either completely or partially through the carbon atoms. It is known from the literature[1] that chelate complexes of chromium dicarbonyl have only been isolated and characterised in cases where the double bond is separated from the aromatic ring by at least two CH_2 units. The general preparation of π-olefin complexes is shown in Reaction 3.1.1. The formation of chelate complexes for a series of manganese dicarbonyl complexes have been reported[2] with cyclopentadienylmethyl allyl ether used as ligand.[3,4] The structure of the manganese complex was confirmed by elemental analysis, IR, ^1H nmr and mass spectrometry.

In this study flash photolysis experiments were carried out on (η^6-allylbenzene)$Cr(CO)_3$. Previous work on this compound carried out by Nesmeyanov *et al.* [1,6] has indicated that continuous irradiation in ether results in degradation of compound.

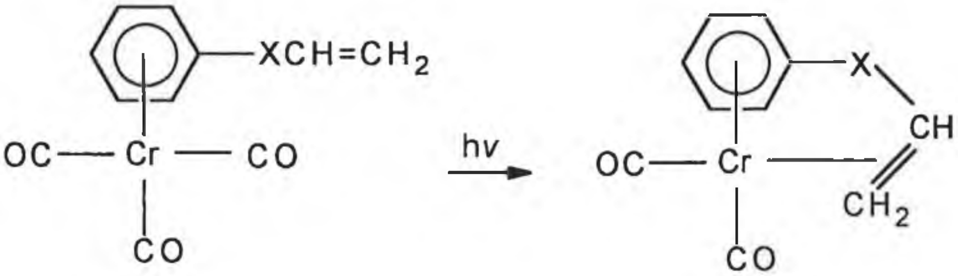

$X = CH_2CH_2,\ (CH_2)_3,\ (CH_2)_4$

Reaction 3.1.1

3.1.1 Electronic absorption spectrum of (η^6-allylbenzene)$Cr(CO)_3$.

The UV/vis. spectrum of (η^6-allylbenzene)$Cr(CO)_3$ is given in Figure 3.1.1.1 and the absorption spectrum of this compound is similar to that of any of the other tricarbonyls previously described in Section 2.1.1, where $\lambda_{max.}$ at 316 nm is assigned to a Cr ----> arene charge transfer transition with some Cr ----> π^* CO character.[5]

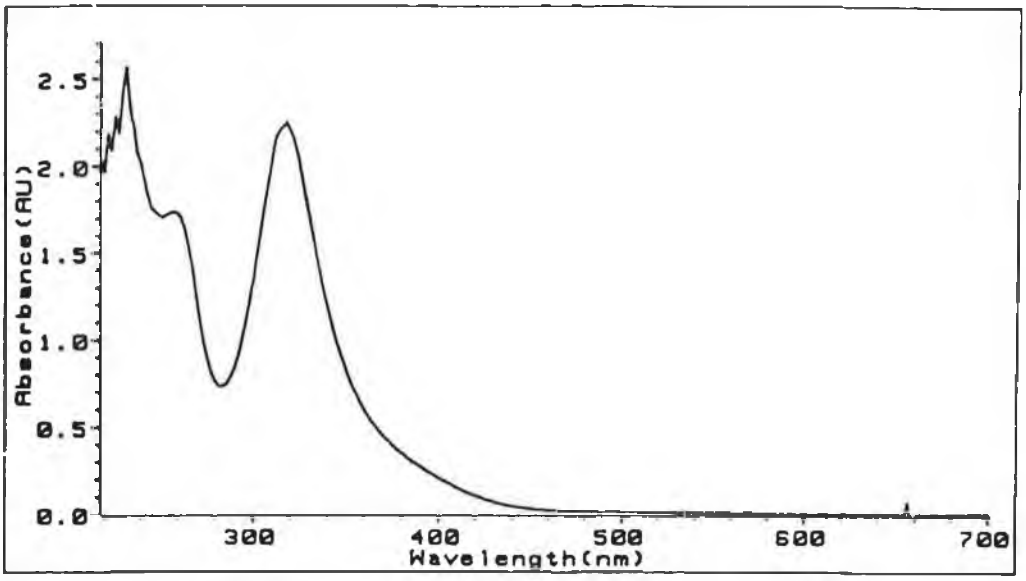

Figure 3.1.1.1 UV/vis. spectrum of (η^6-allylbenzene)Cr(CO)$_3$ in cyclohexane (2.9 x 10^{-4}M).

3.1.2 Photolysis studies.

3.1.2.1 Laser flash photolysis using UV/vis. detection.

Following laser flash photolysis of (η^6-allylbenzene)Cr(CO)$_3$ in cyclohexane under 1 atm. of CO at 355 nm excitation (ε_{355} = 2695 dm^3 mol^{-1} s^{-1}) a transient absorption was observed at 280 nm. The transient was formed within the duration of the flash (see Figure 3.1.2.1.1). No decay of the transient species was evident even on the longest time-scale available with the current equipment. Concurrent with formation of this species, changes in the UV/vis. spectrum were evident with the valley in the absorption spectrum disappearing, as presented in Figure 3.1.2.1.2. Two isosbestic points were maintained at 308 and 354 nm during the course of the experiment. $\lambda_{max.}$ at 316 nm decreased in intensity along with an increase in the region of 400 nm. On allowing the solution to stand for 60 minutes in the dark the spectrum reverted to that of the unphotolysed material.

(a)

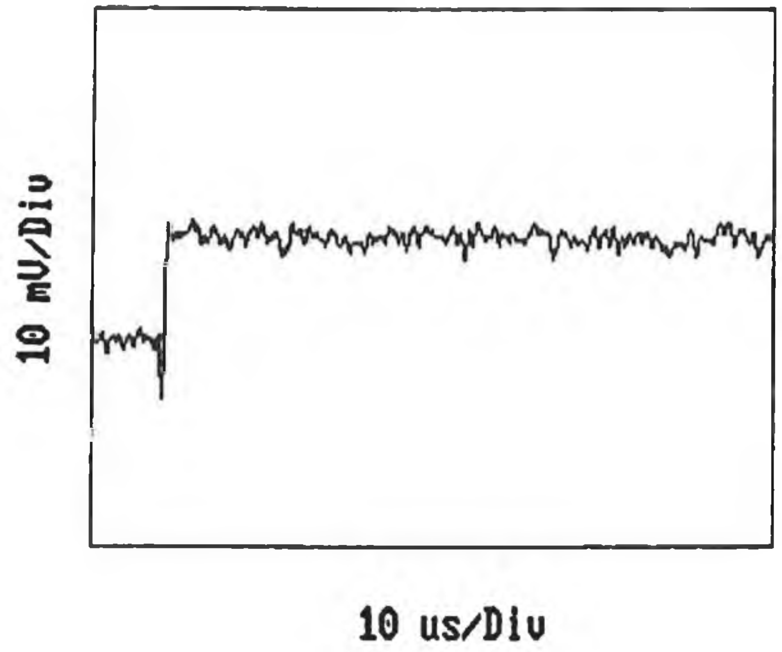

(b)

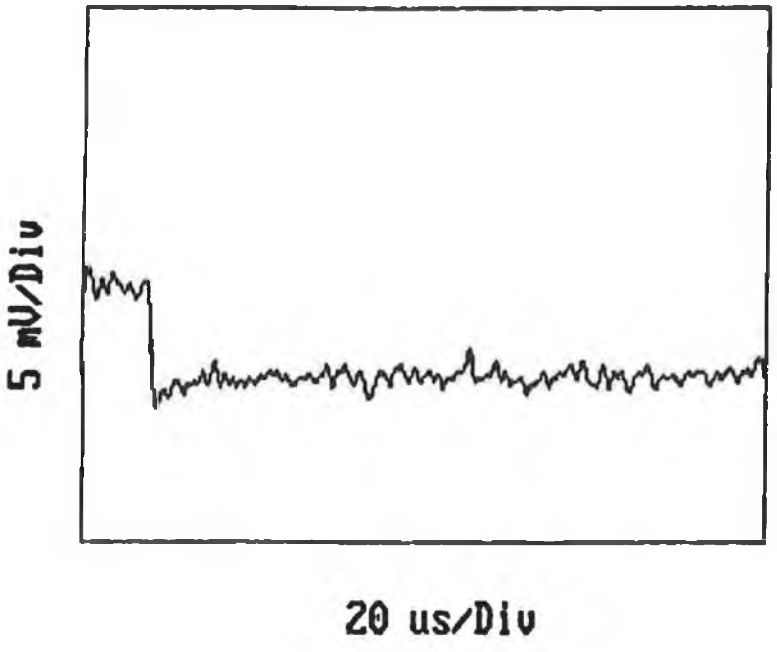

Figure 3.1.2.1.1 Transient spectra following flash photolysis of (η^6-allylbenzene)Cr(CO)$_3$ in cyclohexane at (a) 280 nm and (b) 340 nm under 1 atm. of CO.

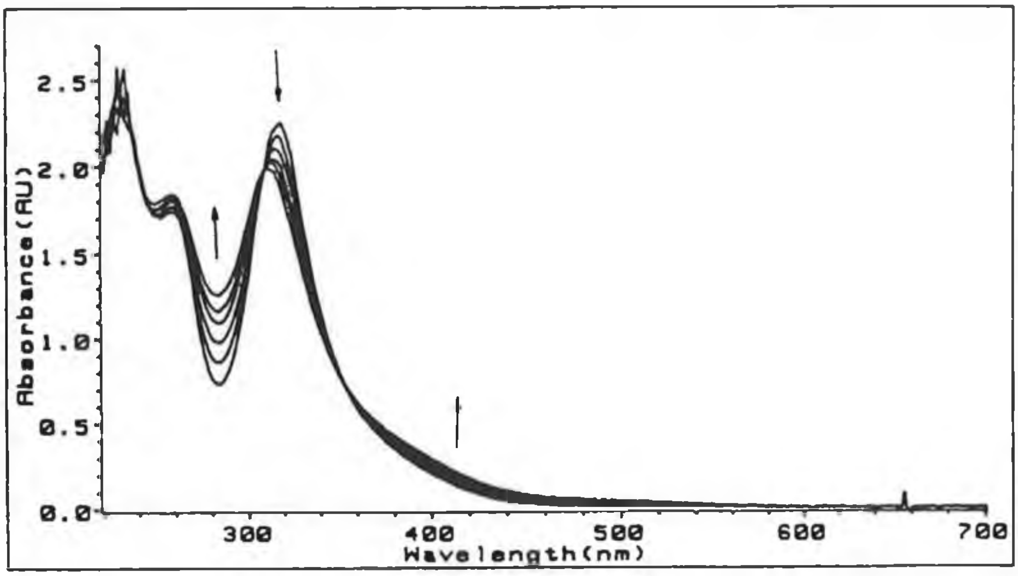

Figure 3.1.2.1.2 Spectral changes observed in the parent absorption spectrum (2.9×10^{-4}M) following flash photolysis under 1 atm. of CO in cyclohexane.

3.1.2.2 Steady state photolysis using IR detection.

A sample of (η^6-allylbenzene)$Cr(CO)_3$ was dissolved in cyclohexane and outgassed with a flow of argon. IR analysis of the sample revealed two intense carbonyl absorptions at 1978 and 1910 cm^{-1}. The sample was photolysed (in the IR solution cell) at $\lambda > 350$ nm and the IR spectrum recorded at various time intervals. The resulting changes in the IR spectrum are given in Figure 3.1.2.2.1.

After irradiating the solution cell for 5 seconds two new bands were seen at 1934 and 1881 cm^{-1}. Along with the growth of these two new bands the intensity if the parent bands at 1978 and 1910 cm^{-1} decreased. On prolonged irradiation a band appeared at 1986 cm^{-1} (not shown in Figure 3.1.2.2.1.) which is most likely the result of $Cr(CO)_6$ formation. To ensure that the same process is being observed in the IR solution cell as the laser experiment, an IR of the laser sample was carried out following a laser flash photolysis experiment. The bands measured from a laser sample agreed with those of the IR solution cell experiment with bands present at 1881, 1934 cm^{-1} and on continued flashing of a laser sample an infrared spectrum indicated a band at 1986 cm^{-1} attributed to the presence of $Cr(CO)_6$.

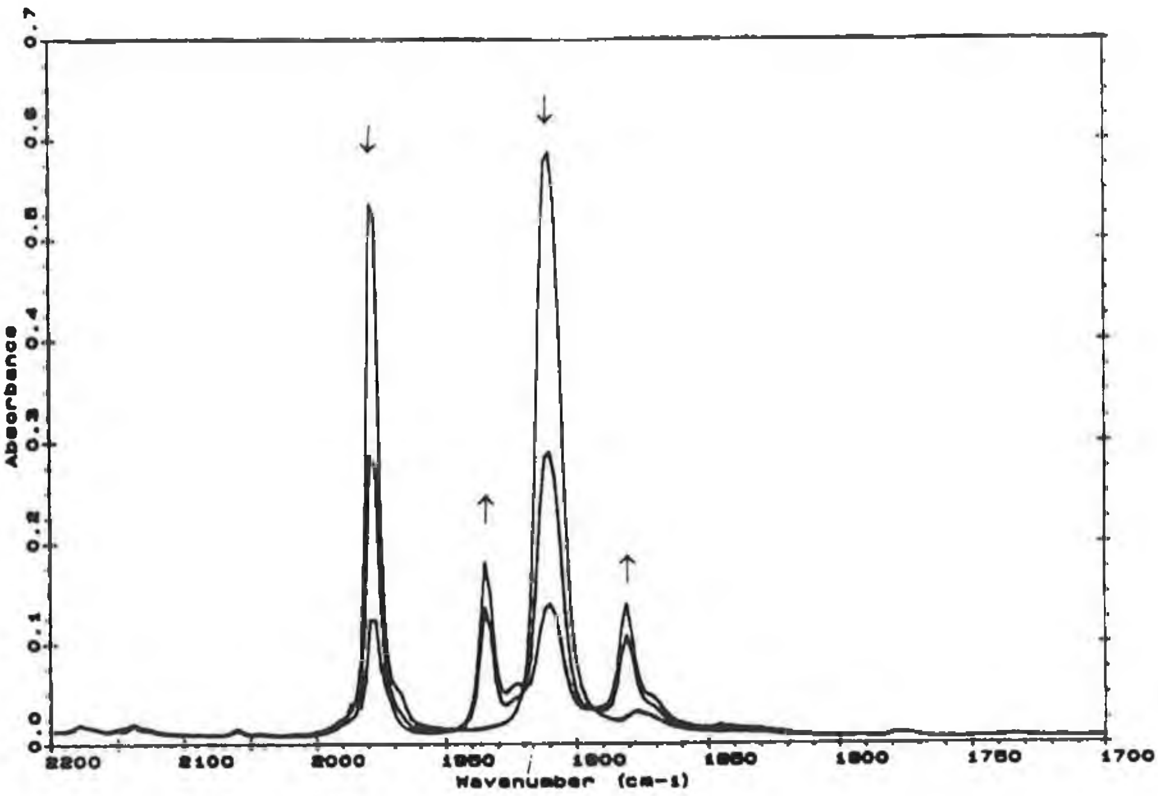

Figure 3.1.2.2.1 Infrared spectral changes observed upon photolysis of (η^6-allylbenzene)$Cr(CO)_3$ in cyclohexane.

Chelate complexes derived from alkenylarenedicarbonyl complexes of Cr, Mo and W have been isolated and characterised by Nesmeyanov and coworkers.[4] When there are four atoms between the phenyl ring and the olefin group the complex which formed was unstable but its formation was proved by IR spectroscopy. UV irradiation of a solution where x = CH_2, *i.e.* the phenyl ring is separated from the double bond by one methylene group did not bring about the formation of the chelate complex but only resulted in gradual decomposition of the initial complex.

Initially it was thought that perhaps in this work that formation of the chelate complex was observed as the difference in frequency of the new bands correspond well with those reported by Nesmeyanov *et al.*[1,6] for other arenedicarbonylolefin complexes (see Table 3.1.2.2.1)

x	cm^{-1}
$(CH_2)_2$	1878, 1930
$(CH_2)_3$	1871, 1923
$(CH_2)_4$	1886, 1920

Table 3.1.2.2.1 Areneolefin complexes of $Cr(CO)_2(\eta^6\text{-}C_6H_5)\text{-x-}CH{=}CH_2$, data taken from reference 6.

In all complexes synthesised by Nesmeyanov *et al.*[1, 6] the carbonyl stretching vibrations of the tricarbonyl complexes are separated by approximately 70 cm^{-1} whereas in the arenedicarbonylolefin complexes the differences decreases to some 50 cm^{-1}. The ν(CO) gradually shifts to lower frequency as the number of bridging CH_2 units increased from two to four in phenyl alkene complexes. This reported difference between tricarbonyl and chelate dicarbonyl is very similar to the data obtained in this study as bands formed at 1934 and 1881 cm^{-1} following irradiation, thus indicating possible formation of this type of species.

3.1.2.3 NMR monitored photolysis.

A NMR sample of the (η^6-allylbenzene)$Cr(CO)_3$ in cyclohexane-d_{12} was prepared in a similar manner to a laser photolysis sample (*i.e.* freeze pump thaw) and 1 atm. of CO was admitted to the NMR tube. As the NMR tube was irradiated with $\lambda > 350$ nm a red oil like product was seen to precipitate from solution. The sample was irradiated until such time that no further precipitation was observed. The cyclohexane was then removed under reduced pressure and benzene-d_6 distilled into the NMR tube. The red product is soluble in aromatic solvents. The ^1H nmr spectrum of this solution was identical to the nmr spectrum of the parent tricarbonyl in benzene-d_6.

3.1.2.4 Low temperature photolysis.

Attempts were made to isolate this new species, hence (η^6-allylbenzene)$Cr(CO)_3$ was dissolved in pentane and this solution was photolysed at -25°C, the photolysis was monitored by infrared spectroscopy. As the irradiation progressed an orange solid was seen to fall out of solution. At the stage when the bands attributed to the tricarbonyl had diminished the photolysis was stopped and excess pentane was removed at -20°C, leaving an orange solid. The solid was very sensitive to O_2. The infrared spectrum of the orange solid when dissolved in aromatic or chlorinated solvent was identical to the parent tricarbonyl compound.

A mass spectrum of this orange product revealed the peak of the molecular ion M^+ 254. The fragmentation pattern was consistent with loss of 3 carbonyl ligands, confirming that the orange solid contains 3 carbonyl groups. These results indicate that the product formed on photolysis does not result in carbonyl loss but rather the ring coordination changes from being η^6-arene to η^4-arene with a subsequent η^2 coordination of the double bond (see Reaction 3.1.2.4.1). Presumably this compound would be very unstable and quickly reverts to the (η^6-arene) compound on dissolving as the only infrared bands measurable are those of the parent tricarbonyl.

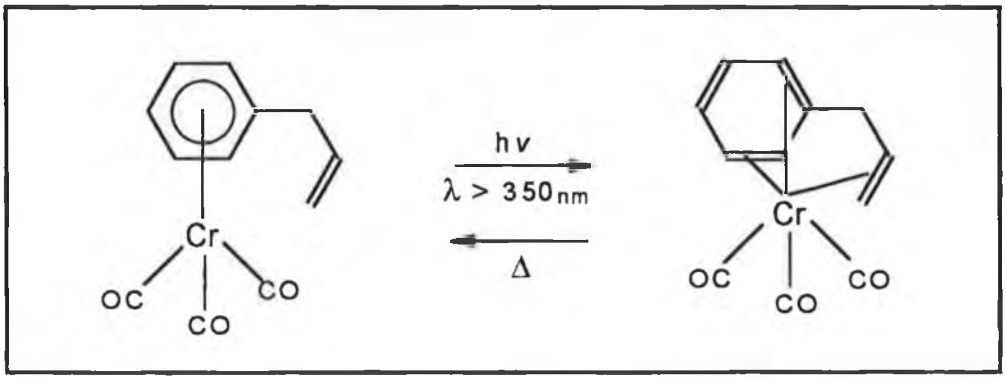

Reaction 3.1.2.4.1

3.2 (η^6-tetrahydronaphthalene)$Cr(CO)_3$.

In the latter part of this chapter the photochemistry of (η^6-tetrahydronaphthalene)$Cr(CO)_3$ is reported. To date, all of the reported photochemistry of (η^6-arene)$Cr(CO)_3$ compounds deals with monoaromatic rings attached to the metal centre[7] with the exception of one report where the arene attached to the metal centre consists of a biphenyl ligand.[8]

3.2.1 Electronic absorption spectrum of (η^6-tetrahydronaphthalene)$Cr(CO)_3$.

The prominent spectral feature of the electronic spectrum of (η^6-tetrahydronaphthalene)$Cr(CO)_3$ consists of a sharp intense band near 330 nm assigned as being a combination of Cr ----> arene charge transfer with some Cr ----> π^* character which is similar to that of (η^6-benzene)$Cr(CO)_3$.[5] The absorption spectrum of (η^6-arene)$Cr(CO)_3$ compounds has previously been described in detail in Section 2.1.1.

3.2.2 Laser flash photolysis using UV/vis. detection.

Photolysis of (η^6-arene)$Cr(CO)_3$ compounds have been found to undergo CO loss as the primary photoprocess. Following laser flash photolysis of (η^6-tetrahydronaphthalene)$Cr(CO)_3$ (ε_{355} = 4263 dm^3 mol^{-1} s^{-1}) in cyclohexane under 1 atm. of CO a transient species was seen to absorb strongly at 280 nm. As with any of the other chromium tricarbonyls investigated in Section 2.1.2 addition of CO to the solution reduced the lifetime of this intermediate but had no effect on it's over all yield. The concentration of CO admitted to the cell was varied, a linear relationship between k_{obs} and concentration of CO was noted, (as presented in Figure 3.2.2.1) and the second order rate constant for the reaction of this species with CO was calculated to be 7.2 x 10^6 dm^3 mol^{-1} s^{-1} at 298K. From these observations and from previous studies on substituted (η^6-arene)$Cr(CO)_3$[9] this transient species is assigned as a solvated dicarbonyl intermediate. The second order rate constant for reaction of the solvated dicarbonyl intermediate towards CO is similar to that of the analogous reaction for (η^6-benzene)$Cr(CO)_3$.[9] Therefore on 355 nm photolysis of (η^6-tetrahydronaphthalene)$Cr(CO)_3$ the first species observed was (η^6-tetrahydronaphthalene)$Cr(CO)_2$(cyclohexane) and this species is formed within the duration of the flash. A typical transient signal obtained is given in Figure 3.2.2.2 where the decay curve corresponds to decay of the (η^6-

tetrahydronaphthalene)$Cr(CO)_2$(cyclohexane). (η^6-Tetrahydronaphthalene)-$Cr(CO)_3$ has been shown to behave similarly to all of the other (η^6-arene)$Cr(CO)_3$ compounds discussed earlier. Thus, the primary photoreaction in solution is given by Reaction 3.2.2.1.

$$(\eta^6\text{-tetrahydronaphthalene})Cr(CO)_3 \xrightarrow{h\nu} (\eta^6\text{-tetrahydronaphthalene})Cr(CO)_2 + CO \qquad (3.2.2.1)$$

As coordinatively unsaturated 16 electron intermediates are extremely reactive and are known to coordinate weakly even to those consisting of inert noble gases[10] the dicarbonyl intermediate readily coordinates to a solvent molecule according to Reaction 3.2.2.2.

$$(\eta^6\text{-tetrahydronaphthalene})Cr(CO)_2 + s \longrightarrow (\eta^6\text{-tetrahydronaphthalene})Cr(CO)_2(s) \qquad (3.2.2.2)$$

In the presence of CO the solvated intermediate recombines with CO to regenerate the parent tricarbonyl according to reaction 3.2.2.3.

$$(\eta^6\text{-tetrahydronaphthalene})Cr(CO)_2(s) + CO \longrightarrow (\eta^6\text{-tetrahydronaphthalene})Cr(CO)_3 + s \qquad (3.2.2.3)$$

The UV/vis. difference spectrum obtained 2 μs after the flash under 1 atm. of CO is given in Figure 3.2.2.3. A $\lambda_{max.}$ is evident at 280 nm and a depletion at 340 nm, which is typical of any of the (η^6-arene)$Cr(CO)_3$ compounds investigated in Chapter 2.

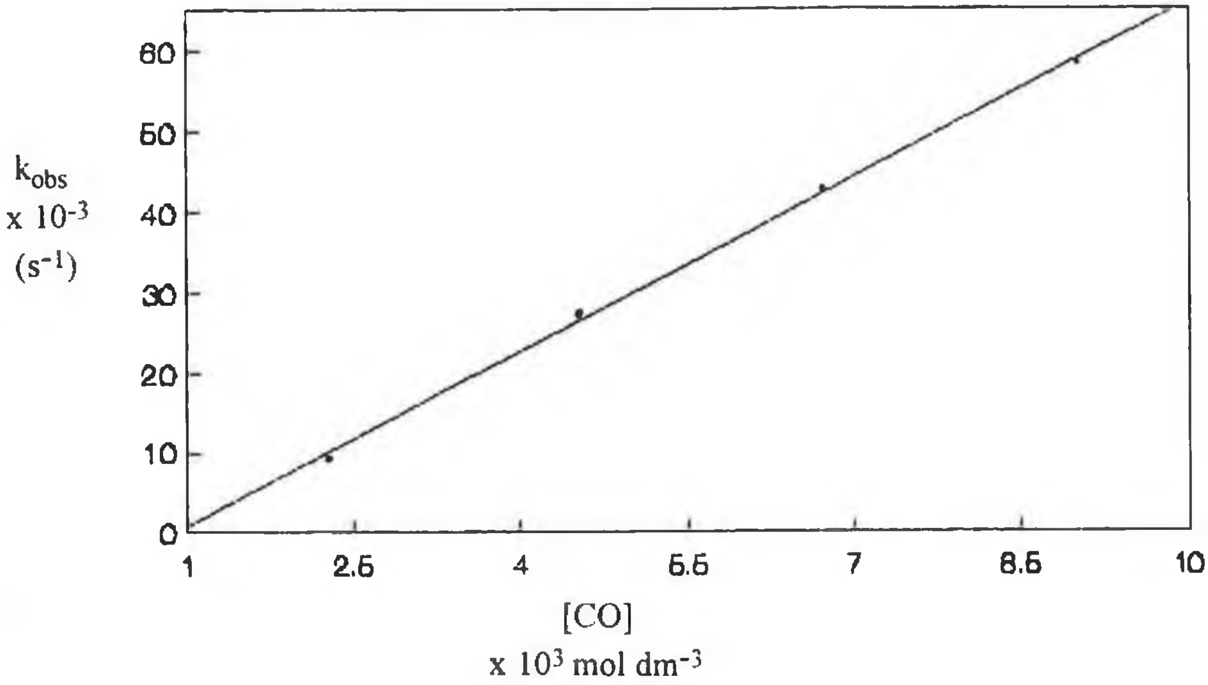

[CO] x 10^3 mol dm^{-3}	k_{obs} (s^{-1}) x 10^{-3}
2.2	9.27
4.5	27.16
6.7	42.52
9.0	58.18

slope = $7.2 \times 10^6 \pm 1.8 \times 10^5$
intercept = $-62.35 \times 10^{-2} \pm 9.07 \times 10^{-2}$
correlation coefficient = 0.99

Figure 3.2.2.1 A plot of CO (mol dm^{-3}) against the observed rate constant for the reaction of CO with (η^6-tetrahydronaphthalene)Cr(CO)$_2$(cyclohexane) at 298K.

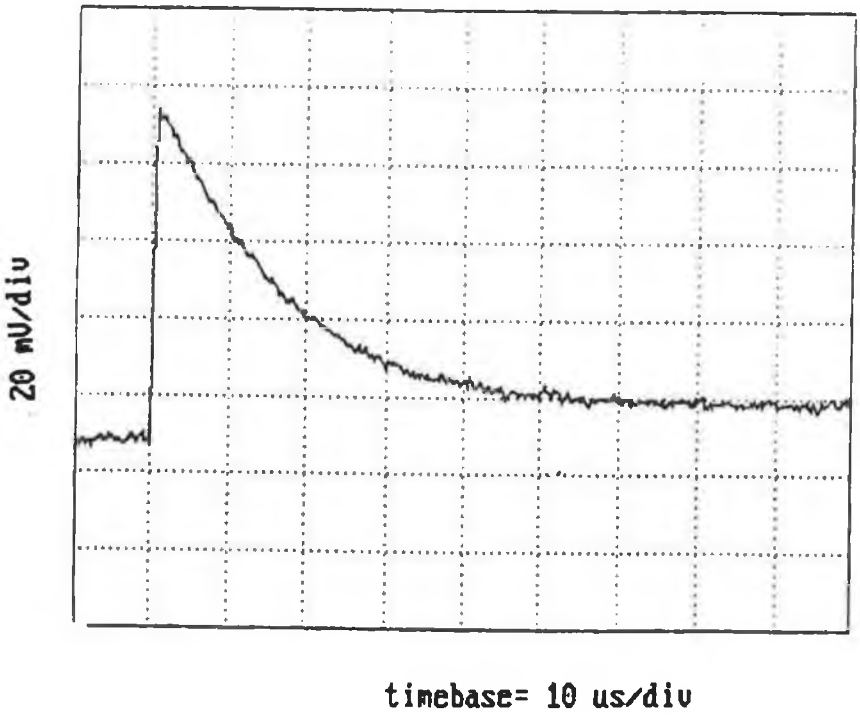

Figure 3.2.2.2. Transient decay of the (η^6-tetrahydronaphthalene)-$Cr(CO)_2$(cyclohexane) complex monitored at 280 nm under 1 atm. of CO.

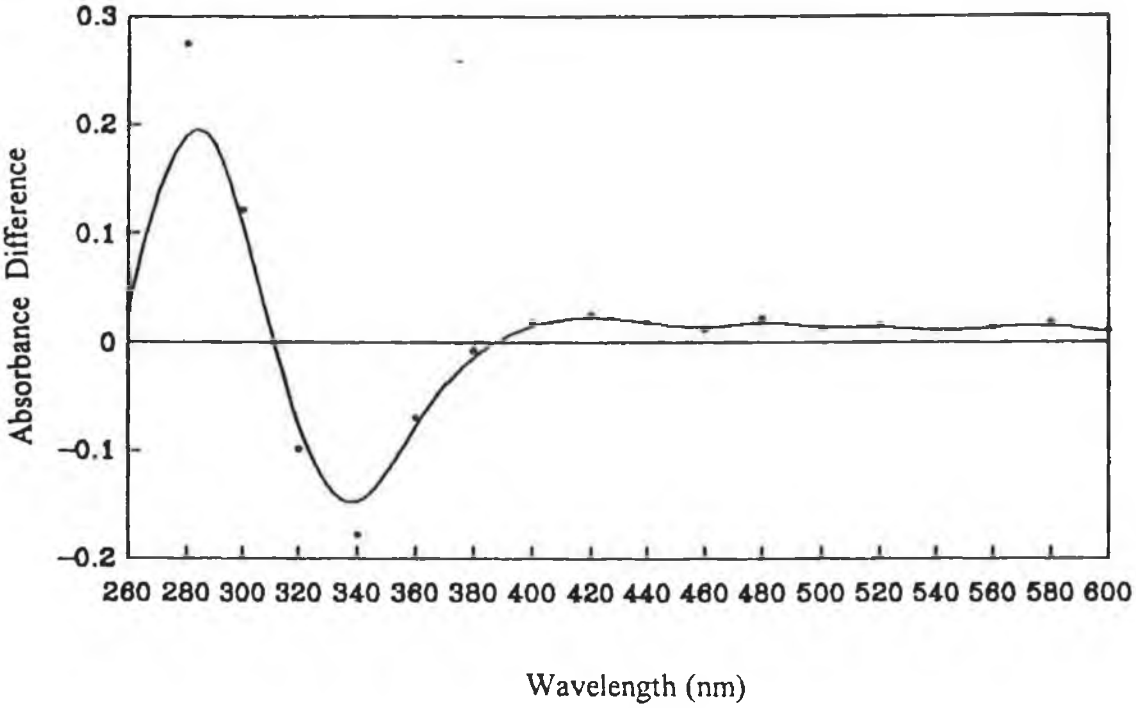

Figure 3.2.2.3 A UV/vis. difference spectrum of (η^6-tetrahydronaphthalene)-$Cr(CO)_2$(cyclohexane) obtained in cyclohexane solution under 1 atm. CO, 2μs after the laser pulse.

Following flash photolysis of (η^6-tetrahydronaphthalene)Cr(CO)$_3$ under 1 atm. of argon a second transient species was seen to absorb in the region 360 to 430 nm. Spectral changes were significant in the parent spectrum (see Figure 3.2.2.4) with a band growing in at approximately 380 nm. Isosbestic points at 276, 296 and 342 nm were maintained throughout the course of the experiment which is indicative of a reaction uncomplicated by side or subsequent reactions. A UV/vis. difference spectrum of this secondary photoproduct is given in Figure 3.2.2.5.

The concentration of (η^6-tetrahydronaphthalene)Cr(CO)$_3$ in solution was varied and the observed rate constants determined at each concentration. The observed rates were plotted against parent concentration. However, a linear relationship was not observed. Thus it would appear that the solvated dicarbonyl species is not reacting with unphotolysed parent.

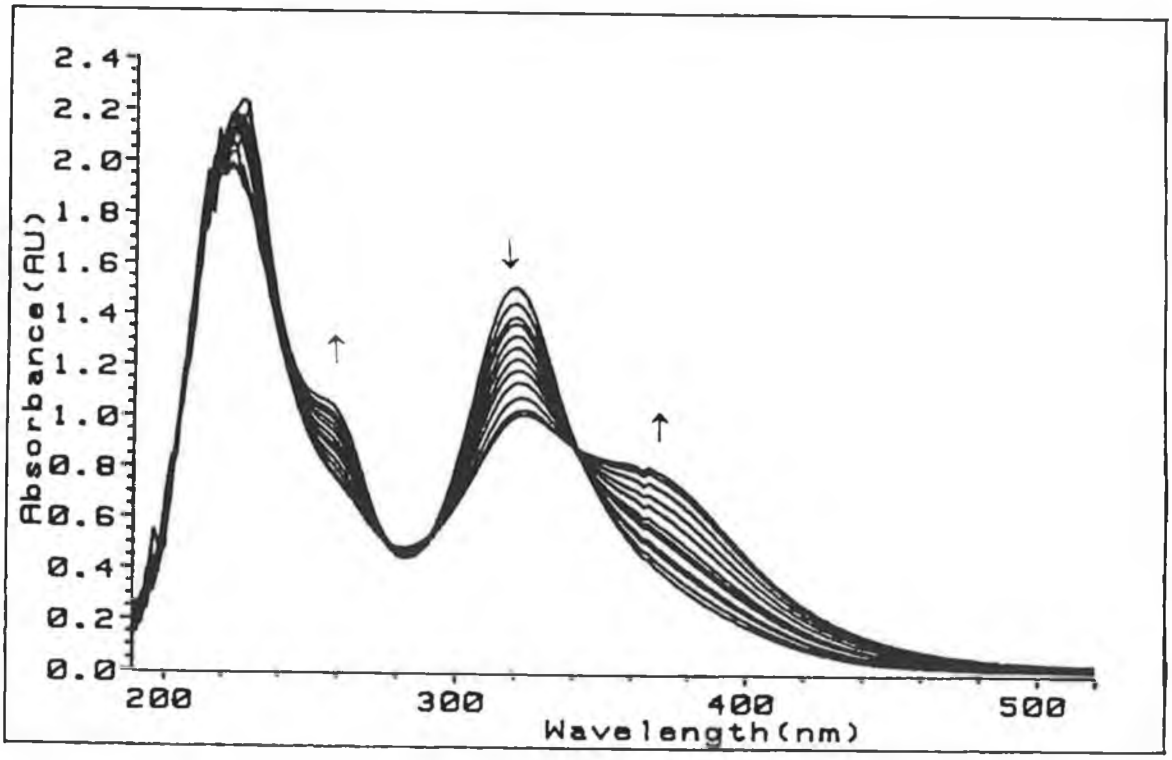

Figure 3.2.2.4 Spectral changes observed following flash photolysis of (η^6-tetrahydronaphthalene)Cr(CO)$_3$ in cyclohexane under 1 atm. of argon.

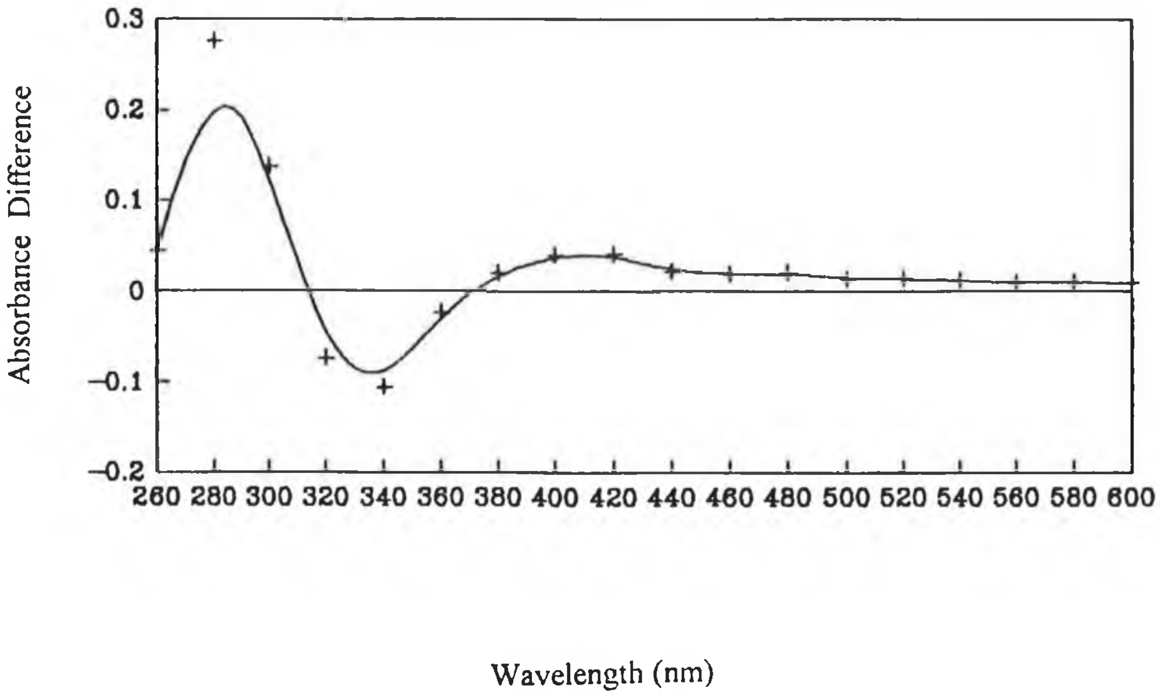

Figure 3.2.2.5 UV/vis. spectrum of the secondary photoproduct formed following photolysis of (η^6-tetrahydronaphthalene)Cr(CO)$_3$ in cyclohexane (150μs) under 1 atm. of argon.

3.2.3 Transient infrared spectroscopy.

As the identity of the second species was unknown following laser flash photolysis it was decided to carry out a number of TRIR experiments. TRIR experiments were conducted in the presence and absence of CO. The TRIR difference spectrum obtained following photolysis under 1 atm. CO is shown in Figure 3.2.2.3.1. Depletion of the parent complex is evident at 1972 and 1900 cm^{-1}, with production of positive bands at 1910 and 1868 cm^{-1}. The latter are assigned to the solvated dicarbonyl intermediate by comparison with the bands for (η^6-benzene)Cr(CO)$_2$(s) which occur at 1927 and 1877 cm^{-1}. Using TRIR the second order rate constant for reaction of the solvated dicarbonyl species was calculated to be 6.7 x 10^6 dm^3 mol^{-1} s^{-1}. This value corresponds well with that derived using UV/vis. detection (*vide supra*). From TRIR it is apparent that the system is not fully reversible under these conditions, as after 20 μs the bands assigned to the dicarbonyl species had decayed completely but the bands at 1972 and 1900 cm^{-1} of the parent tricarbonyl complex remained slightly depleted, thus indicating formation of a further species.

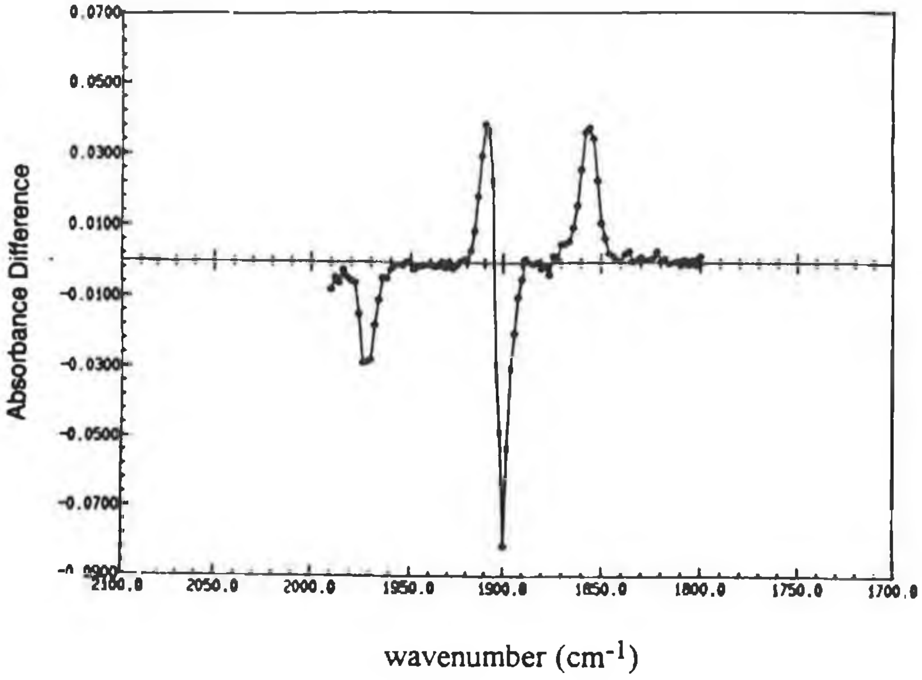

Figure 3.2.3.1 TRIR difference spectrum after 2μs following flash photolysis ($\lambda_{exc.}$ = 308 nm) of (η^6-tetrahydronaphthalene)Cr(CO)$_3$ under 1 atm. of CO.

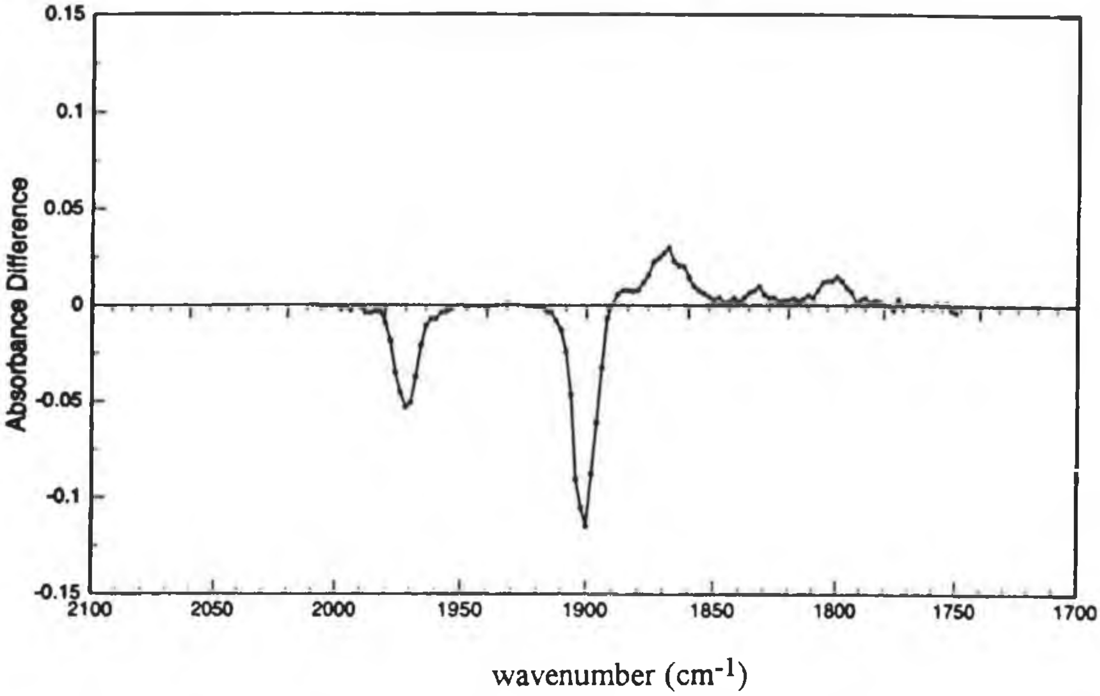

Figure 3.2.3.2 TRIR difference spectrum after 120μs following photolysis of (η^6-tetrahydronaphthalene)Cr(CO)$_3$ under 1 atm. of argon.

On conducting a similar experiment, but this time under 1 atm. of argon, bands were initially observed at 1910 and 1868 cm^{-1} (assigned to the dicarbonyl species). These bands decayed concurrent with formation of four new bands at approximately 1890, 1870, 1832 and 1804 cm^{-1} as presented in Figure 3.2.3.2. The observed rate constant for formation of these new bands is similar to the rate of decay of the dicarbonyl species. The average k_{obs} was calculated to be 2.6 x 10^{4} s^{-1} for rate of grow-in of the 'new' bands. After initial depletion of parent further depletion is not observed, hence ruling out the possibility of unphotolysed starting material reacting with the dicarbonyl as was observed previously for the Mo system. Close examination of the individual transients suggests a slight regeneration of parent, however.

The identity of this species remains unknown. From UV/vis. results, it does not appear to react with unphotolysed (η^6-tetrahydronaphthalene)$Cr(CO)_3$ in solution, as a linear relationship between k_{obs} and concentration of parent does not exist. Also, if a dinuclear species is formed, further depletion of parent should be evident, but this does not occur according to the transient infrared data experiments carried out on this system.

Domogatskaya *et al.*[8] have studied the photochemistry of η^6-arenetricarbonyl complexes by IR, UV and NMR spectroscopy. Experimental data obtained during photolysis of (η^6-arene)$Cr(CO)_3$ favoured the formation of a multicentre complex which photodecays to yield $Cr(CO)_6$. From their results they proposed that the multicentre complex contains bridging carbonyl groups bonded to the metal atom, and terminal CO groups bonded to the metal atoms which are either coordinated or uncoordinated to the arene (Figure 3.2.3.3 and 3.2.3.4).

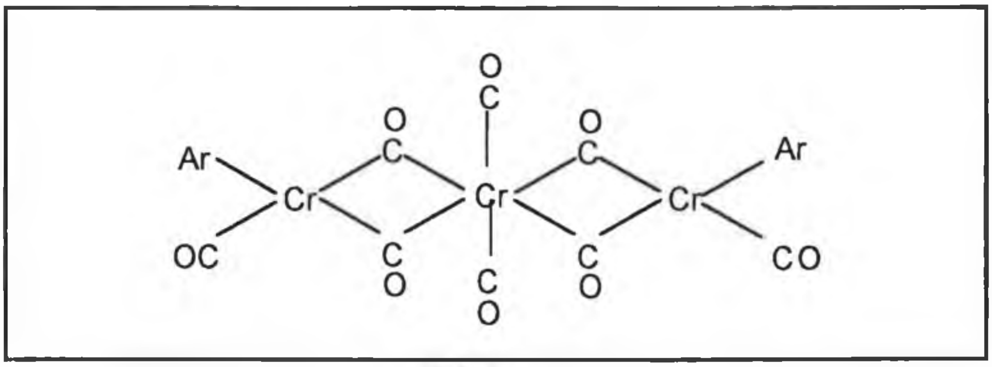

cis form

Figure 3.2.3.3

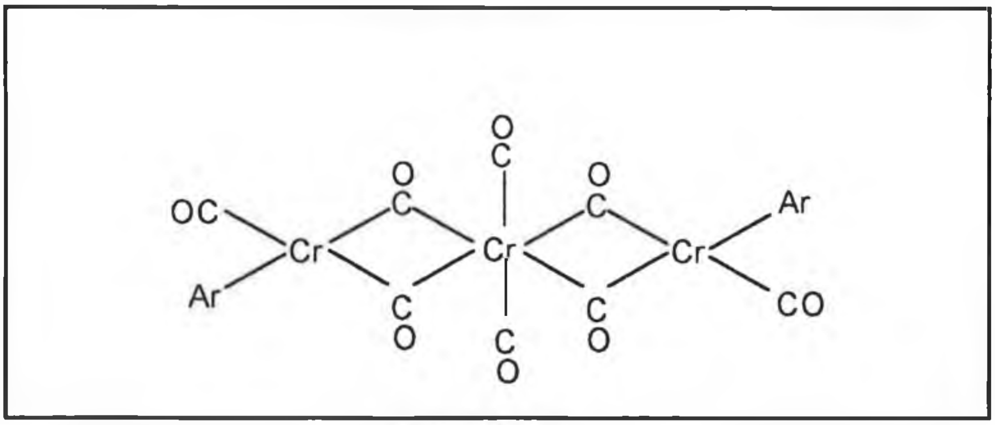

trans form

Figure 3.2.3.4

The electronic absorption spectrum of irradiated (η^6-biphenyl)Cr(CO)$_3$ showed an optical density increase in the region $\lambda > 375$ nm, similar to the observation in this study. They reported that formation of Cr(CO)$_6$ under irradiation of the supposed multinuclear complex is related to breaking of the Cr–CO (bridging) bond.

Another notable feature of this system was that this secondary photoproduct was only formed when samples were freeze pump thawed and liquid pumped. Degassing alone was not sufficient to generate this product, as on photolysing a degassed solution of (η^6-tetrahydronaphthalene)Cr(CO)$_3$ resulted in degradation. This factor made it very difficult to attempt any preparative work to aid in characterising this secondary photoproduct. It may be possible that the ligand is present in the sample, perhaps as a cocrystallite, and this may be removed by liquid pumping, hence the systems are not equivalent. The identity of this species remains unknown and further experiments are required to elucidate the nature of this secondary photoproduct.

3.2.4 Activation parameters for the reaction of (η^6-tetrahydronaphthalene)-$Cr(CO)_3$ with CO.

Activation parameters were obtained using Arrhenius and Eyring plots over a temperature range of 288-313K for Reaction 3.2.4.1.

$$(\eta^6\text{-tetrahydronaphthalene})Cr(CO)_2(s) \quad + \quad CO \quad \longrightarrow$$

$$(\eta^6\text{-tetrahydronaphthalene})Cr(CO)_3 \quad + \quad s \qquad (3.2.4.1)$$

The second order rate constant k_2 was used in the calculations ($k_2 = k_{obs}/[CO]$), where $[CO] = 9.0 \times 10^{-3}M$. The activation parameters are listed in Table 3.2.4.1 and the experimental values given in Table 3.2.4.2 and the corresponding graphs in Figure 3.2.4.1.

$\Delta H^{\neq}$	28 ± 2 kJmol^{-1}
$\Delta S^{\neq}$	-17 ± 5 Jmol^{-1}K^{-1}
$\Delta G^{\neq}_{(298K)}$	33 ± 2 kJmol^{-1}

Table 3.2.4.1 Activation parameters for the reaction of η^6-tetrahydronaphthalene)$Cr(CO)_2$(cyclohexane) with CO.

The enthalpy of activation $\Delta H^{\neq}$ for CO recombination at 28 kJmol^{-1} is similar to that of the analogous systems described in Chapter 2. The activation entropy is close to zero at -17 Jmol^{-1}K^{-1} which is indicative of a interchange mechanism.[11] Hence the reaction of (η^6-tetrahydronaphthalene)$Cr(CO)_2$(cyclohexane) with CO involves an transition state in which the CO molecule binds to the metal centre simultaneously to loss of cyclohexane. This mechanism has previously been postulated for all the substituted (η^6-arene)$Cr(CO)_3$ compounds discussed in Chapter 2.

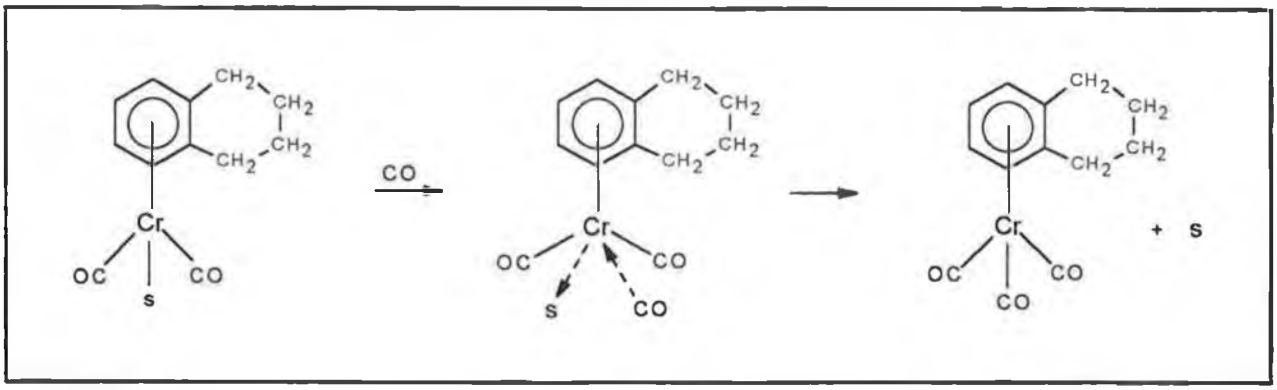

Scheme 3.2.4.2

Interchange mechanism for the recombination of η^6-tetrahydronaphthalene)Cr(CO)$_2$(cyclohexane) with CO to regenerate parent tricarbonyl.

Temp. (K)	1/T x 10^3 (K^{-1})	k_{obs} (s^{-1}) x 10^{-4}	Ln(k_{obs}/[CO])	Ln(k_{obs}/[CO] . T)
288	3.47	4.50	15.42	9.75
293	3.41	5.30	15.59	9.91
298	3.35	7.05	15.87	10.18
303	3.30	8.62	16.07	10.36
308	3.25	10.04	16.23	10.50
313	3.19	12.2	16.42	10.68

Arrhenius Plot

Slope	= -3698 ± 133
Intercept	= 28.21 ± 0.03
Correlation coefficient	= 0.99

Eyring Plot

Slope	= -3421 ± 135
Intercept	= 21.62 ± 0.03
Correlation coefficient	= 0.99

$E_a^{\neq} = 30 \pm 2$ kJmol^{-1}
$\Delta H^{\neq} = 28 \pm 2$ kJmol^{-1}
$\Delta S^{\neq} = -17 \pm 5$ Jmol^{-1}K^{-1}
$\Delta G^{\neq} = 33 \pm 2$ kJmol^{-1}

Table 3.2.4.2 Experimental data for the determination of the activation parameters for the reaction of (η^6-tetrahydronaphthalene)Cr$(CO)_2$(cyclohexane) towards CO.

(a)

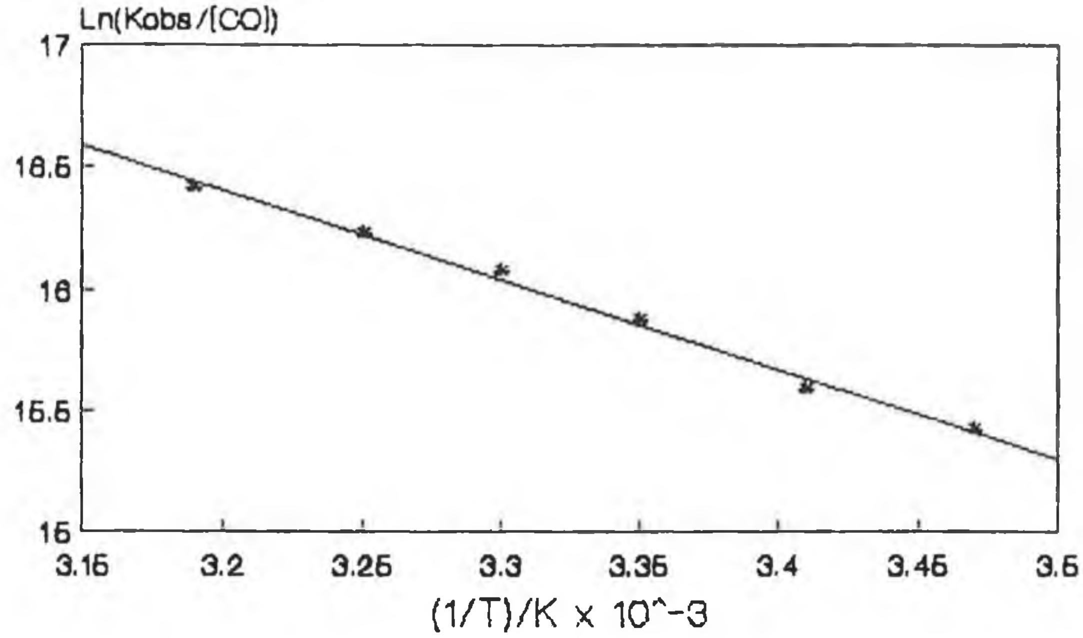

(b)

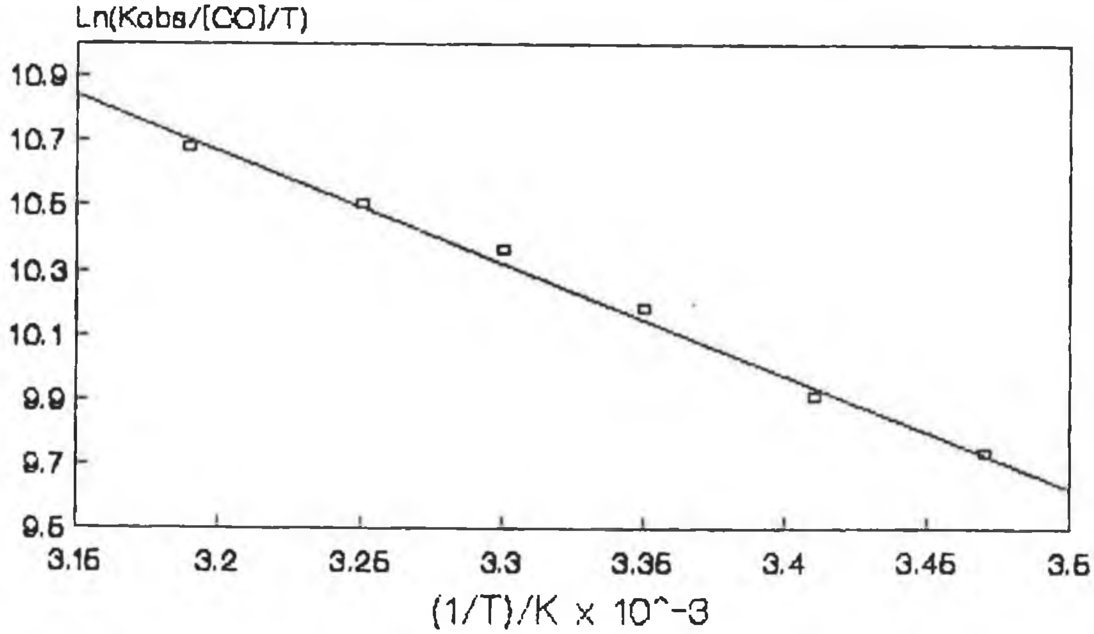

Figure 3.2.4.1 Arrhenius(a) and Eyring(b) plots for the reaction of (η^6-tetrahydronaphthalene)Cr(CO)$_2$(cyclohexane) with CO to regenerate tricarbonyl.

3.3 Conclusion.

A number of chelate complexes of chromium, molybdenum and tungsten have been isolated with intramolecular cyclisation being most suitable where a two or three atom bridge between the arene and olefin exists.[1, 6] Conversion of tricarbonyl was found to be most successful for chromium, followed by molybdenum and tungsten, yielding smaller amounts of the dicarbonyl olefin compound even after prolonged irradiation. When a one CH_2 unit bridge was used, as in the case of (η^6-allylbenzene)$Cr(CO)_3$, only decomposition was observed following irradiation. When no bridge was used, as in the case of (η^6-styrene)$Cr(CO)_3$, μ-olefin bridged dinuclear complexes were formed because of the withdrawing action of the (η^6-arene)$Cr(CO)_3$ moiety attached to the vinyl group.[6]

In this study flash photolysis experiments with (η^6-allylbenzene)$Cr(CO)_3$ were carried out under 1 atm. of CO. Under these conditions a rapid depletion was observed with no apparent recovery. Attempts were made to measure the rate of formation of this transient species but the response time of the instrumental set-up was not adequate. Steady state photolysis was monitored using infrared spectroscopy. Initially two bands were observed at 1934 and 1881 cm^{-1} concomitant with a decrease in intensity of the bands of the starting material at 1978 and 1910 cm^{-1}. On prolonged photolysis a further absorption was visible at 1985 cm^{-1} which is assigned to $Cr(CO)_6$. Initially it was thought that formation of an olefin dicarbonyl compound was occurring because of the similarity in product bands with those previously reported for other olefin-dicarbonyl compounds.[1, 6]

However, mass spectrometry indicated a fragmentation pattern consistent with loss of three carbonyl fragments thereby ruling out the possibility of a dicarbonylolefin compound. The possibility of a dinuclear species comparable with the (η^6-styrene)$Cr(CO)_3$ photolysis product, was considered but as only two carbonyl stretching frequencies were present this product was ruled out. Hence, from the data available it is proposed that on photolysis a hapticity change from $\eta^6 \longrightarrow \eta^4$ occurs with subsequent coordination of the olefin bond, but CO loss does not appear to result upon irradiation.

TRIR and UV/vis. flash photolysis studies were carried out on (η^6-tetrahydronaphthalene)$Cr(CO)_3$ both under CO and argon atmospheres. The primary photoproduct has been identified as the CO loss solvated intermediate. A further secondary photoproduct was also observed, the identity of which is unknown. However, Domogatskaya *et al.*[8] have investigated the photochemistry of (η^6-arene)$Cr(CO)_3$ compounds using a number of spectroscopic techniques. Experimental data suggested formation of a multicentre complex following photolysis. Photodecay of this complex then led to formation of $Cr(CO)_6$. The changes observed in the electronic absorption spectra of (η^6-tetrahydronaphthalene)$Cr(CO)_3$ following photolysis under argon are very similar to those observed by Domogatskaya and coworkers,[8] but in this study freeze pump thaw together with liquid pumping of the sample was required to observe formation of the secondary photoproduct. Further studies are required before any conclusive results can be determined regarding the nature of this product.

3.4 References

1 Nesmeyanov,A.N.;Aerybinskaya,M.I.;Krivykh,V.V.; Kaganovich,V.S.; *J. Organomet. Chem.*; 1978,**93**,C8.

2 Rybinskaya,M.I.;Koeneva,L.M.; *J. Organomet. Chem.*;1982,**231**,25.

3 Nesmeyanov,A.N.;Korneva,L.M.; *Dokl. Akad. Nauk. SSSR*; 1977,**237**, 1373.

4 Nesmeyanov,A.N.;Anisisov,K.N;Valnyeva,Z.P.; *Dokl. Akad. Nauk. SSSR*; 1964,**157**,662.

5 Carroll,D.G.;McGlynn, S.P.; *Inorg. Chem.*; 1968,**7**,1285.

6 Nesmeyanov,A.N.;Krivyktt,V.V.;Petrovskii,P.V.;Kaganovich,V.S.; Rybinskaya,M.I.; *J. Organomet. Chem.*; 1978,**162**,323.

7 (a) Strohmeier,W.;von Hobe,D.; *Z. Naturforsch;* 1963,**18B**,770.
(b) Gilbert,A.;Kelly,J.M.;Budzwait,M..;Koerner von Gustorf,E.; *Z. Naturforsch;* 1976,**31B**,1091.
(c)Zheng,Y.;Wang,W.;Lin,J.;Fu,F.-J.; *J. Phys. Chem.*; 1992,**96**,9821.

8 Domogatskaya,E.A,;Setkina,V.N.;Baranetskaya,N.K.,Tremboveler,V.N.; Yavorskii,B.M.;Shteinshneider,A.Ya.;Petrovskii,P.V.; *J. Organomet. Chem.;* 1983,**248**,161.

9 Creaven,B.S.;George,M.W.;Ginzburg,A.G.;Hughes,C.;Kelly.J.M.;Long,C. ;McGrath,I.M.;Pryce,M.T.; *Organometallics*;1993,**12**,3127.

10 Perutz.R.N.;Turner,J.J.; *J. Am. Chem. Soc.*; 1977,**97**,4791.

11 (a)Lees, A.J.;Adamson,A.; *Inorg. Chem.*; 1981,**20**,4381.
(b)Dobson,G.R.;Spradling,M.D.; *Inorg. Chem.*; 1990,**29**,880.
(c)Zhang,S.;Dobson,G.R.; *Inorg. Chem.Acta*; 1989,**165**,L11.

Chapter 4

Photochemical investigation of η^6-polyaromatic compounds of chromium tricarbonyl.

4.1 Photolysis of (η^6-polyaromatic)$Cr(CO)_3$ compounds.

Photolysis of (η^6-benzene)$Cr(CO)_3$ in frozen gases at 12K has been reported to form the dicarbonyl species.[1] Solution photochemistry has also indicated CO loss to be the primary photoprocess,[2] as the resulting photoproduct has been identified by TRIR spectroscopy as the coordinatively unsaturated 16 electron intermediate.[3] Highly reactive, unsaturated fragments of $Cr(CO)_6$ are known to coordinate weakly either to inert matrices[4] or to a solvent molecule.[5] Much of the photochemistry concerning (η^6-arene)$Cr(CO)_3$ compounds has dealt with monoaromatic systems, however the thermal chemistry of these complexes has covered a greater range of arenes.[6] While photochemically CO is apparently exclusively lost,[7] the thermal reaction is somewhat different and is dominated by arene exchange.[8] Activation of the arene–chromium bonds was first noted when arene exchange in (η^6-arene)$Cr(CO)_3$ was observed in various arene solutions[8, 9] (reaction 4.1.1).

$$(\eta^6\text{-arene})Cr(CO)_3 + \text{arene*} \longrightarrow (\eta^6\text{-arene*})Cr(CO)_3 + \text{arene} \qquad (4.1.1)$$

The displacement of the one arene by another takes place in the following order, going from the most to the least reactive arene:

hexamethylbenzene > mesitylene > xylene > toluene = benzene > chlorobenzene = fluorobenzene > naphthalene.

The driving force in Reaction 4.1.1 is the greater thermodynamic stability of (η^6-arene*)$Cr(CO)_3$ relative to (η^6-arene)$Cr(CO)_3$ because of the increased electron donating capability of arene*.[10] This situation is reflected in greater ease of displacement with increasing alkyl substitution on the arene*.

The aim of this study was to investigate the photochemistry of a number of substituted η^6-polyaromatic chromium tricarbonyl compounds using a combination of UV/vis., TRIR and luminescence data to aid in characterising the photoproducts formed.

4.1.1 Electronic absorption spectrum of (η^6-naphthalene)$Cr(CO)_3$.

Absorption spectra of (η^6-benzene)$Cr(CO)_3$ and related compounds that have been studied are dominated by metal to ligand charge transfer absorptions.[11] On examining the electronic absorption spectrum of (η^6-

naphthalene)Cr(CO)$_3$, it is obvious that this compound absorbs much further into the visible than any of the alkyl or halogenated compounds investigated in Chapter 2. The UV/vis. spectrum of (η^6-naphthalene)Cr(CO)$_3$ in cyclohexane is given in Figure 4.1.1.1. Similar to the benzene analogue, λ_{max} at 345 nm is assigned to being predominantly a Cr ----> arene charge transfer (CT) transition with some Cr ----> π^* CO CT character. A further maximum at approximately 432 nm is thought to be essentially Cr ----> arene CT. With this compound a shoulder at 305 nm is present, which may be masked in any of the previous (η^6-arene)Cr(CO)$_3$ compounds investigated. The low energy region of (η^6-benzene)Cr(CO)$_3$ has not been studied in detail but it is thought that the low lying absorptions are probably ligand field in character.[12] As the shoulder at 305 nm is not observable in the previous arene tricarbonyls investigated, it is possible that this band may be the result of a ligand field transition, however there is no evidence to support this hypothesis.

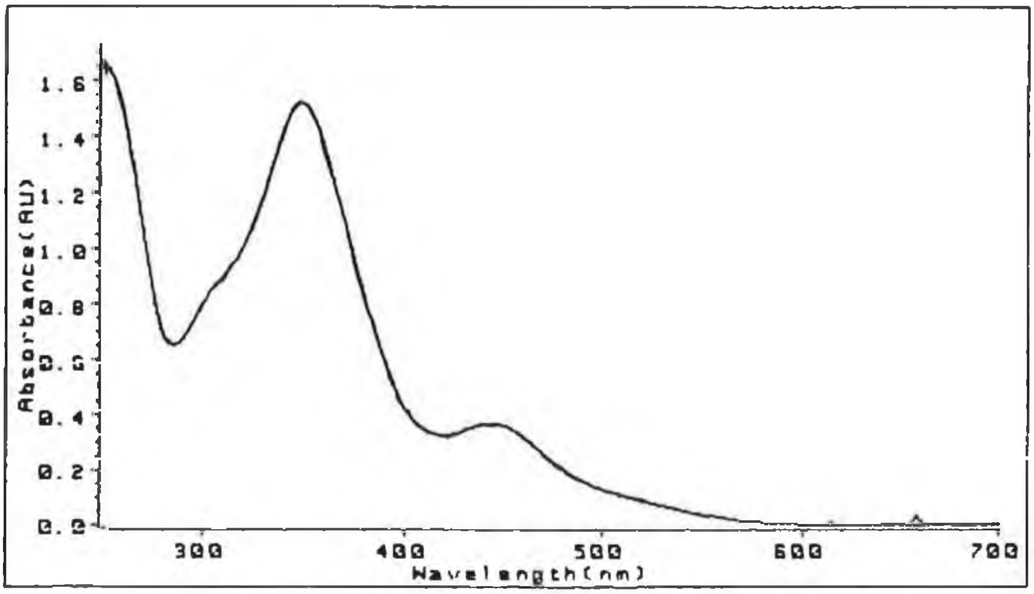

Figure 4.1.1.1 UV/vis. spectrum of (η^6-naphthalene)Cr(CO)$_3$ (1.5 x 10^{-4}M) in cyclohexane.

4.1.2 Laser flash photolysis of (η^6-naphthalene)$Cr(CO)_3$.

Following 266 nm laser flash photolysis of (η^6-naphthalene)$Cr(CO)_3$ in cyclohexane (ε_{266} = 8261 dm^3 mol^{-1} s^{-1}) under 1 atm. of CO a transient species was seen to absorb at 300 nm. Based primarily on previous studies carried out on (η^6-benzene)$Cr(CO)_3$ compounds this transient species was assigned to being the solvated dicarbonyl intermediate. A typical transient species monitored at 300 nm is given in Figure 4.1.2.1 where the decay curve represents decay of the solvated complex. The dependence of the life-time of the solvated dicarbonyl (η^6-naphthalene)$Cr(CO)_2$(cyclohexane) on CO was investigated. As with (η^6-benzene)$Cr(CO)_2$(cyclohexane) (see Chapter 2.) addition of CO to the solution reduced the life-time of the solvated complex but had little effect on its overall yield. The second order rate constant was calculated by plotting k_{obs} *versus* concentration of CO, and as a linear relationship existed, the slope of the line was used to generate the second order rate constant as given in Figure 4.1.2.2 which was calculated to be 5.08 x 10^6 dm^3 mol^{-1} s^{-1} at 298K. This value is smaller than that measured for the reaction of (η^6-benzene)$Cr(CO)_2$(cyclohexane) towards CO which was reported to be 9.8 x 10^6 dm^3 mol^{-1} s^{-1}.[2d] Hence the primary photoreaction of this system is given by Reaction 4.1.2.1 and 4.1.2.2.

$$(\eta^6\text{-naphthalene})Cr(CO)_3 \xrightarrow{h\nu} (\eta^6\text{-naphthalene})Cr(CO)_2 + CO \qquad (4.1.2.1)$$

$$(\eta^6\text{-naphthalene})Cr(CO)_2 + s \longrightarrow (\eta^6\text{-naphthalene})Cr(CO)_2(s) \qquad (4.1.2.2)$$

When in an CO environment this solvated intermediate recombines with CO to regenerate parent the tricarbonyl complex:

$$(\eta^6\text{-naphthalene})Cr(CO)_2(s) + CO \longrightarrow (\eta^6\text{-naphthalene})Cr(CO)_3 + s \qquad (4.1.2.3.)$$

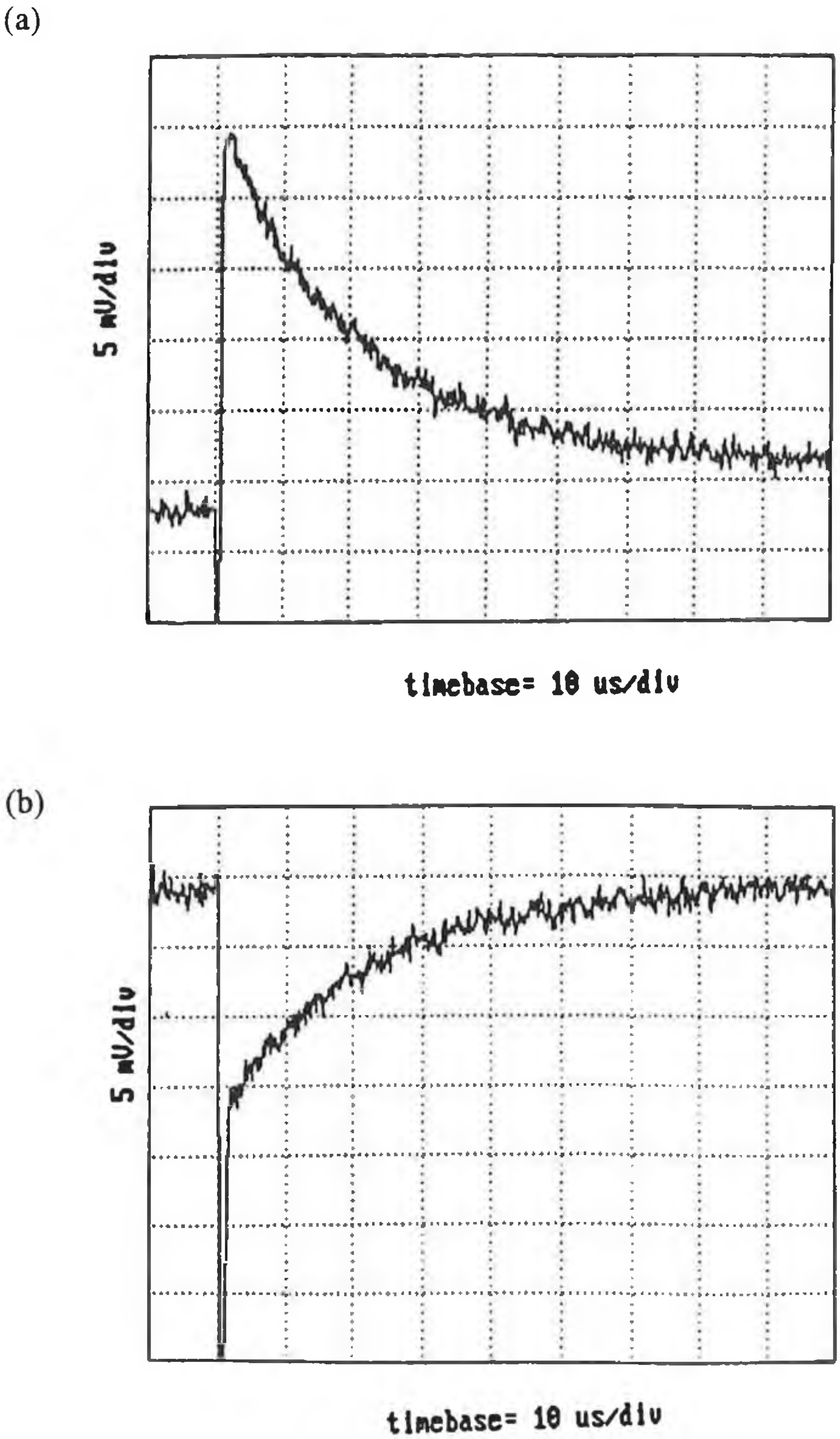

Figure 4.1.2.1 A typical transient signal obtained for (a) the decay of (η^6-naphthalene)$Cr(CO)_2$(cyclohexane) and (b) rate of recovery of the tricarbonyl compound under 1 atm. CO (9.0×10^{-3}M).

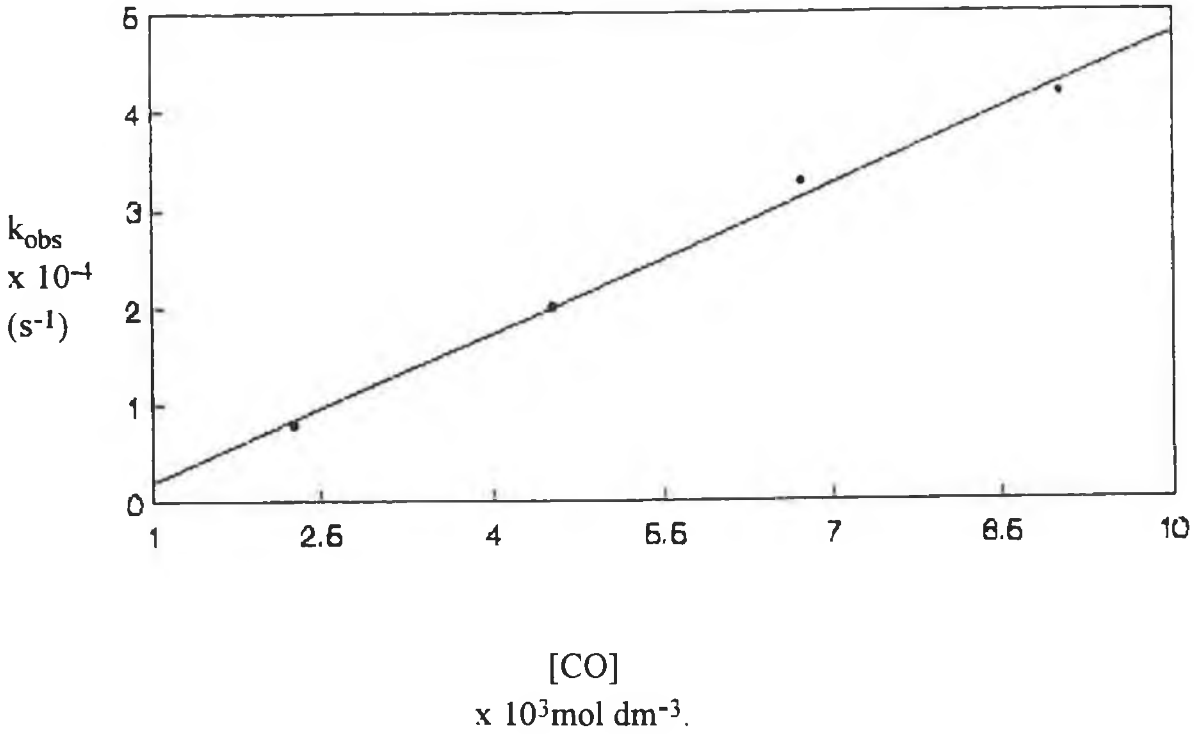

[CO] x 10^3 mol dm^{-3}	k_{obs} (s^{-1}) x 10^{-4}
2.25	0.78
4.50	1.99
6.75	3.27
9.00	4.17

slope = 5.08 x 10^6 ± 2.59 x 10^5
intercept = 31.00 x 10^{-2} ± 13.06 x 10^{-2}
correlation coefficient = 0.99

Figure 4.1.2.2 A plot of concentration of CO (mol dm^3) against the observed rate constant for the reaction of CO with the (η^6-naphthalene)$Cr(CO)_2$(cyclohexane) at 298K.

The UV/vis. difference spectrum under 1 atm. of CO is given in Figure 4.1.2.3. A maximum is evident at 300 nm and a depletion at 350 nm. The positive band at 300 nm represents formation of the solvated dicarbonyl intermediate whereas the negative absorption signifies depletion of parent tricarbonyl. Noticeable for this system is the red shift for formation of the solvated intermediate as opposed to the methyl or ethyl substituted tricarbonyl compounds discussed in Chapter 2.

The UV/vis. absorption spectrum of the sample solution was recorded throughout the experiment and it was evident during the flash photolysis experiment that the nature of the sample was changing. Total reversibility did not occur under a CO atmosphere, as the absorption of λ_{max} at approximately 345 nm decreased in intensity together with an increase in the absorption in the region 290 to 310 nm. The change in the spectrum may appear to be of minor consequence but it does indicate the formation of a further species. An infrared spectrum of the sample at the end of the experiment indicated formation of $Cr(CO)_6$. Further experiments were required to confirm the presence of uncomplexed naphthalene.

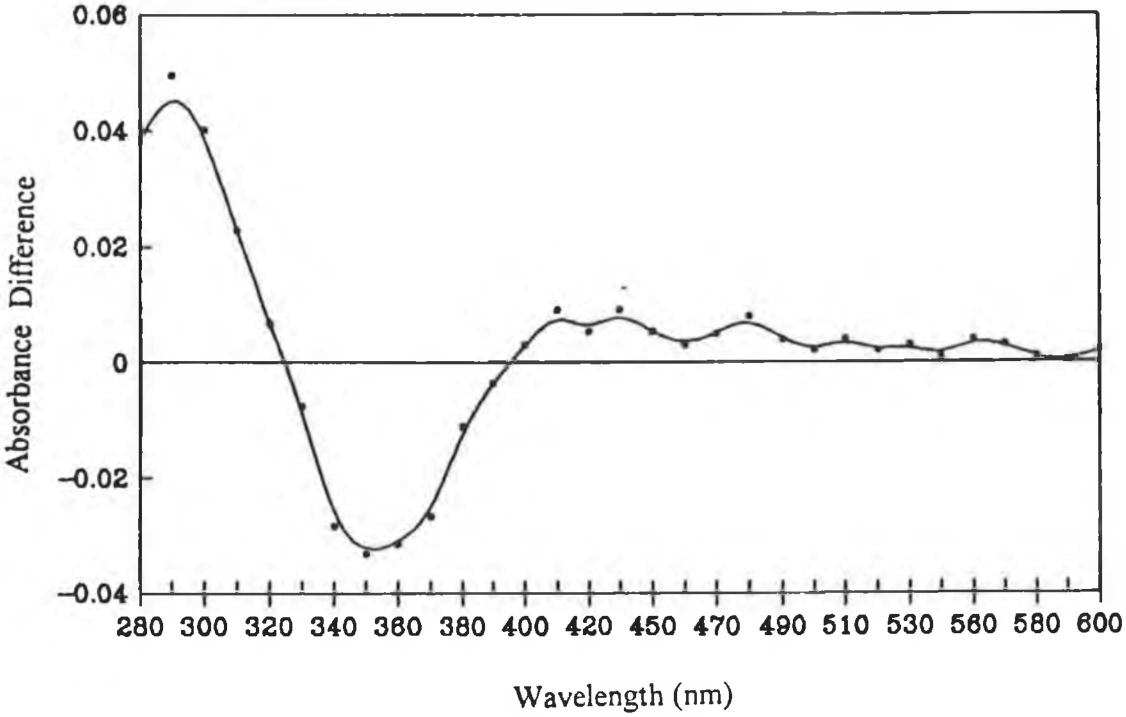

Figure 4.1.2.3 UV/vis. difference spectrum following flash photolysis of (η^6-naphthalene)$Cr(CO)_3$ in cyclohexane at 266 nm under 1 atm. of CO (9.0×10^{-3}M) at 298K.

Laser experiments were originally conducted at $\lambda_{exc.}$ 266 nm (33mJ per pulse) as no transient species were observed following 355 (20mJ per pulse) excitation. However, subsequently it was possible to conduct experiments using 355 nm excitation as the laser setup was serviced, which resulted in the energy of the system almost tripling, being 60-70 and 70-80 mJ per pulse for 355 and 266 nm excitation respectively.

Experiments were also carried out with 532 nm excitation as (η^6-naphthalene)$Cr(CO)_3$ absorbs in this region but no transients species were observed. If the low lying transition were ligand field in character, transients would be expected at this excitation wavelength, but this result further substantiates the likelihood that the lowest lying transition in this compound is metal to ligand charge transfer.

4.1.3 Luminescence monitored photolysis.

(η^6-Naphthalene)$Cr(CO)_3$ does not luminescence at room temperature, however the luminescence properties of naphthalene are well documented.[13] As (η^6-naphthalene)$Cr(CO)_3$ absorbs well into the visible to approximately 540 nm, it was initially decided to carry out long wavelength irradiation of this system. Room temperature photolysis of (η^6-naphthalene)$Cr(CO)_3$ at $\lambda > 345$ nm under 1 atm. of CO revealed the production of uncomplexed naphthalene as monitored by luminescence spectroscopy.

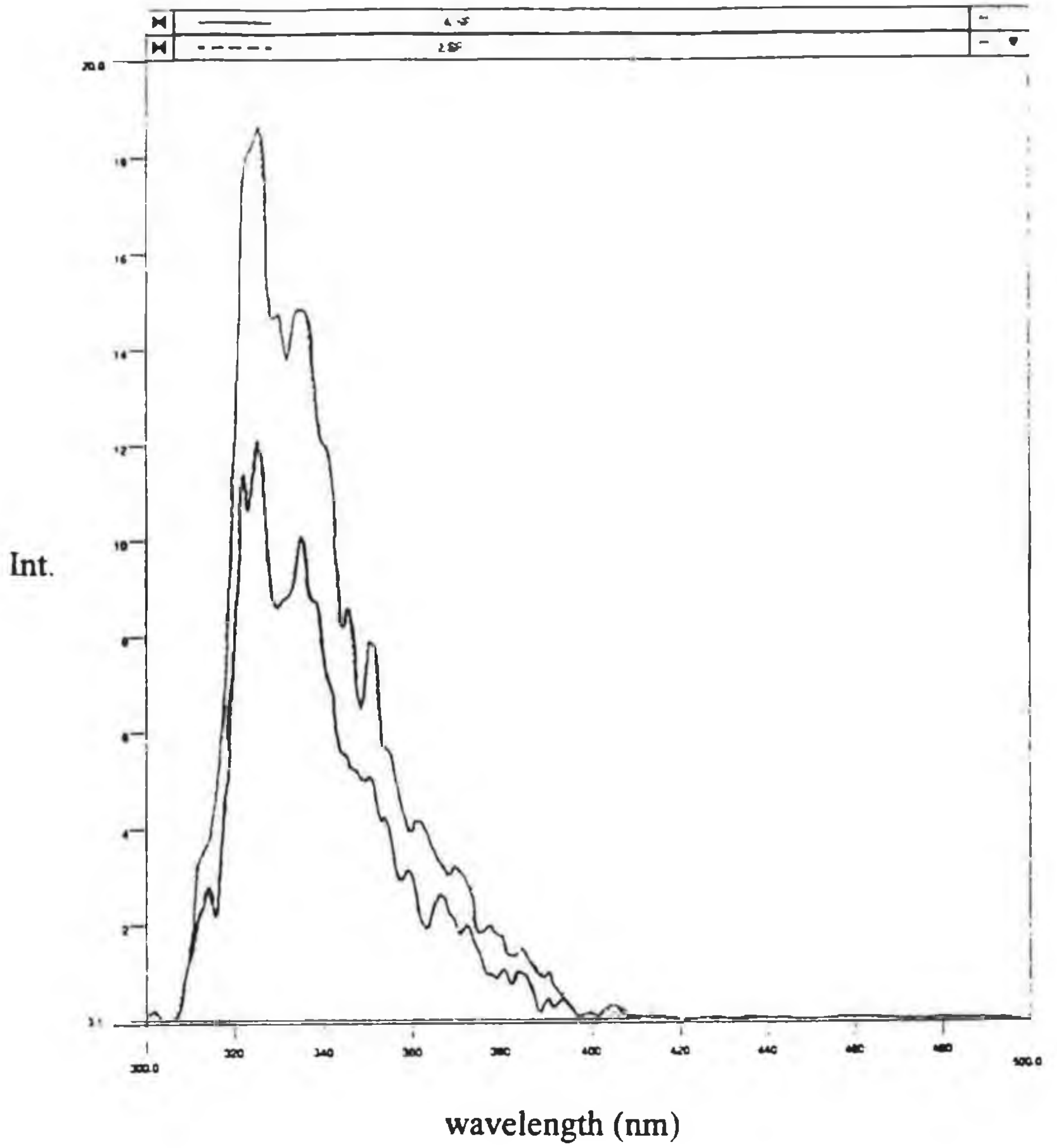

Figure 4.1.3.1 Luminescence spectra obtained after 10 and 20 minutes photolysis of (η^6-naphthalene)$Cr(CO)_3$ at $\lambda > 345$ nm in cyclohexane under 1 atm. of CO.

Luminescence spectra recorded after 10 and 20 minutes photolysis are given in Figure 4.1.3.1. Together with these measurements the absorption spectrum of the parent tricarbonyl was also monitored as presented in Figure 4.1.3.2 and this time the changes in the parent are much more pronounced. Decay of the absorbance at $\lambda_{max.}$ (345 nm) is evident, concurrent with an increase in the absorption at approximately 290 nm. An isosbestic point at 330 nm was maintained throughout the photolysis experiment which is indicative of a relatively clean reaction. At the end of the experiment an infrared spectrum of the sample solution indicated the presence of $Cr(CO)_6$.

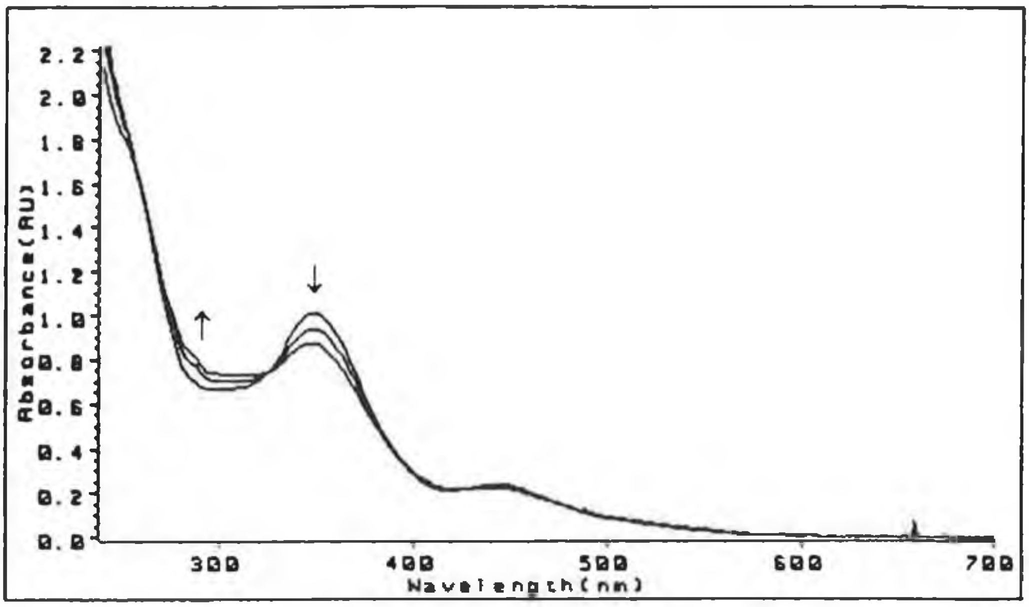

Figure 4.1.3.2 Changes observed in the UV/vis. spectrum of (η^6-naphthalene)$Cr(CO)_3$ (1.02×10^{-4}M) following photolysis at $\lambda > 345$ nm.

From these results long wavelength photolysis indicated the following reaction occurring:

$$(\eta^6\text{-naphthalene})Cr(CO)_3 \xrightarrow[\substack{\lambda > 345\ \text{nm} \\ CO}]{h\nu} \text{naphthalene} + Cr(CO)_6 \qquad (4.1.3.1)$$

This observation raised many questions as to exactly how did formation of $Cr(CO)_6$ occur. Is it possible that the metal to arene bond was cleaved upon photolysis which would then result in the initial formation of $Cr(CO)_3$ and naphthalene. The formation of $Cr(CO)_3$ would indicate the presence of essentially a 12 electron species which, if formed, would be extremely reactive. However, the exact mechanism of Reaction 4.1.3.1 is unknown and it is merely speculation that a $Cr(CO)_3$ fragment is produced following irradiation.

Initially, when the photochemistry of (η^6-benzene)$Cr(CO)_3$ was investigated, Strohmeier and von Hobe reported that upon photolysis formation of $Cr(CO)_6$ and uncomplexed benzene resulted.[2a] However these observations were later disputed,[2b] but in light of the experiments conducted on (η^6-

naphthalene)$Cr(CO)_3$ it appears that formation of $Cr(CO)_6$ does occur when experiments are carried out under CO.

At this stage it was decided to carry out a number of matrix isolation experiments, as this technique should give a better insight into the exact nature of the photochemistry of this compound.

4.1.4 Matrix isolation.

The matrix isolation technique was originally developed in order to study unstable molecular species, as with this experimental method the life-time of the trapped species is much longer. The main aim of matrix isolation is for the product formed to be present as an isolated species hence, a series of matrix isolation experiments were carried out at the Max-Planck-Institute in Mulheim. A number of matrices were used: Xe, Ar, N_2, CH_4 and CH_4/CO (10:1), to aid in characterising the observed photochemistry of this system. Matrix isolation has proved to be very apt at characterising unstable species, particularly unstable organometallic species some of which have been proposed as intermediates in thermal and photochemical reactions.

4.1.4.1 Xenon matrix.

The parent bands for (η^6-naphthalene)$Cr(CO)_3$ are present at 1975, 1914 and 1899 cm^{-1} in a Xe matrix. Upon photolysis at $\lambda = 460$ nm new bands were observed at 1970, 1906 and 1903 cm^{-1} - the latter two bands being as a result of what is known as the matrix splitting effect (see Figure 4.1.4.1.1). On irradiating the matrix at wavelength of 340 nm new bands were produced at 1918 and 1862 cm^{-1} as presented in Figure 4.1.4.1.2. On long wavelength photolysis these two bands decrease in intensity together with an increase in the parent bands which is typical of a reversible CO loss process.

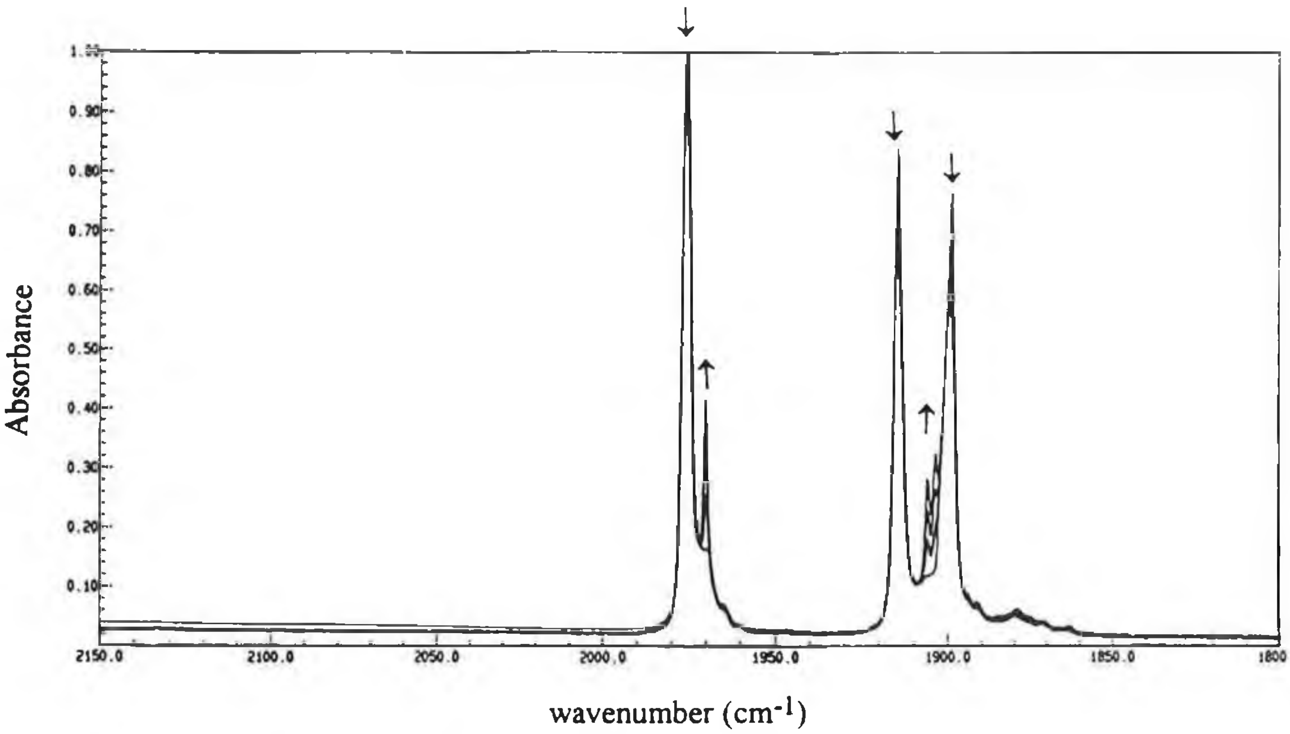

Figure 4.1.4.1.1 Spectral change of (η^6-naphthalene)$Cr(CO)_3$ in a xenon matrix following irradiation at 460 nm at 10K.

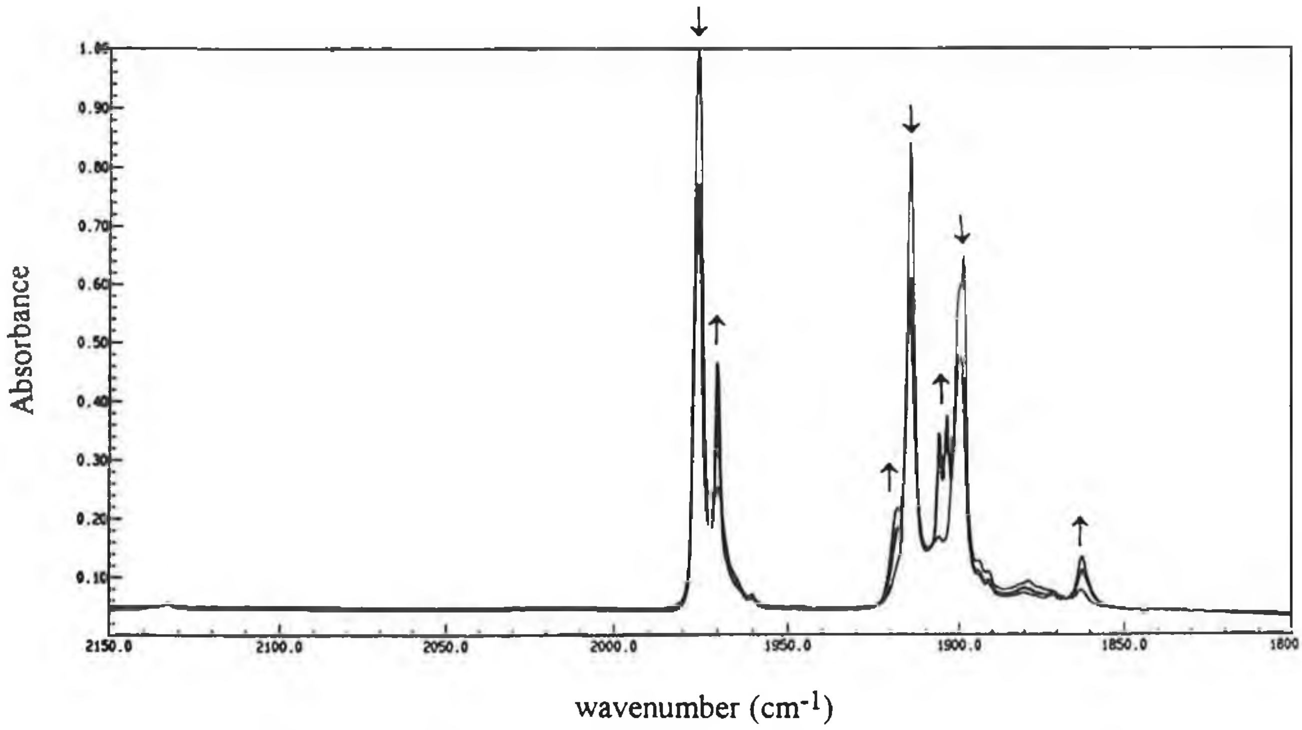

Figure 4.1.4.1.2 Spectral change of (η^6-naphthalene)$Cr(CO)_3$ in a xenon matrix following irradiation at 340 nm at 10K.

4.1.4.2 Argon matrix.

Parent absorptions bands for (η^6-naphthalene)$Cr(CO)_3$ are present at 1983, 1923 and 1907 cm^{-1} in an argon matrix. On photolysing the sample at 460 nm new bands were seen to form at 1979, 1916 and 1914 cm^{-1} (again the latter two as a result of matrix splitting), but the intensity of these two bands are extremely weak in comparison to the previous work carried out in the xenon matrix. On irradiating the matrix with wavelength of 340 nm bands at 1930 and 1872 cm^{-1} were produced as shown in Figure 4.1.4.2.1. On short wavelength photolysis both photoproducts are formed.

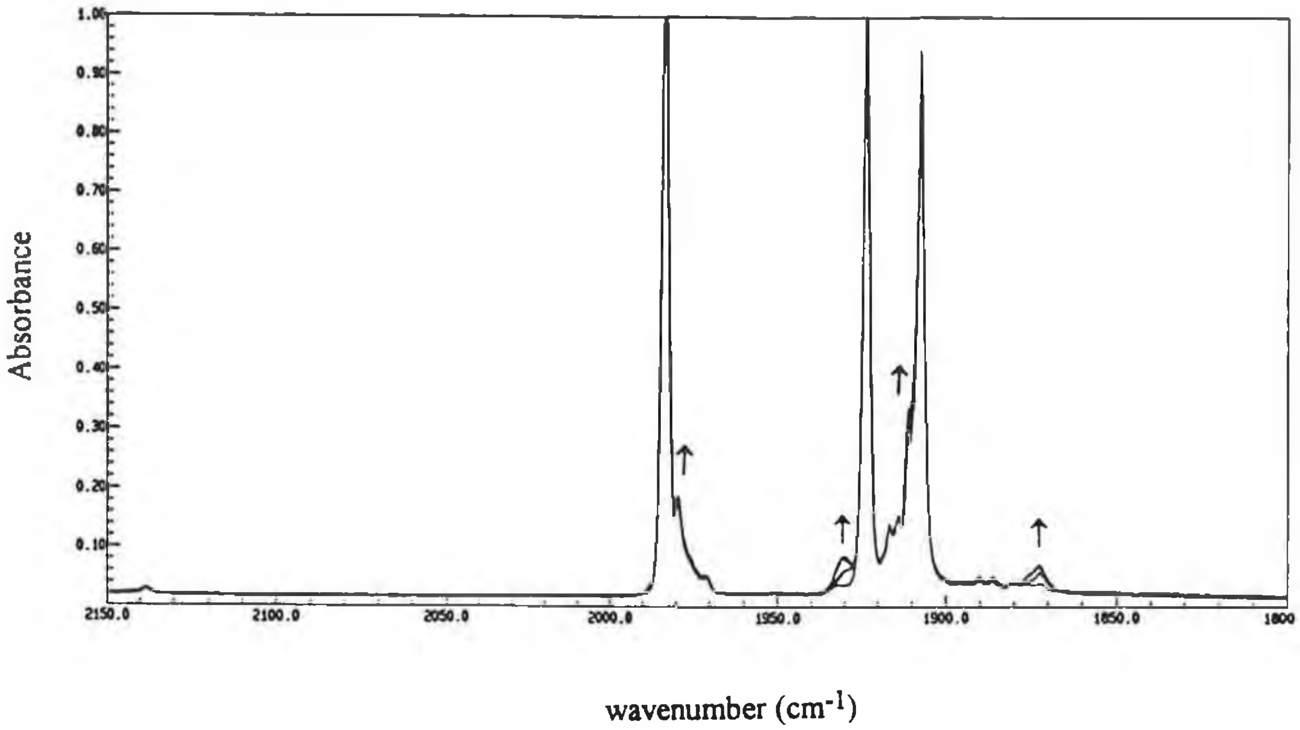

Figure 4.1.4.2.1 Spectral changes of (η^6-naphthalene)$Cr(CO)_3$ in a argon matrix following irradiation at 340 nm at 10K.

4.1.4.3 Dinitrogen matrix.

The bands for (η^6-naphthalene)Cr(CO)$_3$ are present at 1980, 1920 and 1903 cm^{-1} in a dinitrogen matrix. When a sample of (η^6-naphthalene)Cr(CO)$_3$ was irradiated in this matrix at long wavelength photolysis with either 460 or 430 nm no new bands were seen to form unlike in the previous matrices. However on photolysing the sample with wavelength of 340 nm new bands were seen to absorb at 1936 and 1888 cm^{-1}, along with a higher absorption at 2139 cm^{-1} which indicates a ν(N=N) vibration. The spectrum obtained is presented in Figure 4.1.4.3.1.

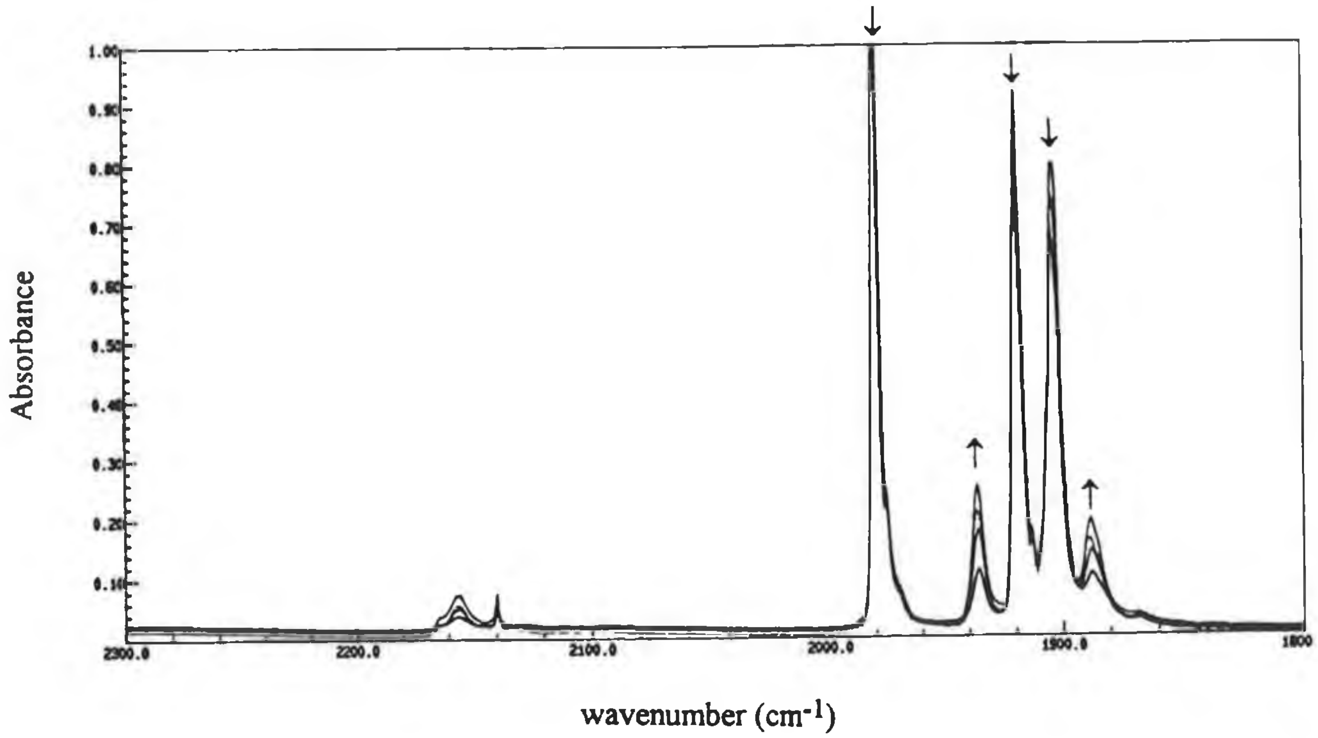

Figure 4.1.4.1 Spectral changes of (η^6-naphthalene)Cr(CO)$_3$ in a dinitrogen matrix following irradiation at 340 nm at 10K.

4.1.4.4 Methane matrix.

The infrared spectrum of (η^6-naphthalene)Cr(CO)$_3$ in a CH$_4$ matrix at 10K consists of four bands in the carbonyl stretching region at 1976, 1914, 1898 and 1896 cm^{-1} - the latter two again being a result of matrix splitting. On irradiation at 460 nm new bands were observed at 1971, 1906 and 1904 cm^{-1} (1906 and 1904 cm^{-1}-matrix splitting). On closer inspection of this spectrum (see Figure 4.1.4.4.1) it appears that the parent bands at 1898 and approximately 1896 cm^{-1} do not decrease at a similar intensity upon irradiation, thus indicating that another band is forming under this parent absorption at 1896 cm^{-1}. Therefore the new species formed on photolysing the sample at wavelength of 460 nm has three absorptions in the infrared region at 1971, 1904.5 and 1896 cm^{-1}. An infrared spectrum in the region 4000 to 1500 cm^{-1} was recorded and no evidence for uncomplexed naphthalene was present. The matrix was then subjected to irradiation at 340 nm which resulted in the formation of a further two bands, one at 1858 cm^{-1} and the other at 1914 cm^{-1}. As the parent band at 1914 cm^{-1} does not decrease at a similar intensity to that of the other parent bands, it is again indicative that further band is present at 1914 cm^{-1} on short wavelength photolysis as presented in Figure 4.1.4.4.2.

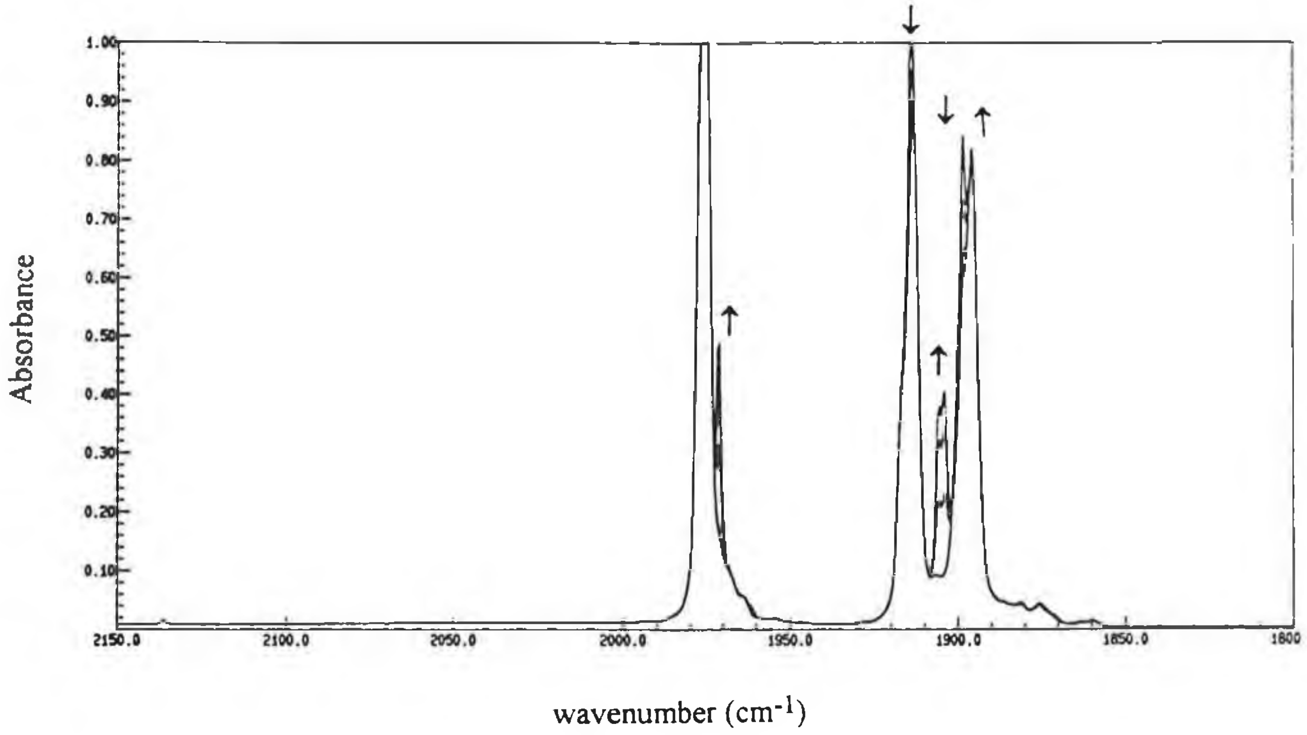

Figure 4.1.4.4.1 Spectral changes of (η^6-naphthalene)Cr(CO)$_3$ in a methane matrix following irradiation at 460 nm at 10K.

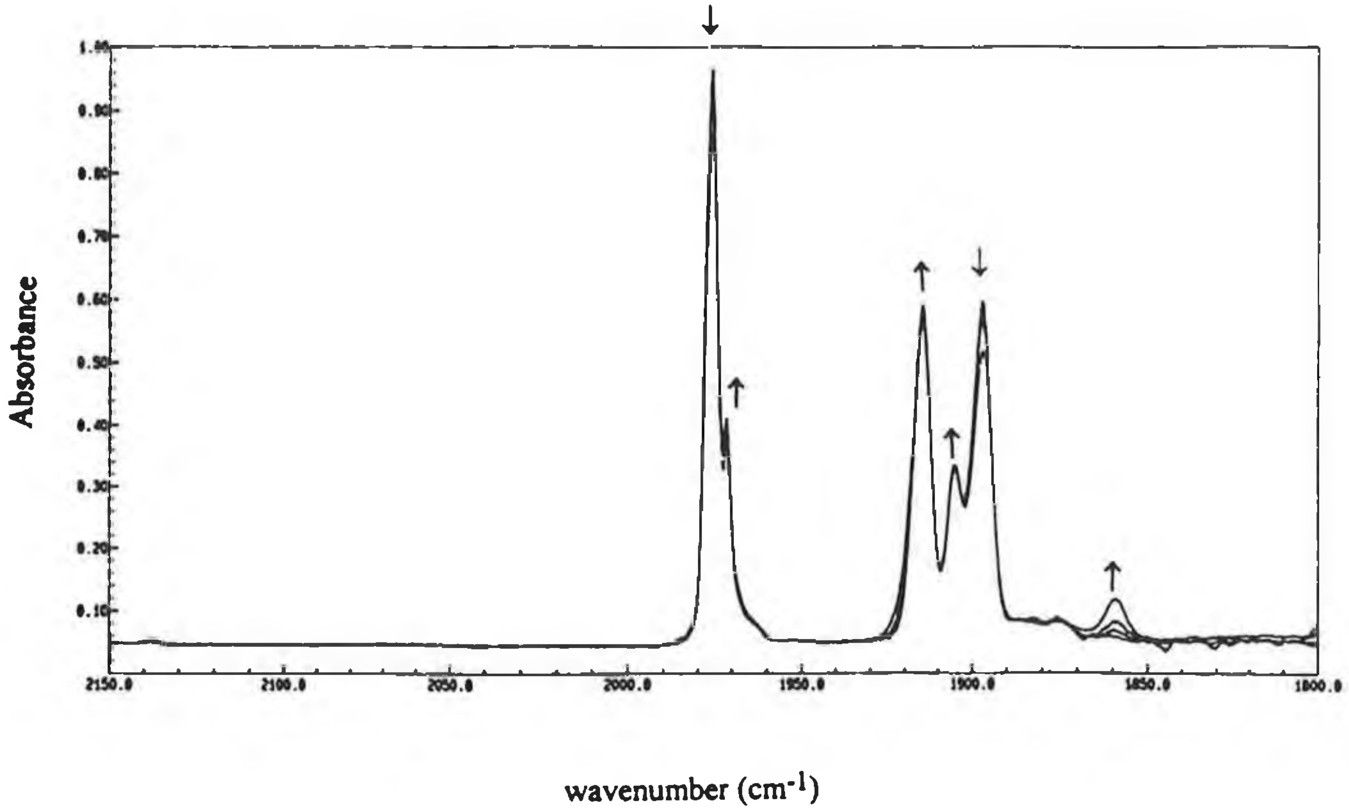

Figure 4.1.4.4.1 Spectral changes of (η^6-naphthalene)$Cr(CO)_3$ in a methane matrix following irradiation at 340 nm at 10K.

4.1.4.5 Methane:CO (10:1) matrix.

The infrared bands for the tricarbonyl compound are slightly shifted to lower frequency in a CO doped matrix, with the carbonyl stretches at 1973, 1911, and 1894 cm^{-1}. Following irradiation for 60 minutes at λ = 460 nm a weak absorption was observed at ~1985 cm^{-1}, which occurs concomitantly with a decrease in the absorption bands of the parent compound. No evidence was detected for the bands at 1971, 1905 and 1896 cm^{-1} previously observed in a methane matrix following irradiation at 460 nm. On photolysing the sample at 340 nm a very weak absorption at 1856 cm^{-1} was detected along with a further band at 1911 cm^{-1}. Because the parent bands at 1911 and 1894 cm^{-1} do not decrease at the same intensity it is indicative the presence of a product band underneath the parent band at 1911 cm^{-1}.

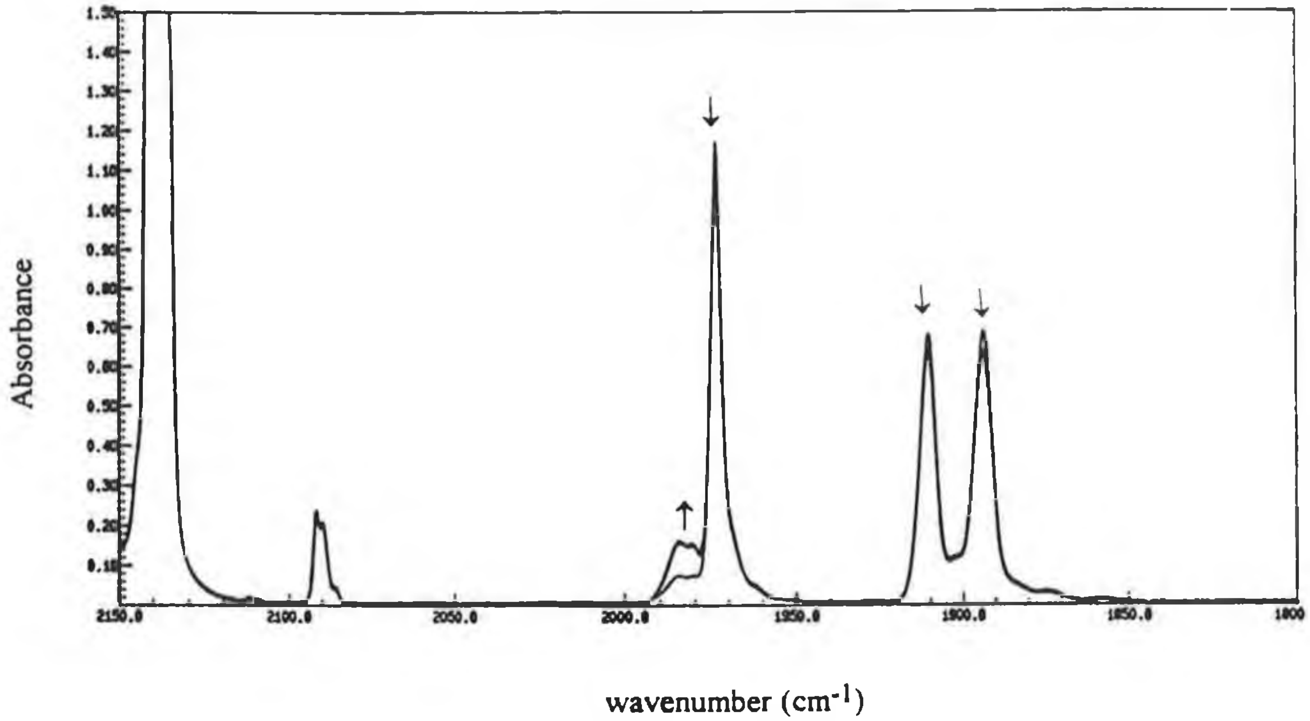

Figure 4.1.4.5.1 Spectral changes of (η^6-naphthalene)Cr(CO)$_3$ in a methane:CO (10:1) matrix following irradiation at 460 nm at 10K.

4.1.5 Discussion of matrix experiments.

The matrix experiments provided much more evidence to aid in characterising the photoproducts of this system. (η^6-Naphthalene)Cr(CO)$_3$ upon deposition has three stretching frequencies in the carbonyl region. On photolysis at λ = 460 nm new absorptions were seen to form in all matrices other than the dinitrogen matrix. On short wavelength photolysis at λ = 340 nm two absorptions were produced in all matrices. The results of the matrix isolation studies are summarised in Table 4.1.5.1.

	Xe cm^{-1}	Ar cm^{-1}	N_2 cm^{-1}	CH_4 cm^{-1}	CH_4:CO cm^{-1}
before irradiation	1975, 1914, 1899	1983, 1923, 1907	1980, 1920, 1903	1976, 1914, 1897	1973, 1911, 1894
λ = 460 nm	1970, 1904	1979, 1915	*	1970, 1905, 1896	1985
λ = 340 nm	1918, 1862	1930, 1872	1936, 1888, 2139	1914, 1858	1911, 1856

Table 4.1.5.1 Differences observed in the carbonyl region of the infrared spectrum following irradiation of (η^6-naphthalene)$Cr(CO)_3$. The bands observed following 460 nm irradiation are also observed following 340 nm irradiation along with the formation of further new bands. * no new bands observed following 460 or 430 nm photolysis.

If upon irradiation cleavage of the chromium to naphthalene bond occurred resulting in formation of a $Cr(CO)_3$ fragment only two bands would be expected in the infrared region based on work carried out by Pertuz and Turner[14] as shown in Table 4.1.5.2. These workers carried out extensive studies on $Cr(CO)_6$ and $Mo(CO)_6$ in a variety of matrices. In a methane matrix two bands at 1979 and 1889 cm^{-1} were observed which they assigned to $Cr(CO)_3$ and on further irradiation a band was observed at 1902 cm^{-1} which was reported to belong to a further CO loss product namely $Cr(CO)_2$, ($Cr(CO)_5$ and $Cr(CO)_4$ were also characterised). This work was repeated in a argon matrix but only one band at 1867 cm^{-1} was observed for the tricarbonyl fragment presumably because the other band was masked by another absorption. Gas phase experiments on $Cr(CO)_6$ were carried out by Church *et al.*[15] and from their work they concluded that coordinatively unsaturated photofragments in the gas phase compare well with those species previously identified in the condensed phase. Subsequently Ishikawa *et al.*[16] carried out gas phase studies on chromium and molybdenum tricarbonyls and their results correlated with that previously reported by Church and coworkers.[15]

metal fragment	Ar matrix cm^{-1}	CH_4 matrix cm^{-1}	Gas phase cm^{-1}
$Cr(CO)_3$	1867[a]	1979[a] 1889[a]	1880[b]
$Cr(CO)_2$		1902[a]	
η^6-benzene$Cr(CO)_2$	1937[c] 1885[c]	1925[c] 1870[c]	1981[d] 1917[d]

Table 4.1.5.2 Carbonyl stretching frequencies for the formation of $Cr(CO)_2$ and $Cr(CO)_3$ following irradiation of $Cr(CO)_6$, and (η^6-benzene)$Cr(CO)_2$ following irradiation of (η^6-benzene)$Cr(CO)_3$. [a] denotes reference 14, [b] reference 15, [c] reference 1, [d] reference 17.

On long wavelength photolysis of (η^6-naphthalene)$Cr(CO)_3$ in an argon matrix, formation of bands at 1979 and 1915 cm^{-1} resulted, which are very similar in frequency to the carbonyl bands obtained by Wang *et al.*[17] following photolysis of (η^6-benzene)$Cr(CO)_3$ in the gas phase. These bands at 1981 and 1917 cm^{-1} were assigned to (η^6-benzene)$Cr(CO)_2$. The absorptions for (η^6-benzene)$Cr(CO)_2$ in the gas phase are considerably shifted to higher frequency with regard to the values reported by Rest *et al.*[1] for formation of (η^6-benzene)$Cr(CO)_2$ in either an argon or methane matrix (Table 4.1.5.2).

Zheng *et al.*[18] investigated the photochemistry of the isoelectronic (η^5-C_5H_5)$Mn(CO)_3$ in the gas phase. Akin to the studies carried out on (η^6-benzene)$Cr(CO)_3$ in the gas phase[17] the bands observed for the dicarbonyl intermediate as presented in Table 4.1.5.3 are at a much higher wavenumber than those in either argon matrix[19], glasses[20] or solution[21].

fragment	argon[a]	glasses		*n*-heptane[d]	gas phase[c]
		MCH/IP[b]	HCH[c]		
	cm^{-1}	cm^{-1}		cm^{-1}	cm^{-1}
(η^5-C_5H_5)-$Mn(CO)_2$	1955 1886	1955 1886	1950 1880	1964 1895	2021 1874

Table 4.1.5.3 Carbonyl stretching frequencies for (η^5-C_5H_5)$Mn(CO)_2$ in various media. [a] reference 1, [b] reference 19, [c] reference 20, [d] reference 21.

From Table 4.1.5.3 it is apparent that the infrared absorption bands of (η^5-C_5H_5)Mn(CO)$_2$ in the gas phase are in disagreement with the corresponding values in condensed phases. Generally, the coordinatively unsaturated transition-metal carbonyls observed in the gas phase have their IR absorptions bands shifted by ~ 10-30 cm^{-1} to higher frequency than those in an argon matrix. In both the chromium and the manganese systems the positions of the dicarbonyl absorptions are shifted to a considerably greater extent in the gas phase. This variation has been explained in terms of the interaction of the dicarbonyl with the host matrix. This theory was based on previous work[22] where it was indicated that interaction with even a relatively inert matrix material can cause distortion. There have been other publications where coordinatively unsaturated molecules show significant differences in structure between matrix and gas phase.[23]

The systems investigated by Wang *et al.*[17], (η^6-benzene)Cr(CO)$_3$ and Zheng *et al.*[18], (η^5-cyclopentadienyl)Mn(CO)$_3$, in the gas phase were reported to be photoreversible as the bands assignable to the dicarbonyl species returned to base-line at a similar rate to the bands for depletion of parent.

In condensed phases the ejection of benzene the ligand from photo-excited (η^6-benzene)Cr(CO)$_3$ is considered to be very inefficient, if it occurs at all. Nevertheless it still remains a concern whether a pathway exists involving the loss of benzene when (η^6-benzene)Cr(CO)$_3$ is in an excited state.[24] The bond energy between the chromium centre and the benzene ligand is estimated to be 180 kJ/mol.[25] Wang and coworkers[17] noted a weak absorption at ~ 1999 cm^{-1} following 355 nm flash photolysis (η^6-benzene)Cr(CO)$_3$ in the gas phase in the presence of CO.[17] The absorption at 1999 cm^{-1} occurred in the latter part of the experiment and only in the presence of CO, hence suggesting that the absorption is due to a secondary product formed *via* the reaction of the primary photoproduct with CO. This absorption they attributed to be as a result of formation of Cr(CO)$_6$[26] formed by the consecutive addition of three CO molecules to the primary Cr(CO)$_3$ fragment.

In view of the observations by Perutz and Turner[14] it is extremely unlikely that cleavage of the Cr-naphthalene bond occurs on irradiating this compound, as in this set of experiments three bands are observed in the infrared region rather than the reported two band pattern for formation of the tricarbonyl fragment. It appears that the product formed on long wavelength photolysis is most probably a tricarbonyl species that is in some way bound to the naphthalene ligand, as the bands observed following irradiation are only shifted slightly to lower frequency to those of the parent bands.

Albright *et al.*[27] reported a detailed theoretical investigation into the minimum energy pathways for shifting of the $Cr(CO)_3$ group from one ring to another in bicyclic polyenes, which has been termed haptotropic rearrangements. One of the systems on which a detailed theoretical investigation was carried out was (η^6-naphthalene)$Cr(CO)_3$. Figure 4.1.5.1 gives a potential energy surface diagram for shifting of the $Cr(CO)_3$ moiety relative the naphthalene ring.

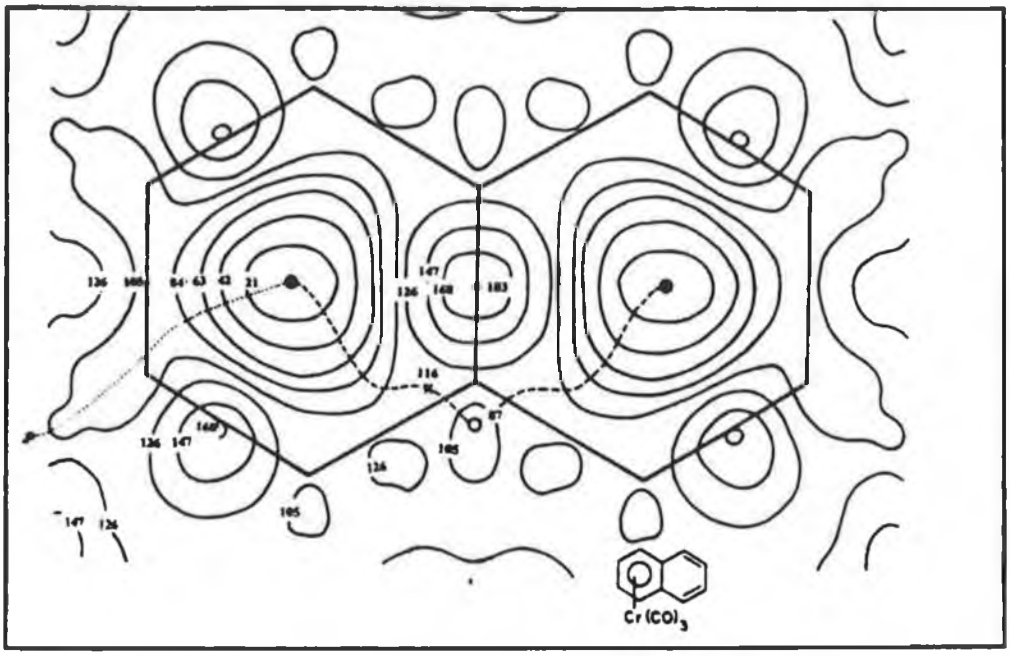

Figure 4.1.5.1 The potential energy surface diagram for shifting of the $Cr(CO)_3$ moiety relative the naphthalene ring. Diagram from reference 27.

The energy contours are given in kJ/mol and are symbolised by solid circles. To attain the central η^2 geometry as presented in Figure 4.1.5.2 requires 183 kJ/mol, which is close to the computed binding energy of $Cr(CO)_3$ to the naphthalene being (197 kJ/mol). The calculated minimum energy pathway is shown by a dashed line. A transition state indicated by a cross and a local minimum shown by a open circle are computed to be 117 and 88 kJ/mol respectively less stable than the ground state. Thus the non-least motion pathway is definitely favoured over a least motion alternative. Hence, a η^2 structure is not on the lowest energy pathway for a haptotropic rearrangement. In view of the location of the lowest energy minimum a η^3 type intermediate is likely which is essentially a 16 electron η^3-allylCr(CO)$_3$ anion with a heptatrienyl cation fused to the allyl portion.

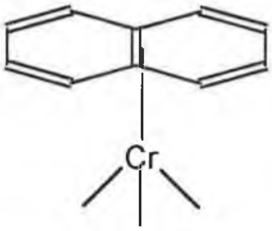

Figure 4.1.5.2

As a consequence of the results obtained by Albright *et al.*[27] it would be plausible to assume that on long wavelength photolysis a η^3 type intermediate as show in Figure 4.1.5.3 is formed.

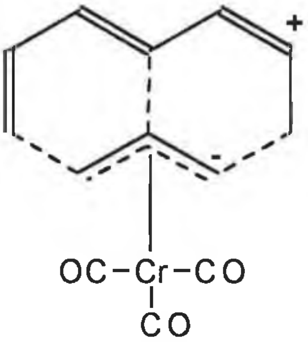

Figure 4.1.5.3

In the matrix experiments this η^3-allyl intermediate is isolated and trapped and three bands are observed for its formation. However the solution photochemistry is somewhat different. In solution this intermediate is most likely extremely unstable and hence the Cr(CO)$_3$ fragment is lost from the aromatic system and in the presence of CO formation of Cr(CO)$_6$ results. The exact mechanism for the formation of Cr(CO)$_6$ is unknown and further experiments are required to ascertain this information.

4.1.6 Activation parameters for reaction of (η^6-naphthalene)$Cr(CO)_2$-(cyclohexane) with CO.

The activation parameters for the reaction of (η^6-naphthalene)$Cr(CO)_2$-(cyclohexane) with CO were calculated using Arrhenius and Eyring plots. The second order rate constant k_2 used in the calculation was calculated by dividing $k_{obs}/[CO]$ where the concentration of CO equals 9.0×10^{-3}M. The activation parameters are listed in Table 4.1.6.1, the experimental data is given in Table 4.1.6.2 and the corresponding graphs in Figure 4.1.6.1.

$\Delta H^{\neq}$	26 ± 2 kJmol^{-1}
$\Delta S^{\neq}$	-27 ± 5 Jmol^{-1}K^{-1}
$\Delta G^{\neq}_{(298K)}$	34 ± 2 kJmol^{-1}

Table 4.1.6.1 Activation parameters for the reaction of (η^6-naphthalene)$Cr(CO)_2$(cyclohexane) towards CO.

The results in Table 4.1.6.1 are in agreement with the results determined in Chapter 2. $\Delta H^{\neq}$ for the recombination of CO was measured to be 26 kJmol^{-1} which is within the error of the data obtained for any of the monoaromatic systems. The activation entropy $\Delta S^{\neq}$ was measured to be -27 kJmol^{-1}K^{-1} which is in agreement with previous reports. This observation along with the $\Delta H^{\neq}$ value is indicative of an interchange mechanism occurring, whereby the solvent molecule is ejected at the same time as the CO ligand forms a bond with the metal as presented in Figure 4.1.6.2.

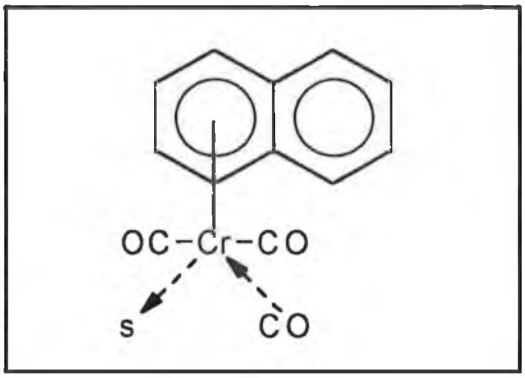

Figure 4.1.6.2

Temp. (K)	$1/T \times 10^3$ (K^{-1})	k_{obs} (s^{-1}) $\times 10^{-4}$	$Ln(k_{obs}/[CO])$	$Ln(k_{obs}/[CO] \cdot T)$
289	3.46	3.2	15.09	9.43
293	3.41	4.2	15.35	9.67
299	3.36	5.1	15.54	9.84
303	3.30	5.9	15.69	9.98
308	3.24	7.1	15.88	10.15
311	3.19	8.6	16.07	10.32

Arrhenius Plot
Slope = -3446 ± 185
Intercept = 27.06 ± 0.04
Correlation coefficient = 0.99

Eyring Plot
Slope = -3129 ± 171
Intercept = ± 0.04
Correlation coefficient = 0.99

$E_a^{\neq} = 29 \pm 2$ kJmol^{-1}
$\Delta H^{\neq} = 26 \pm 2$ kJmol^{-1}
$\Delta S^{\neq} = -27 \pm 5$ Jmol^{-1}K^{-1}
$\Delta G^{\neq} = 34 \pm 2$ kJmol^{-1}

Table 4.1.6.2 Experimental data for the determination of the activation parameters the reaction of (η^6-naphthalene)$Cr(CO)_2$(cyclohexane) towards CO to regenerate parent tricarbonyl.

(a)

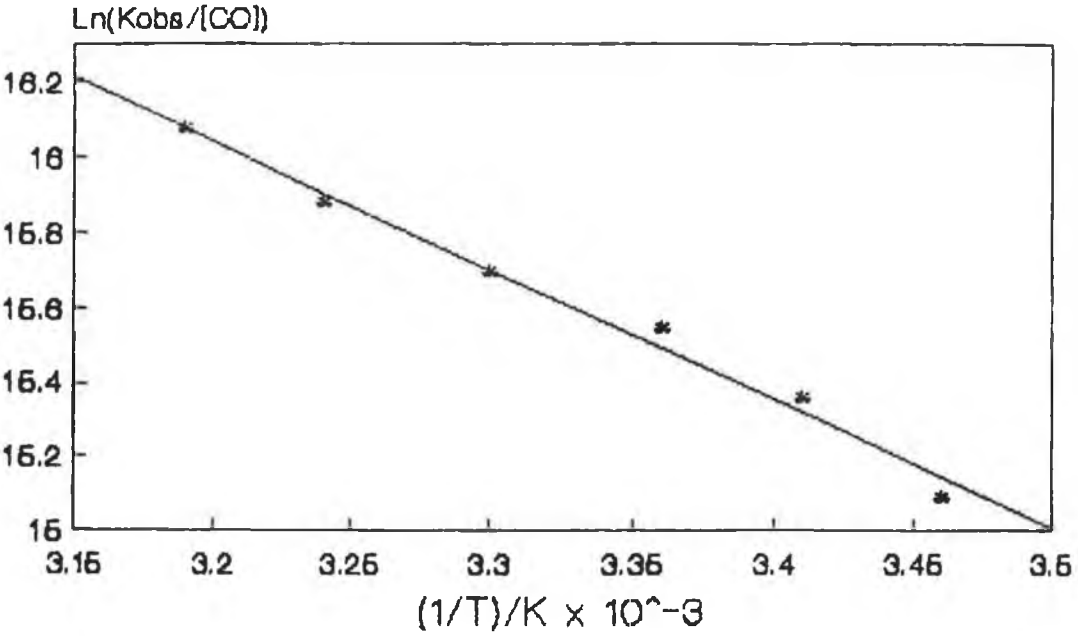

(b)

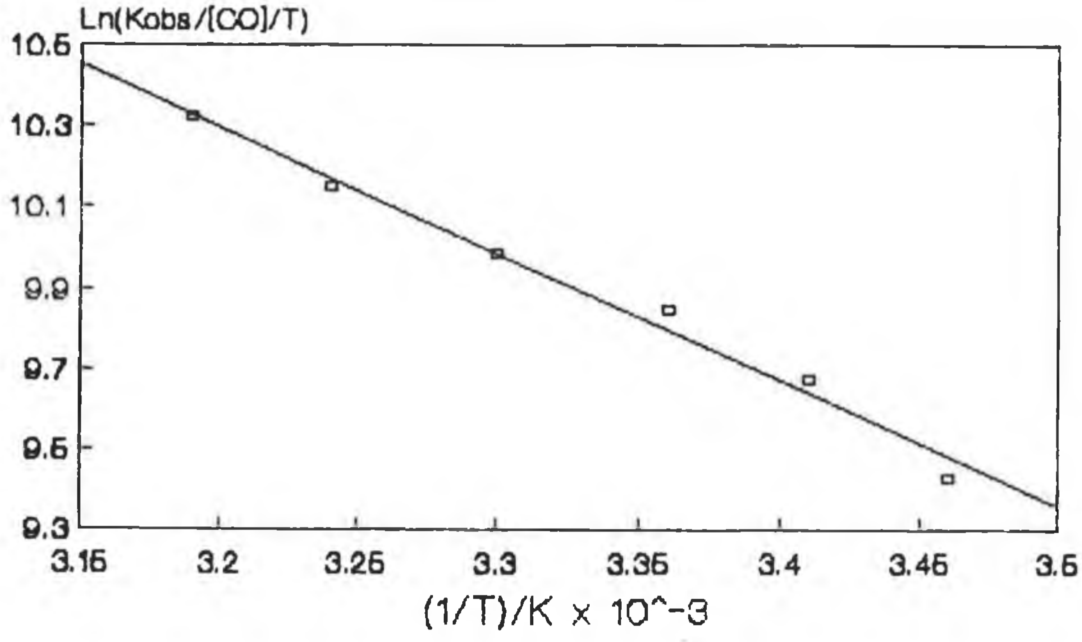

Figure 4.1.6.1 Arrhenius(a) and Eyring(b) plots the reaction of (η^6-naphthalene)Cr(CO)$_2$(cyclohexane) with CO to regenerate the parent complex.

4.2 (η^6-Phenanthrene)$Cr(CO)_3$.

4.2.1 Electronic absorption spectrum of (η^6-phenanthrene)$Cr(CO)_3$.

The UV/vis. spectrum of (η^6-phenanthrene)$Cr(CO)_3$ in cyclohexane is given in Figure 4.2.1.1. A $\lambda_{max.}$ is prominent at approximately 370 nm which is assigned to a chromium ----> arene charge transfer transition with some chromium ----> π^* CO charge transfer character. These assignments are based primarily on investigations into the electronic absorption spectrum of (η^6-benzene)$Cr(CO)_3$.[11] There is also a shoulder centred about 290 nm which is assigned to being metal ----> π^* CO CT. In the valley of the spectrum there is an absorption at approximately 310 nm, which was not previously observed in the alkyl substituted monoaromatic systems, but in the naphthalene analogue a similar absorption was visible at ~ 305 nm which was speculated to be a ligand field transition. There is a shoulder at 450 nm which could possibly be MLCT in nature but again this is merely speculation. The differences in the spectra between naphthalene and phenanthrene are quite marked, in so far as naphthalene tricarbonyl absorbs further into the visible than the phenanthrene compound.

4.2.2 Laser flash photolysis of (η^6-phenanthrene)$Cr(CO)_3$.

For this compound all laser flash photolysis experiments were conducted at 355 nm excitation. Following laser flash photolysis in cyclohexane (ε_{355} = 7730 $dm^3 mol^{-1} s^{-1}$) under 1 atm. of CO a transient species absorbed at 290 nm. A typical transient signal observed at this wavelength is presented in Figure 4.2.2.1 along with depletion of parent which occurs at 370 nm.

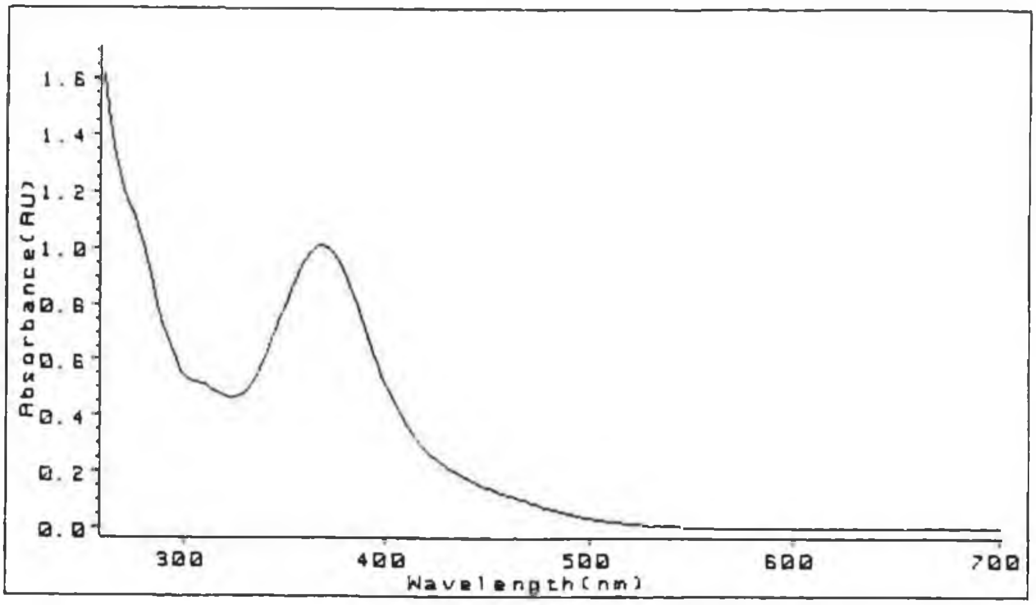

Figure 4.2.1.1 UV/vis. spectrum of (η^6-phenanthrene)$Cr(CO)_3$ (1.07 x10^{-4}M) in cyclohexane.

The concentration of CO admitted to the cell was varied, no change in yield was observed but as the concentration of CO increased the life-time of the species at 290 nm decreased. This transient species was assigned to the dicarbonyl intermediate as a linear relationship exists between the concentration of CO and the observed rate constant. The second order rate constant was calculated by plotting k_{obs} *versus* concentration of CO, the slope of the line represents the second order rate constant, 5.93 x 10^6 dm^3 s^{-1} mol^{-1}. This value is very similar to that obtained for the reaction of (η^6-naphthalene)$Cr(CO)_2$(cyclohexane) towards CO.

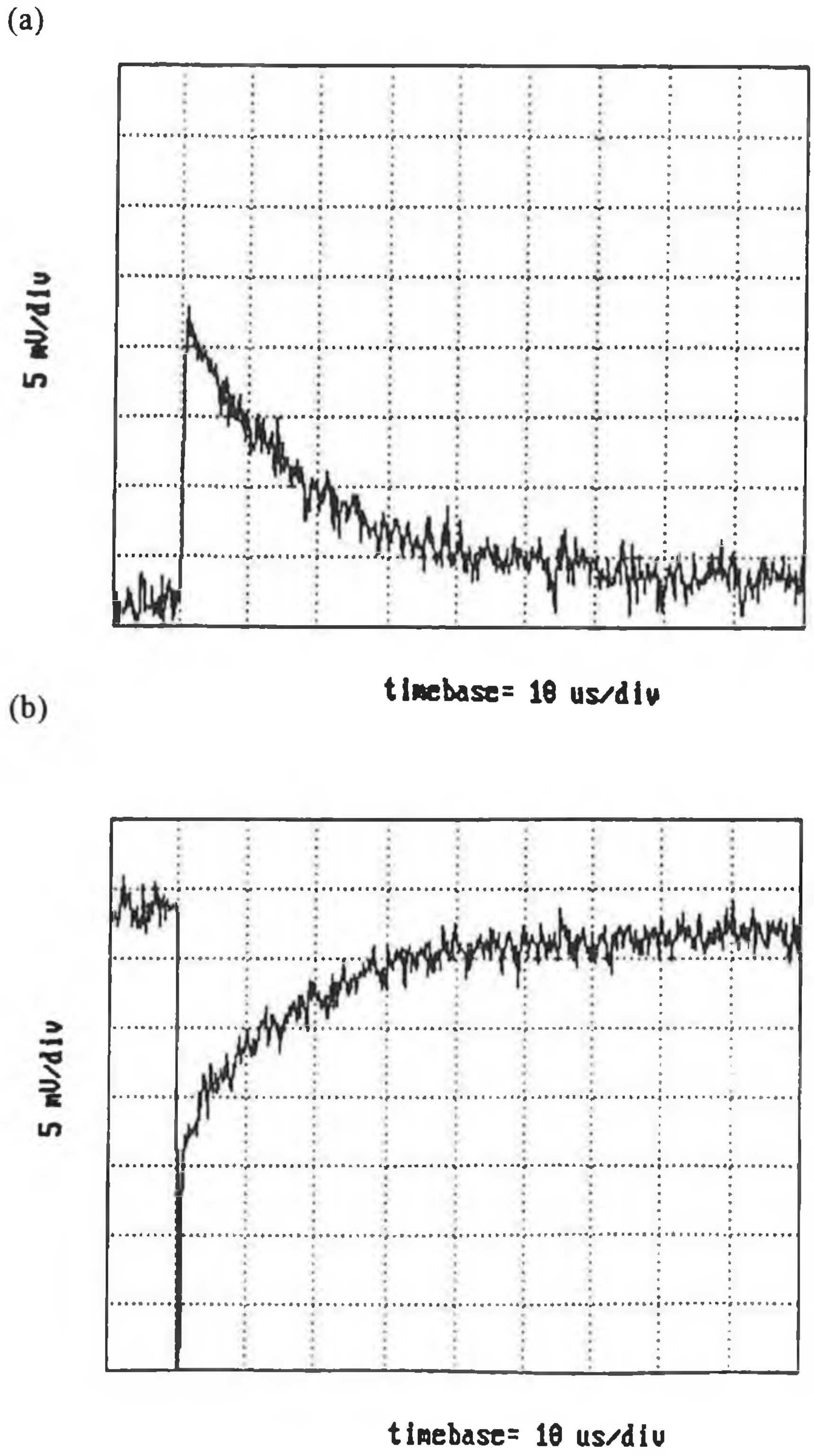

Figure 4.2.2.1 A typical transient signal obtained for (a) the decay of (η^6-phenanthrene)Cr(CO)$_2$(cyclohexane) at 290 nm and (b) the recovery of the tricarbonyl compound at 370 nm under 1 atm (9.0 x 10^{-3}M) CO.

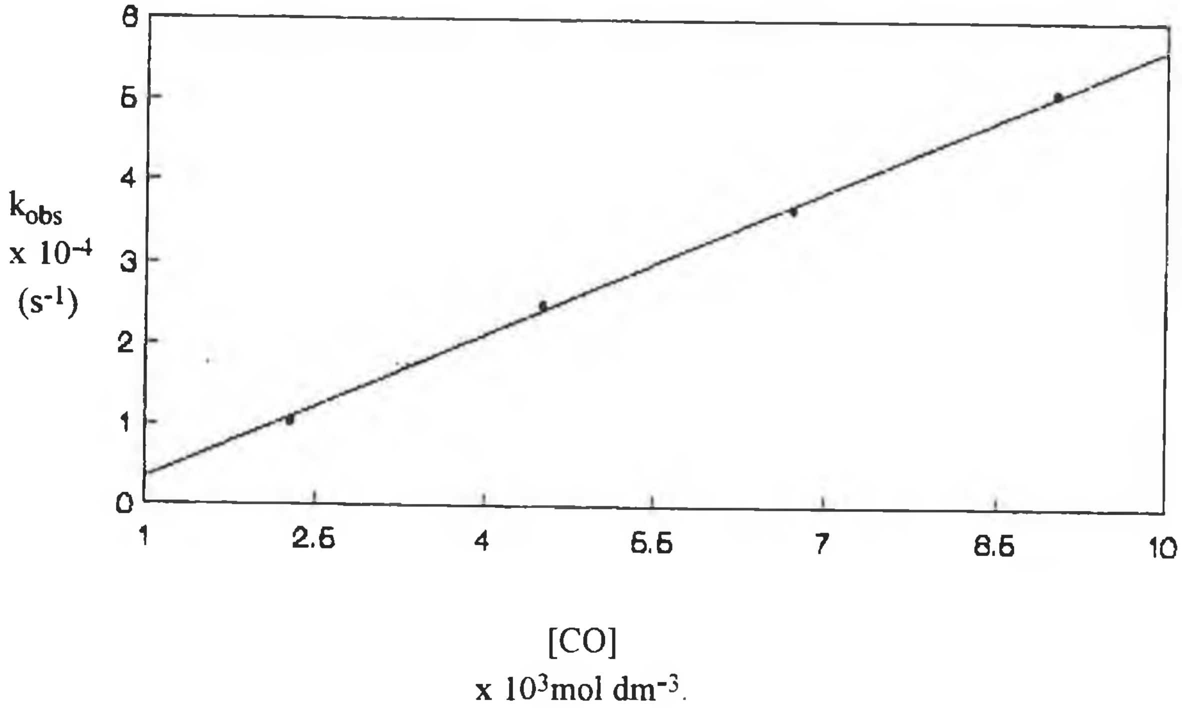

[CO] x 10^3 mol dm^{-3}	k_{obs} (s^{-1}) x 10^{-4}
2.25	1.05
4.50	2.4
6.75	3.6
9.00	5.1

slope = 5.93 $10^6 \pm 2.03 \times 10^{-5}$
intercept = -30.00 x $10^{-2} \pm 8.87 \times 10^{-2}$
correlation coefficient = 0.99

Figure 4.2.2.2 A plot of concentration of CO (mol dm^{-3}) against the observed rate constant for the reaction of CO with the (η^6-phenanthrene)$Cr(CO)_2$(cyclohexane) at 298K.

The UV/vis. difference spectrum obtained following flash photolysis under 1 atm. of CO is given in Figure 4.2.2.3. An absorption occurs at 290 nm which is assignable to the solvated dicarbonyl species together with a depletion of parent at 370 nm.

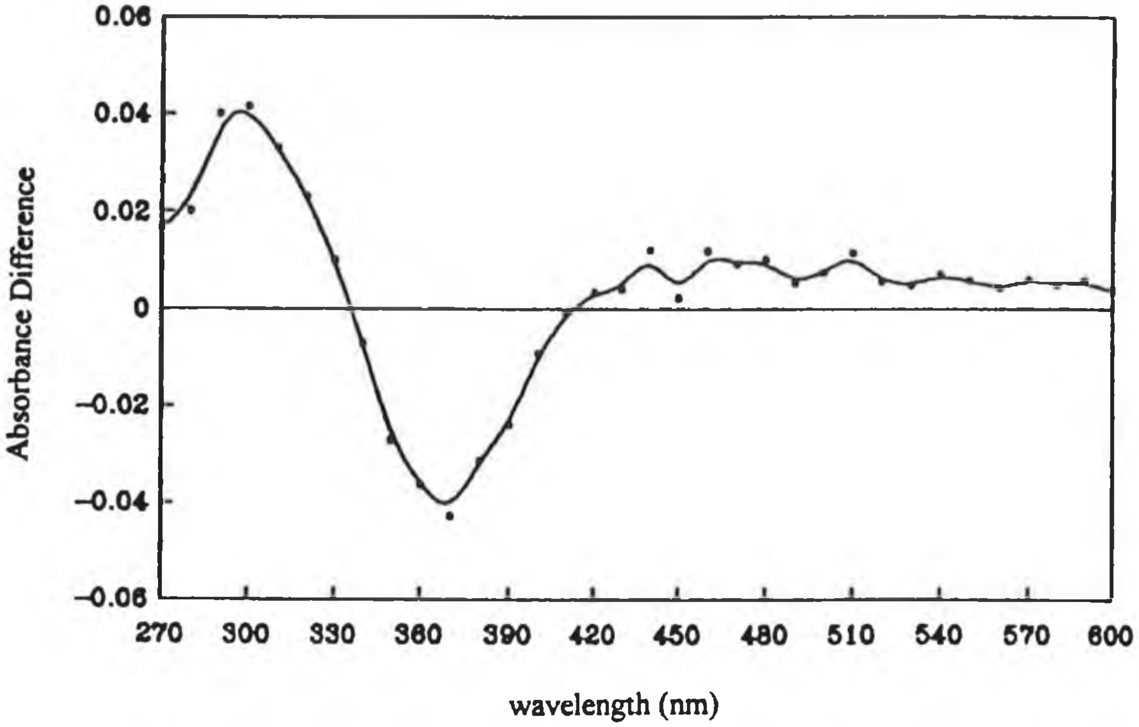

Figure 4.2.2.3 UV/vis. difference spectrum following flash photolysis of (η^6-phenanthrene)$Cr(CO)_3$ in cyclohexane at 355 nm under 1 atm. of CO (9.0×10^{-3}M) at 298K.

4.2.3 Steady state photolysis with monitoring by luminescence spectroscopy.

Phenanthrene luminesces strongly[28] however on complexation to $Cr(CO)_3$, luminescence is quenched. Hence, if on photolysis the aromatic ring is lost, it's presence can be monitored by luminescence spectroscopy. As before it was decided to carry out long wavelength photolysis on this system as it absorbs in the visible region. Room temperature photolysis of (η^6-phenanthrene)$Cr(CO)_3$ at $\lambda > 345$ nm under 1 atm. of CO resulted in the formation of uncomplexed phenanthrene as monitored by luminescence spectroscopy. Given in Figure 4.2.3.1. are luminescence spectra of phenanthrene obtained after 10 and 20 minutes photolysis of (η^6- phenanthrene)$Cr(CO)_3$. Throughout the photolysis the electronic absorption spectrum was recorded. again slight changes in absorbance were obvious as shown in Figure 4.2.3.2. At the end of the experiment an infrared spectrum indicated formation of $Cr(CO)_6$.

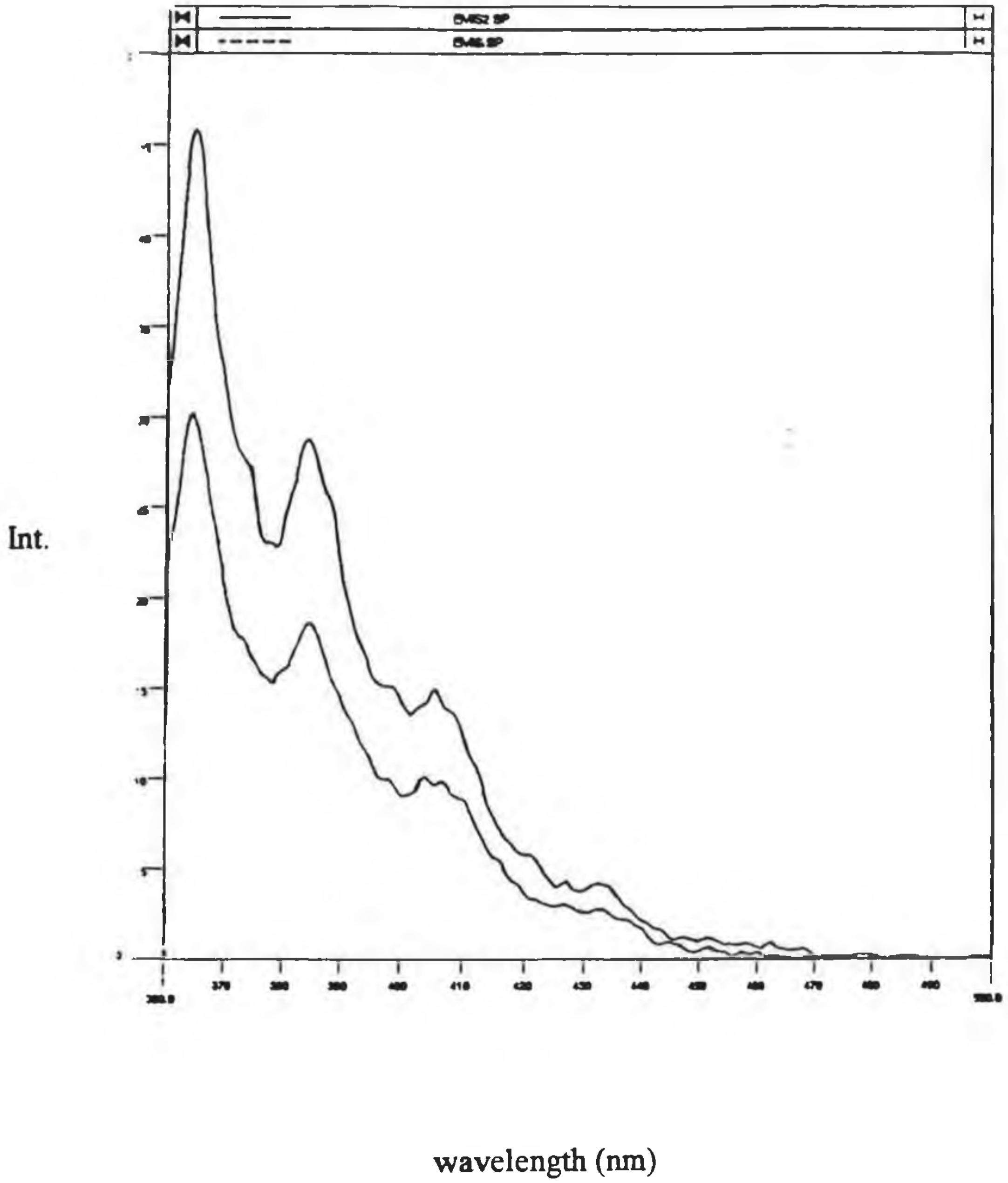

Figure 4.2.3.1 Luminescence spectra obtained after 10 and 20 minutes photolysis of (η^6- phenanthrene)$Cr(CO)_3$ at $\lambda > 345$ nm in cyclohexane under 1 atm. of CO.

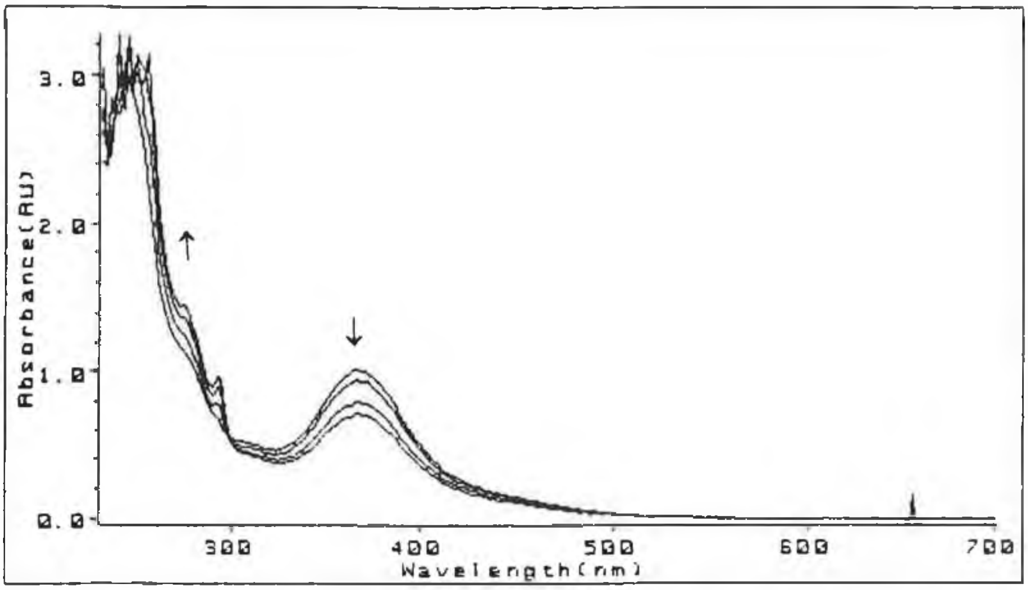

Figure 4.2.3.2 Changes observed in the UV/vis. spectrum of (η^6-phenanthrene)$Cr(CO)_3$ following photolysis at $\lambda > 345$ nm.

These results indicate that on long wavelength photolysis the following reaction occurs:

$$(\eta^6\text{- phenanthrene})Cr(CO)_3 \xrightarrow[\lambda > 345\ nm\ \ CO]{h\nu} \text{phenanthrene} + Cr(CO)_6 \qquad (4.2.3.1)$$

Matrix isolation experiments were not carried out on this system but from both the laser experiments and the continued photolysis as monitored by luminescence it appears that similarly to the experiments carried out on the naphthalene analogue, arene loss is the predominant photochemical reaction on long wavelength photolysis.

Consequently, two photochemical reactions are occurring on 355 nm flash photolysis, loss of CO to generate the dicarbonyl intermediate which in the presence of CO recombined to regenerate the parent compound and arene loss to form $Cr(CO)_6$ and uncomplexed phenanthrene. In the case of the naphthalene compound arene loss was proposed to occur through a "η^3" type allyl naphthalene intermediate. In a matrix environment this intermediate is stabilised but in solution this is not so and therefore recombines with CO to form $Cr(CO)_6$ which was detected by infrared spectroscopy. Infrared spectra of (η^6-phenanthrene)$Cr(CO)_3$ before and after a laser experiment carried out under 1 atm. of carbon monoxide are given in Figure 4.2.3.3. Presumably, in the case of the phenanthrene compound a similar reaction occurs as the laser experiments and luminescence studies yield similar results to those of the naphthalene system. In the haptotropic rearrangement the $Cr(CO)_3$ fragment is lost from the metal centre resulting in the formation of the products observed.

Migration of tricarbonyl groups in phenylanthracenes between two non-adjacent six membered rings is not unusual and has been reported by Cunningham *et al.*[29] On heating a solution of I in dioxane a colour change from yellow to purple was noted which indicated migration of the tricarbonyl group from one aromatic ring to another as shown by ^1H NMR to form product II as given in Reaction 4.2.3.1.

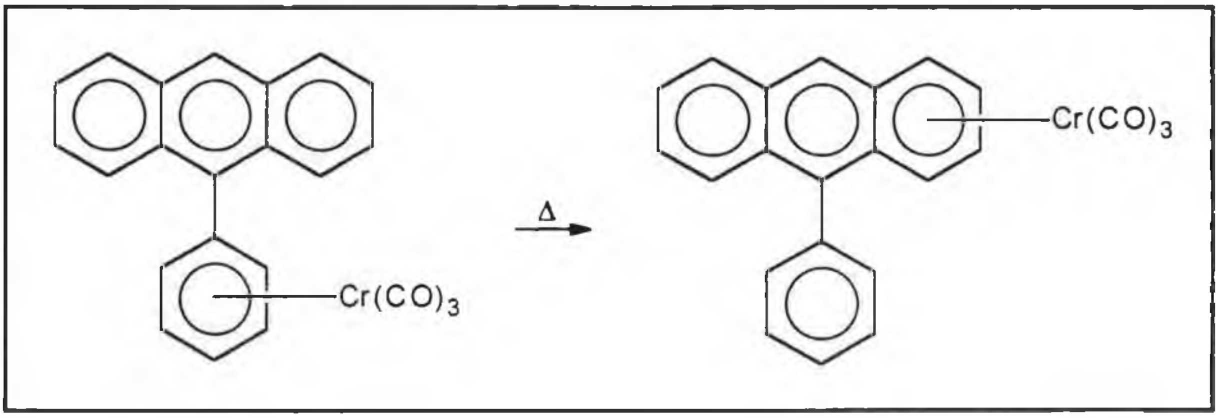

I II

Reaction 4.2.3.1.

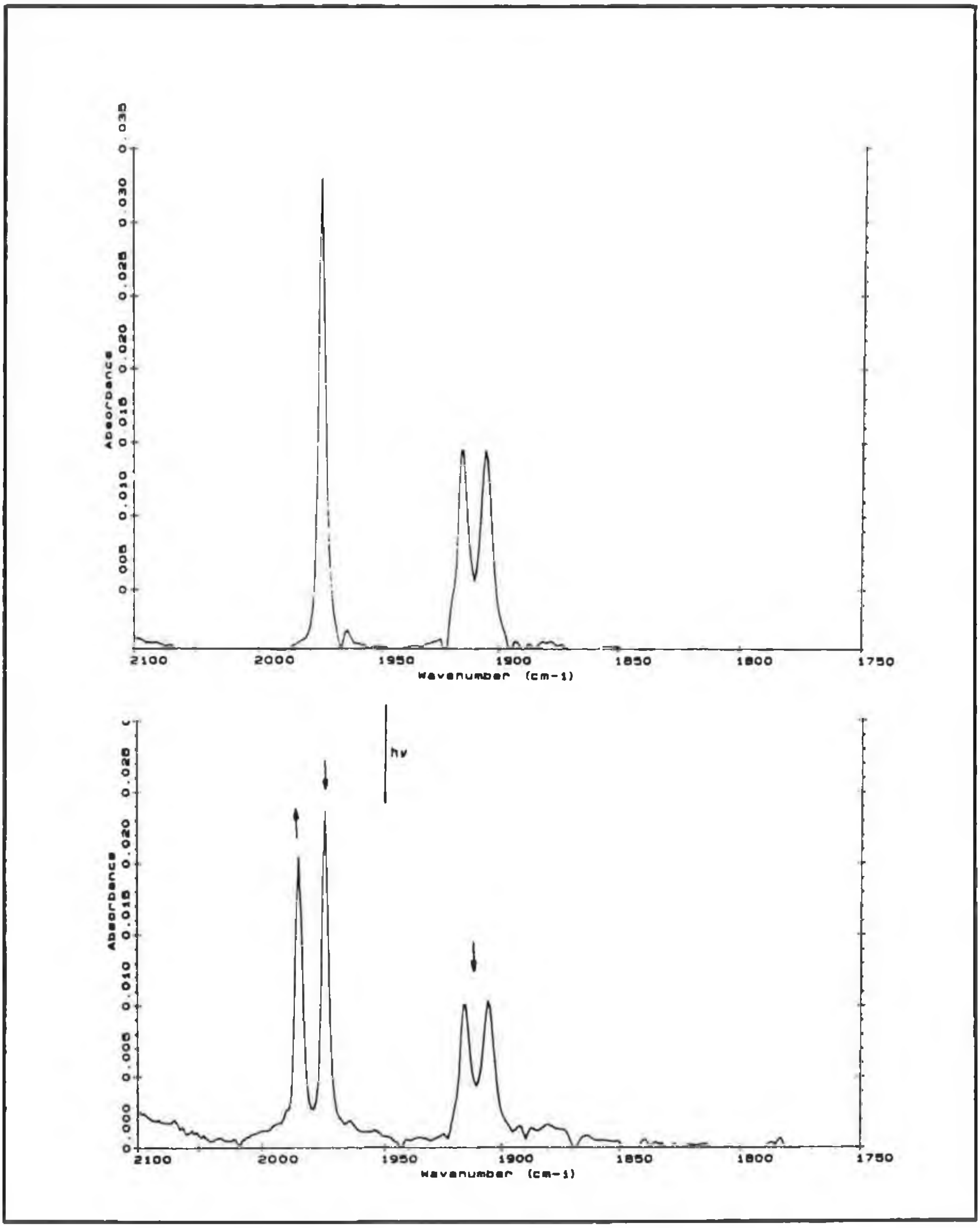

Figure 4.2.3.3 Infrared spectra of (η^6- phenanthrene)$Cr(CO)_3$ before and after a laser experiment carried out under one atmosphere of CO.

4.2.4 Activation parameters for reaction of (η^6- phenanthrene)Cr(CO)$_2$-(cyclohexane) with CO.

The activation parameters for the reaction of (η^6-phenanthrene)-Cr(CO)$_2$(cyclohexane) with CO were calculated using Arrhenius and Eyring plots. The second order rate constant k_2 used in the calculation was calculated by dividing k_{obs}/[CO] where the concentration of CO equals 9.0 x 10^{-3}M. The activation parameters are listed in Table 4.2.4.1, the experimental data is given in Table 4.2.4.2 and the corresponding graphs in Figure 4.2.4.1.

$\Delta H^{\neq}$	25 $\pm$ 2 kJmol^{-1}
$\Delta S^{\neq}$	- 30 $\pm$ 5 Jmol^{-1}K^{-1}
$\Delta G^{\neq}_{(298K)}$	34 $\pm$ 2 kJmol^{-1}

Table 4.2.4.1 Activation parameters for the reaction of (η^6-phenanthrene)Cr(CO)$_2$(cyclohexane) towards CO.

The results in Table 4.2.4.1 are similar to the results obtained for the activation parameters calculated for (η^6-naphthalene)Cr(CO)$_3$. $\Delta H^{\neq}$ for the recombination of CO was measured to be 25 kJmol^{-1} for this compound as opposed to 26 kJmol^{-1} for the likewise reaction for (η^6-naphthalene)Cr(CO)$_3$. The activation entropy $\Delta S^{\neq}$ was measured to be -30 kJmol^{-1}K^{-1} which is in agreement with the naphthalene system and previous reports,[3] thus agreeing with an interchange mechanism occurring as presented in Figure 4.2.4.2.

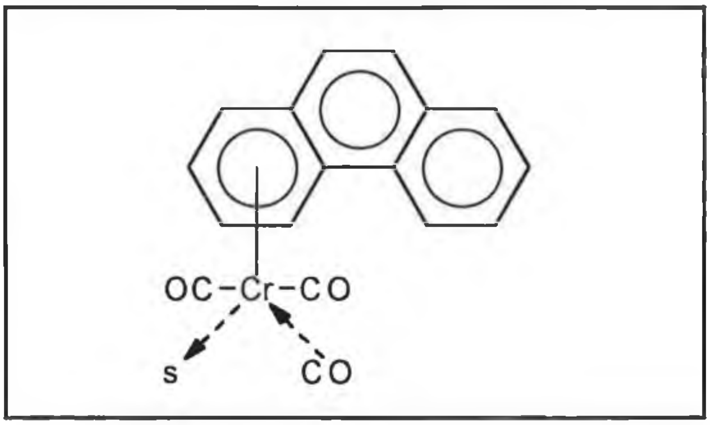

Figure 4.2.4.2

Temp. (K)	1/T x 10^3 (K^{-1})	k_{obs} (s^{-1}) x 10^{-4}	Ln(k_{obs}/[CO])	Ln(k_{obs}/[CO] . T)
283	3.53	2.61	14.88	9.23
289	3.46	3.28	15.11	9.45
293	3.41	4.43	15.41	9.73
299	3.36	5.31	15.59	9.89
303	3.30	5.63	15.65	9.9
308	3.24	6.95	15.86	10.13
311	3.19	8.49	16.06	10.31

Arrhenius Plot	
Slope	= -3373 ± 184
Intercept	= 26.83 ± 0.05
Correlation coefficient	= 0.99

Eyring Plot	
Slope	= - 3074 ± 184
Intercept	= 10.13 ± 0.05
Correlation coefficient	= 0.99

$E_a^{\neq}$ = 28 ± 2 $kJmol^{-1}$
$\Delta H^{\neq}$ = 25 ± 2 $kJmol^{-1}$
$\Delta S^{\neq}$ = -30 ± 5 $Jmol^{-1}K^{-1}$
$\Delta G^{\neq}$ = 34 ± 2 $kJmol^{-1}$

Table 4.2.4.2 Experimental data for the determination of the activation parameters for the reaction of (η^6-phenanthrene)$Cr(CO)_2$(cyclohexane) with CO to regenerate the parent tricarbonyl complex.

(a)

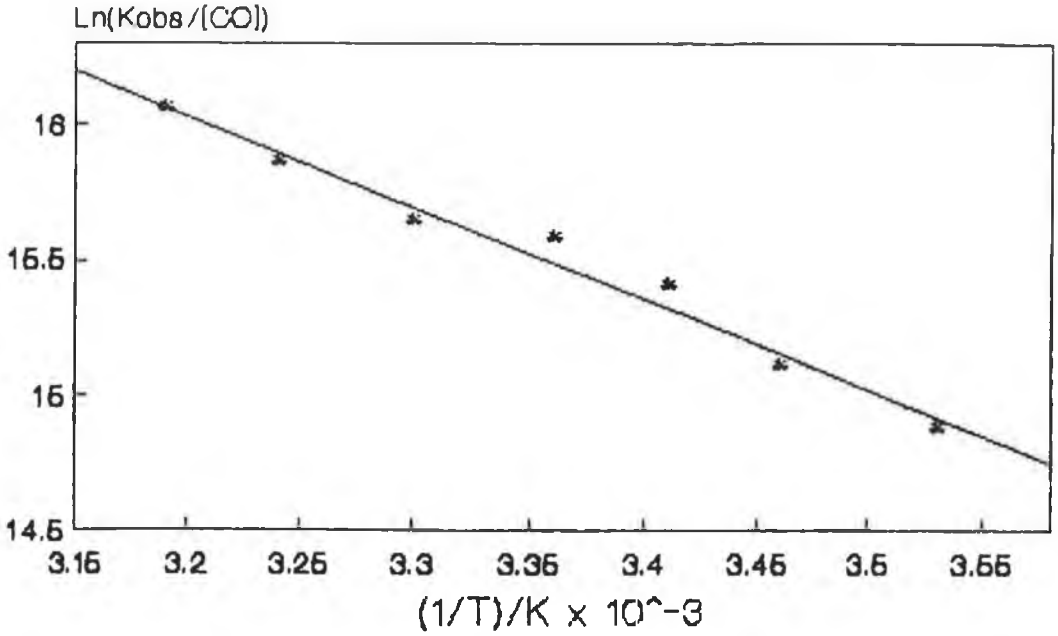

(b)

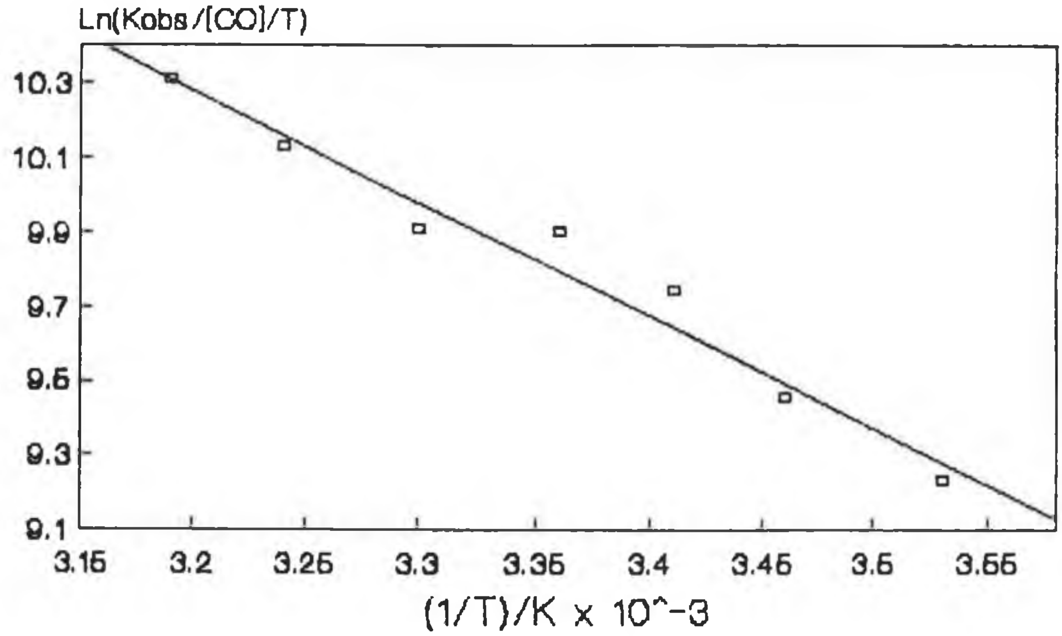

Figure 4.2.1 Arrhenius(a) and Eyring(b) plots the reaction of (η^6-phenanthrene)Cr$(CO)_2$(cyclohexane) with CO to regenerate the parent tricarbonyl complex.

4.3 (η^6-Pyrene)$Cr(CO)_3$.

4.3.1 Electronic absorption spectrum of (η^6-pyrene)$Cr(CO)_3$.

The UV/vis. spectrum of (η^6-pyrene)$Cr(CO)_3$ in cyclohexane is given in Figure 4.3.1.1. A $\lambda_{max.}$ is prominent at approximately 310 nm which is assigned to being predominantly chromium ----> arene charge transfer with some chromium ----> π^* CO charge transfer character. Once again, these assignments are based primarily on investigations into the electronic absorption spectrum of (η^6-benzene)$Cr(CO)_3$.[11] There are two further maxima at 380 and 490 nm which are thought to be metal to ligand charge transfer transitions. (η^6-Pyrene)$Cr(CO)_3$ absorbs further into the visible than any of the other polyaromatic carbonyl compounds previously discussed.

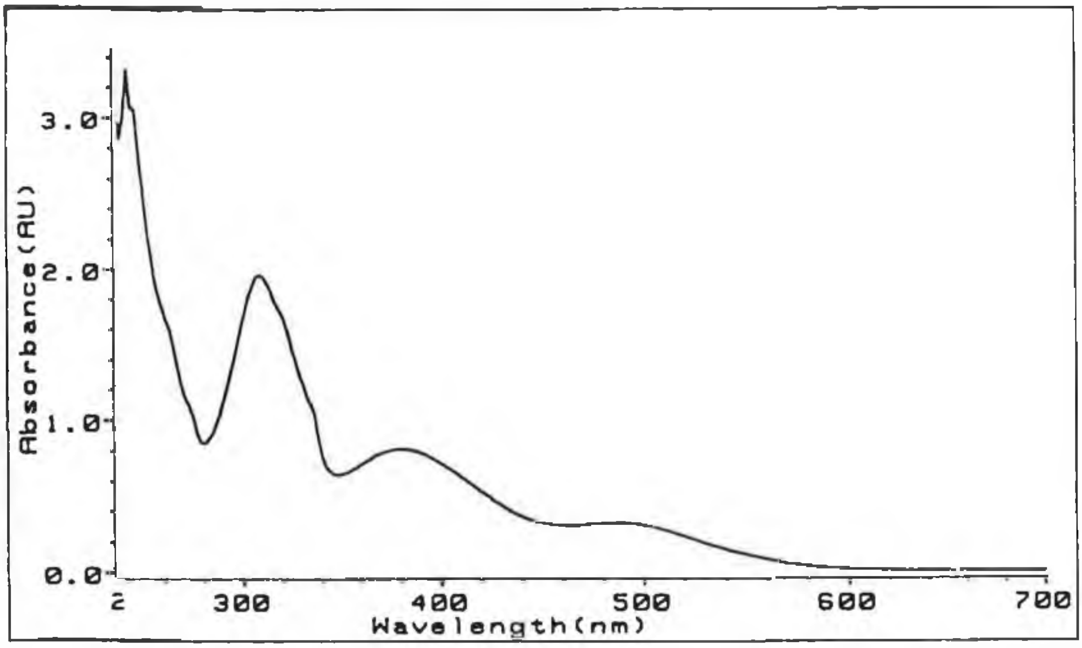

Figure 4.3.1.1 UV/vis. spectrum of (η^6-pyrene)$Cr(CO)_3$ (1.3×10^{-4}M) in cyclohexane.

4.3.2 Laser flash photolysis of (η^6-pyrene)Cr(CO)$_3$.

All laser flash photolysis experiments were conducted at 355 nm excitation (ε_{355} = 4748 dm^3 mol^{-1} s^{-1}) under 1 atm. of carbon monoxide. Following flash photolysis a transient species was measured at 300 nm as presented in Figure 4.3.2.1. This transient species was identified as being the solvated dicarbonyl intermediate which reacts with CO with a second order rate constant of 3.2 x 10^6 dm^{3}mol^{-1}s^{-1}. The changes in the UV/vis. were monitored throughout the experiment and are presented in Figure 4.3.2.2. The absorption maxima of the parent complex decreased in intensity along with an increase in absorption in the region around 340 nm. A UV/vis. difference spectrum was not recorded for this compound as above 340 nm there were problems with luminescence as the sample decomposes rapidly, much more noticeably than either of the previous compounds investigated.

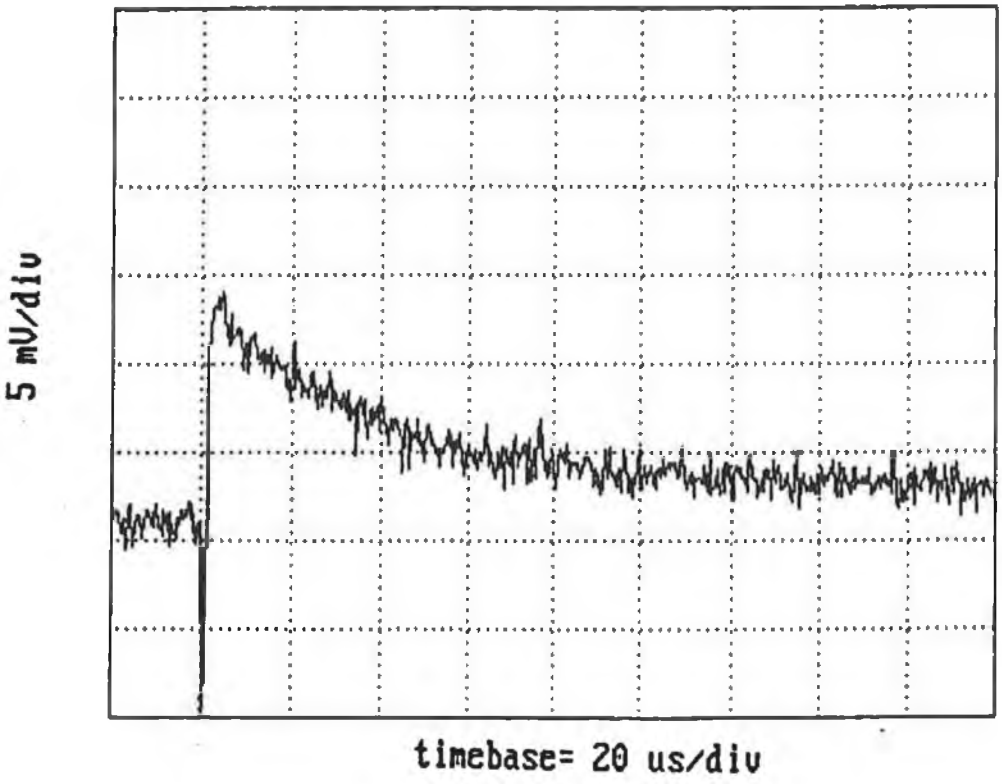

Figure 4.3.2.1 A typical transient signal observed at 300 nm following flash photolysis of (η^6-pyrene)Cr(CO)$_3$ at 355 nm under 1 atm. of CO (9.0 x 10^{-3}M) at 298K.

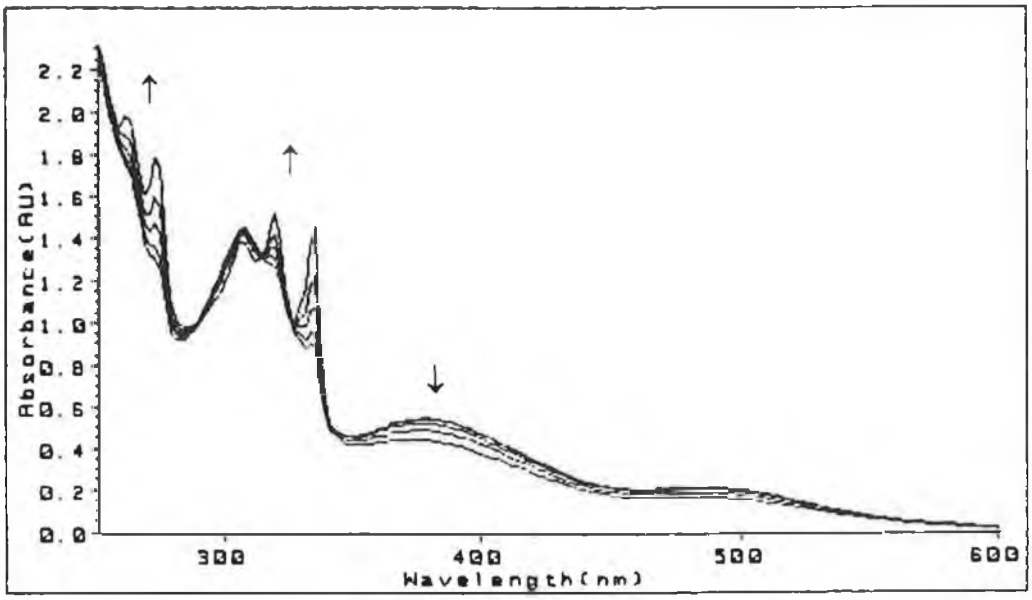

Figure 4.3.2.2 Changes in the UV/vis. absorption spectrum observed upon flash photolysis of (η^6-pyrene)Cr(CO)$_3$.

4.3.3 Steady state photolysis with monitoring by luminescence spectroscopy.

As before it was decided to carry out luminescence studies as uncomplexed pyrene luminesces whereas (η^6-pyrene)Cr(CO)$_3$ does not.[13] Room temperature photolysis of (η^6-pyrene)Cr(CO)$_3$ at $\lambda > 400$ nm and under 1 atm. of CO resulted in the formation of uncomplexed pyrene as determined by luminescence measurements. Presented in Figure 4.3.3.1 are luminescence spectra recorded after 5 and 10 minutes photolysis. As before the UV/vis. absorption spectrum was recorded and similar changes were observed to that seen in Figure 4.3.2.2.

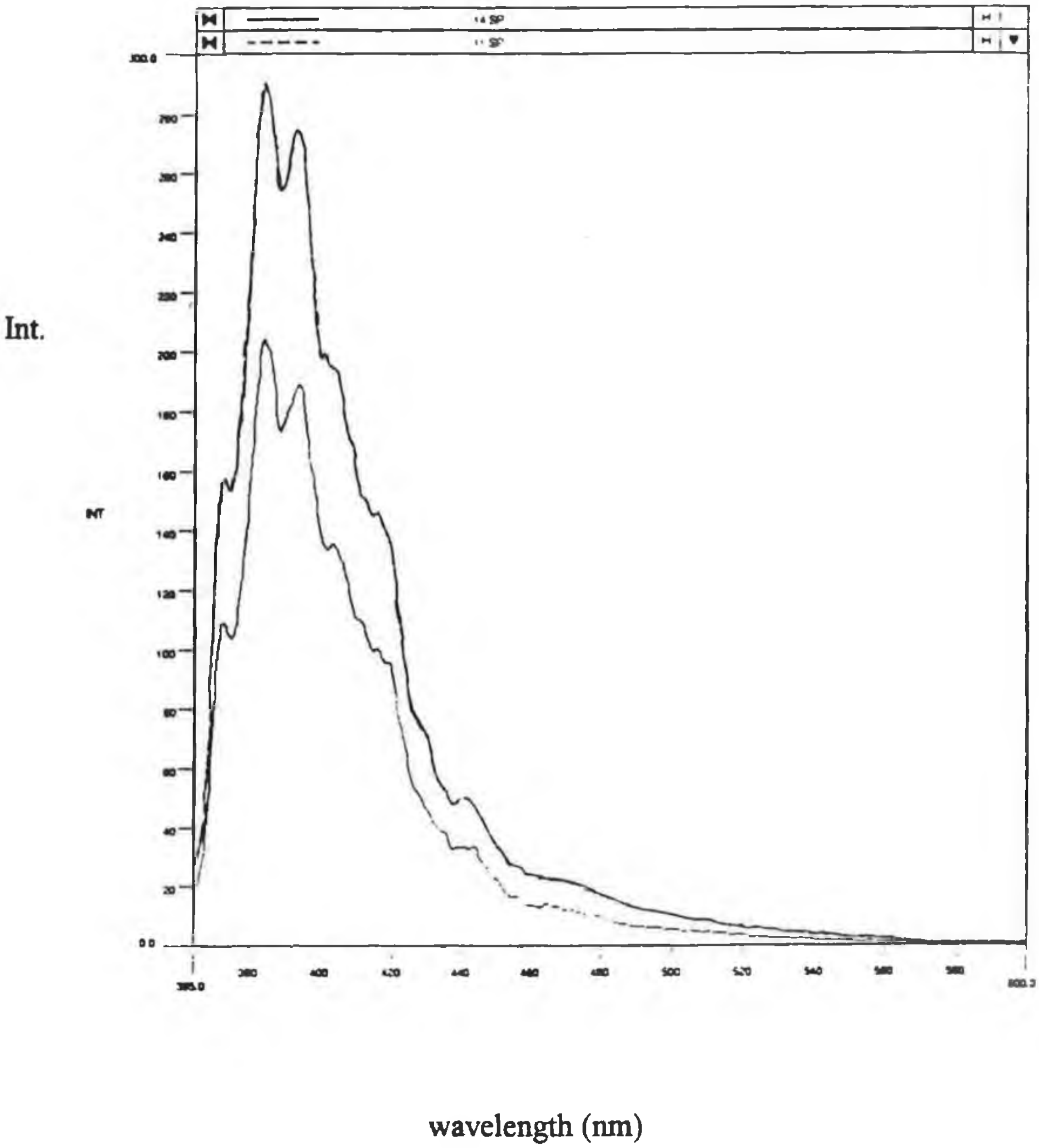

Figure 4.3.3.1 Luminescence spectra obtained after 5 and 10 minutes photolysis of (η^6-pyrene)Cr(CO)$_3$ at λ > 400 nm in cyclohexane under 1 atm. of CO.

4.4 Conclusion.

Solution photochemistry of the polaromatic chromium tricarbonyl compounds investigated in this study resulted in the formation of $Cr(CO)_6$. However laser flash photolysis experiments provide evidence for the presence of a dicarbonyl intermediate which is presumably solvated similarly to other dicarbonyl fragments.[3] The matrix isolation study carried out on the naphthalene system further substantiates the formation of a dicarbonyl species on short wavelength photolysis. On long wavelength photolysis of (η^6-naphthalene)$Cr(CO)_3$ in either a xenon, argon or methane matrix a further photoproduct is observed. This photoproduct is thought to be of an "η^3" type intermediate which is stabilised in the matrix because of its rigid nature, but this is not so in solution where the $Cr(CO)_3$ fragment is lost from the aromatic ligand and results in the formation of $Cr(CO)_6$. Experiments conducted in a dinitrogen matrix only resulted in the formation of a dicarbonyl product, no evidence was found for a second photoproduct. The CO doped methane matrix provides evidence for the formation of $Cr(CO)_6$ which is in agreement with solution photochemistry and hence indicates that a similar reaction pathway exists in both a matrix and in solution for (η^6-naphthalene)$Cr(CO)_3$. Work is ongoing on these systems in so far as matrix isolation studies have to be carried out on both (η^6-phenanthrene)$Cr(CO)_3$ and (η^6-pyrene)$Cr(CO)_3$ compounds. Previously it has been thought that the photochemistry (η^6-arene)$Cr(CO)_3$ compounds results solely in CO loss, but this study has demonstrated that by varying the nature of the arene ligand it is possible to alter the photochemistry. The quantum yield for CO loss has been measured to be relatively efficient ($\Phi = 0.72$) for (η^6-benzene)$Cr(CO)_3$[2b], and because of this efficiency it is of the opinion that the lowest energy transition is ligand field in character. If this were so for the polyaromatic tricarbonyls a transient signal for the CO loss product would have been expected following 532 nm flash photolysis, however this was not the case as no transient signals were detected. Matrix isolation studies provide evidence for a photoproduct following long wavelength photolysis which has been identified as an "η^3" type intermediate and this result further confirms that the ligand field is no longer the lowest lying energy transition as it now appears to be metal to ligand charge transfer in origin. If the ligand field excited state were the lowest in energy these polyaromatic systems would most probably be photoreversible as is for (η^6-benzene)$Cr(CO)_3$. An overall view of the reaction pathway for the polyaromatic systems in both solution and matrix is given in Scheme 4.4.1.

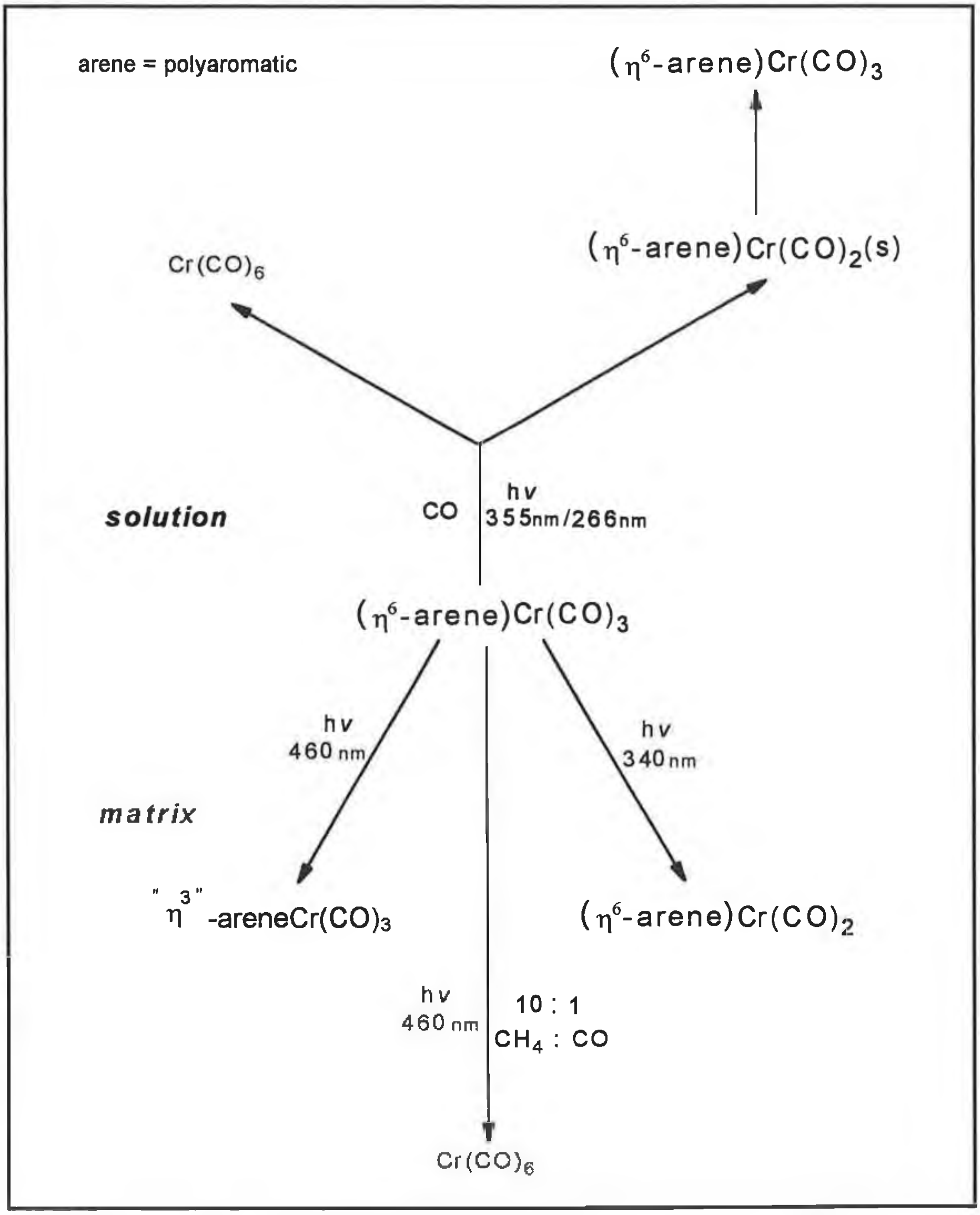
arene = polyaromatic
(η⁶-arene)Cr(CO)3
(η⁶-arene)Cr(CO)2(s)
Cr(CO)6
solution
CO
hv
355nm/266nm
(η⁶-arene)Cr(CO)3
hv
460 nm
hv
340 nm
matrix
"η3" -areneCr(CO)3
(η⁶-arene)Cr(CO)2
hv
460 nm
10 : 1
CH4 : CO
Cr(CO)6

Scheme 4.4.1

4.5 References

1 Rest,A.J.;Sodeau,J.R.;Taylor,D.J.; *J. Chem. Soc., Dalton Trans.*; 1978,651.

2 (a) Stohmeier,W.;von Hobe,D.; *Z. Naturforsch*;1963,**18B**,770.
(b) Gilbert,A.;Kelly,J.M;Budzwait,M.;Koerner von Gustorf,E.; *Z. Naturforsch*; 1976,**31B**,1091.
(c) Zheng,Y.;Wang,W.;Lin,j.;She,Y.;Fu,F-J.; *J. Phys.Chem.*; 1992,**96**,9821.
(d) McGrath,I.M. Ph.D *Thesis*, Dublin City University; 1993.

3 Creaven,B.S.;George,M.W.;Ginzburg,A.G.;Hughes,C.;Kelly.J.M.;Long,C.;McGrath,I.M.;Pryce,M.T.; *Organometallics*; 1993,**12**,3127.

4 Perutz,R.N.;Turner,J.J.,; *J. Am. Chem. Soc.*; 1975,**97**,4791.

5 (a)Bonneau,R.;Kelly,J.M.; *J. Am. Chem. Soc.*; 1980,**102**,1220.
(b)Kelly,J.M.;Long,C.;Bonneau,R.; *J. Chem. Phys.*; 1983,**87**,3344.

6 (a)Strohmeier,S.;Starrico,E.; *Z. Phyzik. Chem. Neue Folge.*; 1966,**38**,315.
(b)Zimmerman,C.L.;Shaner,J.L.;Royh,S.A.;Willeford,B.R.; *J. Chem. Res.(S)*;1980,108.
(c)Traylor,T.G.;Stewart,K.J.;Goldberg,M.J.; *J. Am. Chem. Soc.*; 1984,**106**,4445.
(d)Traylor,T.G.;Stewart,K.J.; *J. Am. Chem. Soc.*; 1986,**108**,6977.
(e)Traylor,T.G.;Goldberg,M.J.; *Organometallics*;1987,**6**,2413.

7 Wrighton,M.S.;Haverty,J.L.; *Z. Naturforsch*; 1975,**B30**,254.

8 Natta,G.;Ercoli,R.;Calderazzo.;Santambrozio,E.; *Chim. Ind. (Milan);* 1958,**40**,1003.

9 Ercoli,R.;Calderazzo,R;Abberola,A.; *Chim. Ind. (Milan);* 1959,**41**,975.

10 (a) Mahaffy,C.A.L,;Pauson,P.L,; *J. Chem. Res.(S);* 1979,126.
(b) Mahaffy,C.A.L,;Pauson,P.L,; *J. Chem. Res.(M);* 1979,1972.

11 (a) Carroll,D.G.;McGlynn, S.P.; *Inorg. Chem.*; 1968,**7**,1285.
(b) Ercoli,R.;Mangini,A.; *Ric. Sci. Suppl.*; 1958,**84**,1167.
(c) Yamada,S.;Nakamura, H.;Tsuchida,R., *Bull. Chem. Soc. Japan*; 1957,**30**,647.

(d) Yamada,S.;Nakamura, H.;Tsuchida,R.; *Bull. Chem. Soc. Japan*; 1960,**33**,481.

12 Geoffroy,G.L;Wrighton,M.S.; *Organometallic Photochemistry*, Academic Press, New York; 1979.

13 Turro,N.J.;*Modern Molecular Photochemistry*, Benjamin/Cummings Publishing Co. Inc.;1978.

14 Perutz,R.R.;Turner,J.J.; *J. Am. Chem. Soc.*; 1975,**97**,4800.

15 Seder,T.A.;Church,S.P.;Weitz,E.; *J. Am. Chem. Soc.*; 1986,**108**,4721.

16 Ishikawa,Y-i,;Brown,C.E.;Hackett,P.A.;Rayner,D.M.; *J. Phys. Chem.*; 1990,**94**,2404.

17 Wang,W.;Jin,P.;Liu,Y.;She,Y.,Fu,K-J.; *J. Phys.Chem.*; 1992,**96**,1279.

18 Zheng,Y.;Wang,W.;Lin,J.;She,Y.;Fu,K-J.; *J. Phys.Chem.*; 1992,**96**,7651.

19 Black,J.D.;Boylan,M.J.;Braterman,P.S.; *J. Chem. Soc., Dalton Trans.*; 1981,673.

20 Hill,R.H,;Wrighton,M.S.; *Organometallics*; 1987,**6**,632.

21 (a) Creaven,B.S.;Dixon,A.J.;Kelly,J.M.;Long,C.;Poliakoff,M.; *Organometallics*;1987,**6**,2600.
(b)Johnson,F.P.A.;George,M.W.;Bagratashvili,V.N.;Vereshchagina,L.N.; Poliakoff,M.; *Mendeleev Commun.*; 1991,26.

22 Poliakoff,M.; *J. Chem. Soc., Dalton Trans.*; 1974,210.

23 Ishikawa,Y.;Hackett,P.A.;Rayner,D.M.; *J. Phys. Chem.*; 1988,**92**,3863.

24 Rooney,D.;Chaiken,J.;Driscoll,D.; *Inorg. Chem.*;1987,**26**,3939.

25 Connor,J.A.; *Top. Curr. Chem.*; 1977,**71**,71.

26 Fletcher,T.R.;Rosenfeld,R.N.; *J. Am. Chem. Soc.*; 1985,**107**,2203.

27 Albright,T.A.;Hofman,P.;Hoffmann,R.;Lillya,C.;Dobosh,P.A.; *J. Am. Chem. Soc.*; 1983,**105**,3396.

28 Yoshihara,K.;Kasuya.;T.;Inoue,A.;Nagakura,S.; *Chem. Phy. Lett.*; 1971,**8**,469.

29 Cunningham,S.D.;Ofele,K.;Willeford,B.R.; *J. Am. Chem. Soc.*; 1983,**105**,3725.

Chapter 5.

Photochemistry of
(η^6-*cis and trans* -1,2 diphenylethene)Cr(CO)$_3$
and
the crystal and molecular structure of
(η^6-*trans*-1,2 diphenylethene)Cr(CO)$_3$.

5.1 Photochemistry of (η^6-1,2 diphenylethene)$Cr(CO)_3$.

There has been much interest in the photochemistry of transition metal complexes that have low lying metal to ligand charge transfer excited states, for *e.g.* $W(CO)_5L$[1] or (η^5-C_5H_5)$Mn(CO)_2L$[2] complexes where L is CO or a Lewis base. The results of these studies have shown that the photochemical and luminescence characteristics of the complexes are dependent on the energy of the low lying MLCT excited state. Small changes in the nature of the ligand(L) have illustrated that this can have a major effect on the properties of the complex. Therefore the ligand substituent can be used to 'tune' the excited states and the photochemical properties of a number of transition metal complexes.[3]

Photochemical studies of [$W(CO)_5L$] (L = N-donor ligand) in solution at room temperature have shown that the quantum yields (Φ) of Reactions 5.1.1 and 5.1.2 are sensitive to the wavelength of irradiation. Short wavelength causes more efficient loss of CO (Φ_{CO} = 0.04 at 254 nm, 0.002 at 436 nm; Φ_L = 0.34 at 254 nm, 0.63 at 436 nm where L = pyridine).[4]

$$[W(CO)_5L] \xrightarrow{h\nu} [W(CO)_4L] + CO \qquad (5.1.1)$$

$$[W(CO)_5L] \xrightarrow{h\nu} [W(CO)_5] + L \qquad (5.1.2)$$

For the ligand 4 styrylpyridine the efficiency of photosubstitution of the ligand is somewhat reduced due to competing *cis* —> *trans* isomerisation of the coordinated ligand. Quantum yields for (styrylpyridine)$W(CO)_5$ were calculated to be Φ_{diss} = 0.16, $\Phi_{c \rightarrow t}$ = 0.31 and $\Phi_{t \rightarrow c}$ = 0.08 ($\lambda_{exc.}$ = 436 nm). In the case of styrylpyridine it was proposed that isomerisation resulted from an intraligand triplet state formed by internal conversion from the lowest lying metal centred ligand field triplet. Argon matrices were used to investigate the photochemistry of (pyridine)$W(CO)_5$ and (3-bromopyridine)$W(CO)_5$.[5] Photolysis ($320 < \lambda < 390$ nm) produced bands attributed to $W(CO)_5$. Long wavelength photolysis (λ = 435 nm) resulted in regeneration of the parent and a decrease in the bands of the starting material. Photolysis with unfiltered light resulted in a complicated spectrum but a band was observed at 2138 cm^{-1} which indicated the presence of 'free' CO.

These observations in low temperature matrices are consistent with those previously observed by Wrighton *et al.*[1] in solution and thus indicate that Reactions 5.1.1 and 5.1.2 can take place in low temperature matrices at 12K with Reaction 5.1.2 being photochromic. In this study the photochemistry of (η^6-*cis* and *trans*-1.2 diphenylethene)Cr(CO)$_3$ was investigated along with preliminary studies on (η^6-*trans,trans*-1,4-diphenyl-1,3-butadiene)Cr(CO)$_3$.

5.1.1 Electronic absorption spectra of (η^6-*cis* and *trans*-1,2 diphenylethene)Cr(CO)$_3$.

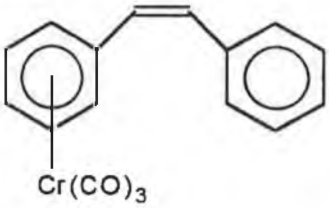

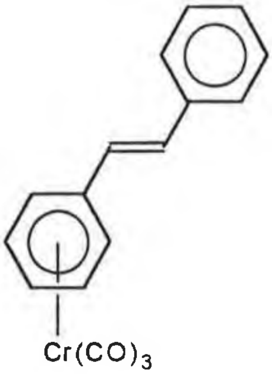

(η^6-
-1,2 diphenylethene)Cr(CO)$_3$

(η^6-*trans*-
1,2 diphenylethene)Cr(CO)$_3$

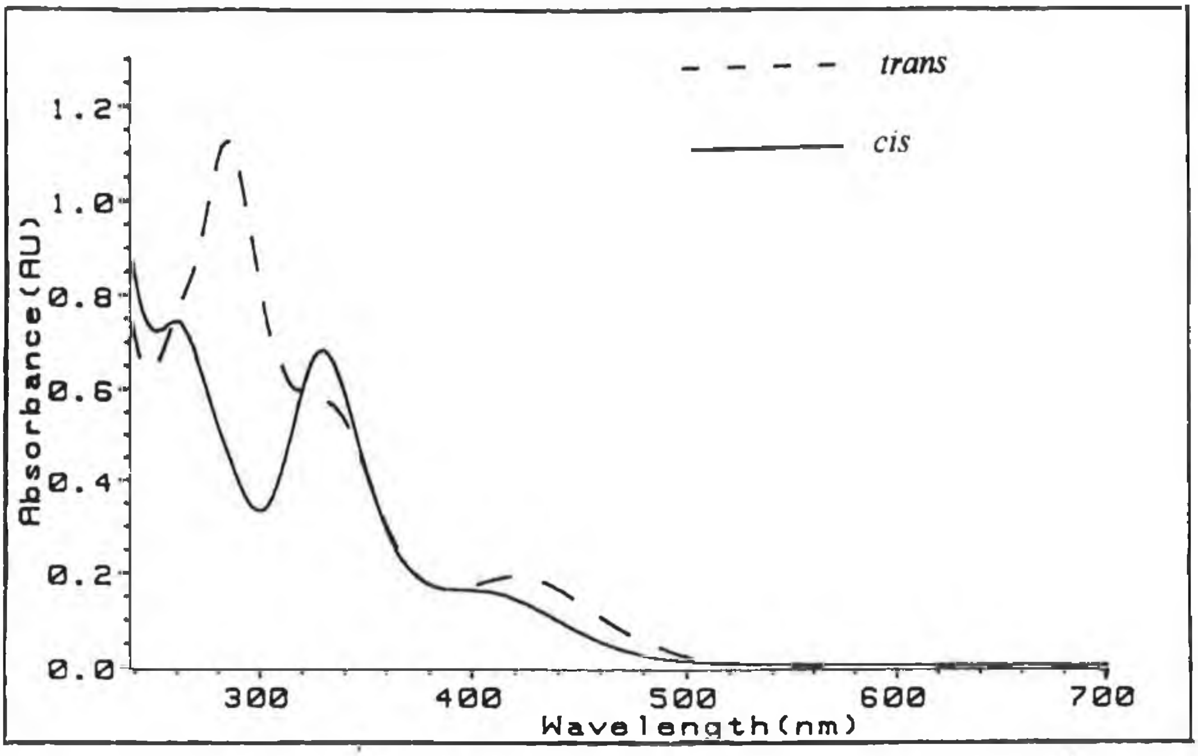

5.1.1.1 Electronic absorption spectra of (η^6-*cis* - and *trans*-1,2 diphenylethene)Cr(CO)$_3$ in cyclohexane (8.1 x 10^{-5} and 8.7 x 10^{-5}M).

The UV/vis spectra for both (η^6-*cis*- and *trans*-1,2 diphenylethene)Cr(CO)$_3$ in cyclohexane are given in Figure 5.1.1.1. The absorption spectra of these complexes are noticeably different to that of (η^6-benzene)Cr(CO)$_3$ in cyclohexane previously described in Chapter 2, especially (η^6-*trans*-1,2 diphenylethene)Cr(CO)$_3$. An absorption maxima at 290 nm for the *trans* isomer is assigned to the chromium ----> arene CT transition with some chromium ----> π* CO CT character.[6] In the case of the *cis* isomer, $\lambda_{max.}$ is shifted to a somewhat lower energy of 330 nm and similarly to the *trans* isomer this transition is assigned to being chromium ----> arene CT with some chromium ----> π* CO CT character. For the *cis*-isomer there is a shoulder at 260 nm which is attributed to being a M ----> π* CO CT transition. In the *trans* isomer this transition is not readily observable and may be the shoulder on the high energy side of the absorption maxima at 290 nm. Two further absorption maxima present at 408 and 430 nm for the *cis* and *trans* isomers respectively are thought to be MLCT transitions as increasing the solvent polarity resulted in a blue shift of these bands, given in Figure 5.1.1.2 and 5.1.1.3 are the spectra for both isomers in cyclohexane and acetone. (η^6-*Cis*-1,2 diphenylethene)Cr(CO)$_3$ has a window in the absorption spectrum at 300 nm which is typical of (η^6-arene)Cr(CO)$_3$ complexes. However in the case of the *trans* complex this valley is absent as $\lambda_{max.}$ occurs in this region.

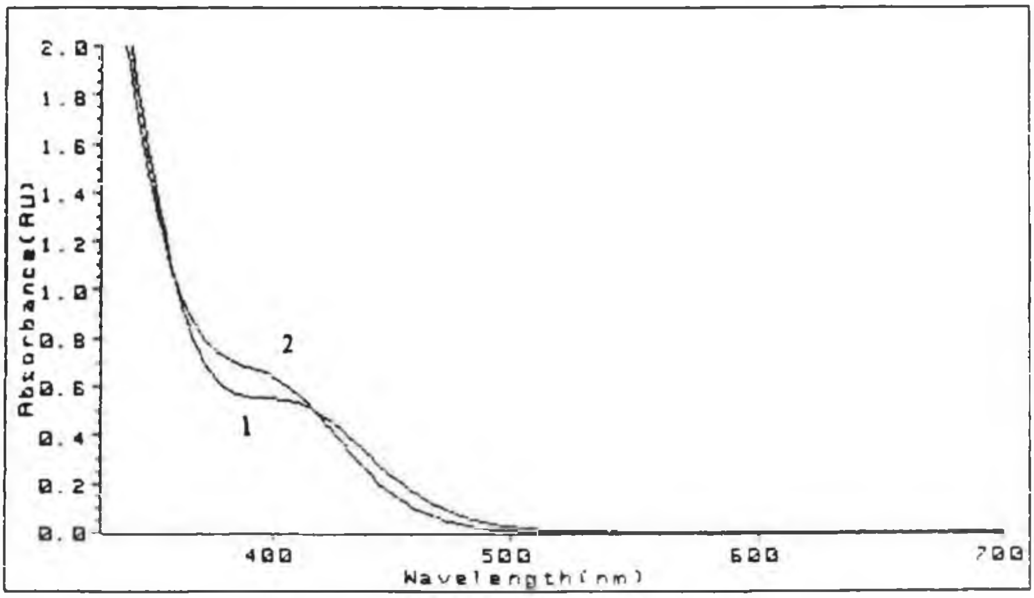

Figure 5.1.1.2 UV/vis. spectrum of (η^6-*cis*-1,2 diphenylethene)Cr(CO)$_3$ in (1) cyclohexane and (2) acetone.

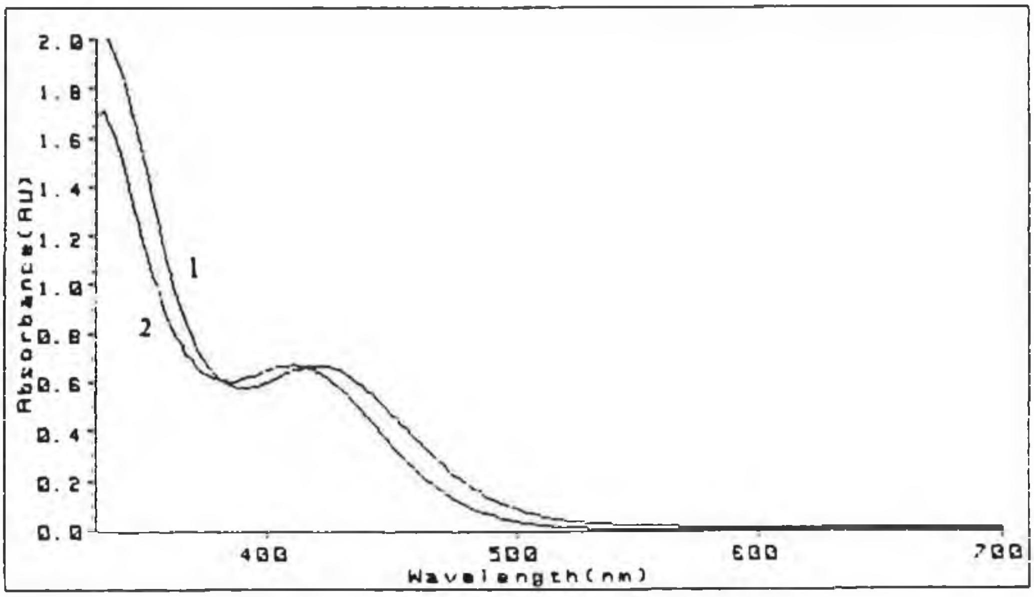

Figure 5.1.1.2 UV/vis. spectrum of (η^6-*trans*-1,2 diphenylethene)$Cr(CO)_3$ in (1) cyclohexane and (2) acetone.

5.1.2.1 Laser flash photolysis of (η^6-*trans* -1,2 diphenylethene)$Cr(CO)_3$.

Following flash photolysis of (η^6-*trans*-1,2 diphenylethene)$Cr(CO)_3$ at 355 nm (ε_{355} = 6268 $dm^3\ mol^{-1}\ s^{-1}$) under 1 atm. of CO a transient species was observed at 310 nm and a depletion at 350 nm as given in Figure 5.1.2.1. From previous studies conducted on (η^6-arene)$Cr(CO)_3$ in cyclohexane under flash photolysis conditions[7] or low temperature work[8] the primary photoproduct has been identified as the coordinatively unsaturated dicarbonyl intermediate. Similarly here the primary photoproduct is assigned to the solvated dicarbonyl species which in the presence of a carbon monoxide reacts to reform the parent tricarbonyl complex with a second order rate constant of $6.0 \times 10^6\ dm^3mol^{-1}s^{-1}$.

Figure 5.1.2.2 contains a UV/vis. difference spectra recorded under 1 atm. of CO. A $\lambda_{max.}$ is evident at 310 nm together with a broad absorption maximum at 470 nm. As the rate of decay of the absorption at 310 nm ($6.0 \times 10^6\ dm^3mol^{-1}s^{-1}$) is similar to that at 470 nm ($6.2 \times 10^6\ dm^3mol^{-1}s^{-1}$) this absorption is attributed to the solvated dicarbonyl intermediate. Along with the absorptions following flash photolysis a depletion occurs at 350 nm which corresponds to an absorption maxima of the parent compound. This system is not fully reversible under 1 atm. of CO, as the UV/vis. absorption spectrum of the parent recorded at various time intervals indicates an increase in the absorption at 250 nm along with a decrease in the absorptions at 290, 335 and 408 nm. An infrared spectrum of this solution indicated the formation of $Cr(CO)_6$ (Figure 5.1.2.3).

(a)

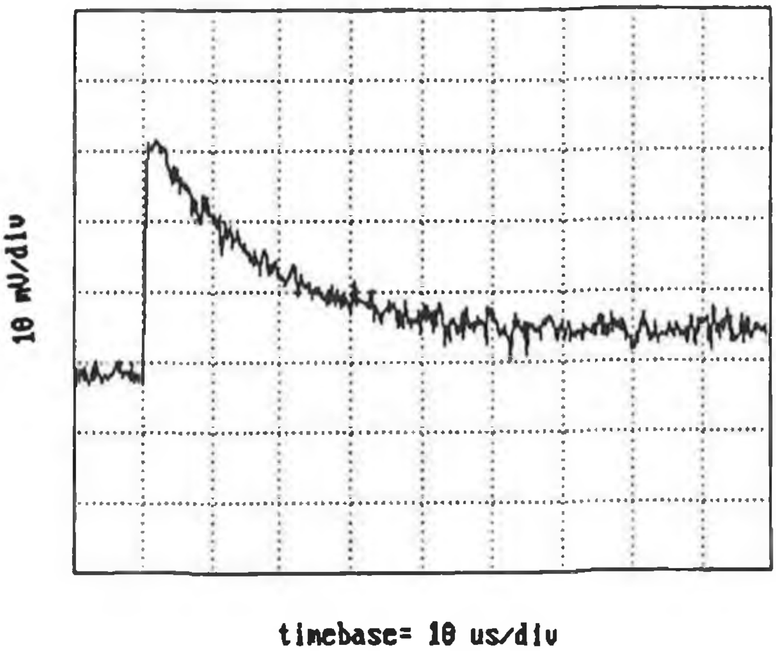

(b)

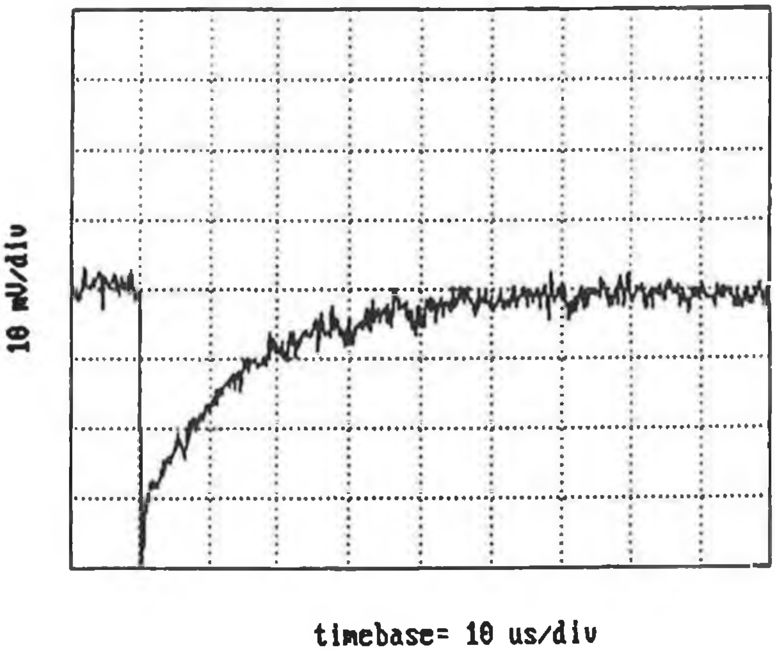

Figure 5.1.2.1 Transient signal recorded at 310(a) and 350 nm(b) following flash photolysis ($\lambda_{exc.}$ = 355 nm)of (η^6- *trans*-1,2 diphenylethene)$Cr(CO)_3$ under 1 atm. of CO.

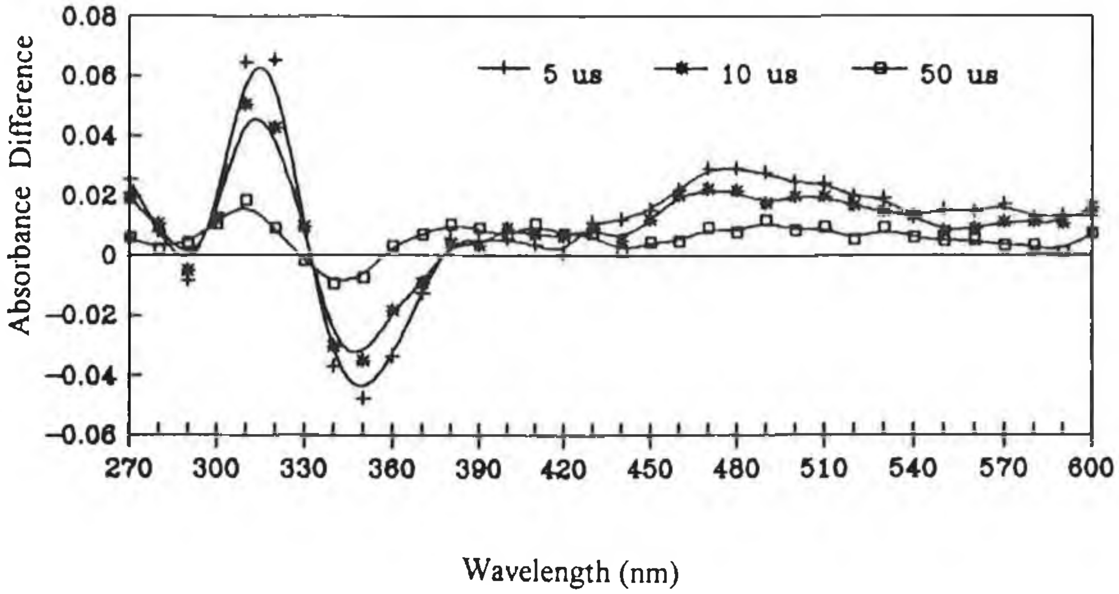

Figure 5.1.2.2 UV/vis. difference spectra of (η^6-*trans*-1,2 diphenylethene)Cr(CO)$_3$ under 1 atm. CO at different time intervals.

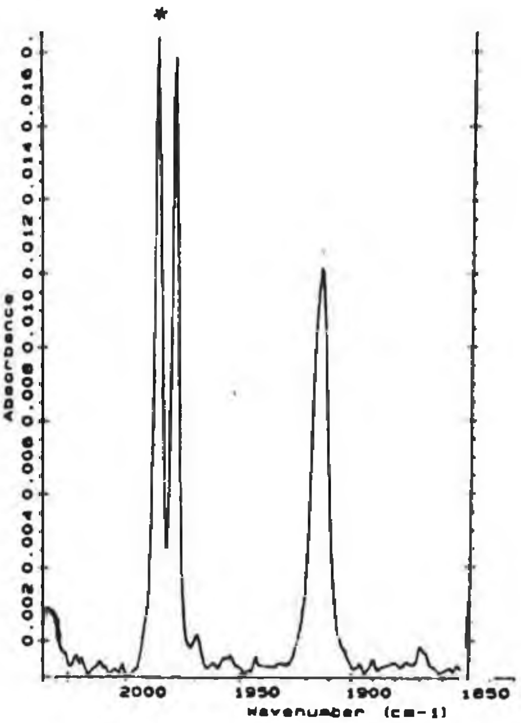

Figure 5.1.2.3 Infrared spectrum of (η^6-*trans*-1,2 diphenylethene)Cr(CO)$_3$ under 1 atm. CO at the end of the experiment. * indicates Cr(CO)$_6$.

5.1.2 NMR monitored photolysis of (η^6-*trans*-1,2 diphenylethene)Cr(CO)$_3$.

Photolysis of (η^6-*trans*-1,2 diphenylethene)Cr(CO)$_3$ was followed by proton NMR in order to investigate the nature of products. The NMR sample was made up in a similar manner to that of any of the laser samples by using a degassable NMR tube and 1 atm. of CO was admitted to the tube. Resonances for the complexed ring in (η^6-*trans*-1,2 diphenylethene)Cr(CO)$_3$ occur in the region between 4.98 – 5.32 ppm, those of the uncomplexed ring between 7.15 – 7.38 ppm and the vinylic protons at ~ 6.54 and ~6.88 ppm. As the sample of (η^6-*trans*-1,2 diphenylethene)Cr(CO)$_3$ in deuterated cyclohexane-d_{12} was irradiated at $\lambda > 400$ nm for intervals of approximately 10 minutes multiplets were seen to grow at ~7.3 ppm together with a doublet at 7.4 ppm. Also evident was a singlet at 7.02 ppm. On comparing the spectrum of photolysed (η^6-*trans*-1,2 diphenylethene)Cr(CO)$_3$ with that of the uncomplexed ligand *trans*-diphenylethene (Figure 5.1.2.1) it appears that upon irradiation at $\lambda > 400$ nm scission of the metal to arene bond occurs with production of the uncomplexed ligand. Presented in Figure 5.1.2.2 is the ^{1}H NMR spectrum of (η^6-*trans*-1,2 diphenylethene)Cr(CO)$_3$ in cyclohexane-d_{12} before and after irradiation at $\lambda >$ 400 nm.

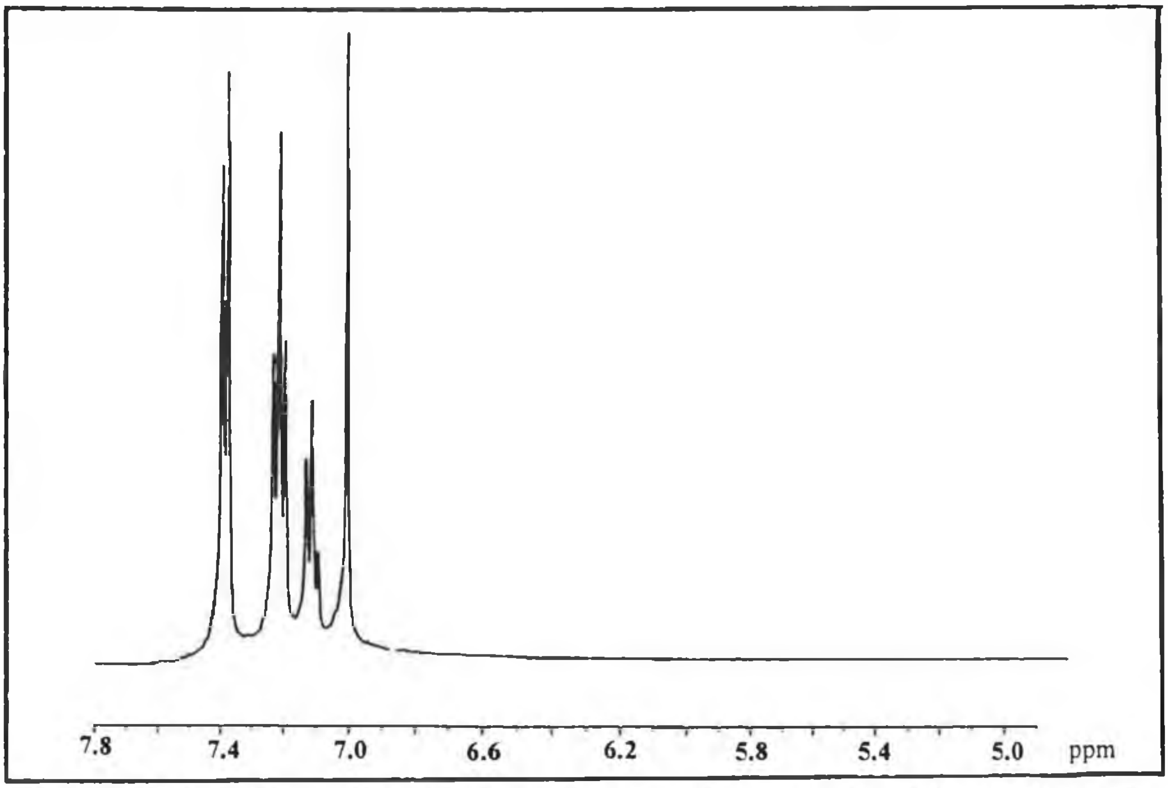

Figure 5.1.2.1 the ^{1}H NMR spectrum of *trans*-1,2 diphenylethene in cyclohexane-d_{12}.

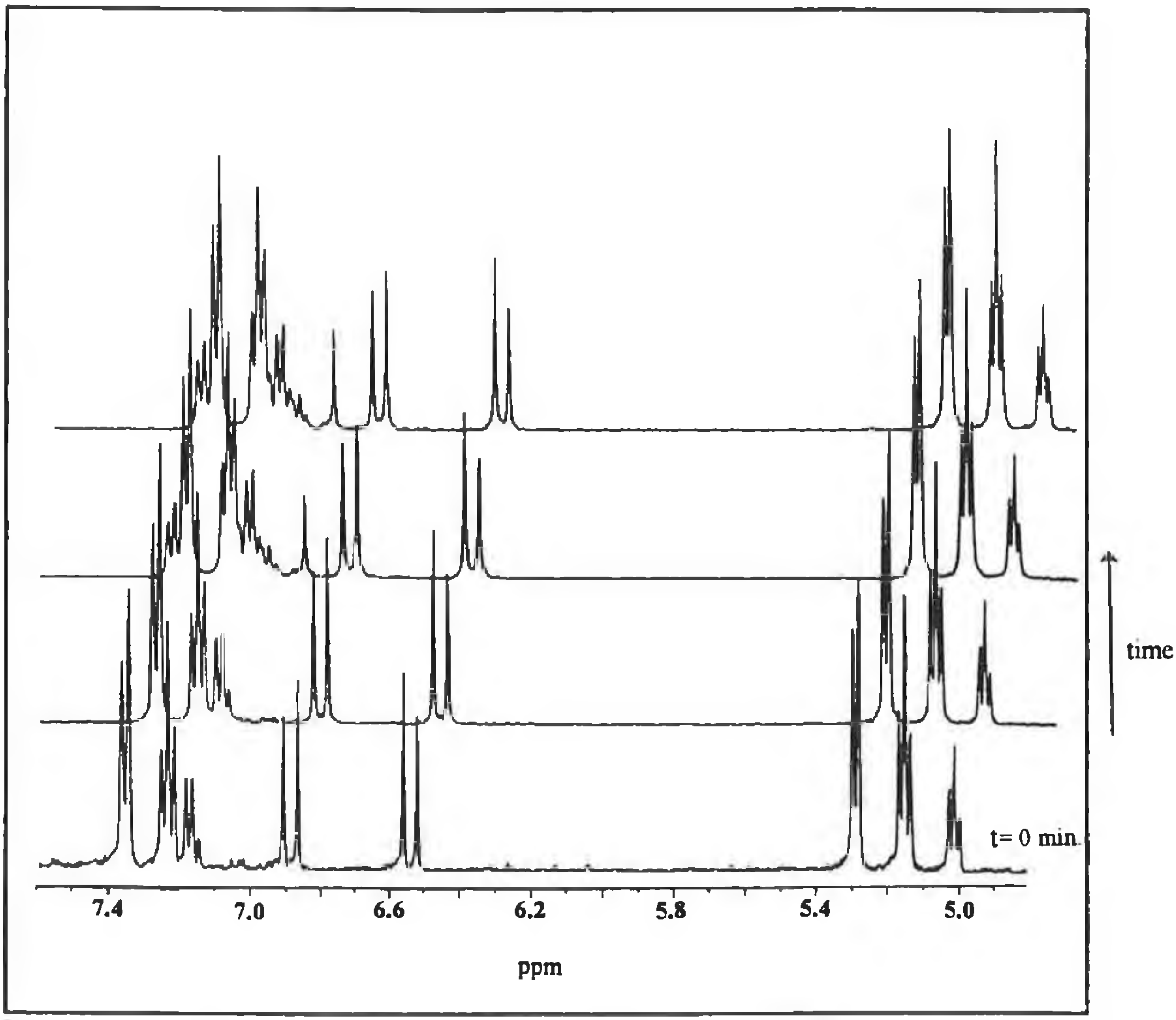

Figure 5.1.2.2, the ^{1}H NMR spectrum of (η^6-*trans*-1,2 diphenylethene)$Cr(CO)_3$ in cyclohexane-d_{12} at different time intervals of irradiation at $\lambda > 400$ nm.

5.1.3 Infrared monitored photolysis of (η^6-*trans*-1,2 diphenylethene)Cr(CO)$_3$.

(η^6-Arene)Cr(CO)$_3$ compounds are known to undergo CO loss upon photolysis and in the presence of a ligand the vacant site on the metal centre is hence occupied.[9] For instance following irradiation in the presence of excess pyridine (η^6-benzene)Cr(CO)$_3$ looses CO to form the complexed dicarbonyl pyridine product as shown in the infrared spectrum in Figure 5.1.3.1. As the irradiation time progressed (spectra recorded at intervals of 3 seconds) the absorptions at 1982 and 1914 cm^{-1} decreased in intensity with corresponding formation of bands at 1902 and 1850 cm^{-1}. These new bands are attributed to (η^6-benzene)Cr(CO)$_2$(pyridine).

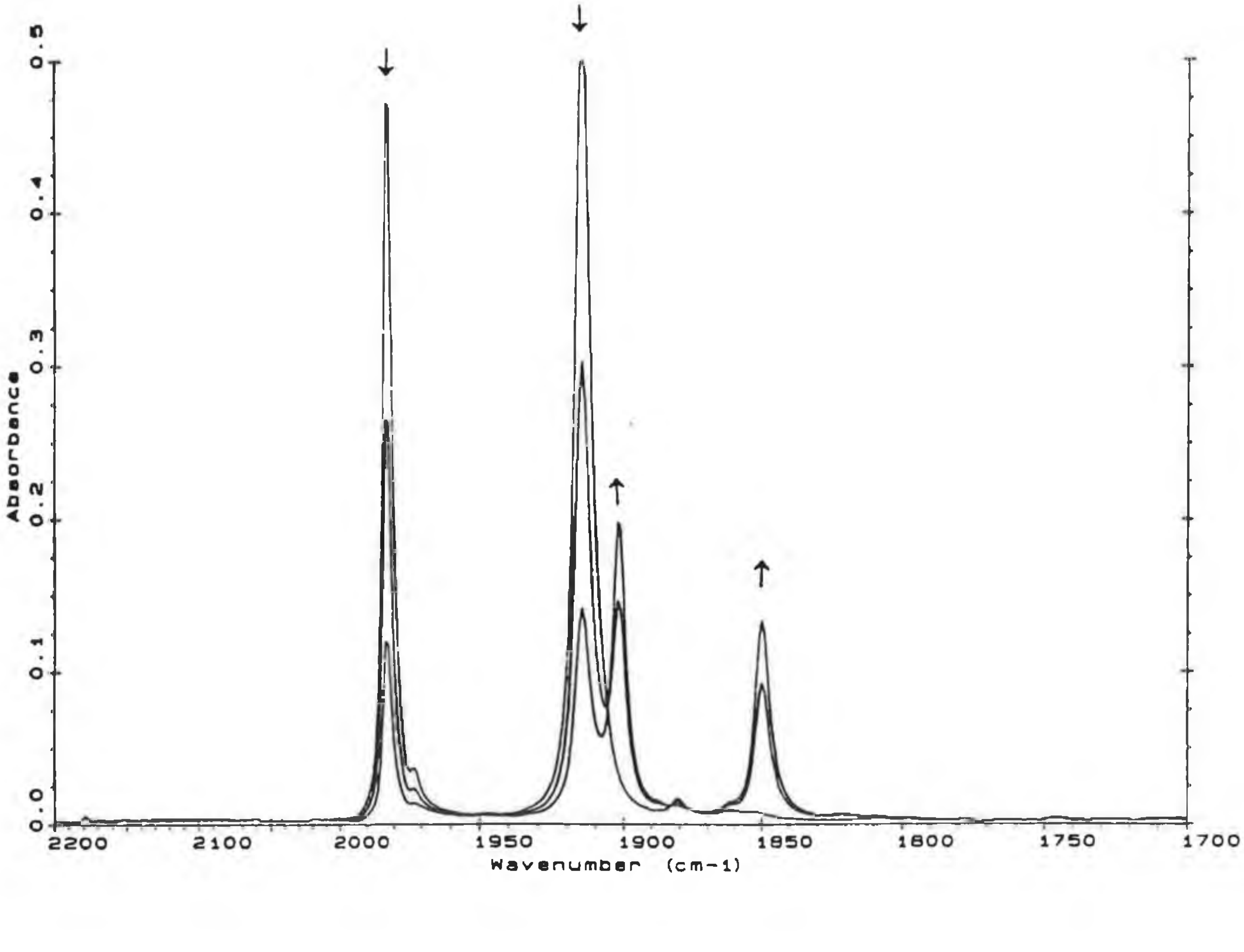

Figure 5.1.3.1 Infrared spectral changes for the reaction of (η^6-benzene)Cr(CO)$_3$ with excess pyridine in argon degassed cyclohexane.

An argon degassed solution of (η^6-*trans*-1,2 diphenylethene)$Cr(CO)_3$ in cyclohexane in the presence of excess pyridine was photolysed (the sample was protected by a Corning filter 7-54). As the photolysis time increased the bands of the parent tricarbonyl at 1978 and 1913 cm^{-1} decreased in intensity together with the formation of bands at 1903 and 1854 cm^{-1} as shown in Figure 5.1.3.2. The infrared spectra were recorded at intervals of approximately 4 seconds. An isosbestic point occurs at 1908 cm^{-1} which is indicative of a clean reaction uncomplicated by side or subsequent reactions taking place. Based on experiments carried out on the analogous (η^6-benzene)$Cr(CO)_3$ compound the bands at 1903 and 1854 cm^{-1} are assigned to (η^6-*trans*-1,2 diphenylethene)$Cr(CO)_2$(pyridine).

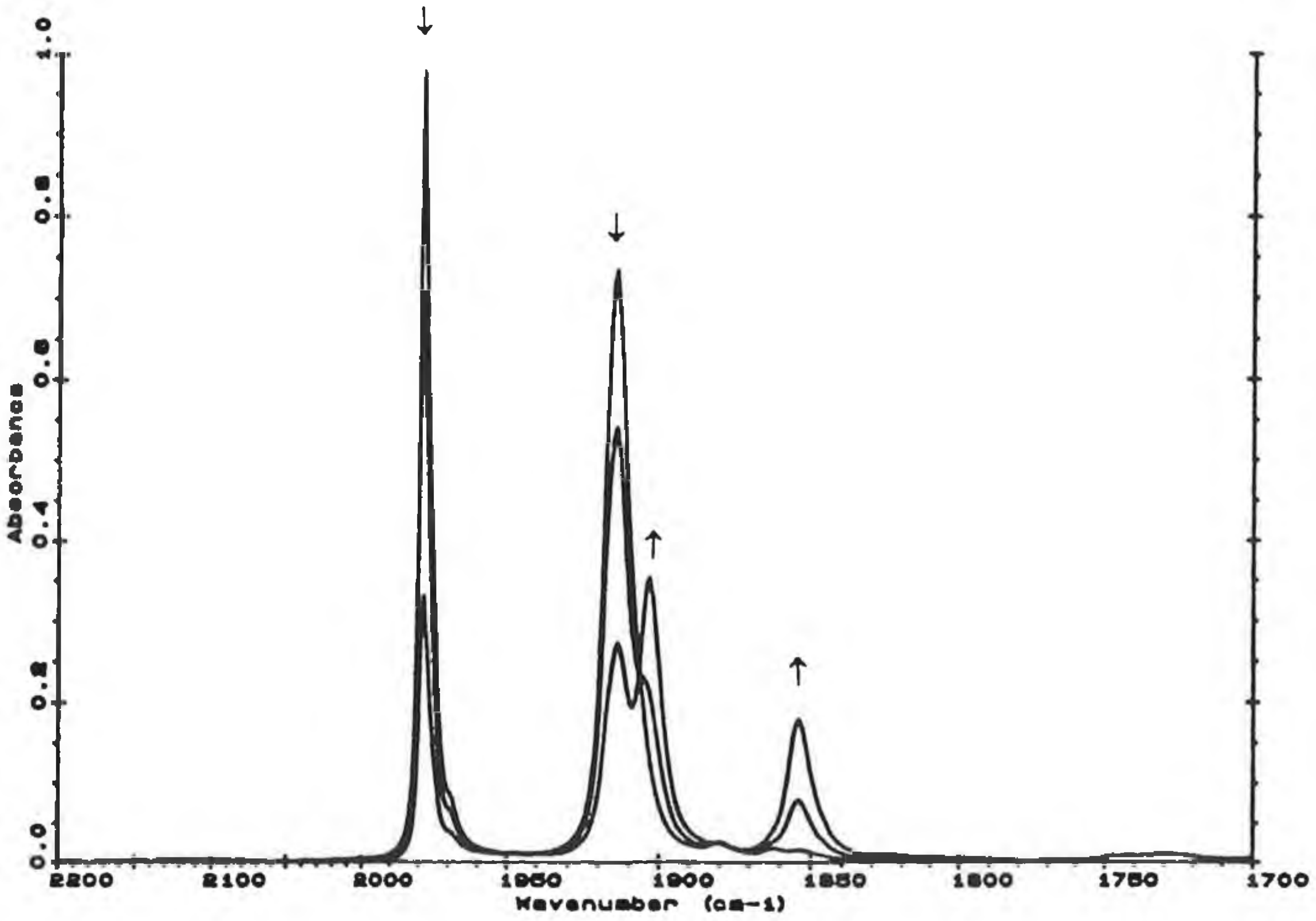

Figure 5.1.3.2 Infrared spectral changes for the reaction of (η^6-*trans*-1,2 diphenylethene)$Cr(CO)_3$ with excess pyridine in argon degassed cyclohexane.

5.2.1 Laser flash photolysis of (η^6-*cis*-1,2 diphenylethene)Cr(CO)$_3$.

Flash photolysis of (η^6-*cis*-1,2 diphenylethene)Cr(CO)$_3$ at 355 nm (ε_{355} = 6734 dm^3 mol^{-1} s^{-1}) under 1 atm. of CO resulted in the formation of a very long lived transient species with a $\lambda_{max.}$ at 300 nm. A UV/vis. difference spectra for (η^6-*cis*-1,2 diphenylethene)Cr(CO)$_3$ is presented in Figure 5.2.1.1. From this difference spectra it can be seen that upon flash photolysis of (η^6-*cis*-1,2 diphenylethene)Cr(CO)$_3$ reversibility of the system is not maintained, as the absorption at 300 and depletion at 330 nm do not return to base-line. Noticeable was a colour change to a much deeper shade of yellow as the experiment proceeded.

Throughout the experiment the UV/vis. spectrum was recorded as given in Figure 5.2.1.2. The absorption at 330 nm decreased in intensity with a concurrent increase in the absorptions at 290 and 430 nm. Two isosbestic points were observed at 322 and 340 nm. From the changes in the UV/vis. absorption spectrum it would appear that upon photolysis conversion from the *cis* to *trans* isomer resulted.

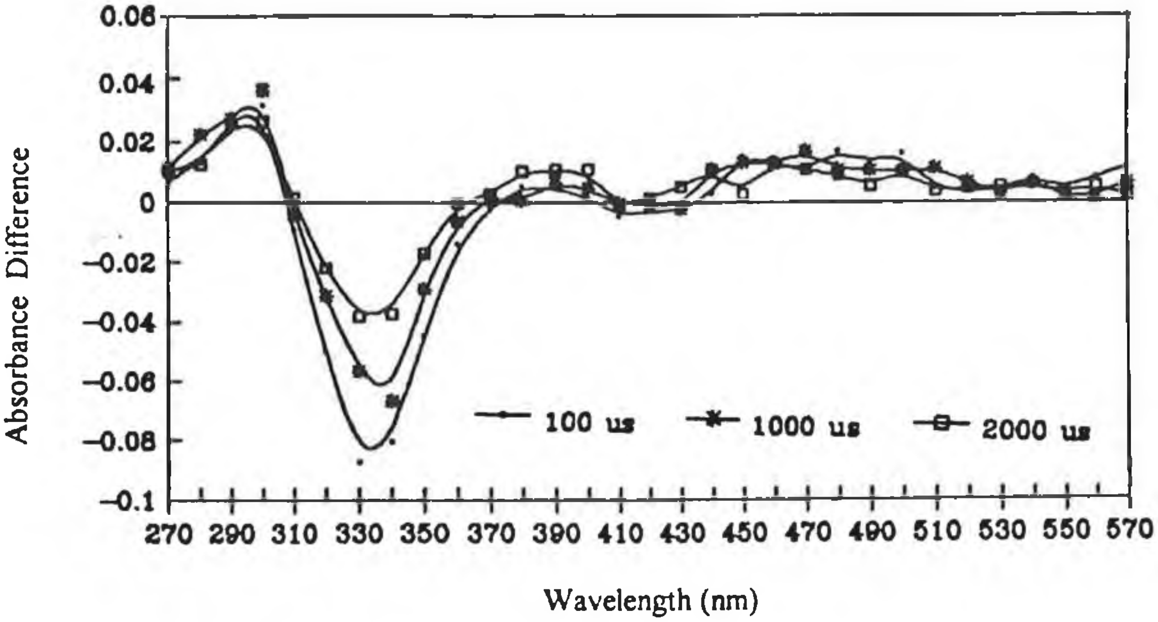

Figure 5.2.1.1 UV/vis. difference spectra observed upon flash photolysis of (η^6-*cis*-1,2 diphenylethene)Cr(CO)$_3$ under 1 atm. of CO at different time intervals after the flash.

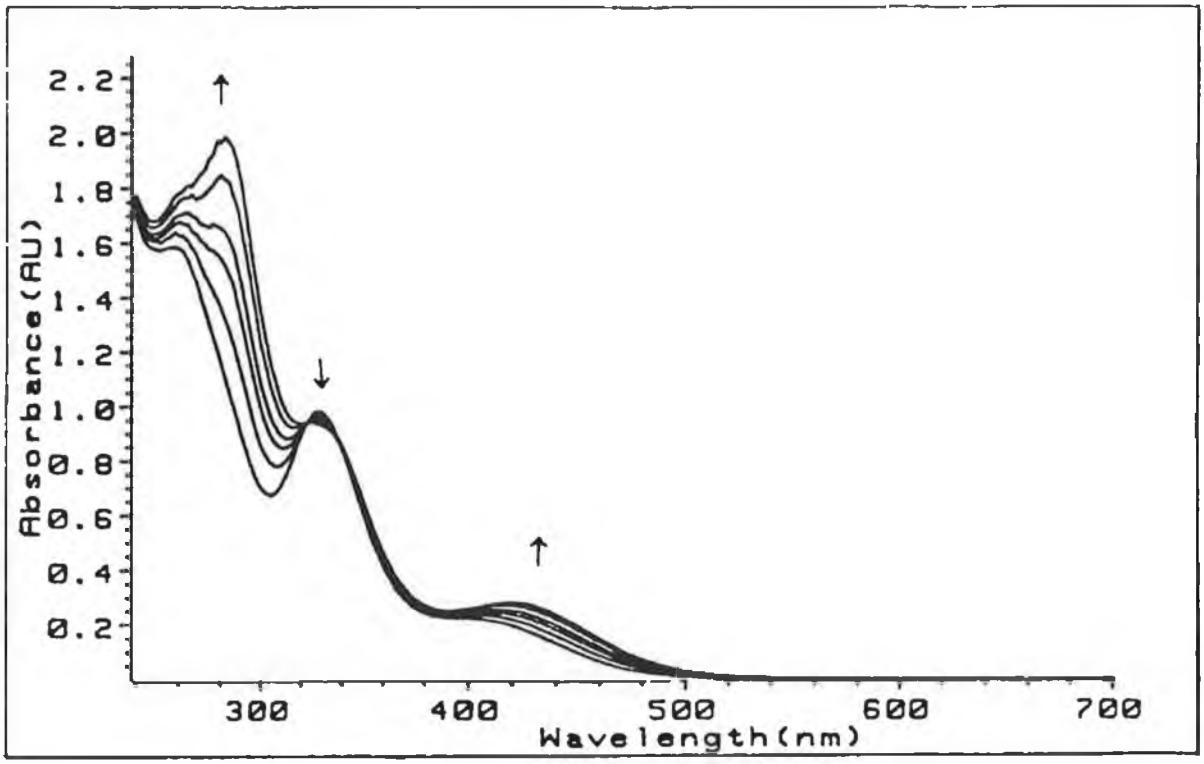

Figure 5.2.1.2 Changes recorded in the electronic absorption spectrum of (η^6-*cis*-1,2 diphenylethene)Cr(CO)$_3$ following laser flash photolysis at 355 nm under 1 atm. of CO.

5.2.2 NMR monitored photolysis of (η^6-cis-1,2 diphenylethene)Cr(CO)$_3$.

Photolysis of (η^6-*cis*-1,2 diphenylethene)Cr(CO)$_3$ was monitored by proton NMR. The sample for NMR was made up in a degassable NMR tube in deuterated cyclohexane following freeze pump thaw procedure and 1 atm. of CO was admitted to the tube. Resonances for the complexed ring in (η^6-*cis*-1,2 diphenylethene)Cr(CO)$_3$ occur between 4.9 – 5.2 ppm with those of the uncomplexed ring in the region 7.10 – 7.24 ppm and the vinylic protons occur at ~6.75 and ~ 6.6 ppm (see Figure 5.2.2.2). As the cyclohexane solution of (η^6-*cis*-1,2 diphenylethene)Cr(CO)$_3$ was irradiated at λ > 400 nm new resonances were seen to form in the region 5.16 – 5.34 together with further resonances in the region 7.2 – 7.4 ppm. Concurrently two sets of doublets appear at ~6.55 and ~6.88 ppm. Singlets are observed at 6.5 ppm and 7.2 ppm as the photolysis proceeded. On comparing the final photolysed sample proton NMR spectrum with that of uncomplexed *trans* and *cis* stilbene (Figures 5.1.2.1 and 5.2.2.1) and with (η^6-*trans*-1,2 diphenylethene)Cr(CO)$_3$ it appears that the main photochemical pathway is isomerisation from (η^6-*cis*-1,2 diphenylethene)Cr(CO)$_3$ to (η^6-*trans*-1,2 diphenylethene)Cr(CO)$_3$. However, this is not the only reaction that is occurring as the NMR resonances of uncomplexed ligands are also present. At 7.2 ppm a singlet increases in intensity together with other resonances, and the singlet at this frequency indicates the formation of uncomplexed *trans* ligand. Also a singlet is observed at 6.5 ppm which is present in the uncomplexed *cis* isomer (see Figure 5.2.2.1). On comparing the relative intensities of the various products it would appear that the *major* photochemical pathway is isomerisation of (η^6-*cis*-1,2 diphenylethene)Cr(CO)$_3$ to (η^6-*trans*-1,2 diphenylethene)Cr(CO)$_3$, also formed are uncomplexed *cis* ligand together with a *minor* amount of uncomplexed *trans* stilbene.

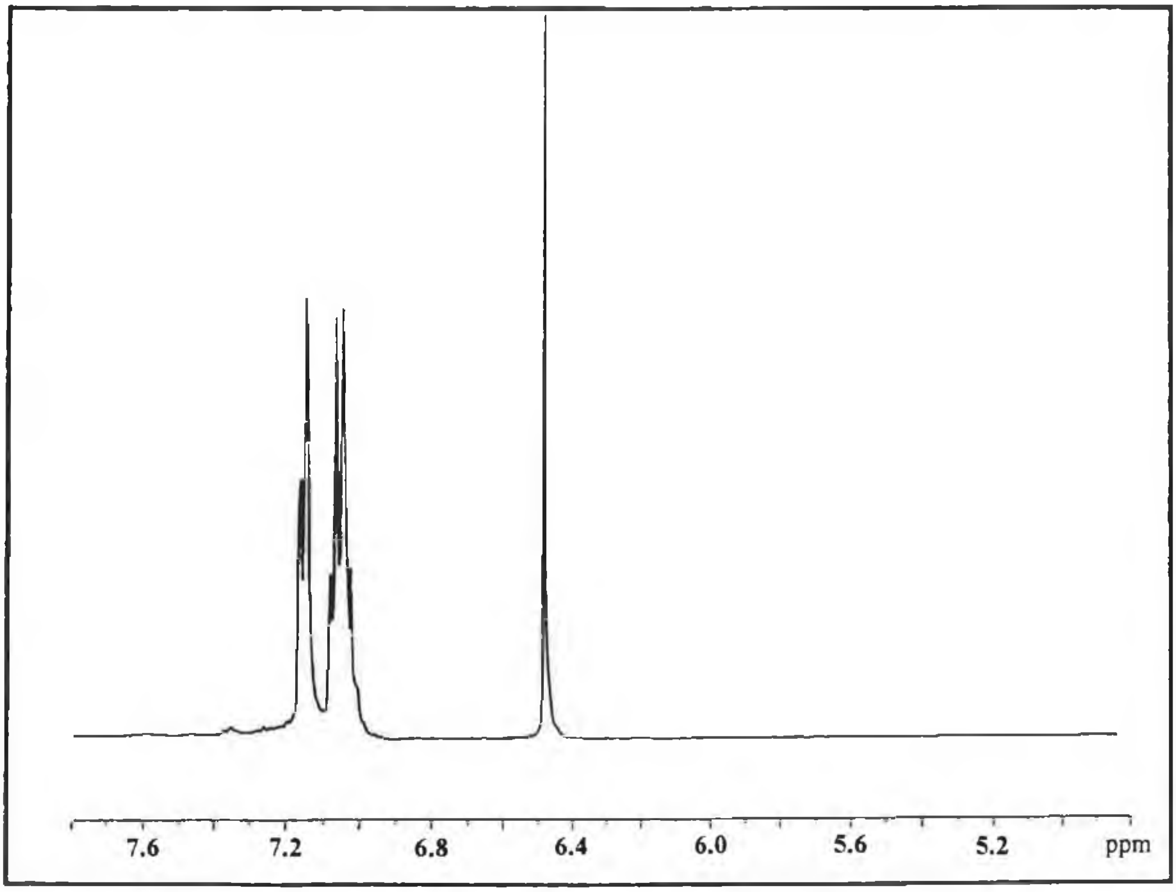

Figure 5.2.2.1. ^{1}H NMR spectrum of *cis*-1,2 diphenylethene in cyclohexane-d_{12}.

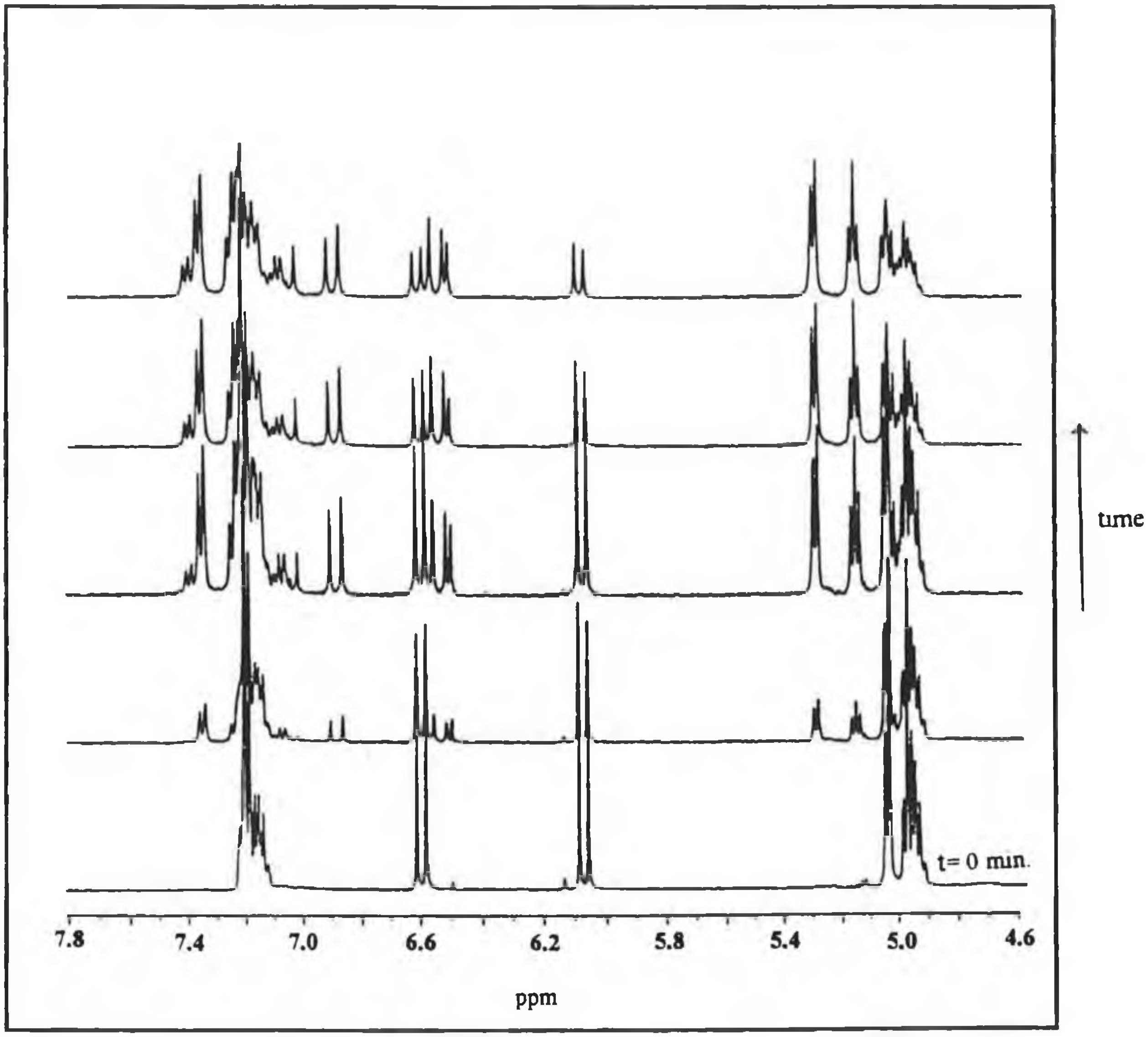

Figure 5.2.2.2. ^{1}H NMR spectrum of (η^6-*cis*-1,2 diphenylethene)Cr(CO)$_3$ in cyclohexane-d_{12} at different time intervals of irradiation at $\lambda > 400$ nm.

5.2.3 Infrared monitored photolysis of (η^6-*cis*-1,2 diphenylethene)Cr(CO)$_3$.

An argon degassed cyclohexane solution of (η^6-*cis*-1,2 diphenylethene)Cr(CO)$_3$ was irradiated in the presence of excess pyridine. As the photolysis proceeded the infrared bands of the tricarbonyl at 1912 and 1978 cm^{-1} decreased in intensity together with the formation of two bands at 1902 and 1853 cm^{-1}. The infrared spectra in Figure 5.2.3.1 was recorded at intervals of 10 seconds. From the previous results of the NMR experiment (*vide supra*) it is probable that (η^6-*trans*-1,2 diphenylethene)Cr(CO)$_2$(pyridine) is formed, rather than the *cis*-complex as at $\lambda > 400$ nm isomerisation from the *cis* to *trans* tricarbonyl occurs. There is only a difference of one wave number in the frequencies of the product formed following photolysis of the *cis* and *trans* compound in the presence of pyridine.

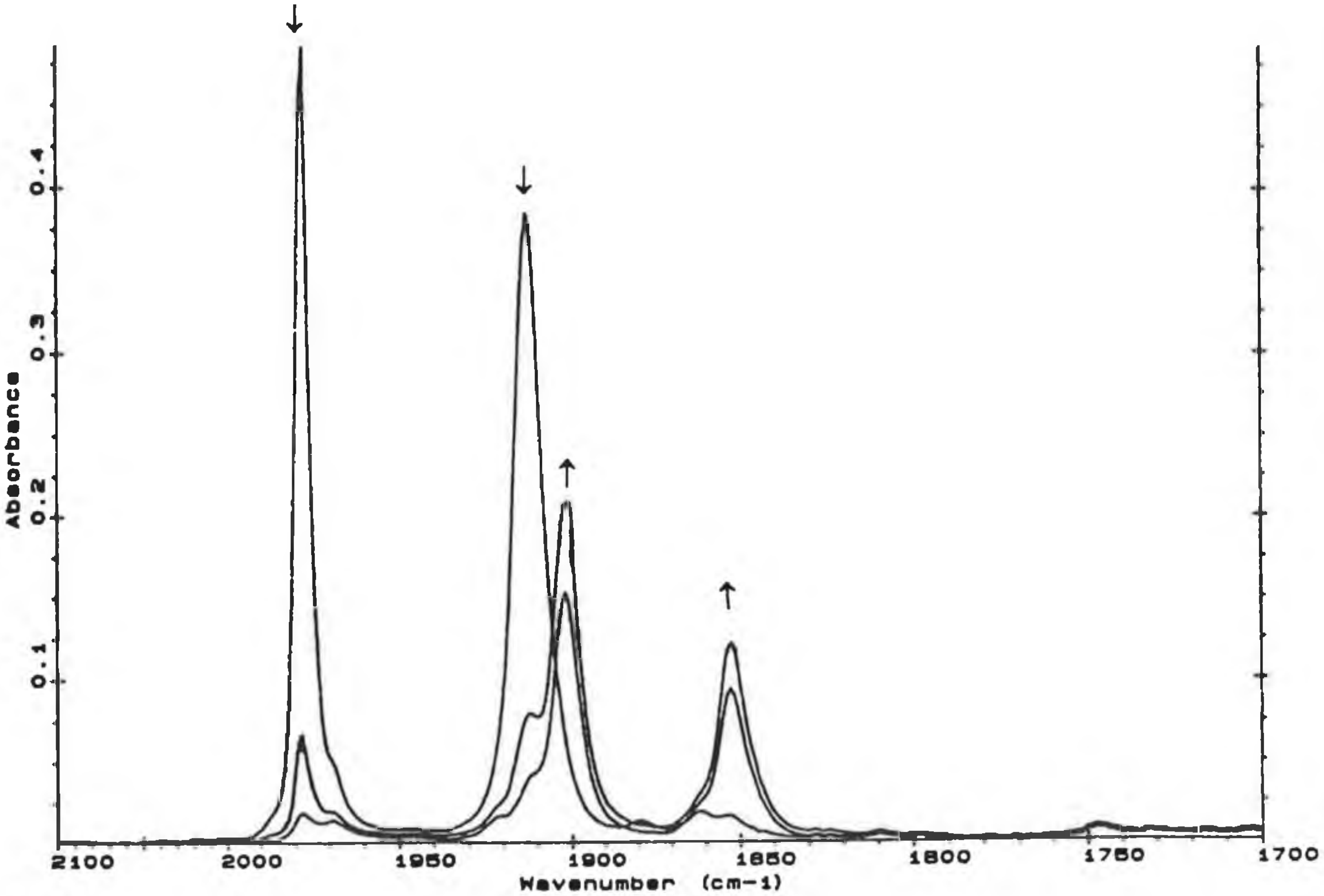

Figure 5.2.3.1 Infrared spectral changes for the reaction of (η^6-*cis*-1,2 diphenylethene)Cr(CO)$_3$ with excess pyridine in argon degassed cyclohexane.

5.2.4 Luminescence studies of (η^6-*cis*- and *trans*-1,2 diphenylethene)$Cr(CO)_3$ in solution at room temperature.

Emission spectra were recorded from (η^6-*cis*- and *trans*-1,2 diphenylethene)$Cr(CO)_3$ in cyclohexane at room temperature. Solutions were deaereated by flushing with argon for 20 minutes. An excitation wavelength of 330 nm was used as it corresponds to $\lambda_{max.}$ in the *cis*-tricarbonyl compound. The emission spectrum recorded for the *cis*-isomer is given in Figure 5.2.4.1. This spectrum has an emission maximum centred at 365 nm with a 'tailing' emission to approximately 420 nm. The emission spectrum for the *trans*-isomer is given in Figure 5.2.4.2. This compound has a much broader emission band than that of the *cis*-isomer with a maximum emission at 350 nm together with a further shoulder at 365 nm.

Metal complexes which do not emit in room temperature solution is because of rapid ligand dissociation and efficient non-radiative relaxation to the ground state. Complexes that possess a MLCT state as the lowest energy excited state undergo relatively slow radiative deactivation which can readily be detected under fluid conditions. Only the $M(CO)_5L$ complexes where M=Mo or W and L = pyridine containing an electron withdrawing substituent have been established to luminesce at room temperature. Emission under fluid conditions has not been observed from $M(CO)_5L$ complexes in which the ligand field excited state has been established as the lowest lying excited state. Most of the emissive properties of metal carbonyls have been recorded at low temperature in a rigid environment, where nonradiative processes are considerably reduced.[10]

As both the *cis* and *trans* compounds luminesce at room temperature it would indicate that the lowest lying state is probably metal to ligand charge transfer which is in agreement with previous studies.

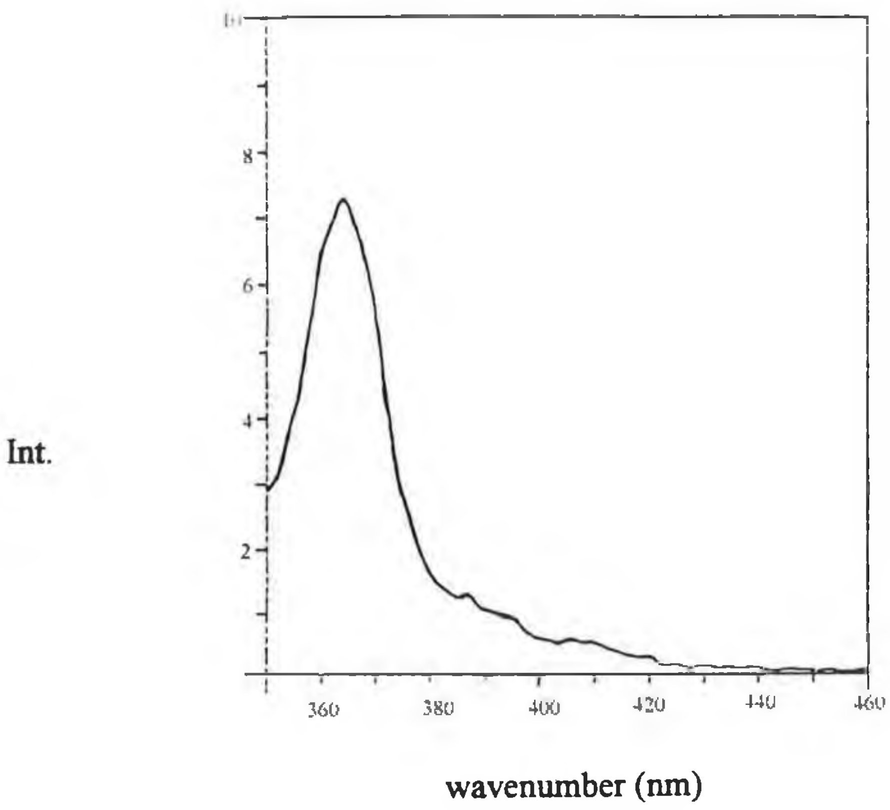

Figure 5.2.4.1 Emission spectrum of (η^6-*cis*-1,2 diphenylethene)Cr(CO)$_3$ at 298K in cyclohexane.

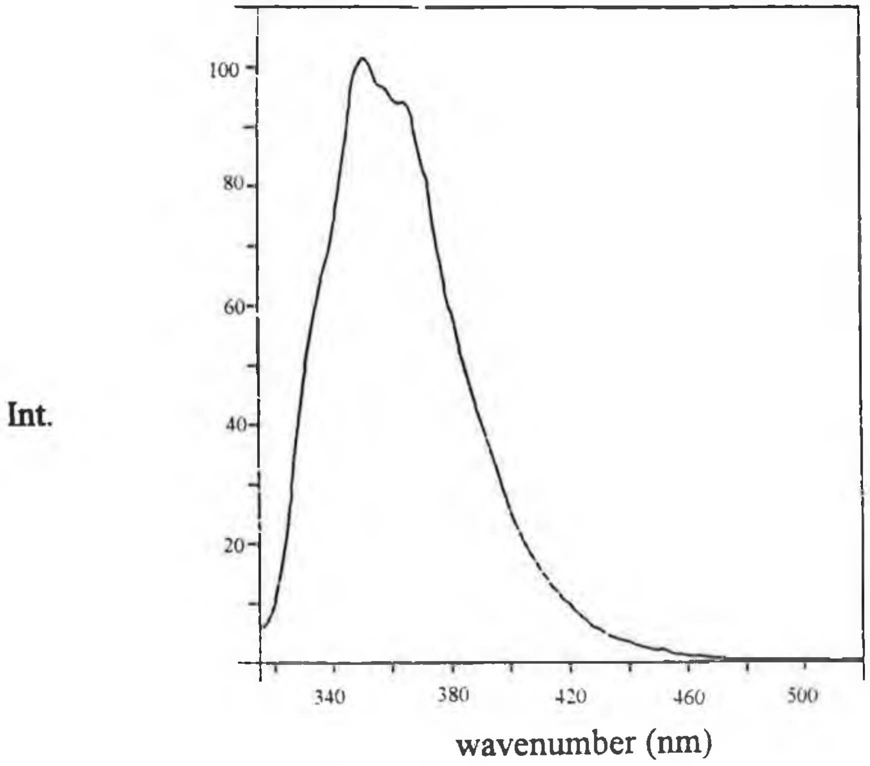

Figure 5.2.4.2 Emission spectrum of (η^6-*trans*-1,2 diphenylethene)Cr(CO)$_3$ at 298K in cyclohexane.

5.3 (η^6-*Trans, trans*-1,4-diphenyl-1,3-butadiene)Cr(CO)$_3$.

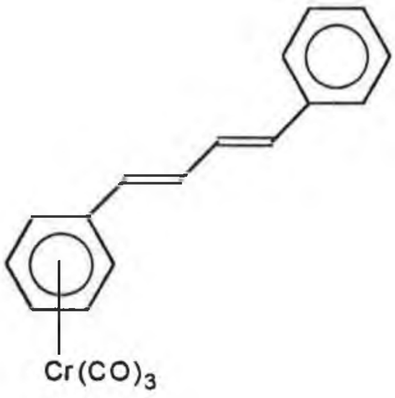

5.3.1 Electronic absorption spectrum of (η^6-*trans, trans*-1,4-diphenyl-1,3-butadiene)Cr(CO)$_3$.

The UV/vis. spectrum of (η^6-*trans,trans*-1,4-diphenyl-1,3-butadiene)Cr(CO)$_3$ in cyclohexane is given in Figure 5.3.1.1. The maximum absorption occurs at 315 nm. This transition is attributed to a metal ----> arene CT with some chromium ----> π^* CO CT character. A further maxima was observed at 435 nm which is tentatively assigned as a MLCT transition because on increasing the solvent polarity a blue shift is observed as shown in Figure 5.3.1.2.

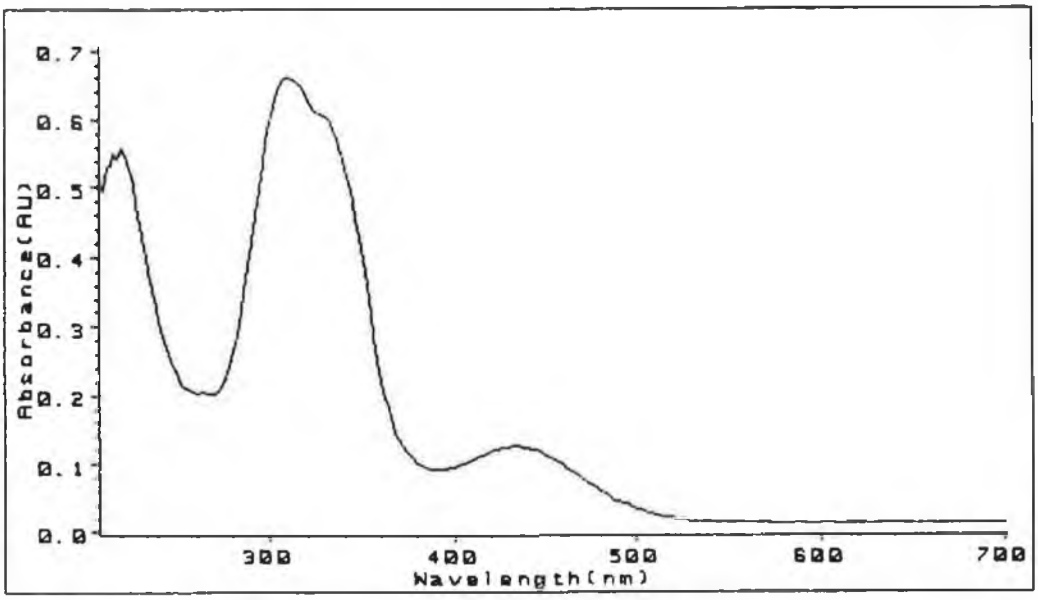

Figure 5.3.1.1 Electronic absorption spectra (η^6-*trans,trans*-1,4-diphenyl-1,3-butadiene)Cr(CO)$_3$ in cyclohexane (1.25 x 10^{-4} M).

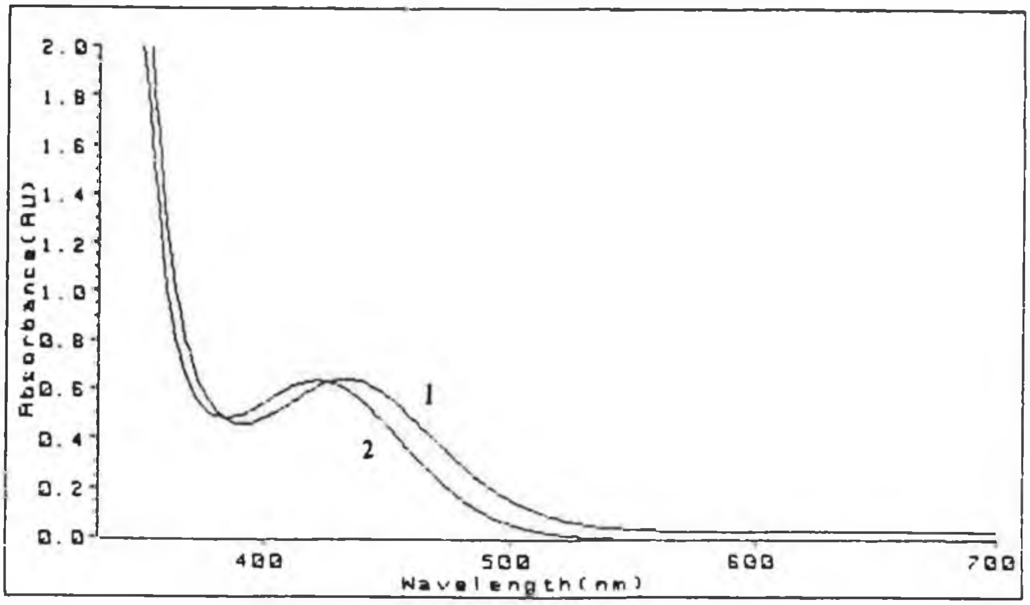

Figure 5.3.1.2 UV/vis. spectrum of (η^6-*trans,trans*-1,4-diphenyl-1,3-butadiene)$Cr(CO)_3$ in (1) cyclohexane and (2) acetone.

5.3.2 Steady state photolysis of (η^6-*trans, trans*-1,4-diphenyl-1,3-butadiene)$Cr(CO)_3$.

Preliminary photolysis experiments were carried out on this compound. A sample was made up in cyclohexane under 1 atm. of CO and irradiated at > 345 nm and irradiated at various time intervals of 5 minutes. Throughout the absorption spectrum was recorded as presented in Figure 5.3.2.1. The absorptions at 315 and 435 nm decrease in intensity concurrent with an increase in the absorption at 228 nm. An infrared spectrum of this sample indicated the formation of $Cr(CO)_6$.

Hence the reaction for this system is as given in Reaction 5.3.2.1

$$(\eta^6\text{-}trans,\ trans\text{-1,4-diphenyl-1,3-butadiene})Cr(CO)_3 \xrightarrow[\lambda > 345\text{ nm. CO}]{h\nu} trans,trans\text{-1,4-diphenyl-1,3-butadiene} + Cr(CO)_6$$

(5.3.2.1)

At present work is continuing on this tricarbonyl compound and as yet laser experiments and NMR photolysis experiments have to be carried out to further elucidate the reaction pathway for this system.

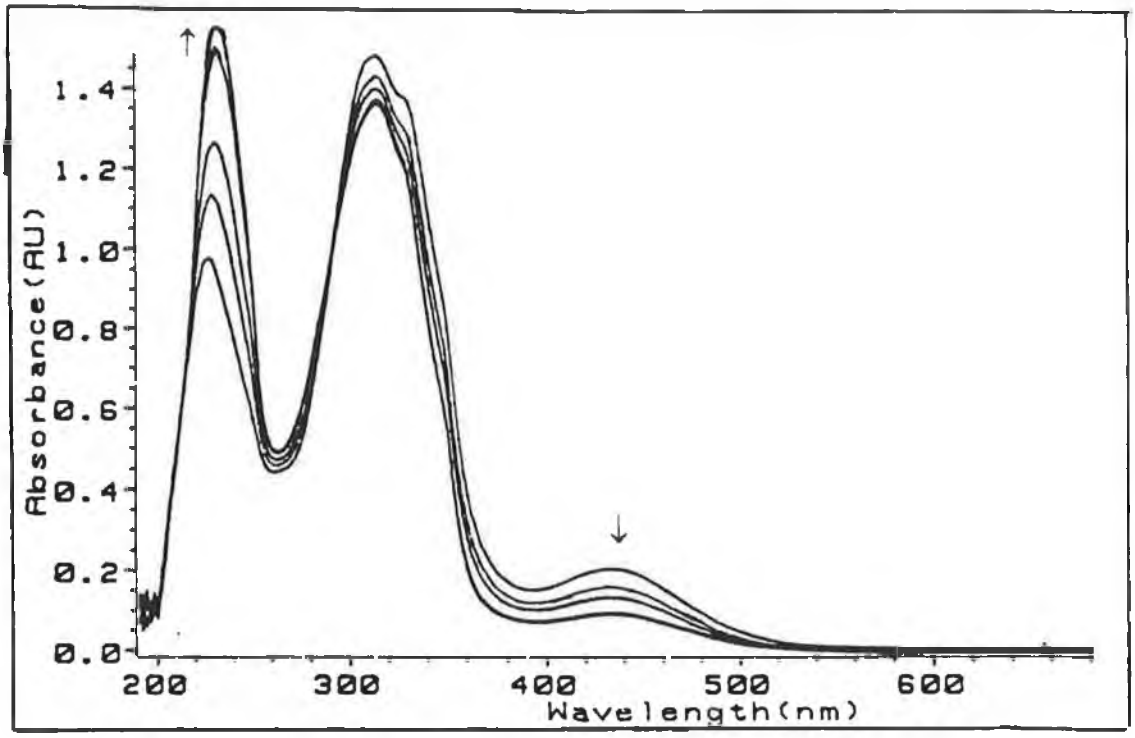

Figure 5.3.2.1 Changes observed in electronic absorption spectra of (η^6-*trans,trans*-1,4-diphenyl-1,3-butadiene)Cr(CO)$_3$ in cyclohexane (1.8 x 10^{-4} M) under 1 atm. CO as the sample is irradiated at > 345 nm.

5.4 Conclusion

From the experimental results obtained on photolysing samples of (η^6-*cis*- or *trans*-1,2 diphenylethene) chromium tricarbonyl it would appear that a wavelength dependent photochemistry exists. The NMR experiments possibly provide the most informative results for this system. Firstly on photolysing the sample of (η^6-*trans*-1,2 diphenylethene)$Cr(CO)_3$ under carbon monoxide at $\lambda >$ 400 nm loss of the stilbene ligand is observed as indicated by NMR but from the flash photolysis experiments (λ = 355 nm) formation of the dicarbonyl intermediate is observed. Secondly, from the NMR data on photolysing a sample of (η^6-*cis*-1,2 diphenylethene)$Cr(CO)_3$ under carbon monoxide at $\lambda >$ 400 nm isomerisation from the *cis* to *trans* isomer is observed as is loss of *cis* and *trans* stilbene ligands. However, from a comparison of the relative intensities of the uncomplexed ligands it would appear that the *trans* ligand is formed in a lower yield than the *cis* ligand. Formation of the dicarbonyl species results from high energy photolysis as confirmed from the infrared measurements. It would appear that in the case of the *cis* ligand it is the *trans* ligated pyridine dicarbonyl product that is formed following irradiation in the presence of pyridine in view of the NMR experiments. Possible reaction mechanisms for the stilbene complexes are given in Schemes 5.4.1 and 5.4.2.

As regards (η^6-*trans,trans*-1,4-diphenyl-1,3-butadiene)$Cr(CO)_3$ only very preliminary studies were carried out on this system but loss of ligand and formation of $Cr(CO)_6$ were the end results following long wavelength photolysis.

All the data available on these compounds indicate the lowest transition as being metal to ligand charge transfer in origin. Similarly to the polyaromatic tricarbonyls discussed in Chapter 4, these complexes indicate that on varying the ligand the system may not be photoreversible as observed here. Also, a wavelength dependent photochemistry exists. On long wavelength photolysis cleavage of the arene ligand occurs while at a shorter wavelength formation of a dicarbonyl species is observed. For the *cis*-isomer isomerisation to the *trans*-isomer results following irradiation.

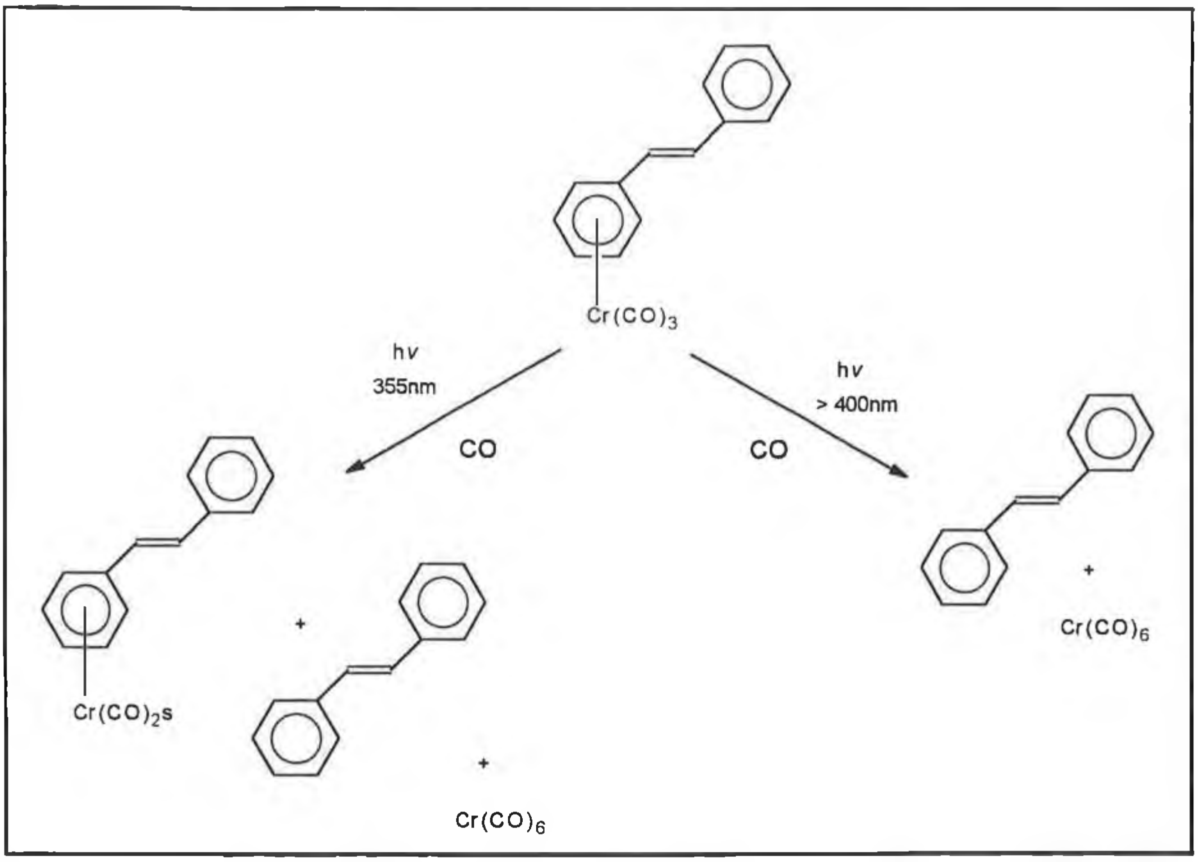

Scheme 5.4.1

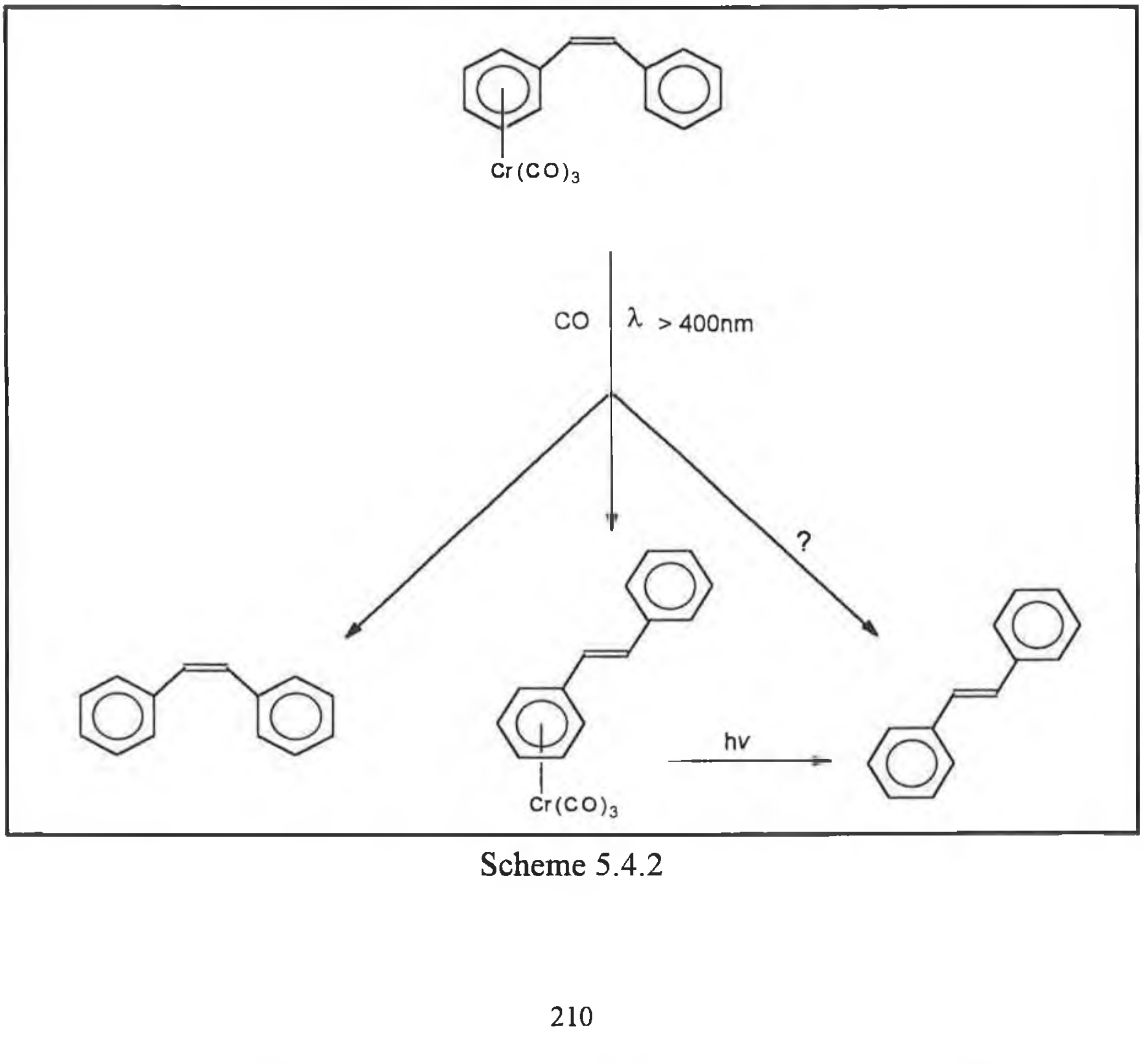

Scheme 5.4.2

5.5 The crystal and molecular structure of (η^6-*trans*-1,2 diphenylethene)Cr(CO)$_3$.

5.5.1 Introduction.

Early this century the newly discovered X-ray diffraction by crystals made a complete change in crystallography and in the whole science of the atomic structure of matter, thus giving a new impetus to the development of solid state physics. The diffraction of X-rays by crystals was discovered by Max von Laue in 1912, who later showed that the phenomenon could be described in terms of diffraction from a three dimensional grating. Crystallographic methods, primarily X-ray diffraction analysis, penetrated into material sciences, molecular physics, and chemistry, and also into many other branches of science. Other important factors promoting the development of crystallography were the elaboration of the theory of crystal growth (which brought crystallography closer to thermodynamics and physical chemistry) and the development of the various methods of growing synthetic crystals dictated by practical needs. The theoretical basis of crystallography is the theory of symmetry, which has been intensively developed in recent years. The study of the atomic structure has been extended to extremely complicated crystals containing hundreds and thousands of atoms in the unit cell.

5.5.2 Data collection for (η^6-*trans*-1,2 diphenylethene)Cr(CO)$_3$.

(η^6-*Trans*-1,2 diphenylethene) Cr(CO)$_3$ was synthesised by the method of *Hrnviar et al.*[11] as described in Chapter 7, and suitable crystals were grown from benzene/pentane solution. Collection of the crystallographic data was carried out at Trinity College Dublin.

A red crystal of dimensions 0.4 x 0.4 x 0.5 mm^3 was selected for the molecular structure determination. Mo Kα radiation (0.71069Å) was used in the analysis of the complex of which 2062 independent reflections were collected. The index range was h - 0 to 12, k - 0 to 16 and l - 1 to 17. Of the reflections measured 282 were rejected leaving 1780 unique reflections. The unit cell was found to be orthrombic with unit cell dimensions :- a = 11.489(12), b = 15.638(11), c = 16.239(2). The density was calculated to be 1.44g/cm^3. The space group Pbca was established with Z = 8.

The structure was solved using the Patterson heavy atom method with partial structure expansion to find all non-hydrogens using SHELXS-86.[12] The atomic coordinates were refined with full matrix least squares refinement using SHELXL-93.[13] Hydrogen atoms were located in their calculated positions and refined with respect to the carbon atoms to which they were attached. The final calculated R values were R = 0.0475 and wR = 0.1107. The final atomic coordinates for all the non hydrogen atoms are given in Table 5.5.3.1 and those for the hydrogen atoms in Table 5.5.3.2. A complete list of bond angles and bond lengths are given in Tables 5.5.3.3 and 5.5.3.4.

5.5.3 Molecular structure of (η^6-*trans*-1,2 diphenylethene)$Cr(CO)_3$.

The complex contains one molecule per asymmetric unit as presented in Figure 5.5.3.1. The six carbon atoms of the complexed ring are coplanar, and their plane is essentially parallel to that of the three oxygen atoms - this is as was reported for the structure of (η^6-benzene)$Cr(CO)_3$.[14]

The distance between the carbon atoms in the complexed ring varied from 1.346-1.399 Å which is similar to that measured in (η^6-benzene)$Cr(CO)_3$[14] where the C-C distances varied from 1.371-1.421 Å. The chromium to complexed carbon ring carbon ring distances range from 2.182-2.240 Å, with an average distance of 2.211 Å. The perpendicular distance of the chromium atom from the plane of the ring to the six carbon atoms is marginally greater than that for (η^6-benzene)$Cr(CO)_3$ (1.72Å), (η^6-1,3,5-mesitylene)$Cr(CO)_3$ (1.72Å)[15] and (η^6-benzene)$_2Cr_2$ (1.60Å).[16] The C=C double bond was measured to be 1.116Å. One noticeable feature of this compound is that the uncomplexed ring is slightly "bent" out of the plane of the complexed ring.

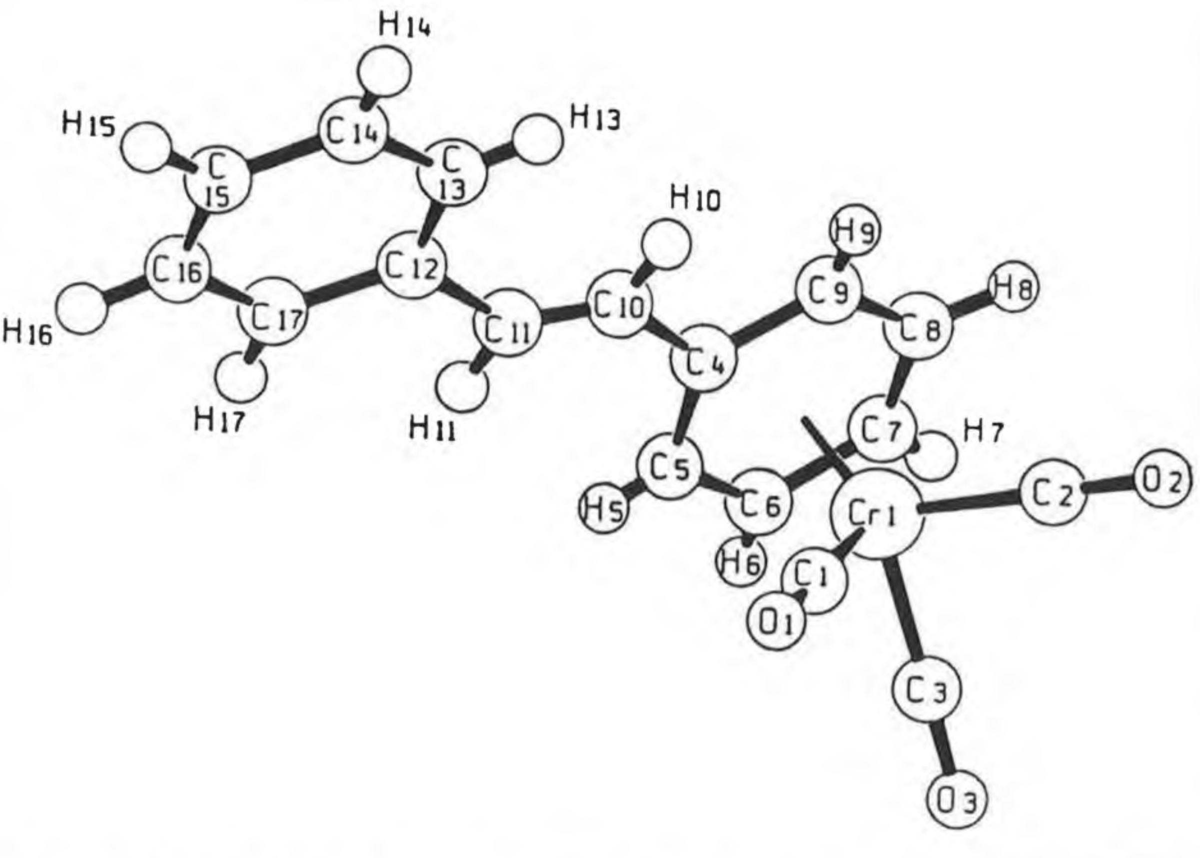

Figure 5.5.3.1 SCHAKAL drawing of the crystal structure of (η^6-*trans*-1,2 diphenylethene)$Cr(CO)_3$.

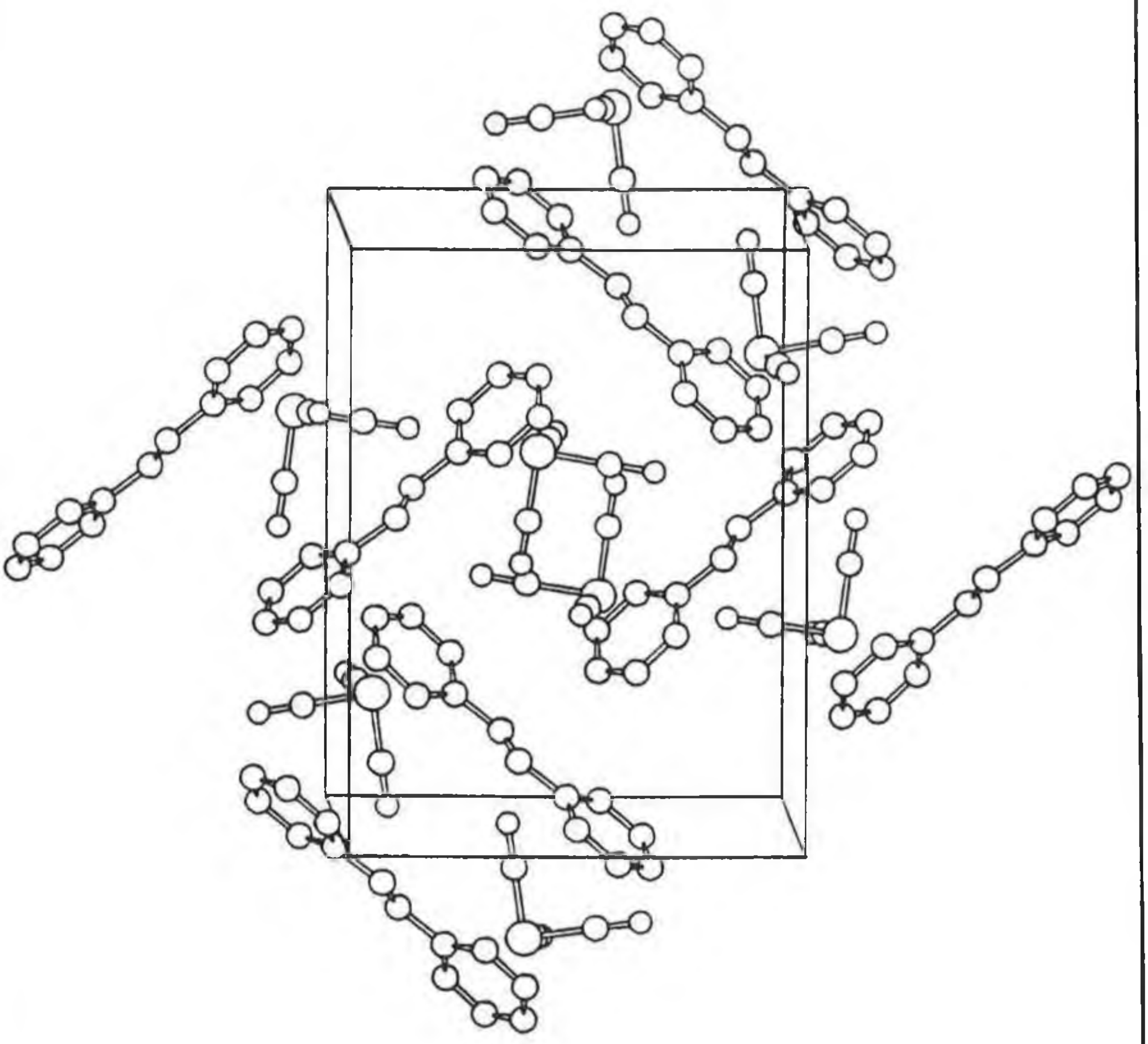

Figure 5.5.3.2 A SCHAKAL representation of the unit cell of (η^6-*trans*-1,2 diphenylethene)Cr(CO)$_3$ (Z=8).

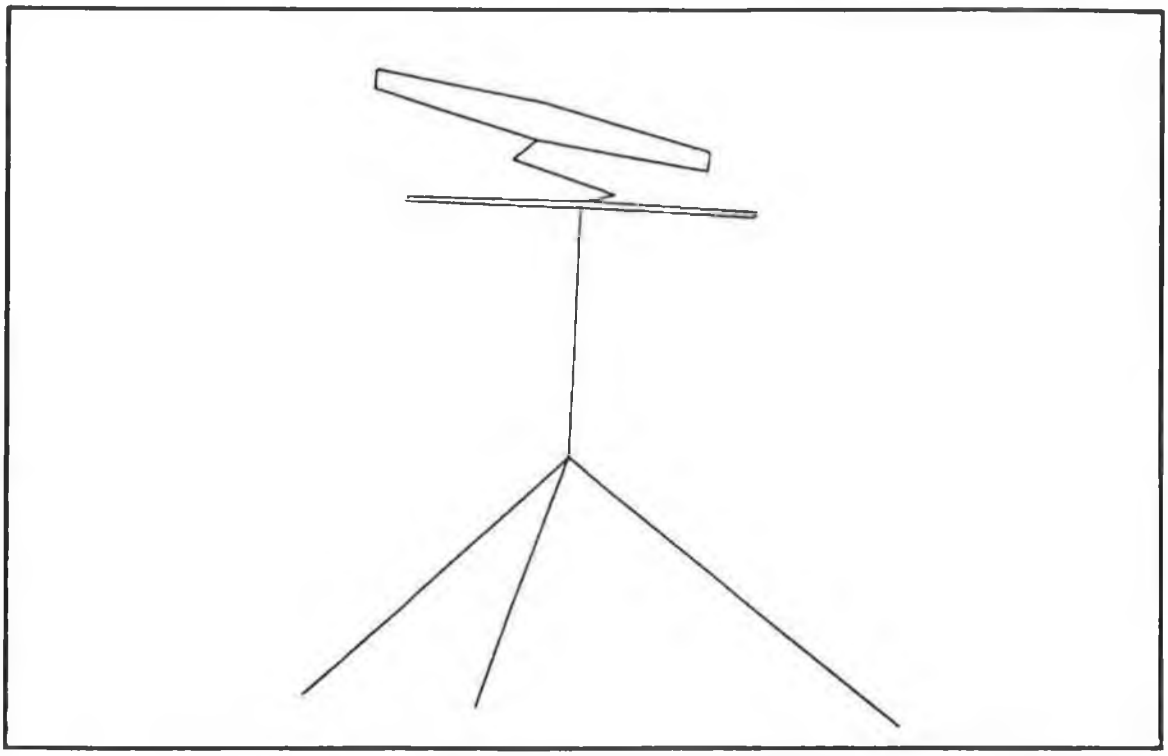

Figure 5.5.3.3 A SCHAKAL drawing of the structure of (η^6-*trans*-1,2 diphenylethene)$Cr(CO)_3$.

	x/a	y/b	z/c	Ueq
Cr(1)	974(1)	1767(1)	789(1)	40(1)
O(1)	1318(4)	-112(2)	536(2)	75(1)
O(2)	496(4)	1913(3)	-1018(2)	80(1)
O(3)	-1557(4)	1464(3)	1086(3)	84(1)
C(1)	1178(4)	606(3)	638(3)	49(1)
C(2)	678(4)	1856(3)	-319(4)	53(1)
C(3)	-580(5)	1578(3)	965(3)	55(1)
C(4)	2737(5)	1820(3)	1376(4)	59(2)
C(5)	1878(6)	1845(4)	1986(4)	63(2)
C(6)	1010(6)	2454(5)	1958(4)	70(2)
C(7)	1005(7)	3055(4)	1322(5)	77(2)
C(8)	1813(6)	3025(4)	723(5)	69(2)
C(9)	2675(5)	2424(4)	749(4)	66(2)
C(10)	3750(7)	1211(5)	1318(6)	107(3)
C(11)	4115(8)	754(4)	1778(7)	112(3)
C(12)	5159(5)	166(3)	1771(4)	61(2)
C(13)	5919(7)	51(4)	1126(5)	80(2)
C(14)	6837(6)	-523(5)	1192(5)	90(2)
C(15)	6987(5)	-974(4)	1894(4)	70(2)
C(16)	6255(6)	-861(4)	2537(4)	70(2)
C(17)	5350(5)	-294(4)	2468(5)	66(2)

Table 5.5.2.1 Atomic coordinates (x 10^4) for non hydrogen atoms with e.s.d.'s in parentheses for *trans*-(η^6-1,2 diphenylethene)Cr(CO)$_3$. Ueq x 10^3. $\{Ueq = (1/3)\Sigma_i\Sigma_j U_{ij} a^*_i . a^*_j . a_i a_j\}$.

H(5)	1870(45)	1499(31)	2324(31)	48(18)
H(6)	519(45)	2478(34)	2294(33)	55(19)
H(7)	487(39)	3344(28)	1312(26)	27(14)
H(8)	1730(55)	3365(39)	228(39)	19(22)
H(9)	3147(46)	2374(34)	342(32)	61(18)
H(10)	4135(7)	1217(5)	814(6)	268(51)
H(11)	3690(8)	730(4)	2265(7)	268(51)
H(13)	5860(45)	304(34)	652(33)	59(16)
H(14)	7271(67)	-524(49)	798(45)	119(30)
H(15)	7665(53)	-1384(67)	1964(34)	84(18)
H(16)	6325(51)	-1182(40)	3055(40)	91(21)
H(17)	4844(51)	-262(35)	2915(35)	75(19)

Table 5.5.2.2 Coordinates x 10^4 for hydrogen atoms *trans*-(η^6-1,2 diphenylethene)$Cr(CO)_3$.

C(3) - Cr(1) - C(2)	89.1(2)
C(3) - Cr(1) - C(1)	89.2(2)
C(2) - Cr(1) - C(1)	88.2(2)
C(3) - Cr(1) - C(6)	87.8(3)
C(2) - Cr(1) - C(6)	144.9(3)
C(1) - Cr(1) - C(6)	126.7(3)
C(3) - Cr(1) - C(7)	95.9(3)
C(2) - Cr(1) - C(7)	108.7(3)
C(1) - Cr(1) - C(7)	162.4(3)
C(6) - Cr(1) - C(7)	37.2(3)
C(3) - Cr(1) - C(8)	125.5(3)
C(2) - Cr(1) - C(8)	88.0(3)
C(1) - Cr(1) - C(8)	145.0(3)
C(6) - Cr(1) - C(8)	65.9(3)
C(7) - Cr(1) - C(8)	35.7(3)
C(3) - Cr(1) - C(5)	109.3(3)
C(2) - Cr(1) - C(5)	161.1(2)
C(1) - Cr(1) - C(5)	96.4(2)
C(6) - Cr(1) - C(5)	36.7(2)
C(7) - Cr(1) - C(5)	66.1(3)
C(8) - Cr(1) - C(5)	77.7(3)
C(3) - Cr(1) - C(9)	160.4(2)
C(2) - Cr(1) - C(9)	95.7(2)
C(1) - Cr(1) - C(9)	109.9(2)
C(6) - Cr(1) - C(9)	77.3(3)
C(7) - Cr(1) - C(9)	64.6(3)
C(8) - Cr(1) - C(9)	36.2(2)
C(5) - Cr(1) - C(9)	65.4(3)
C(3) - Cr(1) - C(4)	145.1(2)
C(2) - Cr(1) - C(4)	125.6(2)
C(1) - Cr(1) - C(4)	88.7(2)
C(6) - Cr(1) - C(4)	66.1(2)
C(7) - Cr(1) - C(4)	77.5(4)
C(8) - Cr(1) - C(4)	65.8(4)
C(5) - Cr(1) - C(4)	36.7(4)

Table 5.5.2.3 A complete list of bond angles (°) for *trans*-(η^6-1,2 diphenylethene)Cr(CO)$_3$.

C(9) - C(1) - C(4)	36.4(2)
O(1) - C(1) - Cr(1)	179.0(5)
O(2) - C(2) - Cr(1)	179.7(5)
O(3) - C(3) - Cr(1)	179.0(5)
C(9) - C(4) - C(5)	117.69(6)
C(9) - C(4) - C(10)	115.0(7)
C(5) - C(4 - C(10)	127.4(7)
C(9) - C(4) - Cr(1)	70.5(3)
C(5) - C(4) - Cr(1)	70.4(3)
C(10) -C(4) -Cr(1)	130.4(4)
C(6) - C(5) - C(4)	120.4(6)
C(6) - C(5) - Cr(1)	70.7(4)
C(4) - C(5) - Cr(1)	73.0(3)
C(5) - C(6) - C(7)	119.5(7)
C(5) - C(6) - Cr(1)	72.7(4)
C(7) - C(6) - Cr(1)	71.8(4)
C(8) - C(7) - C(6)	120.6(7)
C(8) - C(7) - Cr(1)	72.2(4)
C(6) - C(7) - Cr(1)	71.0(4)
C(7) - C(8) - C(9)	120.1(7)
C(7) - C(8) - Cr(1)	72.1(4)
C(9) - C(8) - Cr(1)	72.5(3)
C(8) - C(9) - C(4)	121.8(7)
C(8) - C(9) - Cr(1)	71.39(3)
C(4) - C(9) - Cr(1)	73.09(3)
C(11) - C(10) -C(4)	130.89(13)
C(10) - C(11) - C(12)	133.1(13)
C(17) - C(12) - C(13)	117.6(6)
C(17) - C(12) - C(11)	116.4(7)
C(13) - C(12) - C(11)	126.0(7)
C(12) - C(13) - C(14)	120.4(6)
C(15) - C(14) - C(13)	120.0(7)
C(14) - C(15) - C(16)	120.2(7)
C(15) - C(16) - C(17)	119.6(7)
C(12) - C(17) - C(16)	122.2(6)

Table 5.5.3.3 (continued): A complete list of bond angles (°) for *trans*-(η^6-1,2 diphenylethene)Cr(CO)$_3$.

Cr1--C3	1.832(6)
Cr1--C2	1.836(6)
Cr1--C1	1.847(5)
Cr1--C6	2.182(6)
Cr1--C7	2.192(6)
Cr1--C8	2.193(6)
Cr1--C5	2.207(6)
Cr1--C9	2.209(6)
Cr1--C4	2.240(5)
O1--C1	1.146(6)
O2--C2	1.158(6)
O3--C3	1.153(6)
C4--C9	1.391(8)
C4--C5	1.399(8)
C4--C10	1.506(10)
C5--C6	1.380(9)
C6--C7	1.396(10)
C7--C8	1.346(10)
C8--C9	1.367(9)
C10--C11	1.116(10)
C11--C12	1.512(9)
C12--C17	1.358(9)
C12--C13	1.376(9)
C13--C14	1.390(10)
C14--C15	1.351(9)
C15--C16	1.353(9)
C16--C17	1.370(8)

Table 5.5.2.4 Selected bond lengths (Å) for *trans*-(η^6-1,2 diphenylethene)$Cr(CO)_3$.

5.6 References

1 (a)Wrighton,M.;Hammond,G.S.;Gray,H.B.; *J. Am. Chem. Soc.*:; 1968,**90**,1187.
(b)Wrighton,M.;Hammond,G.S.;Gray,H.B.; *J. Am. Chem. Soc.*; 1971,**93**,4336.
(c)Mastubara,T.;Ford,P.C.; *Inorg.Chem.*;1978,**17**,1747.
(d)Wrighton,M.;Abrahamson,H.B.;Morse,D.L.; *J. Am. Chem. Soc.*; 1976,**98**,4105.

2 Giordano,P.J.;Wrighton,M.S.; *Inorg.Chem.*; 1977,**16**,160.

3 Ford,P.C.; *Rev. Chem. Intermed.*; 1976,**2**,267.

4 Wrighton,M.;Hammond,G.S.;Gray,H.B.; *Mol. Photochem.*; 1973,**5**,179.

5 Rest,A.J.;Sodeau,J.R.; *J. Chem. Soc., Chem. Comm.*; 1975,696.

6 Caroll,D.G.;McGlynn.S.P.;*Inorg. Chem.*;1968,**7**,1285.

7 Gilbert,A.;Kelly,J.M.;Budzwait,M.;Koerner von Gustorf,E.; *Z. Naturforsch.*; 1976,**31B**,1091.

8 Rest,A.J.;Sodeau,J.R.;Taylor,D.J.; *J. Chem. Soc., Dalton Trans.;* 1978,651.

9 Wrighton,M.S.;Haverty,J.L.; *Z. Naturforsch.*; 1974,**30B**,254.

10 Calvert,J.G.;Pitts,J.N.;*Photochemistry*; Wiley-Interscience: New York; 1966.

11 Hrnviar,P;Hudeck,M.;Magomedov,G.K.I.;Toma,S.; *Collect. Czech. Comm.*; 1991,**56**,1477.

12 Sheldrick,G.M.;*Acta Cryst.*; 1990,**A46**,467.

13 Sheldrick,G.M.;SHELX-93, Program for crystal structure determination;1993.

14 Bailey,M.F.;Dahl,L.F.; *Inorg. Chem.*; 1965,**4**,1314.

15 Ibers,J.A.; *J. Chem. Phy.*; 1964,**40**,3129.

16 Bailey,M.F.;Dahl,L.F.; *Inorg. Chem.*; 1965,**4**,1298.

Chapter 6

Photochemistry of bimetallic carbonyl compounds and acyclic pentadienyl manganese carbonyl compounds.

6.1 Photochemistry of bimetallic carbonyl compounds and acyclic pentadienyl manganese carbonyl compounds.

The photochemistry of the heteronuclear complex $Mn(CO)_4(\eta^3-C_3H_4-\eta^6-C_6H_5)Cr(CO)_3$ was investigated by laser flash photolysis to determine at which metal centre the photochemistry orignated. To date, there are no reports in the literature concerning flash photolysis of heteronuclear compounds where the metal centres are not directly bonded. This is in contrast to the area of binuclear complexes such as $Mn_2(CO)_{10}$[1] or heteronuclear $MnRe(CO)_{10}$,[2] where there is an ample volume of literature, but in both these systems the metal centres are directly bonded through M-M bonds. Previously the photochemistry of (η^6-benzene)$Cr(CO)_3$ has been discussed where the photochemical reaction is loss of a CO ligand, which results in a coordinatively unsaturated 16 electron intermediate, which in the presence of CO reacts to reform the tricarbonyl parent complex (Chapter 2).

Initially the photochemistry of the phenyl allyl manganese compound $(\eta^3-C_3H_4-C_6H_5)Mn(CO)_4$ was investigated so as to observe the photochemistry of the manganese centre. Flash photolysis was then carried out on the heterodinuclear complex but as the results obtained were difficult to interpret it was decided to further the study of the manganese fragment. $(\eta^1-C_5H_7)Mn(CO)_5$, $(\eta^3-C_5H_7)Mn(CO)_4$ and $(\eta^5-C_5H_7)Mn(CO)_3$ were investigated in the hope of elucidating the photochemistry of the heterodinuclear system.

6.2 Photochemistry of $(\eta^3-C_3H_4-C_6H_5)Mn(CO)_4$.

6.2.1 Electronic Absorption Spectrum of $(\eta^3-C_3H_4-C_6H_5)Mn(CO)_4$.

The UV/vis. spectrum of $(\eta^3-C_3H_4-C_6H_5)Mn(CO)_4$ in cyclohexane is presented in Figure 6.2.1.1. The principal feature of this spectrum is an absorptions centred at 240 nm and a lower energy absorptions centred at 300 nm. Studies of the electronic structure of low symmetry Mn derivatives are not well developed.[3] By analogy with the spectrum of $(\eta^1-C_3H_5)Mn(CO)_5$,[4] however, these absorption bands may be assigned as Mn ----> π^* CO charge transfer bands.

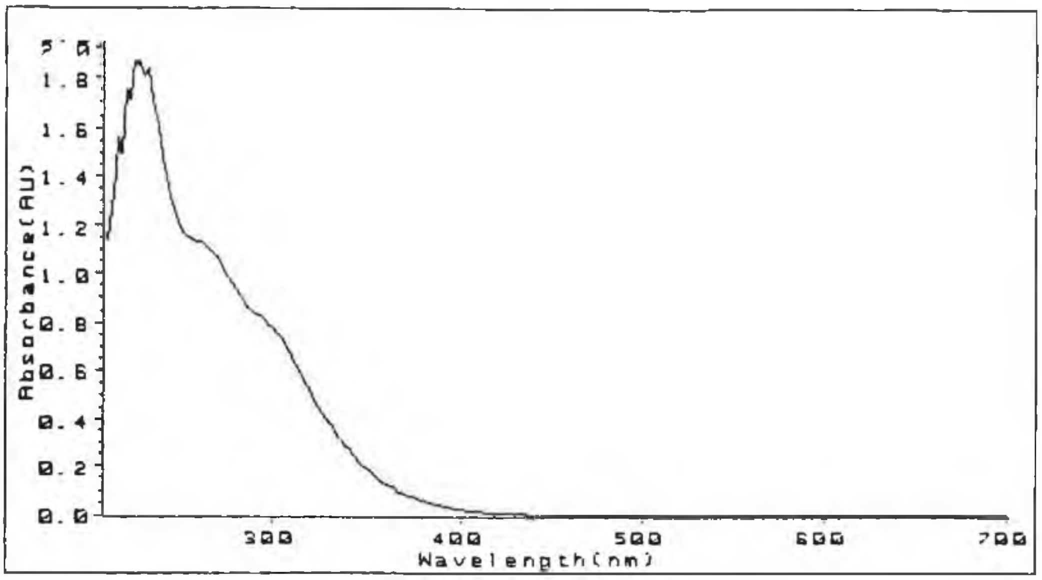

Figure 6.2.1.1 UV/vis. absorption spectrum of (η^3-C_3H_4-C_6H_5)Mn(CO)$_4$ (7.3 x 10^{-5} mol dm^{-3}) in cyclohexane.

6.2.3 Laser flash photolysis of (η^3-C_3H_4-C_6H_5)Mn(CO)$_4$.

Under 1 atm. of CO no transient absorptions could be detected upon photolysis of (η^3-C_3H_4-C_6H_5)Mn(CO)$_4$. However, as the concentration of CO was reduced to 0.2 atmosphere a weak transient signal was detected. The decay curves were difficult to analyse. Hence no rate data could be gathered from these experiments. Problems were also encountered because the transient signals were prone to interference from shock waves which are thought to result from local heating effects. A similar experiment under an argon atmosphere permitted the observation of a weakly absorbing transient species (λ_{max} 410 nm) following flash photolysis at 355 nm as shown in Figure 6.2.3.1. These results indicate that the transient species observed is not a primary photoproduct as the presence of CO quenches its formation and indeed at high concentrations of CO (9.0 x 10^{-3}M) its formation cannot be observed. The UV/vis. difference spectrum of this species is shown in Figure 6.2.3.2. The formation of two species is proposed, initially a very reactive intermediate (species 1) which subsequently produces a secondary product (species 2). The observed rate constant of formation of species 1 was measured to be 6.9 x 10^6 s^{-1} under 1 atmosphere of argon and a grow-in for this signal is given in Figure 6.2.3.3.

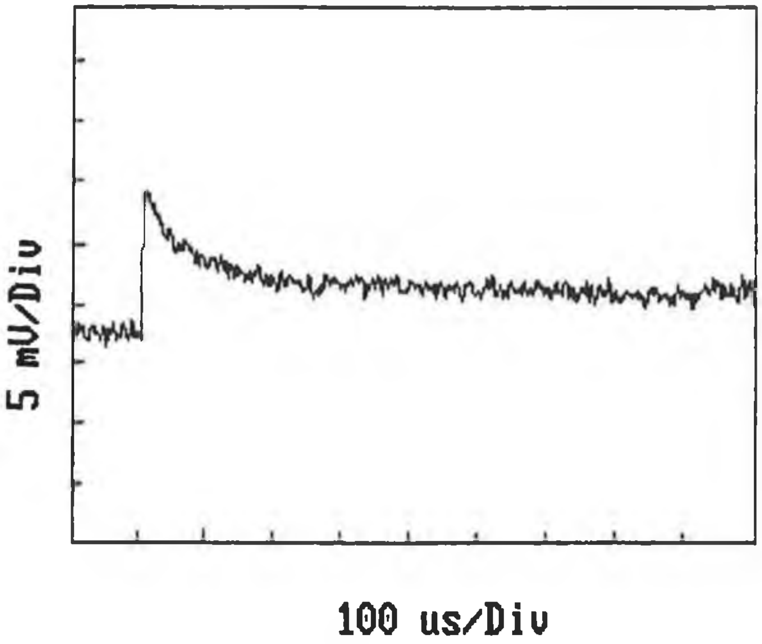

Figure 6.2.3.1 The transient species observed following flash photolysis of (η^3-C_3H_4-C_6H_5)Mn(CO)$_4$ under 1 atm. of argon at 410 nm.

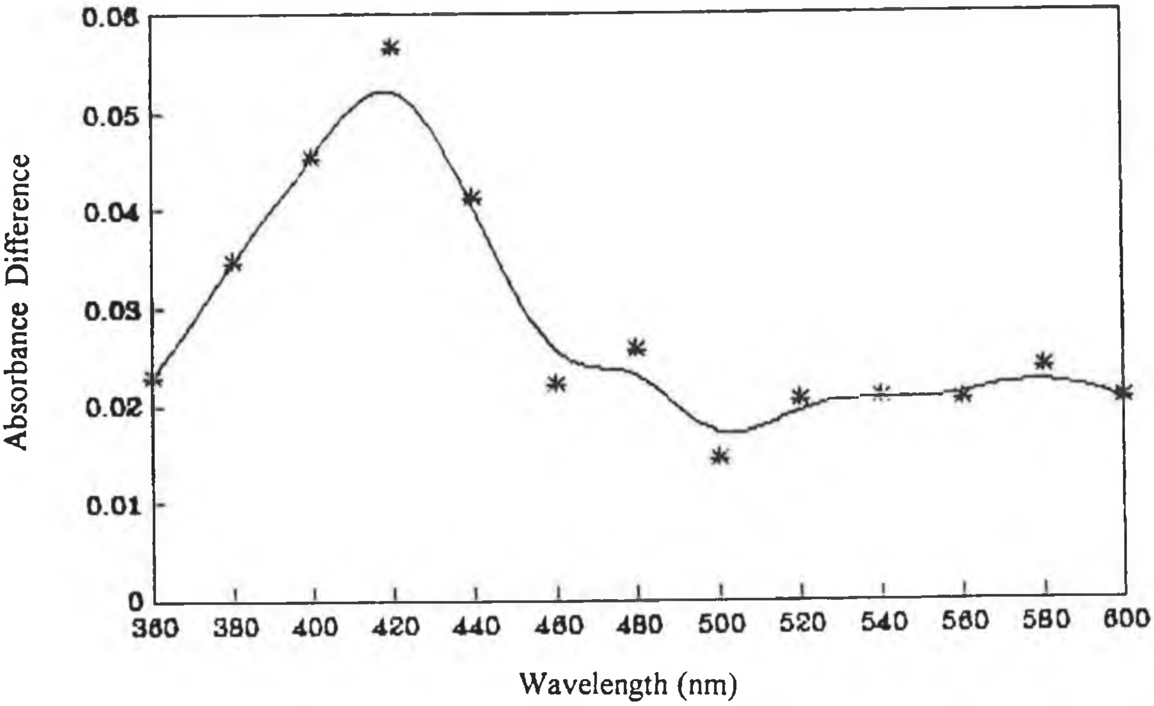

Figure 6.2.3.2 The UV/vis. difference spectrum following flash photolysis of (η^3-C_3H_4-C_6H_5)Mn(CO)$_4$ under 1 atm. of argon at 355 nm at 298K.

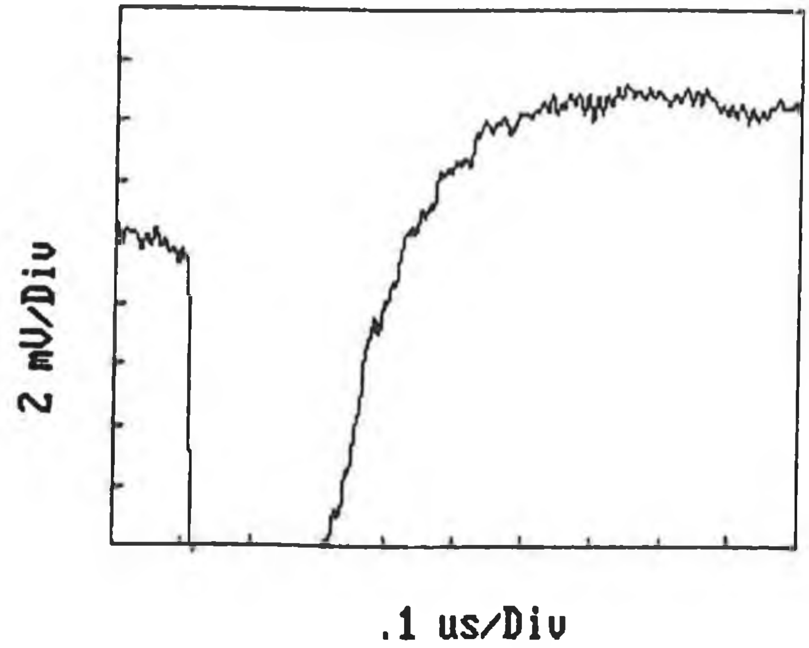

Figure 6.2.3.3 The transient signal indicating formation of the primary photoproduct under 1 atm. of argon at 410 nm.

Belt *et al.*[5] have previously reported a similar behaviour following photolysis of $CH_3Mn(CO)_5$ studied by time-resolved infrared spectroscopy. When $CH_3Mn(CO)_5$ was irradiated in cyclohexane under CO rather than argon the yield of *cis*-$CH_3Mn(CO)_4$(s) was reduced by a factor of 5. To account for these observations it was concluded that photolysis of $CH_3Mn(CO)_5$ in C_6H_{12} results in CO labilisation to give an intermediate that can react competitively with either C_6H_{12} to form *cis*-$CH_3Mn(CO)_4$(s) or with CO to regenerate $CH_3Mn(CO)_5$. Perhaps either steric or electronic constraints might give such species sufficient life-time to demonstrate selectivity in coordinating a sixth ligand. A similar selectivity toward CO over C_6H_{12} has been observed for the 16 electron fragment $(\eta^5\text{-}C_5H_5)Rh(C_2H_4)$.[6] However, in a more recent report[7] it has been confirmed that the highly reactive species formed following flash photolysis of $CH_3Mn(CO)_5$ in cyclohexane is the highly reactive but still selective cyclohexane tetra carbonyl complex, rather than the unsaturated intermediate $CH_3Mn(CO)_4$ as was originally proposed.

The observed rate constant for the decay of species 2 at 410 nm shows a linear dependence on the parent tetracarbonyl concentration under argon as shown in Figure 6.2.3.4. This dependence indicates the possible formation of a dinuclear species where the second order rate constant from the slope of the line was determined to be 1.36 x 10^7 $dm^3mol^{-1}s^{-1}$. This value is similar to the rate of formation of the dinuclear species for (η^6-benzene)$Cr(CO)_3$ where a rate constant of 4.8 x 10^7 $dm^3mol^{-1}s^{-1}$ was measured.[8]

The experimental observations signify that species 1 is an extremely short lived photoproduct that does not appear to be solvated. This species has been assigned as the carbonyl loss product (η^3-C_3H_4-C_6H_5)$Mn(CO)_3$. The efficiency of recombination of this species under 1 atm. of CO is so great that no transient species are observed under these conditions. Presumably, the bulky phenyl group hinders the solvent molecule from coordinating to the vacant site on the manganese atom. Similar arguments have previously been reported for $CH_3CpMn(CO)_2PPh_3$,[9] where the first species was identified from reaction kinetics as the non solvated $CH_3CpMn(CO)PPh_3$ complex. The bulky triphenylphosphine ligand is proposed to prevent the cyclohexane molecule from coordinating to the metal centre. The second order rate constant for the reaction of $CH_3CpMn(CO)PPh_3$ with CO indicates that the CO molecule is able to coordinate to the manganese atom whereas the larger cyclohexane is not. The coordinatively unsaturated complex was thought to be stabilised by an intramolecular reaction, the exact nature of which is uncertain but proposed to be an orthometallated intermediate.

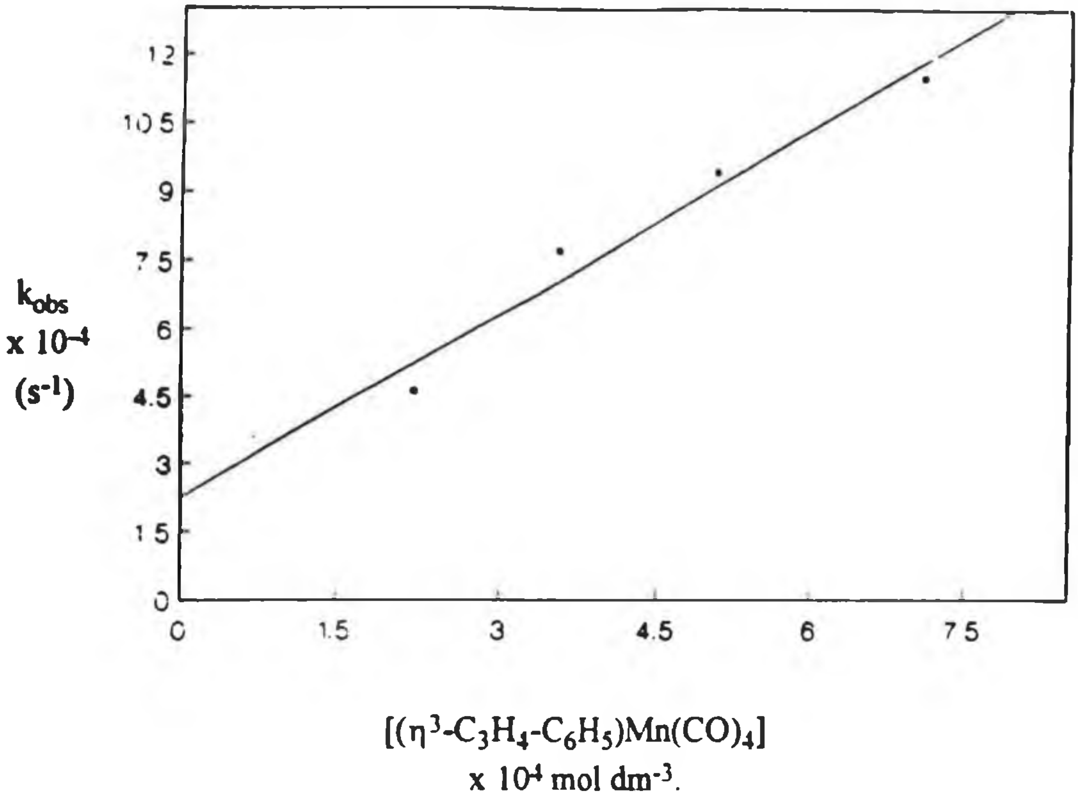

[(η^3-C_3H_4-C_6H_5)Mn(CO)$_4$] x 10^4 dm^3 mol^{-1}	k_{obs} x 10^{-4} (s^{-1})
2.2	4.6
3.54	7.7
5.07	9.4
7.1	11.5

Slope = 1.36 x 10^7 ± x 2.01 10^6 dm^3 mol^{-1} s^{-1}
Intercept = 2187 ± 732 s^{-1}
corr. coeff. = 0.98

Figure 6.2.3.4 K_{obs} *versus* concentration of (η^3-C_3H_4-C_6H_5)Mn(CO)$_4$ for decay of the second species at 410 nm.

Species 2 is assigned to the acyclic pentadienyl complex $(\eta^5\text{-}C_3H_4\text{-}C_6H_5)Mn(CO)_3$ formed by a conformational change at the allyl ligand involving rotation about the C-C single bond, which results in a rapid η^3 ----> η^5 hapticity change to stabilise the coordinatively unsaturated fragment. Young and Wrighton[10] observed a similar reaction in their studies into the photochemistry of $(\eta^1\text{-}C_6H_5CH_2)Mn(CO)_5$. These workers observed rapid formation of $(\eta^3\text{-}C_6H_5CH_2)Mn(CO)_4$ following irradiation of $(\eta^1\text{-}C_6H_5CH_2)Mn(CO)_5$. When experiments were conducted under 1 atm. of CO no transient signals were observed as in this study.

The third species is postulated to be a dinuclear complex- the exact structure of which is unknown. The only evidence for this species is that decay of the second species appears to be dependent on the parent complex concentration which generally signifies reaction of this intermediate (species 2) with unphotolysed parent material. Whatever the precise nature of this species, it appears to be long lived and eventually reforms parent complex as the UV/vis. spectrum of the sample indicated little, if any, variation throughout the experiment. Presented in Scheme 6.2.3.1 is an overview of the proposed photochemical pathway for this system.

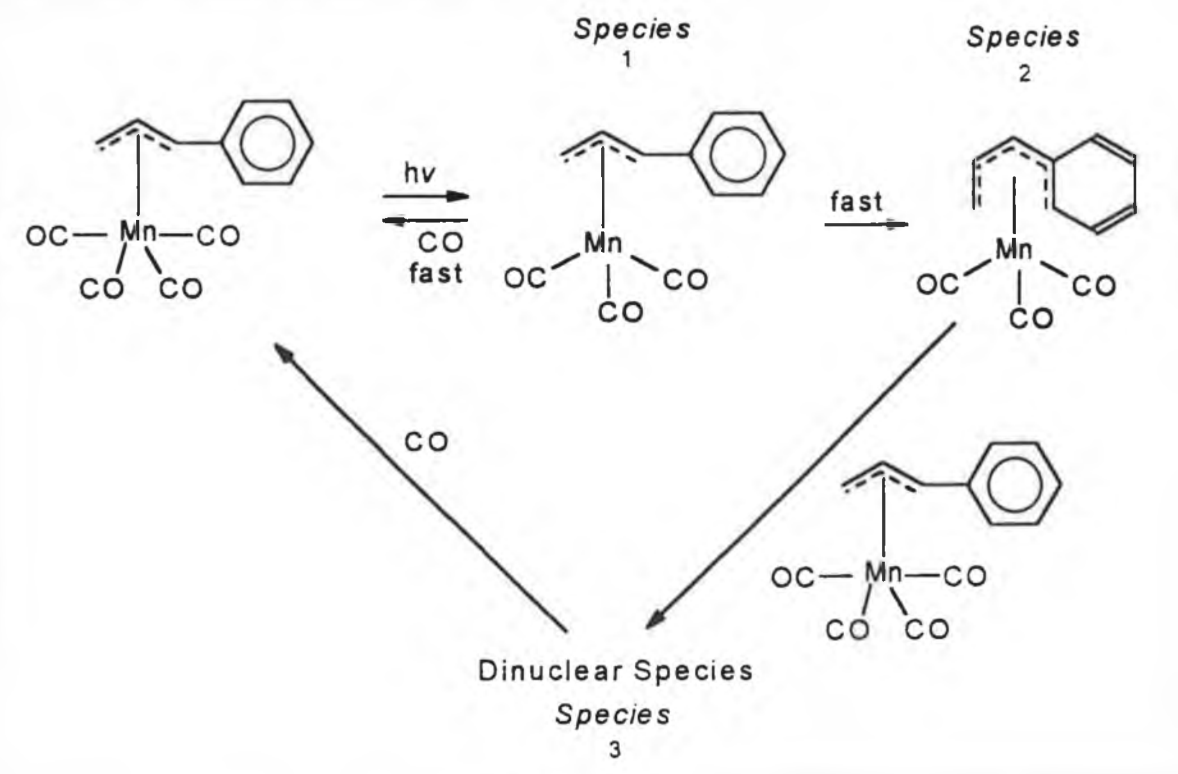

Scheme 6.2.3.1

6.3 Photochemistry of $Mn(CO)_4(\eta^3\text{-}C_3H_4\text{-}\eta^6\text{-}C_6H_5)Cr(CO)_3$.

6.3.1 Electronic absorption spectrum of $Mn(CO)_4(\eta^3\text{-}C_3H_4\text{-}\eta^6\text{-}C_6H_5)Cr(CO)_3$.

The UV/vis. spectrum of $Mn(CO)_4(\eta^3\text{-}C_3H_4\text{-}\eta^6\text{-}C_6H_5)Cr(CO)_3$ in cyclohexane is given in Figure 6.3.1.1. The assignments of bands in relatively large organometallic compounds is difficult and hence are tentative. The most intense band 220 nm is assigned to being Cr ----> CO π^* charge transfer by analogy with the spectrum of $(\eta^6\text{-}C_6H_6)Cr(CO)_3$.[11] A shoulder on the low energy side of this absorption maximum at 252 nm may be assigned to being a blue shift of either the 262 nm absorption of $(\eta^6$-benzene$)Cr(CO)_3$ or the 290 absorption band of $(\eta^3\text{-}C_3H_5)Mn(CO)_4$ species. Gogan and Chu have reported that π complexing of the $Cr(CO)_3$ group onto the arene ring causes a blue shift in the Mn-C band.[12] The band centred at 330 nm is presumably Cr ----> arene charge transfer with some Cr ----> π^* CO charge transfer. The band present at 406 nm is not present in the uncomplexed compounds and is tentatively assigned to being a charged transfer band from Cr ----> C, based on assignments with the reported UV/vis. spectrum of $Cr(CO)_3$-(benzolcyclopentadienyl)$Mn(CO)_3$.[13]

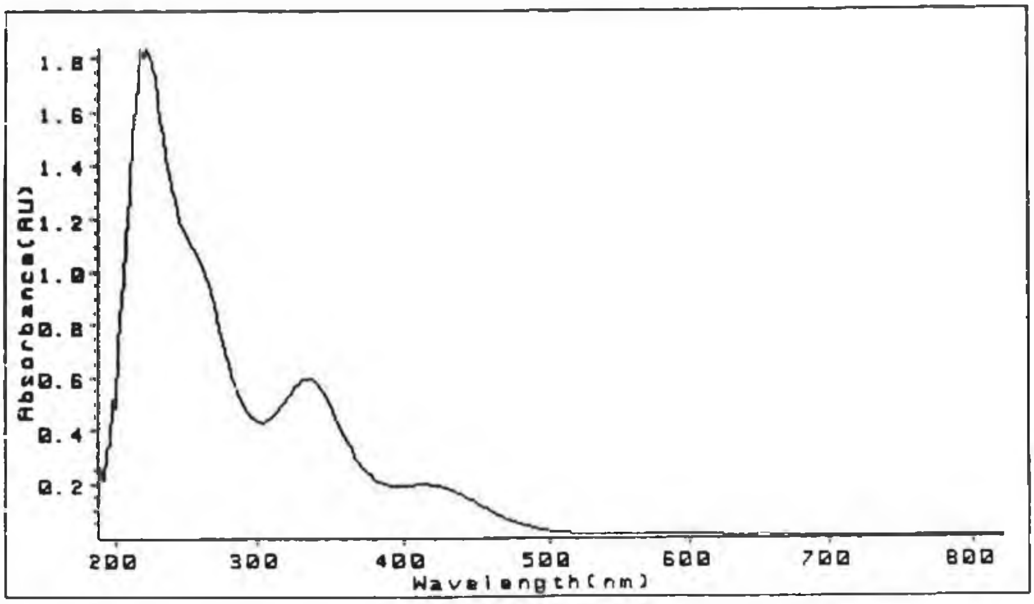

Figure 6.3.1.1 UV/vis. spectrum of $Mn(CO)_4(\mu^3\text{-}C_3H_4\text{-}C_6H_5)Cr(CO)_3$ (4.3 x 10^{-4} mol dm^3) in cyclohexane.

6.3.2 Laser flash photolysis of $Mn(CO)_4(\eta^3-C_3H_4-\eta^6-C_6H_5)Cr(CO)_3$.

From the experimental results obtained in this study it is proposed that the photochemistry of $Mn(CO)_4(\eta^3-C_3H_4-\eta^6-C_6H_5)Cr(CO)_3$ originates at the manganese centre. The UV/vis. difference spectrum obtained 500 ns after the flash under either 1 atmosphere of CO or argon is given in Figure 6.3.2.2. These spectra are identical thus indicating that the transient signal presented in Figure 6.3.2.1 is most probably associated with a primary photoproduct. The difference spectra indicate negative bands at 340 and 425 nm which occur at absorption maxima in the parent compound. This transient species exhibits an absorption in the UV region of the spectrum at 300 nm which occurs at an absorption minimum in the parent compound.

A typical transient signal at 300 nm under 1 atm. of argon is given in Figure 6.3.2.1. This signal indicates the presence of 2 transient species - the first of which is formed within the laser flash. The rate of decay of the first species was unaffected by varying the concentration of parent. Also, the rate of decay of this transient species was unaffected by the concentration of carbon monoxide and the yield of the species was unaltered on addition of CO.

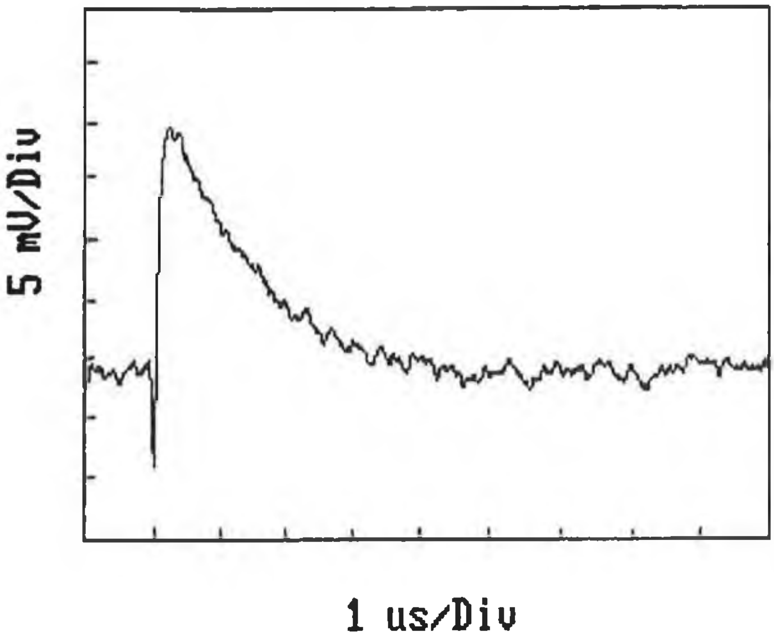

Figure 6.3.2.1 The transient species observed at 300 nm following flash photolysis of $Mn(CO)_4(\eta^3-C_3H_4-\eta^6-C_6H_5)Cr(CO)_3$ under argon.

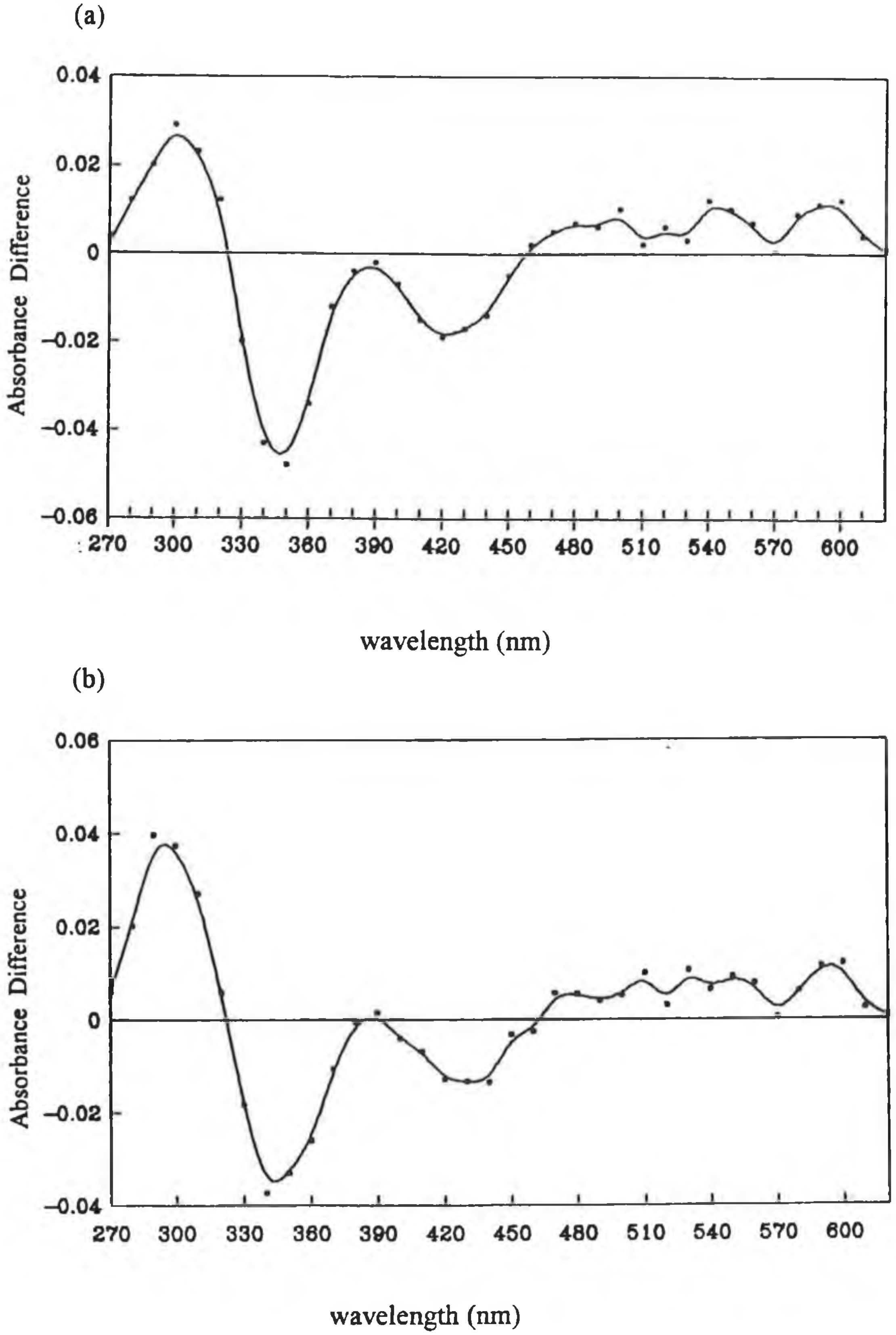

Figure 6.3.2.2 The UV/vis. difference obtained at 500ns following flash photolysis of $Mn(CO)_4(\eta^3\text{-}C_3H_4\text{-}\eta^6\text{-}C_6H_5)Cr(CO)_3$ under (a) argon and (b) CO.

From these observations it was difficult to determine which of the metal centres were giving rise to the transient species observed, thus experiments were conducted in the presence of pyridine as a trapping ligand. A UV/vis. difference spectrum obtained following flash photolysis of $Mn(CO)_4(\eta^3\text{-}C_3H_4\text{-}\eta^6\text{-}C_6H_5)Cr(CO)_3$ in the presence of excess pyridine under 1 atmosphere of argon shows an absorption in the visible region of the spectrum at 480 nm (Figure 6.3.2.3). The rate of formation of this transient species at 480 nm was measured to be independent of pyridine concentration with an observed rate constant of 1.2×10^7 s^{-1}. A typical signal obtained at 480 nm is given in Figure 6.3.2.4. Throughout the experiment the UV/vis. spectrum of the parent compound was recorded as shown in Figure 6.3.2.5 and an isosbestic point occurs at 456 nm which reflects a clean reaction with no side products.

On photolysing $(\eta^6\text{-}C_6H_6)Cr(CO)_3$ in the presence of excess pyridine an absorption is observed at 500 nm as given in Figure 6.3.2.6. On viewing the differences observed in the electronic absorption spectra for both systems following irradiation in the presence of pyridine it would appear that the substituted metal centre was chromium. Previously, the second order rate constant for formation of $(\eta^6\text{-}C_6H_6)Cr(CO)_2(C_6H_5N)$ has been determined to be 3.7×10^7 $dm^3mol^{-1}s^{-1}$,[14] and the rate of formation of this species is dependent on the concentration of pyridine which is in contrast to the results of this study.

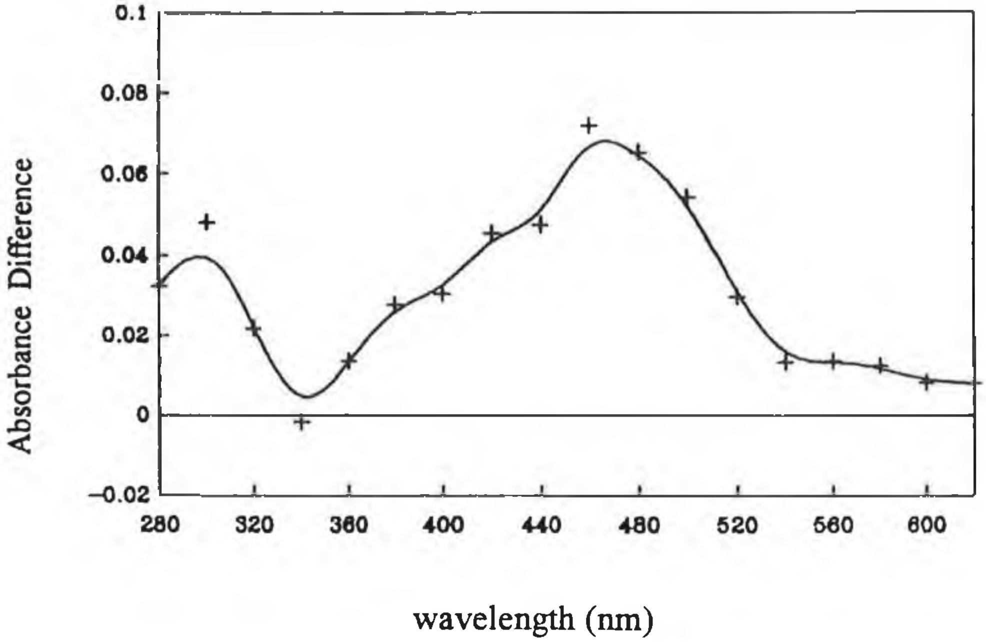

Figure 6.3.2.3 The UV/vis. difference spectrum after 5μs following irradiation of $Mn(CO)_4(\eta^3\text{-}C_3H_4\text{-}\eta^6\text{-}C_6H_5)Cr(CO)_3$ in cyclohexane with excess pyridine.

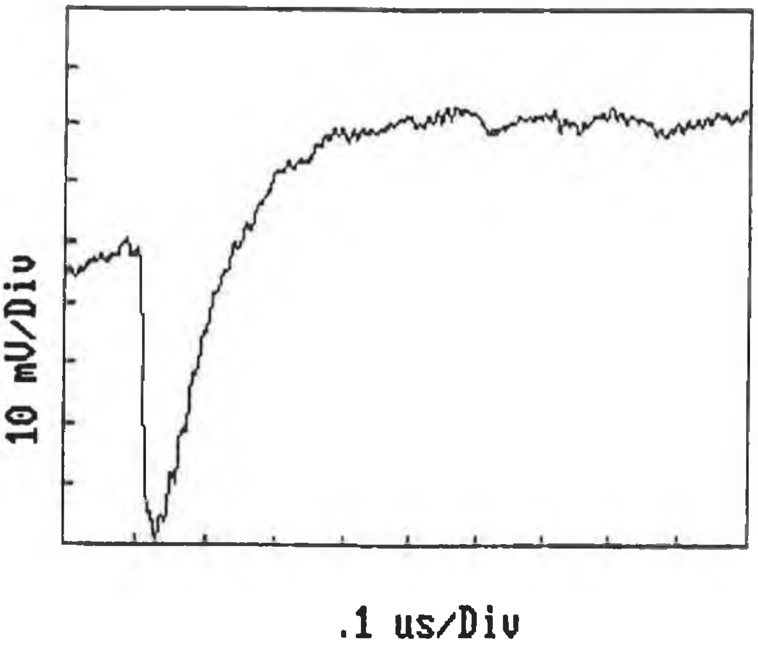

Figure 6.3.2.4 Transient signal observed at 480 nm following irradiation of $Mn(CO)_4(\eta^3-C_3H_4-\eta^6-C_6H_5)Cr(CO)_3$ in the presence of excess pyridine.

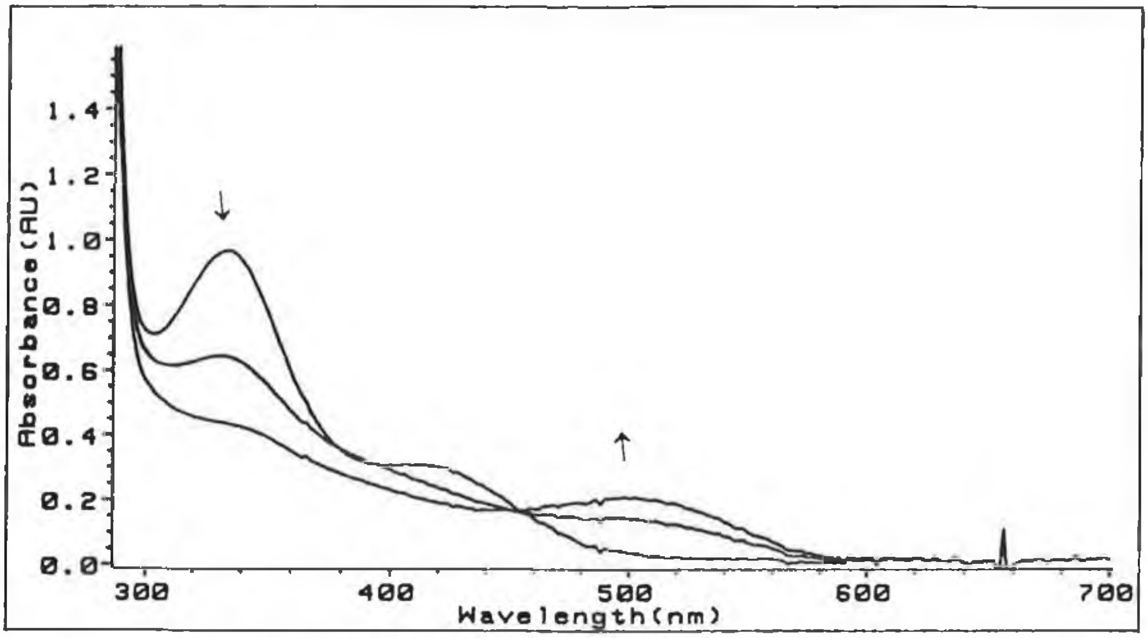

Figure 6.3.2.5 The differences observed in the absorption spectrum of $Mn(CO)_4(\eta^3-C_3H_4-\eta^6-C_6H_5)Cr(CO)_3$ as the sample is irradiated in the presence of pyridine.

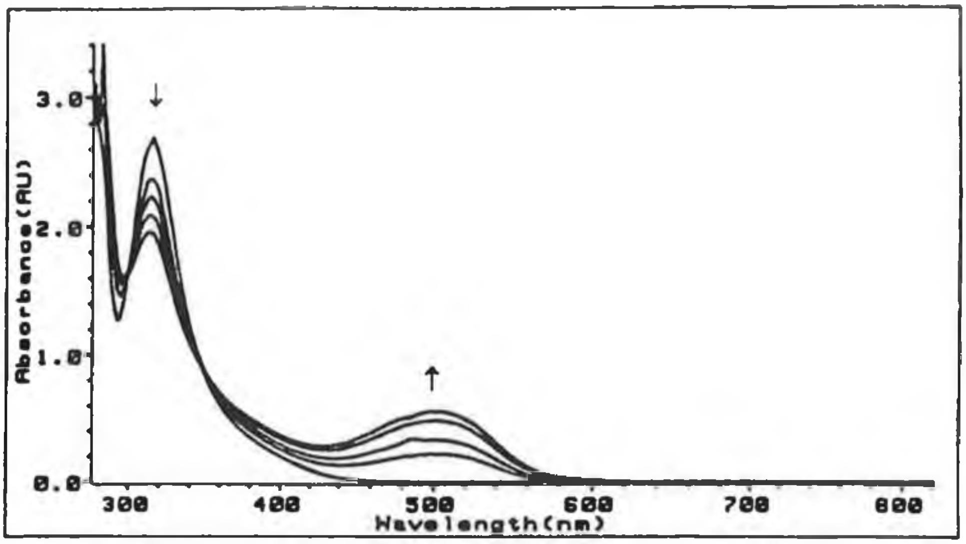

Figure 6.3.2.6 The differences observed in the parent spectrum of (η^6-C_6H_6)$Cr(CO)_3$ as the sample is irradiated in the presence of pyridine.

Hence from these observations the first species formed following flash photolysis of $Mn(CO)_4(\eta^3$-C_3H_4-η^6-$C_6H_5)Cr(CO)_3$ is attributed to the carbonyl loss product of the manganese centre. As the rate of decay of the first species was observed to be independent of concentration of parent complex or carbon monoxide it implies that species 2 results from an intramolecular rearrangement by rotation of the C-C single bond. This rotation allows the manganese centre to interact with chromium and abstract a CO ligand to return to coordinative saturation, thus leaving the chromium centre as a coordinatively unsaturated 16 electron intermediate.

The experiments carried out in the presence of pyridine indicate formation of a substituted chromium centre based on the similarity of the differences observed in the electronic absorption spectrum when photolysing samples in the presence of pyridine. However, k_{obs} for formation of $Mn(CO)_4(\eta^3$-C_3H_4-η^6-$C_6H_5)Cr(CO)_2(C_6H_5N)$ was observed to be independent of pyridine concentration. This indicates that loss of CO from the chromium centre is not the primary photoprocess because if it were an increase in k_{obs} would be observed as was the case in the formation of (η^6-C_6H_6)$Cr(CO)_2(C_6H_5N)$.[14]

Consequently, the rate determining step is proposed to be loss of CO at the manganese centre and not at chromium, but, because the manganese centre abstracts CO from the chromium metal coordinative unsaturation is transferred to the chromium metal.

Under 1 atmosphere of argon a third transient species is seen to form. The rate of formation of this species was impossible to measure accurately as formation of this intermediate is superimposed on species 1 and 2 as shown in Figure 6.3.2.7. However this species is totally suppressed when experiments are performed under 1 atmosphere of CO, thereby suggesting that whatever the exact identity of this complex, results would suggest to it being a secondary photoproduct whose formation is possibly dependent on the second species.

The proposed overall pathway for the photochemistry of this system is as presented in Scheme 6.3.2.1, however this mechanism is subject to speculation.

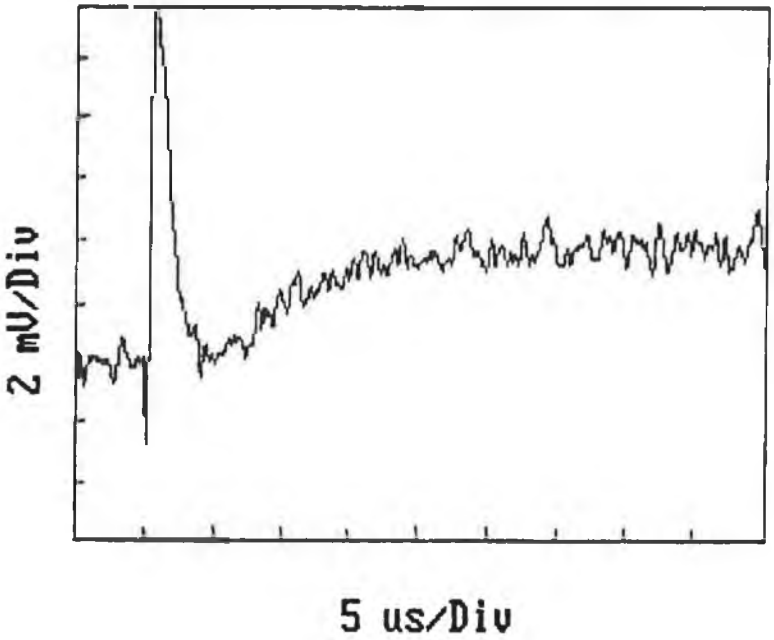

Figure 6.3.2.7 Transient trace of the third species recorded following flash photolysis of $Mn(CO)_4(\eta^3\text{-}C_3H_4\text{-}\eta^6\text{-}C_6H_5)Cr(CO)_3$ under 1 atm. of argon.

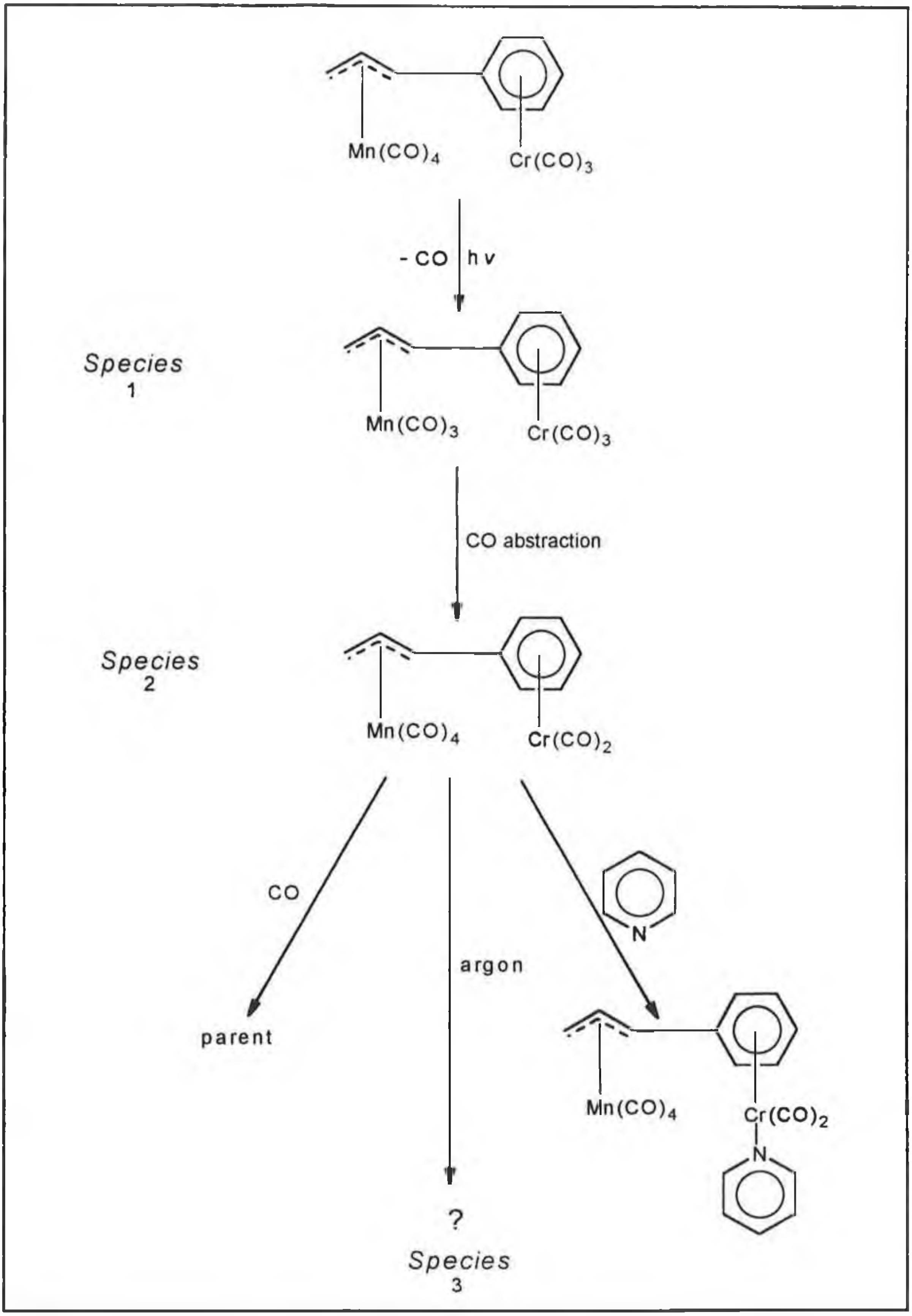
Mn(CO)4
Cr(CO)3
- CO
h v
Species 1
Mn(CO)3
Cr(CO)3
CO abstraction
Species 2
Mn(CO)4
Cr(CO)2
CO
argon
N
parent
Mn(CO)4
Cr(CO)2
N
?
Species 3

Scheme 6.3.2.1

6.4 Photochemistry of (η^1-C_5H_7)Mn(CO)$_5$.

6.4.1. Electronic absorption spectrum of (η^1-C_5H_7)Mn(CO)$_5$.

The UV/vis. spectrum of (η^1-C_5H_7)Mn(CO)$_5$ in cyclohexane is given in Figure 6.4.1.1. By analogy with (CH_3)Mn(CO)$_5$ the strong and medium absorptions at 235 and 320 nm, respectively, may be assigned as metal to ligand[15] charge transfer bands.

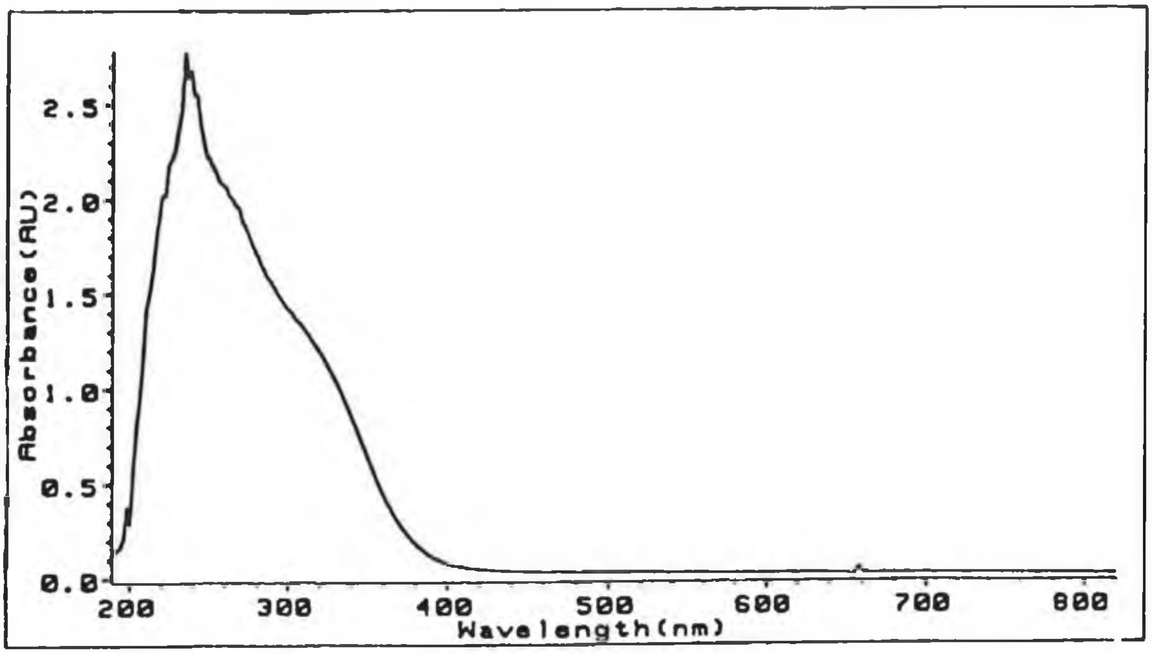

Figure 6.4.1.1 Electronic absorption spectrum of (η^1-C_5H_7)Mn(CO)$_5$ (2.2 x 10^{-4}M) in cyclohexane.

6.4.2 Laser flash photolysis of (η^1-C_5H_7)Mn(CO)$_5$.

Laser flash photolysis (λ = 355 nm) of (η^1-C_5H_7)Mn(CO)$_5$ under 1atm. of CO produced one transient species. Following photolysis a 'rapid' depletion was observed at 320 nm as shown in Figure 6.4.2.1. However, on recording this transient species on a much shorter time-base of 100 ns (see Figure 6.4.2.2) the depleted absorbance was found to recover. k_{obs} for this grow-in was measured to be 1.19 x 10^7 s^{-1} under 1 atmosphere of CO. When a similar experiment was conducted under an atmosphere of argon the same result was obtained and k_{obs} was measured to be 1.09 x 10^7 s^{-1} at 320 nm. These results indicate that formation of this species is independent of CO concentration. No recovery of parent was observed. Throughout the experiment the UV/vis. spectrum of the solution was recorded and a reduction in the intensity of the shoulder at 320 nm was observed as in Figure 6.4.2.3.

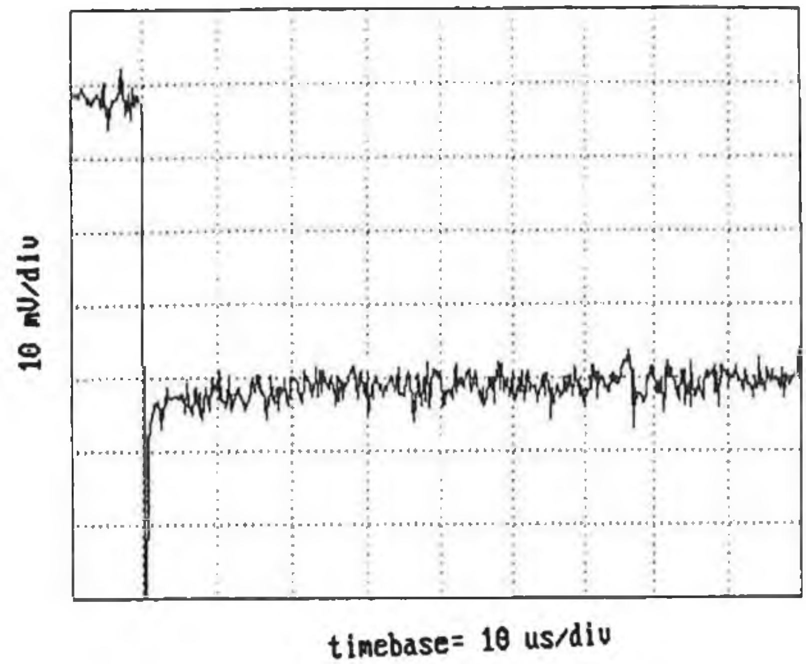

Figure 6.4.2.1 Transient signal recorded 10μs after the flash following photolysis of (η^1-C_5H_7)Mn(CO)$_5$ at 320 nm.

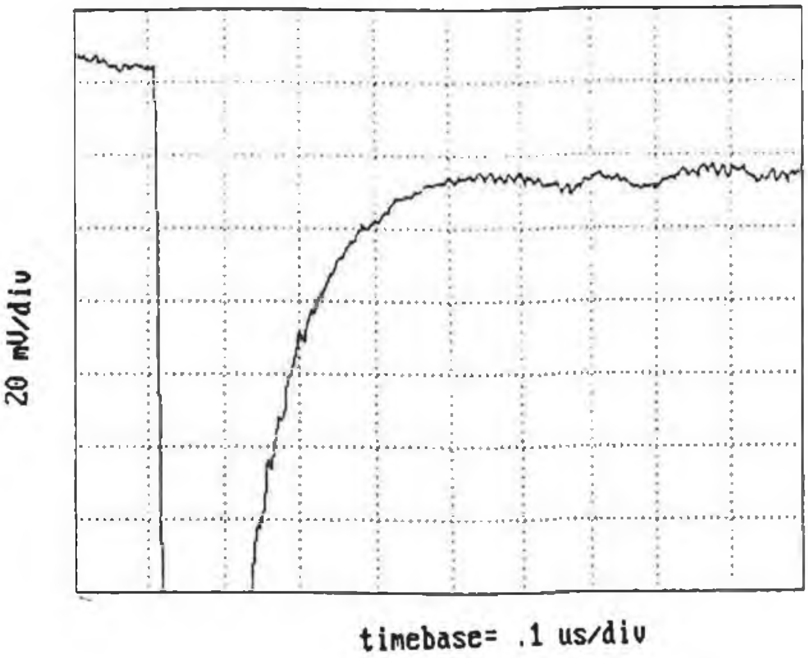

Figure 6.4.2.2 Transient signal recorded 100ns after the flash following photolysis of (η^1-C_5H_7)Mn(CO)$_5$ at 320 nm.

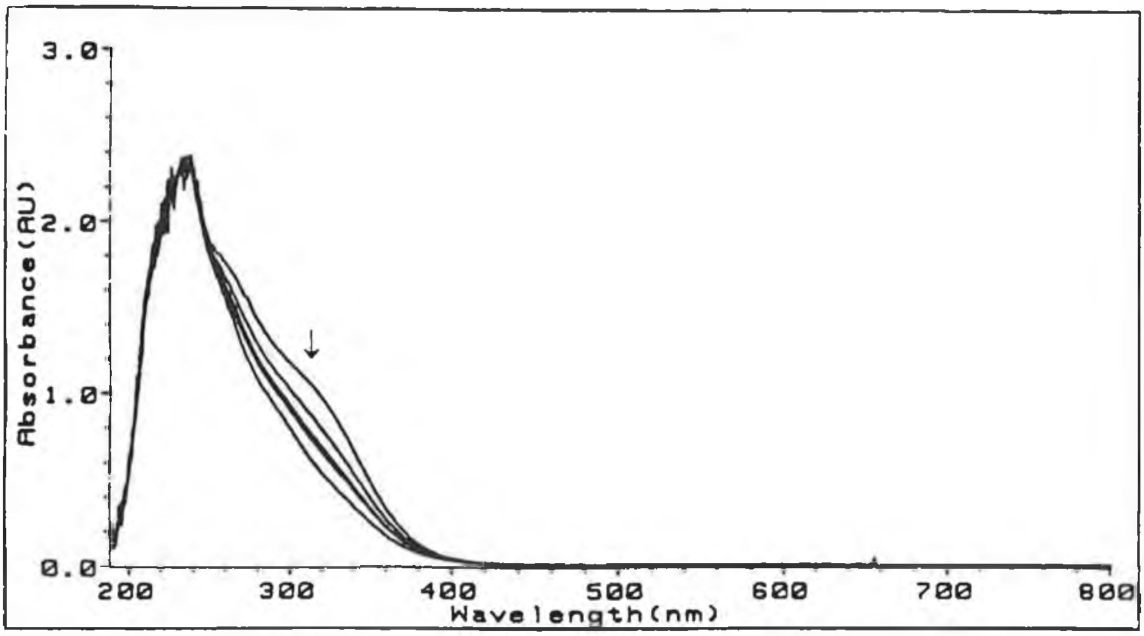

Figure 6.4.2.3 UV/vis. spectrum of $(\eta^1\text{-}C_5H_7)Mn(CO)_5$ and the differences observed during an experiment.

As there appeared to be no difference in observed rate value, flash photolysis of $(\eta^1\text{-}C_5H_7)Mn(CO)_5$ was carried out in toluene as in general this solvent coordinates much more strongly to a 16-electron intermediate (assuming this is produced) as it is a much stronger nucleophile than cyclohexane.[16] Results this time again yielded a similar value for k_{obs} of 1.13×10^7 s^{-1}.

6.4.3 Infrared monitored steady state photolysis of $(\eta^1\text{-}C_5H_7)Mn(CO)_5$.

$(\eta^1\text{-}C_5H_7)Mn(CO)_5$ was dissolved in cyclohexane and degassed with argon. The sample was photolysed at various time intervals (in the solution cell) at $\lambda > 330$ nm and the resulting changes in the $\nu(CO)$ stretching region recorded as shown in Figure 6.4.3.1. After irradiating the solution for a number of minutes the intensity of the parent bands at 2105, 2011 and 1991 cm^{-1} decreased and four bands at 2068, 1994, 1976 and 1965 cm^{-1}, increased in intensity. The bands of the product compare well with those of the previously isolated $(\eta^3\text{-}C_5H_7)Mn(CO)_4$.[17] A FTIR difference spectrum of the photolysed sample is given in Figure 6.4.3.2. The 1994 cm^{-1} band of the product is clearer here as it is partially masked in the previous IR, by the parent absorption at 1991 cm^{-1} (see Figure 6.4.3.1).

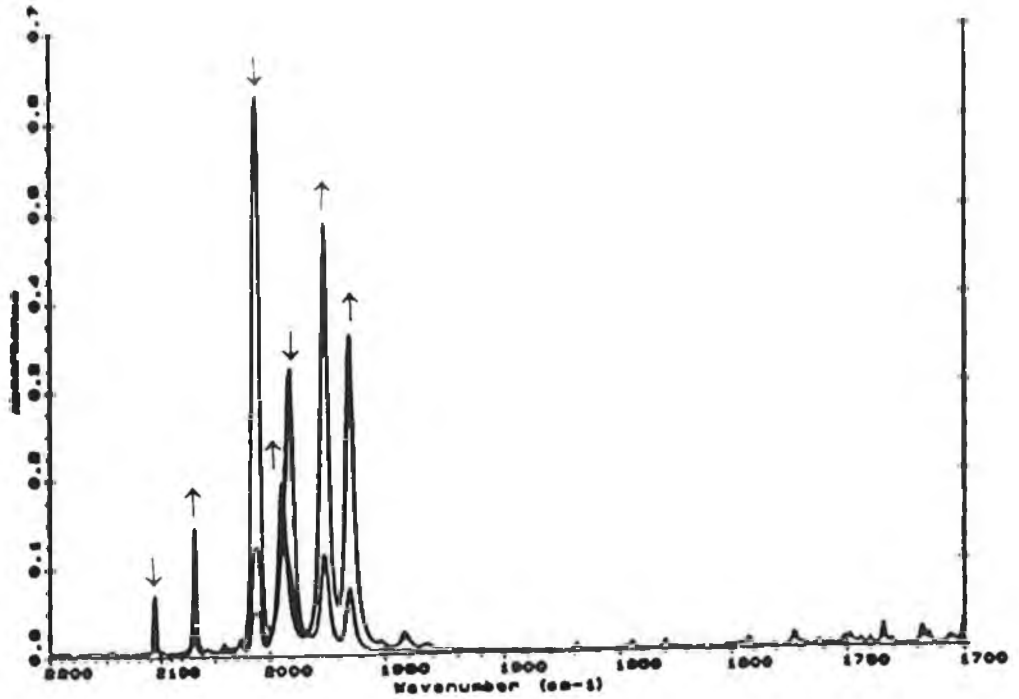

Figure 6.4.3.1. Resultant changes in the IR spectrum as $(\eta^1\text{-}C_5H_7)Mn(CO)_5$ is irradiated with λ > 320 nm in cyclohexane at 298K.

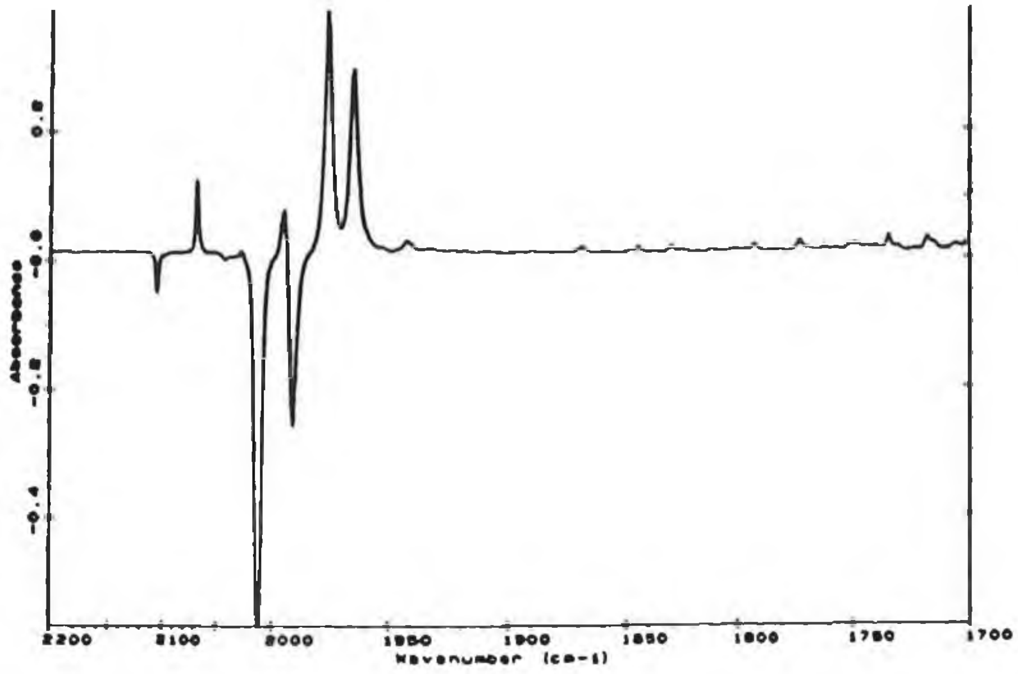

Figure 6.4.3.2. FTIR difference spectrum following photolysis of $(\eta^1\text{-}C_5H_7)Mn(CO)_5$ in cyclohexane at 298K.

On prolonged irradiation (approximately 35 minutes) at $\lambda > 330$ nm complete conversion from the $\eta^1 \longrightarrow \eta^3$ coordinated species occurred.

These results indicate that upon flash photolysis the starting compound $(\eta^1\text{-}C_5H_7)Mn(CO)_5$ is converted to $(\eta^3\text{-}C_5H_7)Mn(CO)_4$ following CO loss. In addition $\eta^1 \longrightarrow \eta^3$ rearrangement appears to occur simultaneously to CO loss. The creation of a vacant site close to the pentadienyl ligand opens the way for donation of a extra electron pair from the double bond of the η^1 ligand to satisfy the 18 electron rule requirement for manganese. Surprisingly, no evidence for a 16 electron intermediate $(\eta^1\text{-}C_5H_7)Mn(CO)_4$ has been observed in this study. Presumably, the bulky pentadienyl ligand prevents a solvent molecule from coordinating to the metal centre.

The observation of a $\eta^1 \longrightarrow \eta^3$ conversion has previously been reported following irradiation of $(\eta^1\text{-}C_3H_5)Mn(CO)_5$ in matrix isolation experiments.[3] No evidence was found for the $(\eta^1\text{-}C_5H_7)Mn(CO)_4$ intermediate. The $\eta^1 \longrightarrow \eta^3$ rearrangement appeared to be irreversible for $(\eta^1\text{-}C_5H_7)Mn(CO)_5$. Hitman and coworkers[3] also reported this stability on formation of their η^3-allyl manganese complex.

A $\sigma \longrightarrow \pi$ rearrangement is an intramolecular reaction in which a organic group σ-bonded (η^1) to a metal becomes π bonded (η^n). In most cases the thermal and photochemical $\sigma \longrightarrow \pi$ rearrangement are irreversible *e.g* Figure 6.4.3.3 but in principle the process should be reversible.

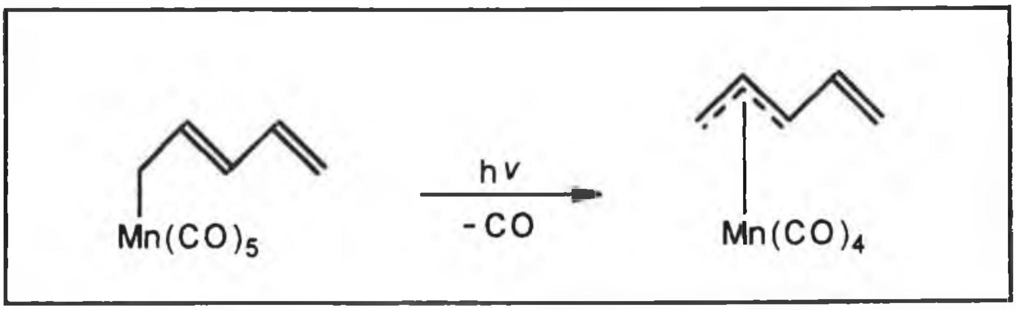

Figure 6.4.3.3 σ ----> π rearrangement observed following photolysis of $Mn(CO)_5\eta^1\text{-}C_5H_7$ in cyclohexane at 298K.

6.5 Photochemistry of (η^3-C_5H_7)Mn(CO)$_4$.

6.5.1 Electronic absorption spectrum of (η^3-C_5H_7)Mn(CO)$_4$.

The UV/vis. spectrum of (η^3-C_5H_7)Mn(CO)$_4$ in cyclohexane is given in Figure 6.5.1.1. Again by analogy with (CH_3)Mn(CO)$_5$ the absorption maxima are attributed to metal to ligand charge transfer bands.[15]

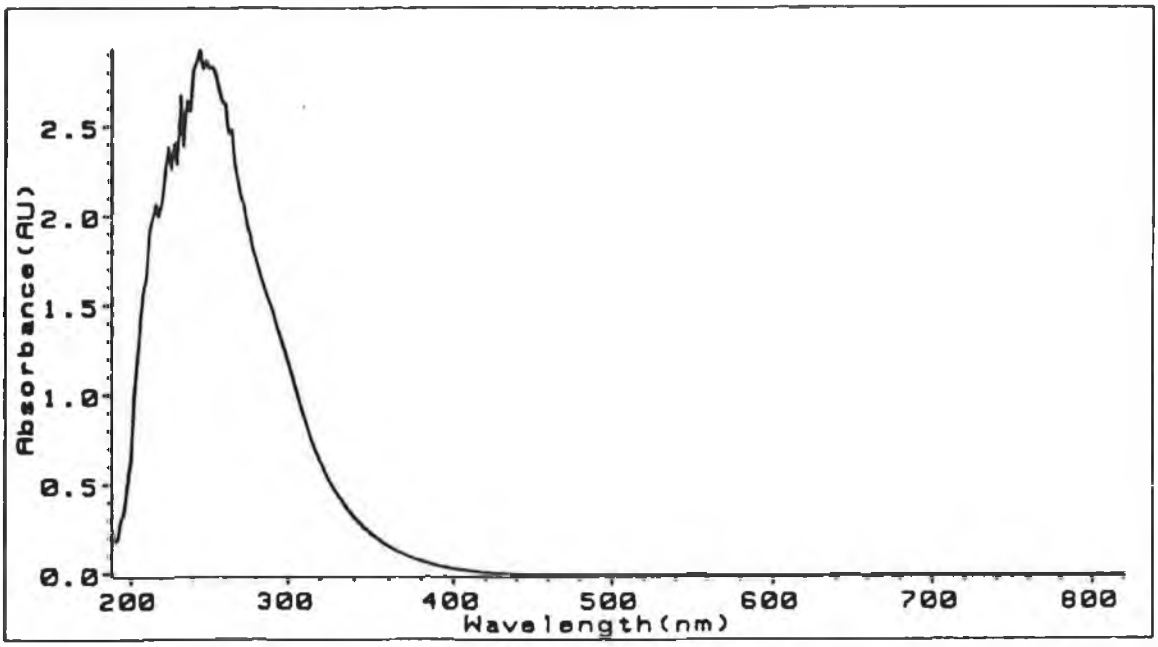

Figure 6.5.1.1 UV/vis. spectrum of (η^3-C_5H_7)Mn(CO)$_4$ (9.4×10^{-4}M) in cyclohexane at 298K.

6.5.2 Laser flash photolysis study of (η^3-C_5H_7)Mn(CO)$_4$.

As laser flash photolysis of (η^1-C_5H_7)Mn(CO)$_5$ resulted in a hapticity change concomitant with CO loss to yield the tetracarbonyl product, it was decided to investigate the photochemistry of the η^3 complex in order to observe if a hapticity change to the η^5 complex occurs upon photolysis. As the absorption of this compound is relatively weak at 355 nm, 266 nm excitation was used in these experiments. Experiments were conducted under CO and argon and in both cases no transient signals were observed. The UV/vis. of the parent spectrum was recorded as the sample was continuously pulsed, but this spectrum indicated only decomposition of compound.

6.5.3 Infrared monitored steady state photolysis of $(\eta^3\text{-}C_5H_7)Mn(CO)_4$.

A sample of $(\eta^3\text{-}C_5H_7)Mn(CO)_4$ was dissolved in cyclohexane which had previously been degassed. The solution IR cell was irradiated at $\lambda > 330$ nm - no new bands were observed hence the solution cell was then irradiated with $\lambda > 230$ nm. On prolonged photolysis new bands were seen to absorb at 2027, 1960 and 1941 cm^{-1} which correspond to $(\eta^5\text{-}C_5H_7)Mn(CO)_3$. As the solution cell had been irradiated for approximately 120 minutes it was very likely that formation of the η^5 species arose from thermal reaction rather than a photochemical reaction, hence a thermal investigation into the reactions of this compound was carried out.

6.5.4 Thermal chemistry of $(\eta^3\text{-}C_5H_7)Mn(CO)_4$ in hexane monitored by infrared spectroscopy.

$(\eta^3\text{-}C_5H_7)Mn(CO)_4$ was dissolved in hexane and the solution brought to its reflux temperature for approximately 20minutes. The infrared spectrum of the sample prior to heating showed four carbonyl bands at 2069, 1996, 1977 and 1966 cm^{-1}. An infrared of the heated sample exhibited three new bands at 2028, 1961 and 1943 cm^{-1}. The new bands are assigned to $(\eta^5\text{-}C_5H_7)Mn(CO)_3$. The FTIR difference spectrum in Figure 6.5.4.1 shows the over all process clearly *i.e.* the positive peaks due to formation of product $(\eta^5\text{-}C_5H_7)Mn(CO)_3$ and the negative bands due to depletion of parent $(\eta^3\text{-}C_5H_7)Mn(CO)_4$.

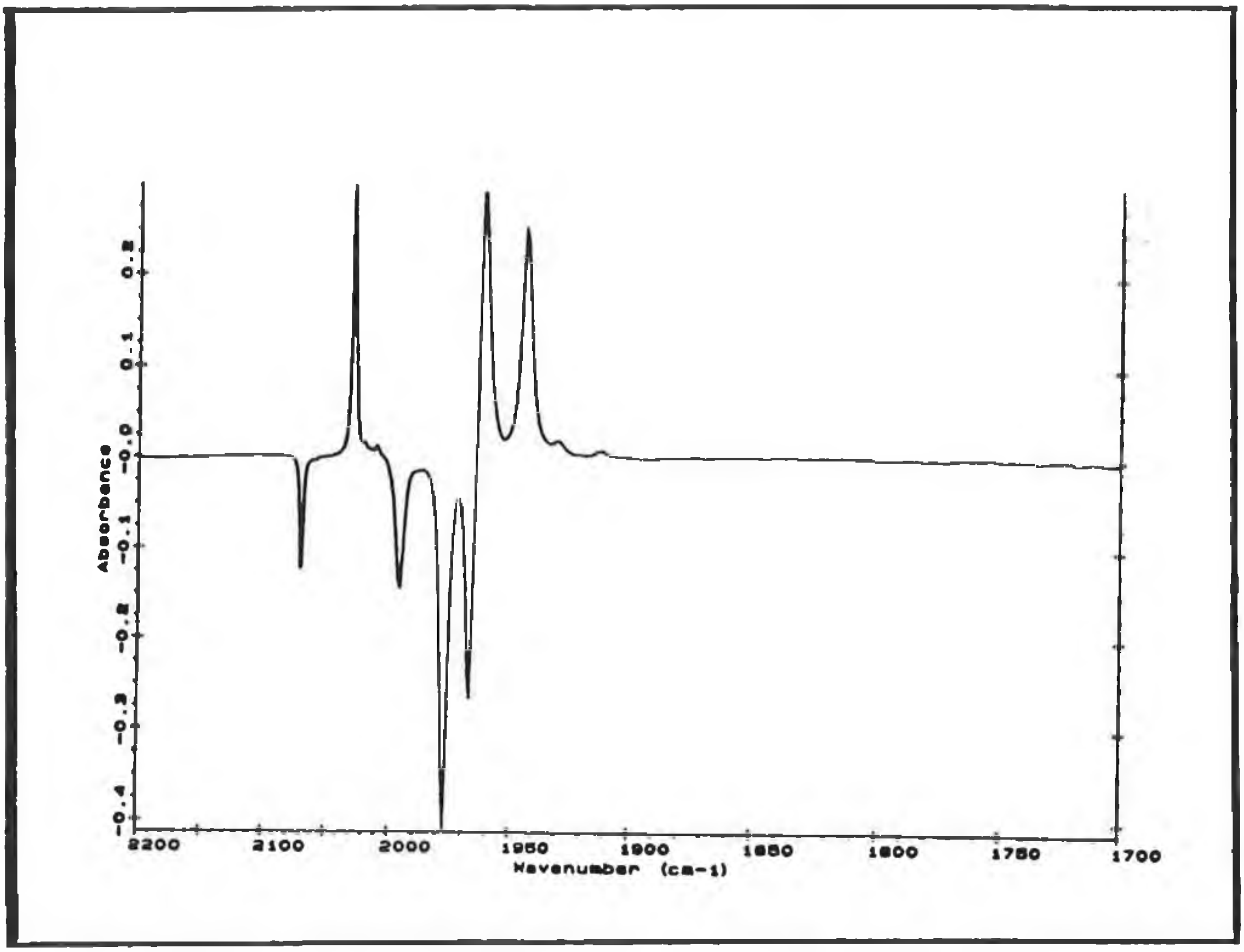

Figure 6.5.4.1 FTIR difference spectrum following the heating of (η^3-C_5H_7)Mn(CO)$_4$ in hexane.

6.6 Photochemistry of $(\eta^5\text{-}C_5H_7)Mn(CO)_3$.

6.6.1 Electronic absorption spectrum of $(\eta^5\text{-}C_5H_7)Mn(CO)_3$.

The UV/vis. spectrum of $(\eta^5\text{-}C_5H_7)Mn(CO)_3$ in cyclohexane is given in Figure 6.6.1.1 By analogy with $CH_3Mn(CO)_5$ the strong absorptions at 238 and 336 nm respectively may be assigned as metal to ligand charge transfer.[15]

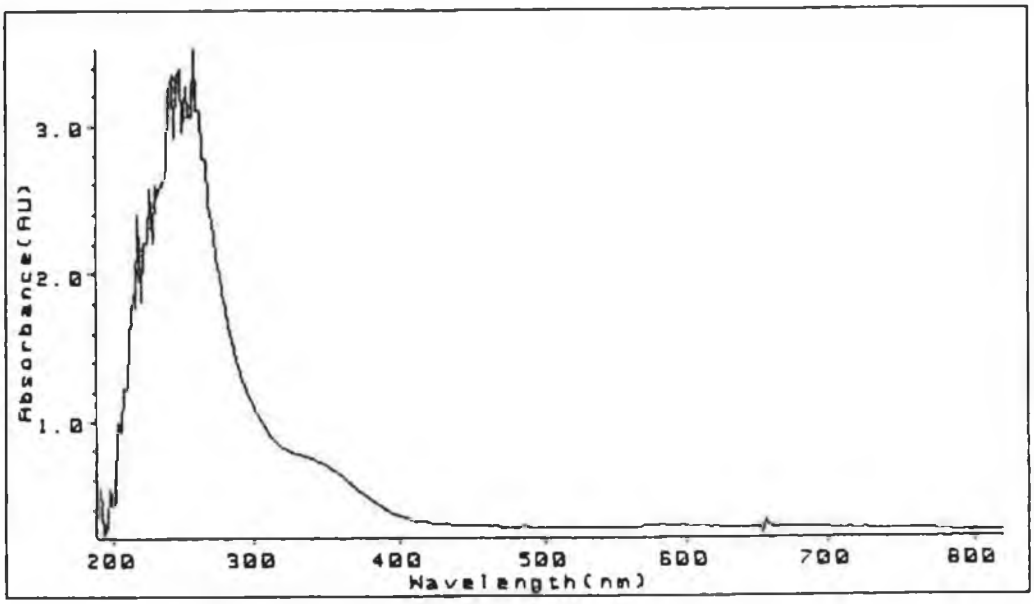

Figure 6.6.1.1 Electronic absorption spectrum of $(\eta^5\text{-}C_5H_7)Mn(CO)_3$ in cyclohexane (2.3×10^{-3}M) at 298K.

6.6.2. Laser flash photolysis of $(\eta^5\text{-}C_5H_7)Mn(CO)_3$.

Following laser flash photolysis of $(\eta^5\text{-}C_5H_7)Mn(CO)_3$ in cyclohexane under 1 atm. of argon at least two transient species were seen to absorb at 280 nm as given in Figure 6.6.2.1. k_{obs} of formation of the first species was measured to be 1.4×10^7 s^{-1}. The decay of this species was difficult to measure and hence no reliable rate data could be obtained. The second species appeared to be long-lived, the UV/vis. of the solution denoted slight variation throughout the experiment with a marginal increase in the region 280-320 nm. On admitting 0.5 atm of CO to the solution cell only one transient species was observed at 280 nm with a decay of 7.1×10^4 s^{-1}.

As no transient species were seen under 1 atm. of CO it would suggest that the primary photoproduct is loss of CO, to yield the dicarbonyl intermediate (Figure 6.6.2.1 and 6.6.2.3, samples were of a similar concentration), and it appears that the yield of the first species decreases in the presence of carbon monoxide. The identity of either of these species are unknown as these are only preliminary studies. It is most probable that one of these species is the CO loss product as on increasing the concentration of CO to half an atmosphere return to base-line of this transient species is observed, and this is quite evident with the second species. Perutz *et al.*[18] have reported that $(\eta^5\text{-}C_5H_7)Mn(CO)_3$ on irradiation for three hours in a CO matrix showed complete consumption of starting material and conversion to essentially only one product which was identified as $(\eta^3\text{-}C_5H_7)Mn(CO)_4$. They then sought to obtain evidence for the formation of the tetracarbonyl complex in solution. Hence, photolysis of $(\eta^5\text{-}C_5H_7)Mn(CO)_3$ in hexane under 1 atm. of CO was carried out and monitored by IR spectroscopy but over 31 hours photolysis was required before any evidence could be obtained for bands attributed to $(\eta^3\text{-}C_5H_7)Mn(CO)_4$. From this study no evidence was found for the formation of the tetra carbonyl species, as no transients were monitored under 1 atm. of CO, and from the previous section it was concluded that $(\eta^3\text{-}C_5H_7)Mn(CO)_4$ is not photolabile, hence if this species were formed changes in the UV/vis. spectrum should occur.

The photochemistry of $(\eta^5\text{-}C_5H_5)Mn(CO)_3$ is dominated by loss of CO to yield a vacant coordination site which 'becomes' coordinated by a solvent molecule. This solvated intermediate was measured to recombine with CO with a second order rate constant of 3.4×10^5 $dm^3mol^{-1}s^{-1}$ to reform the parent tricarbonyl.[19] Evidence was also reported for the formation of a dinuclear species, $(\eta^5\text{-}C_5H_5)_2Mn_2(CO)_5$ which formed in the absence of CO. Transient spectra for this intermediate showed an absorption in the visible region of the spectrum which is common for metal-metal bonding.

As regards $(\eta^5\text{-}C_5H_7)Mn(CO)_3$ no transients were observed beyond 380 nm, which would question whether or not a dinuclear species were formed for this compound. The observed rate constant for formation of the first species under argon was measured to be 1.4×10^7 s^{-1} which is a similar value to that measured for a hapticity change from η^1 ----> η^3 (*vide supra*). If in this case a hapticity were occurring formation of the tetra carbonyl product would be expected but this does not appear tp be the case.

No conclusive results were obtained for this particular compound and further experiments are required to elucidate the photoreactivity of $(\eta^5\text{-}C_5H_7)Mn(CO)_3$, but from the results obtained and the studies that are currently being carried out it appears that the photochemistry of this compound is very different to that of the cyclic analogue. Outlined in Scheme 6.6.2.1 is an overview of the photochemical pathway of the η^1, η^3, and η^5 - manganese complexes.

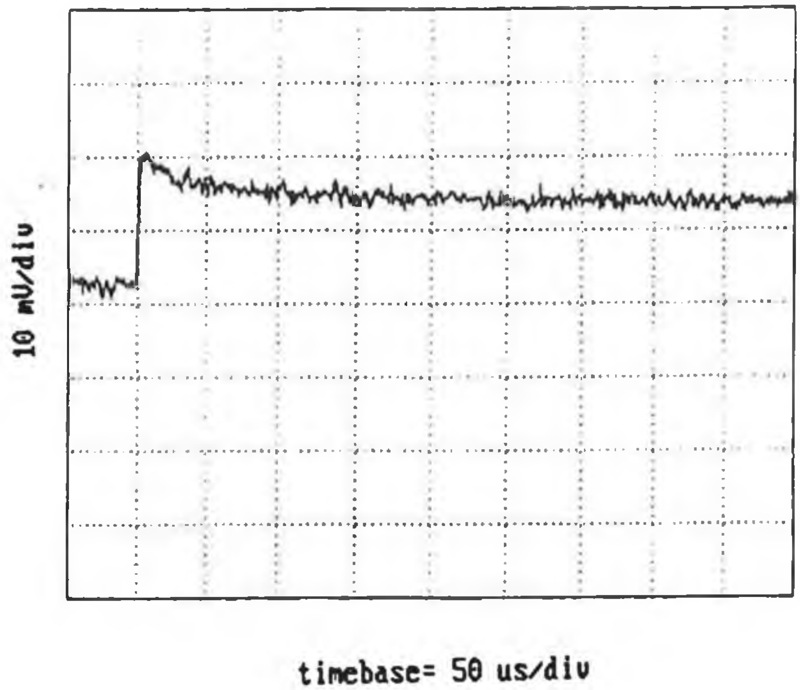

Figure 6.6.2.1 The transient signal observed following flash photolysis of (η^5-C_5H_7)$Mn(CO)_3$ under 1 atm. of argon at 280 nm.

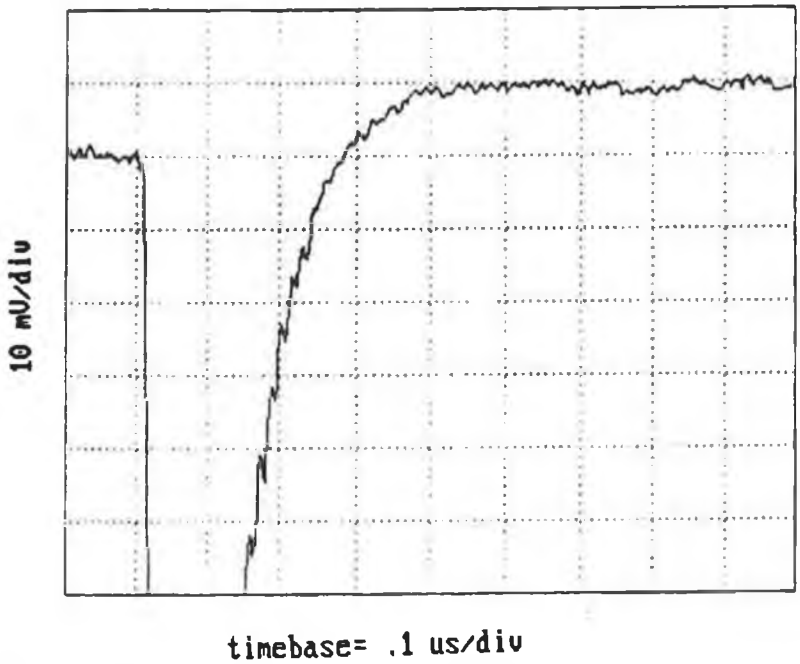

Figure 6.6.2.2 The transient signal indicating formation of the primary photoproduct under 1 atm. of argon at 280 nm.

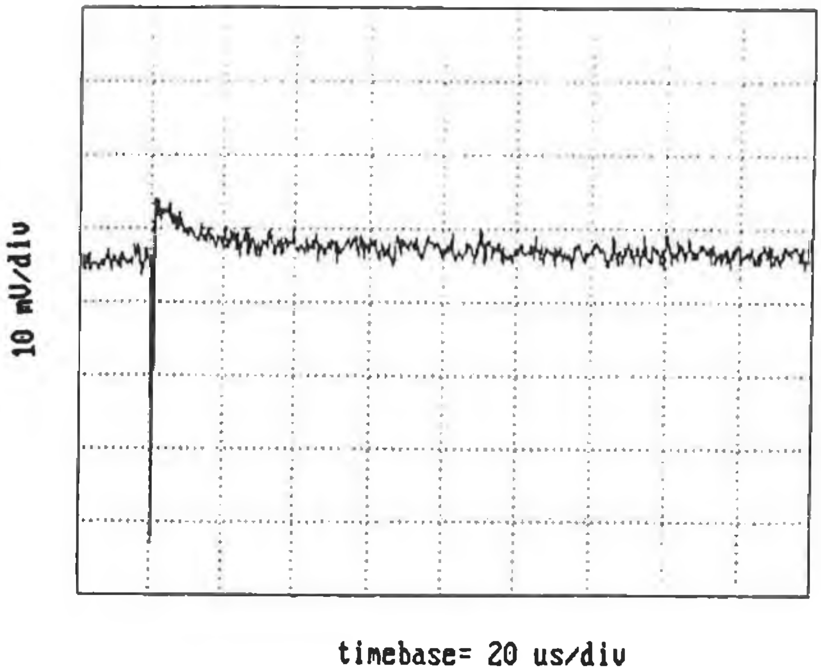

Figure 6.6.2.3 Transient signal under 0.5 atm. of CO at 280 nm.

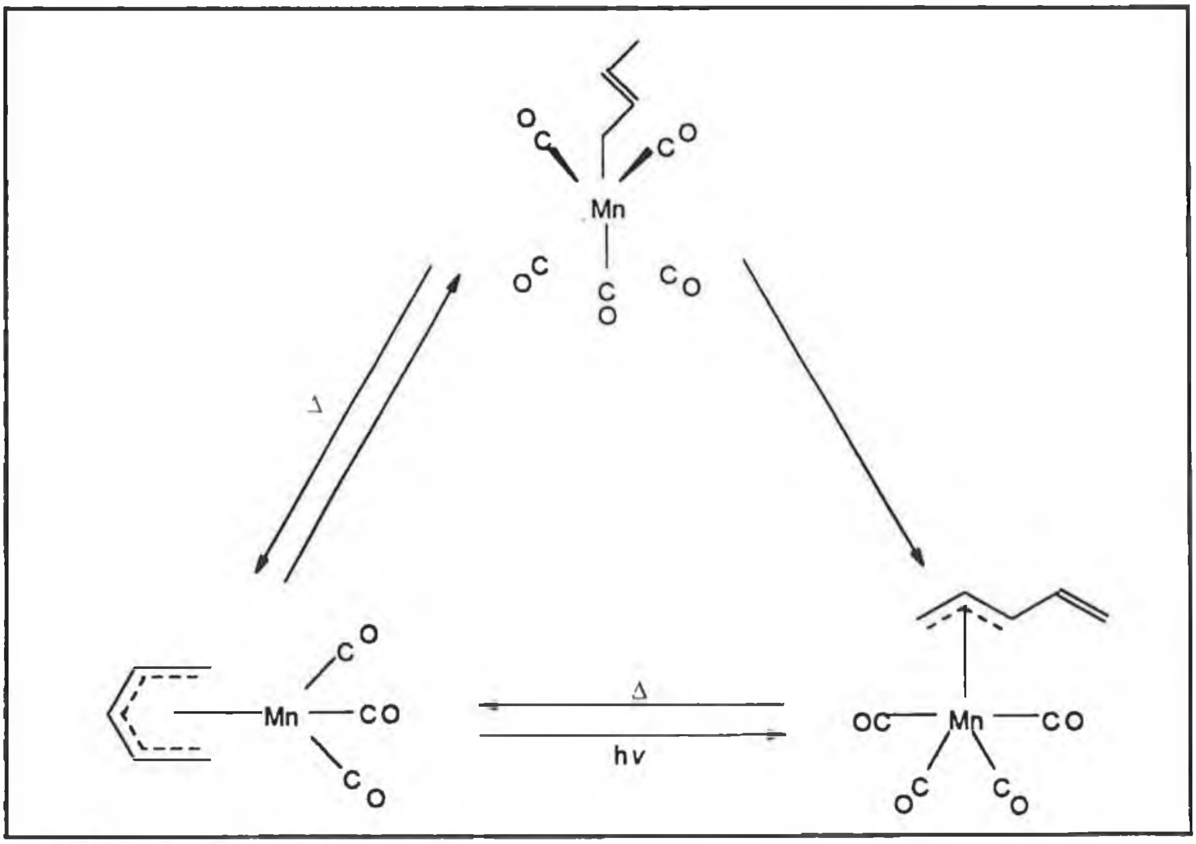

i Reference 20, ii Reference 18.

Scheme 6.6.2.1

6.7 Conclusion.

On irradiation of $(\eta^1\text{-}C_5H_7)Mn(CO)_5$ complete conversion to the $(\eta^3\text{-}C_5H_7)Mn(CO)_4$ compound occurs. The observed rate for formation of the tetracarbonyl following flash photolysis at 355 nm was unaffected by either solvent (cyclohexane or toluene) or the surrounding atmosphere (CO or argon). The fact that no 16 electron CO loss species was observed prior to hapticity change indicates that such a 'change' occurs extremely readily or occurs as a concerted process along with CO loss. From the results obtained in this study, $(\eta^3\text{-}C_5H_7)Mn(CO)_4$ did not appear to be photolabile though it can be thermally converted to the tricarbonyl analogue resulting in a hapticity change from η^3 ----> η^5. As only preliminary studies were carried out on $(\eta^5\text{-}C_5H_7)Mn(CO)_3$ no conclusive results were obtained. However, Perutz and colleagues have carried out matrix isolation studies and indicated CO loss to be the photochemical reaction in a CO matrix, but photolysis in the presence of various phosphine ligands resulted in the formation of a substituted dicarbonyl compound.[18]

The initial aim of this study was to identify, which of the metal centres of $Mn(CO)_4(\eta^3\text{-}C_3H_4\text{-}\eta^6\text{-}C_6H_5)Cr(CO)_3$ is the most photoreactive. From the results obtained it is proposed that the thermal chemistry at the chromium centre occurs subsequent to photochemistry at the manganese centre. There appears to be no literature available to correlate these results with at present.

6.8 References

1 Meyer,T.L.;Caspar,J.V.; *Chem. Rev.*; 1985,**85**,187.

2 (a)Oyer,T.J.;Wrighton,M.S.;*Inorg. Chem.*; 1988,**27**,3690.
(b)Firth,S.;Hodges,P.M.;Poliakoff,M.;Turner,J.J.;*Inorg. Chem.*; 1986,**25**,4680

3 Hitman,R.B.;Mahmound,K.A.;Rest,A.J.; *J. Organomet. Chem.*; 1985,**291**,321

4 Geoffroy,G.L.;Wrighton,M.S.; *Organometallic Photochemistry*; Acamedic Press, New York, 1979.

5 Belt,S.T.;Ryba,D.W.;Ford,P.C.; *Inorg. Chem.*;1990,**29**,3633.

6 Daniel,C.; *Coord. Chem. Rev.*; 1990,**97**,141.

7 Boese,W.T.;Ford,P.C.; *Organometallics*; 1994,**13**,3525.

8 McGrath,I.M.; *Ph.D. Thesis*; Dublin City University; 1993.

9 Crocock,B.; *Ph.D. Thesis*; Dublin City University; 1992.

10 Young,K.M.;Wrighton,M.S.; *J. Am. Chem. Soc.*; 1990,**112**,157.

11 Carroll,D.G.;McGlynn, S.P.; *Inorg. Chem.*; 1968,**7**,1285.

12 (a)Gogan.J.;Chu.C.K.; J. Organomet. Chem.; 1975,**93**,363.

(b)Gogan.J.;Chu.C.K.; Organometallics.; 1990,**9**,1970.

13 Gogan.J.;Chu.C.K.; *J. Organomet. Chem.*; 1977,**132**,103.

14 Walsh,M.M.; *Ph.D. Thesis*; Dublin City University; 1993.

15 Blakney,G.B.;Allen,W.F.; *Inorg. Chem.*; 1971,**10,**2763.

16 (a)Asali,K.J.;van Zyl,G.J.;Dobson,G.R.; *Inorg. Chem.*; 1988,**27**,3314.
(b)Zhang,S.;Bajaj,H.C.;Dobson,G.R.;van Eldik,R.; *Organometallics*; 1992,**11**,3901.

17 Kreiter,C.G.;Leyendecker,M.; *J. Organomet. Chem.*; 1985,**280**,225.

18 Paz-Sandoval,M.;Powell,P.;Drew,M.G.B.;Perutz,R.N.; *Organometallics.*; 1984,**3**,1026.

19 Creaven,B.S.;Dixon,A.J.;Kelly,J.M.;Long,C.;Poliakoff,M.; *Organometallics*; 1987,**6**,2600.

20 Lee,F.W.;Liu,R-S.; *J. Organomet. Chem.*; 1987,**320**,211.

Chapter 7

Experimental section.

7. Experimental Section.

7.1 Materials.

The following solvents were of spectroscopic grade and used without further purification: cyclohexane, cyclooctane, pentane, heptane, decane, dodecane, 1,1,2-trichlorotrifluoroethane, toluene, mesitylene (Aldrich Chemicals Co.), and perfluoromethylcyclohexane 98% (Aldrich). Argon and carbon monoxide were supplied by air products and IIG respectively. (η^6-benzene)$Cr(CO)_3$, (η^6-tetrahydronaphthalene)$Cr(CO)_3$, $Cr(CO)_6$, $BrMn(CO)_5$, $Mn_2(CO)_{10}$ (Strem chemicals), $Mo(CO)_6$, allylbenzene (Riedel de Haen), *o*-xylene, ethylbenzene, chlorobenzene, 1,2-dichlorobenzene, *t*-butylbenzene, naphthalene, phenanthrene (BDH), pyrene, *trans*-1,2 diphenylethene, *cis*-1,2 diphenylethene, *trans,trans*-1,4-diphenyl-1,3-butadiene, hexamethylbenzene, 1,4-pentadiene-3-ol, (Aldrich Chemicals Co.), were used without further purification. THF was distilled from $LiAlH_4$ and stored over CaH_2 under argon.

(η^6-Hexaethylbenzene)$Cr(CO)_3$ was a gift from A.G Gingburg as were the samples of (η^6-p-chlorotoluene)$Cr(CO)_3$ and (η^6-p-fluorotoluene)$Cr(CO)_3$ from Dr. Graham Russell. The manganese compounds:- η^3-C_3H_4-$C_6H_5Mn(CO)_4$ and η^3-C_3H_4-$C_6H_5Cr(CO)_3Mn(CO)_4$ were gifts from Dr. A. Wright.

7.2 Equipment.

Infrared spectra were recorded on a Perkin Elmer 983-G or a Nicloet 205 FTIR spectrometer using 0.1mm sodium chloride solution cells. UV/vis spectra were recorded on a Hewlett Packard 8452A Photodiode array spectrophotometer using a quartz cell of 1cm pathlength. NMR measurements were performed on a Bruker model AC 400 MHz Spectrometer. Luminescence spectra were recorded on a Perkin Elmer LS 50.

7.3 Photolysis apparatus.

Preparative photolysis experiments were performed using an Applied Photophysics 400 watt medium pressure mercury vapour lamp as given in Figure 7.3.1. The double walled pyrex glass vessels houses the lamp which is water cooled or in the case of low temperature photolysis, methanol at the desired temperature circulates around the lamp. The external vessel contains the sample solution to be irradiated. The photolysis solution was purged with argon for 15 minutes prior to irradiation. Argon is constantly bubbled through the solution in order to expel carbon monoxide liberated during the course of the reaction. The products were isolated by removing the solvent under reduced pressure (sometimes at a low temperature of -30°C) and purified by recrystallisation and/or classical chromatography depending on the air sensitivity of the compound.

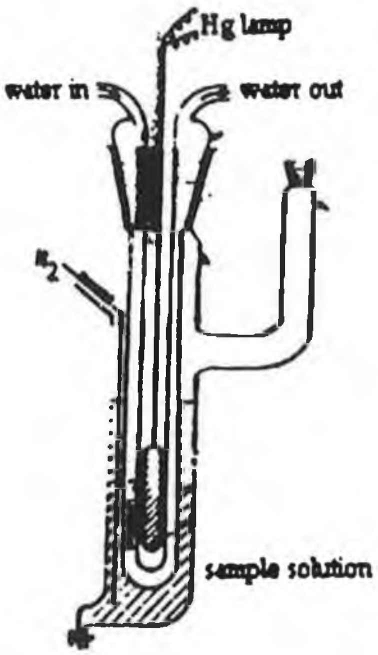

Figure 7.3.1 Photolysis apparatus used for the synthesis of metal carbonyls.

7.4 Synthesis of chromium compounds.

7.4.1 (η^6-mono-arene) chromium tricarbonyls.

The tricarbonyls were synthesised in a similar way to that used by Mahaffy *et al.* with minor alterations.[1] The chlorinated arene tricarbonys were synthesised in the following manner: $Cr(CO)_6$ (1 g,4.5 mmol), THF (5 mL), arene (~40 mL) were added to a round bottomed flask, and heated to reflux for

24 hours under an atmosphere of argon. The yellow solution was then filtered through silica using a glass centred crucible and the solvent removed from the filtrate under vacuum. The products were recrystallised from diethyl ether. The other monoaromatic chromium tricarbonyls were synthesised by refluxing $Cr(CO)_6$ in the desired arene (quantities similar to above) for 24 hours, solvent was removed under reduced pressure and the product purified by column chromatography using pet ether/ethyl acetate and finally recrystallised from diethyl ether. (η^6-Allylbenzene)$Cr(CO)_3$ was synthesised by refluxing $Cr(CO)_6$ (4 g, 18 mmol), allylbenzene (10 mL,75 mmol), butyl ether (125 mL) and THF (10 mL) in a round bottomed flask for 72 hours. Solvent was removed under reduced pressure, the remaining oil-like residue was taken up into hexane which in turn was vacuumed off to leave a yellow oil. In all of the above syntheses the solutions were purged with argon for 30 minutes prior to reflux.

7.4.2 (η^6-Poly-arene) chromium tricarbonyls.

(η^6-Naphthalene)$Cr(CO)_3$ was synthesised by using the method of Hudeck *et al.*[2] : $Cr(CO)_6$ (1.1 g,5 mmol), naphthalene (1.28 g,10 mmol) in decalin was brought to reflux temperature for 3 hours, the solution was then allowed to cool to room temperature and placed at -20 °C overnight. A red product precipitated out which was recrystallised from benzene/pet ether. (η^6-Phenanthrene)$Cr(CO)_3$ was made and purified by a similar manner. (η^6-Pyrene)$Cr(CO)_3$ was made in the same way however column chromatography using pet ether / chloroform in the ratio of 4:1 was required for separation of the starting materials from product. All solutions were purged with argon for 30 minutes prior to reflux.

7.4.3 (η^6- 1,2 Diphenylethene)chromium tricarbonyls.

These compounds were made in the same manner as was (η^6-naphthalene)$Cr(CO)_3$ and recrystallised from benzene/pentane. However in the case of the *cis* isomer temperatures as low as -70°C were required in order to precipitate the productfrom the solution. Again all solutions were purged for 30 minutes with argon prior to reflux.

7.5 Synthesis of molybdenum compounds.

7.5.1 (η^6-mono-arene) molybdenum tricarbonyls.

Both the benzene and mesitylene complexes were synthesed by heating $Mo(CO)_6$ (1 g, 3.7 mmol) and arene (40 mL) to reflux temperature for 3 hours. In the case of (η^6-benzene)$Mo(CO)_3$ the solvent was removed under reduced pressure and prolonged vacuum removed any remaining $Mo(CO)_6$. On allowing the mesitylene solution to cool to room temperature after reflux for three hours the product precipitated from the solution, It was then filtered off and recrystallised from chloroform/hexane. The hexamethylbenzene derivative was synthesised by the method of Pidcock and Smith[3] which involves heating of $Mo(CO)_6$ (1.5 g, 5 mmol), with hexamethylbenzene (3 g, 22.5 mmol) under reflux in ~ 80mL. of heptane for 10 hours. The mixture was cooled, filtered and the solvent evaporated under reduced pressure at room temperature. The excess $Mo(CO)_6$ was sublimed under vacuum and the product recrystallised from iso-propyl ether.

7.5.2 Attempted synthesis of (η^6-hexamethylbenzene)$_2Mo_2(CO)_5$.

Because of the apparent life-time of the dinuclear product formed upon photolysis, attempts were made to isolate this compound. Initially low temperature photolysis was carried out in pentane, unfortunately molybdenum tricarbonyl compounds are not readily soluble in hydrocarbon solvents, hence solutions were always in very low concentrations. This route was not successful. As the photolysis proceeded, a brown product was observed, which could be a photolysis product of the dinuclear compound, assuming it is photolabile, or a photodecomposition product, yielding oxides of molybdenum. The photolysis was monitored by UV/vis. Spectroscopy and the changes observed, were consistent with those previously described following laser flash photolysis. A photolysis experiment was also carried out in toluene as (η^6-hexamethylbenzene)$Mo(CO)_3$ is readily soluble in aromatic solvents. However, again this did not prove to be successful and similar observations were made as before.

Attempts were made to synthesise the dinuclear species *via* (η^6-hexamethylbenzene)$Mo(CO)_2$(*cis*-cyclooctene). Synthesis of this dicarbonyl intermediate was carried out by irradiating (η^6-hexamethylbenzene)$Mo(CO)_3$

with excess *cis*-cyclooctene in pentane at room temperature. the reaction was followed by infrared as presented in Figure 7.5.2.1. Various ligands (CO and PPh_3) were added to displace the *cis*-cyclooctene ligand as this is a known method of synthesising many compounds of chromium pentacarbonyl.^{4} However in no case was the ligand displaced and a brown insoluble product was formed. On allowing (η^6-hexamethylbenzene)$Mo(CO)_2$(*cis*-cyclooctene) to stand overnight in the presence of CO, the major product was found to be $Mo(CO)_6$. An alternative route was attempted *via* (η^6-hexamethylbenzene)$Mo(CO)_2$(ethene) but as before ethene was not displaced either by other ligands or the parent tricarbonyl complex.

Irradiation of (η^6-hexamethylbenzene)$Mo(CO)_3$ in dichloromethane at -70 °C resulted in no detectable changes in its infrared spectrum.

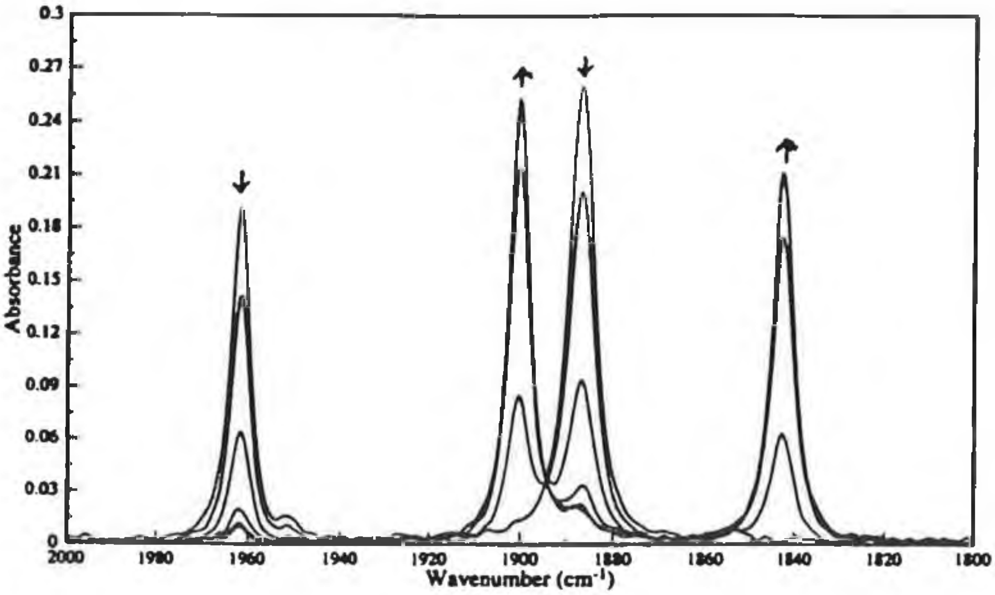

Figure 7.5.2.1 Changes in the infrared spectrum upon irradiation of (η^6-hexamethylbenzene)$Mo(CO)_3$ in the presence of excess *cis*-cyclooctene in pentane.

7.6 Synthesis of manganese compounds.

7.6.1 (η^1-C_5H_7)Mn(CO)$_5$.

To a 1% Na-Hg amalgam was added 100 mL of dried THF followed by 0.62 g $Mn_2(CO)_{10}$. The solution was constantly stirred and kept under argon. This mixture was allowed to stir overnight at room temperature. The mercury was then drained off leaving a solution containing $NaMn(CO)_5$.[5] To this solution was then added 0.5 g *trans*-1-bromo-2,4-pentadiene[6] at -78°C and allowed to warm to 0°C. The solvent was removed at 0°C under reduced pressure leaving a yellowish-brown residue. This residue was then reconstituted in THF, passed through alumina leaving a yellow solution, solvent was removed under reduced pressure leaving a yellow residue.[7]

7.6.2 (η^3-C_5H_7)Mn(CO)$_4$.

(η^3-C_5H_7)Mn(CO)$_4$ was synthesised by irradiating a solution of the previously prepared (η^1-C_5H_7)Mn(CO)$_5$ in pentane. The solution was purged with argon for about 30 minutes prior to photolysis, and during the irradiation time a constant stream of argon flowed through the solution. A medium pressure mercury lamp was used to photolyse the solution. The conversion from η^1 to η^3 was monitored by IR spectroscopy. When complete conversion of the pentacarbonyl was observed the photolysis was stopped which was about 30 minutes and excess solvent was removed at -30°C.[7]

7.6.3 (η^5-C_5H_7)Mn(CO)$_3$.

The method of McDaniel and coworkers[8] was used for the synthesis of the tricarbonyl derivative. To a 250 mL three necked round bottomed flask filled with argon was added 0.3 g, 1.04 mmol $BrMn(CO)_5$, 50 mL of dichloromethane, 0.9 g, 2.8 mmol Bu_4NBr in 50 mL 5N aqueous NaOH and 0.28 g, 2.0 mmol *trans*-1-bromo-2,4-pentadiene. This solution was purged with argon for approximately 30 minutes and then refluxed under argon for 24 hours. The solution was allowed to cool to room temperature and the organic layer removed. The aqueous layer was washed with 25 mL of dichloromethane. The organic layers were combined, washed with 25 mL water, filtered and dried over $MgSO_4$. After filtration the solvent was removed under vacuum where upon a deep orange coloured oil remained. This residue was dissolved in pentane and passed through alumina. Most of the pentane was removed and the product was recrystallised at -78°C yielding a yellow powder.

7.7 Laser flash photolysis.

7.7.1 Sample preparation for flash photolysis experiments.

With the exception of several experiments in Chapter 6 all flash photolysis studies were carried out in hydrocarbon solvents S (where S = cyclohexane, cyclooctane, pentane, heptane, decane, dodecane, perfluoromethyl-cyclohexane and 1,1,2-trichlorotrifluoroethane). All samples were adjusted such that the absorbance values were ideally between 0.5 and 2.0 at the wavelength of excitation (266 or 355 nm). All absorbance readings were recorded on a Hewlett-Packard 8452a UV/vis spectrophotometer. The concentration of the solution could then be determined from the previously calculated extinction coefficient. Samples were degassed by three cycles of a freeze-pump-thaw procedure, followed by liquid-pumping (to remove unwanted impurities such as water) in a specially designed degassing bulb attached to a fluorescence cell. Argon or the required carbon monoxide pressure was then added to the cell to prevent boiling of the solutions and to check the reversibility of the photochemical reactions investigated. The concentration of carbon monoxide was calculated to be 1.6×10^{-2}, 1.2×10^{-2}, 8.5×10^{-3}, 6.8×10^{-3}, 9.0×10^{-3} and 6.3×10^{-2}M in n-pentane, *n*-heptane, *n*-decane, *n*-dodecane, cyclohexane and cyclooctane, respectively, at one atmosphere of CO in the temperature range the experiments were conducted.[9]

7.7.2 Laser flash photolysis with UV/vis monitoring.

A schematic diagram of the flash photolysis instrumentation is given in Figure 7.7.2.1. The excitation source is a Q-switched Nd-Yag (neodynium yittrium aluminium garnet) laser which operates at 1064 nm, but can be frequency doubled, tripled or quadrupled to generate a second, third or fourth harmonic frequency at 532, 355 and 266 nm respectively. The power of the laser can be varied by applying different voltages across the amplifier flash tube. The pulse time is approximately 10 ns. At the frequencies employed the energy is

45 mJ and 60 mJ per pulse at 355 and 266 nm respectively. The circular laser pulse is directed *via* two Pellin-Broca prisms onto the sample cuvette. When the pulse passes through the power meter situated after the first prism but before the sample cuvette the oscilloscope is triggered. The monitoring light source is a air cooled 275 Watt Xenon arc lamp arranged at right angles to the laser beam. The monitoring beam passes through the sample and is directed to the entrance slit of an Applied Photophysics f/3. monochromator *via* a circular lens. UV/vis filter were used ($\lambda > 400$ nm or $\lambda > 345$ nm) between the monitoring source and the sample to prevent excessive photolysis of the sample solution. At the exit slit of the monochromator a Hamatsu five stage photomultiplier operating at 850V, detected absorbance changes and relayed the output to a transient digitiser (oscilloscope) *via* a variable load resistor. The digitiser, a Hewlett Packard HP 54510A oscilloscope is interfaced to an Olivetti PcS286 microcomputer *via* an IEEE bus. All signals were stored on floppy disks. The resultant transient signals were analysed using first order kinetics. Typical traces for transient absorption and decay are given in Figure 7.7.2.2. A transient signal was recorded in the following manner.

Initially, I_0 was recorded, which corresponds to the amount of light passing through the solution before the flash. It is measured by obtaining the difference in mV of the amount of light transmitted by the solution and detected by the photomultipler when the shutter is open and closed on the monitoring beam. A typical trace as given in Figure 7.7.2.2. shows the change in voltage with time which corresponds to the change in optical density. All traces are stored together with the time bases and voltage settings. The stored data can then be used to calculate I_t, the amount of light being transmitted at any time t. A 2-D spectrum is recorded in a 'point by point' manner, whereby a series of transients are accumulated at fixed time intervals after the flash.

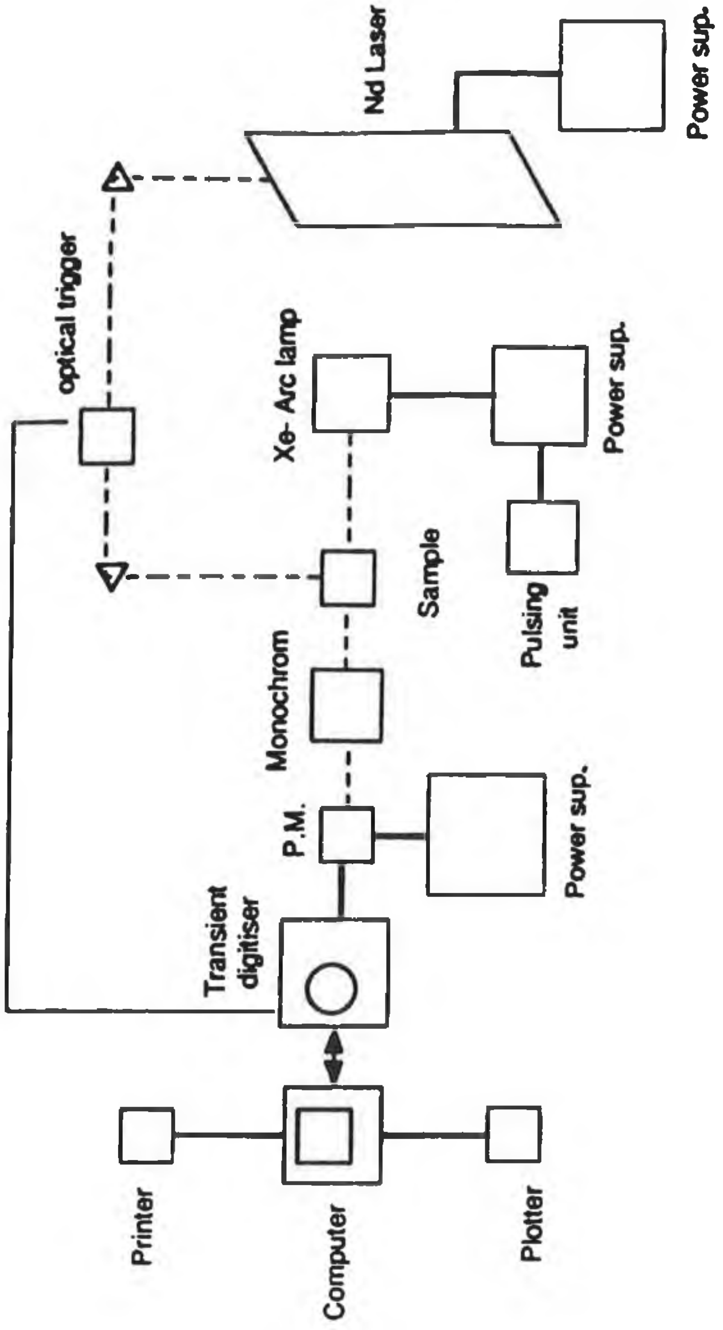

Figure 7.7.2.1 A schematic diagram of the instrumentation used in the laser flash photolysis experiments.

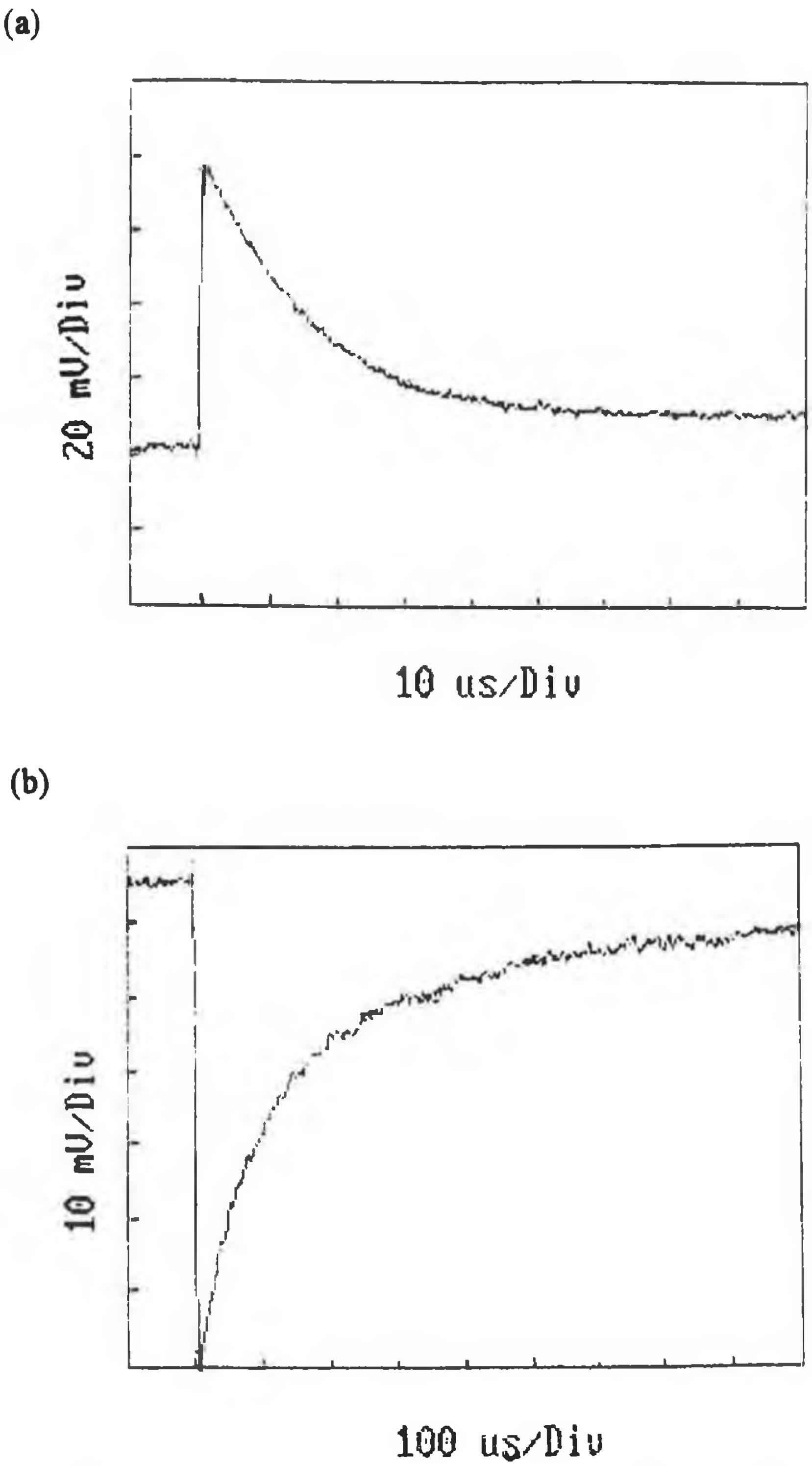

Figure 7.7.2.2 Typical signals obtained from an oscilloscope for (a) decay of transient species and (b) recovery of parent compound.

7.7.3 Laser Flash Photolysis with TRIR detection.

The instrumentation used for the flash photolysis studies using time-resolved-infrared detection has been described elsewhere.[10] The actual set-up used in these studies involves a Lambda Physik EMG 200 excimer laser (λ = 308 nm with XeCl; output attenuated to 80-90 mJ/pulse) as the excitation source. The system has a response time of 1-2 μs and a spectral resolution of 3-4 cm^{-1}. All flash photolysis experiments were performed at room temperature. Stock solution was prepared by three freeze-pump-thaw cycles, then a liquid pumping stage - followed by saturation with the desired gas atmosphere in the reservoir (1 atm.) In the intervals between the laser shot, the cell was emptied and refilled with fresh solution from the reservoir through a magnetic valve system. TRIR difference spectra were built up by a 'point by point' method.

7.7.4 Matrix isolation.

The low temperature matrix isolation apparatus has previously been described.[11] The system consists of an Air Products model CS202 Displex closed-cycle helium refrigerator, which cools a NaCl spectroscopic window to 10-12 K. The temperature of the window is monitored separately by a thermocouple embedded in a cavity close to the window centre. The flow of gases is controlled by a calibrated micrometer needle valve and a vacuum assembly. A thermotron gauge continuously checks the pressure in the gas inlet line. Evaporation rates for deposition of each sample is controlled in each experiment by first depositing onto a quartz crystal microbalance mounted in good thermal contact to the side of the target window holder. Infrared spectra were recorded on a Perkin-Elmer model 1720 fourier transform spectrometer.

7.8 Determination of Activation Parameters.

The activation parameters were calculated from Arrhenius and Eyring plots. The Arrhenius equation is:

$$\text{In } k = \text{In } A - E_a / RT$$

where k = rate constant
E_a = activation energy ($kJmol^{-1}$)
R = universal gas constant (8.314 $JK^{-1}mol^{-1}$)
T = absolute temperature (^oK)
A = frequency factor (the number of collisions between the reactant molecules)

A plot of In k *versus* 1/T gives a straight line with the slope = $-E_a/R$ and the intercept In A. ($k = k_{obs} / [CO]$).

The Eyring equation is:

$$\text{In}(k/T) = -(\Delta H^{\neq}/RT) + (\Delta S^{\neq}/R) + \text{In}(k/h)$$

where k = rate constant
$\Delta H^{\neq}$ = enthalpy change of activation ($kJmol^{-1}$)
$\Delta S^{\neq}$ = entropy change of activation ($Jmol^{-1}K^{-1}$)
k = Boltzmans constant ($1.38066 \times 10^{-23} JK^{-1}$)
h = Planks constant ($6.62618 \times 10^{-34} Js$)
T = absolute temperature (^oK)
R = universal gas constant (8.314 $JK^{-1}mol^{-1}$)

A plot of In k/T *versus* 1/T gives a straight line with slope $-\Delta H^{\neq}/RT$ and the intercept $\Delta S^{\neq}/R$ + In k/h. ($k = k_{obs} / [CO]$).

Activation parameters were calculated by recording the increase in observed rate constant with increasing temperature. Temperatures changes were achieved by immersing the cell in a temperature controlled water bath for a period of 15 minutes at the required temperature. The temperature of the bath was increased in approximately increments of 5 K in the temperature range 280-318 K.

7.9 Determination of extinction coefficients

Extinction coefficients were determined at the wavelength of excitation for all compounds in order to calculate the concentration of the sample. By knowing the absorbance and utilising the Beer-Lambert law the concentration of the sample was calculated. The Beer-Lambert law is given by:

$$A = \varepsilon cl$$

where A = absorbance at excitation wavelength (A.U)
ε = molar extinction coefficient ($dm^3 mol^{-1} cm^{-1}$)
c = concentration ($mol\ dm^{-3}$)
l = pathlength of cell (cm)

7.10 Solubility of CO in alkane solvent.

The solubility of CO in hydrocarbon solvents was calculated using the mole fraction data, reported by Makranczy *et al.*[9] The calculation for cyclohexane is given as a representative example.

Solubility of CO at 298K expressed in mole fraction = 9.94×10^{-4}
1 litre of cyclohexane = 779g
1 mole of cyclohexane = 84g

$$\Rightarrow \quad [CO] = 9.94 \times 10^{-4} \times \frac{779}{84}$$

$$= 9.1 \times 10^{-3}\ mol\ L^{-1} \text{ at 1 bar CO.}$$

7.11 Determination of the quantum yield for the photosubstitution of CO by pyridine in (η^6-benzene)$Mo(CO)_3$ in cyclohexane.

Previously the quantum yield for the photosubstitution of CO by ^{13}CO or pyridine of (η^6-benzene)$Cr(CO)_3$ had been determined and the value $\Phi = 0.72$ was used as a reference for the determination of the quantum yield. Samples were prepared such that the concentration of (η^6-benzene)$Mo(CO)_3$ and (η^6-benzene)$Cr(CO)_3$ was the same in both cuvettes, and then a large excess of pyridine was added to each sample. Solutions were then purged for approximately 15 minutes and sealed. The irradiation wavelength used was 313 nm which was obtained by using a 200 Watt mercury lamp (Applied Photophysics) in combination with a Corning 7-54 filter and a solution filter of an aqueous solution of potassium chromate (0.2 g/L) containing 1% NaOH. The samples were then irradiated for fixed periods of time on a merry-go round apparatus (Applied Photophysics Ltd.). UV/vis absorption spectra were recorded at fixed time intervals for both samples. The formation of (η^6-benzene)$Mo(CO)_2$(pyridine) was compared to that of (η^6-benzene)$Cr(CO)_2$(pyridine) which had previously been determined.[12]

7.11 References

1 Mahaffy,C.A.L.;Pauson,P.L.; *Inorg. Synth.*, 1979,**19**,154.

2 Hrnviar,P;Hudeck,M.;Magomedov,G.K.I.;Toma,S.; *Collect. Czech. Comm.*; 1991,**56**,1477.

3 Pidcock,A.;Smith,S.D.; *J. Chem. Soc. (A)* ; 1967,872.

4 Grevels,F-W.;Skibbe,V.; *J. Chem. Soc.*; 1984,681.

5 Kaesz,H.D.;King,R.B.;Stone,F.G.A.; *Z. Naturforsch.* 1960,**15B**,682.

6 Prevost,C.;Miginiac,P.;Miginiac-Groizeleau,L.; *Bull. Soc. Chim. Fr.*; 1964,2485.

7 Lee,T-W.;Liu,R-S.; *J. Organomet. Chem.*; 1987,**320**,211.

8 McDaniel,K.F.;Afif Abu-Baker,A.B.A.; *J. Organomet. Chem.*; 1993,**443**,107.

9 Makranczy,J.;Megyery-Balog,k.;Rosz,L.;Patyt,D.; *Hungarian J. Indust. Chem.*,;1976,**4**,269.

10 Schaffner,K.;Grevels,F.-W..; *J. Mol. Struct.*; 1988,**173**,51.

11 (a)Grevels,F.-W.;Klotzbucher,W.E.; *Inorg. Chem.*; 1981,**20**,3002.
(b) Klotzbucher,W.E.; *Cryogenics*; 1983,**23**,554.

12 Wrighton,M.S.;Haverty,J.L.; *Z. Naturforsch.*; 1975,**30B**,254.

Appendix A

Data for the determination of the second order rate constants at 298K.

$[CO] \times 10^3$ mol dm^{-3}	k_{obs} (s^{-1}) x 10^{-3}
2.25	17.83
4.50	33.16
6.75	48.97
9.00	62.59

slope = $6.67 \times 10^6 \pm 1.46 \times 10^5$
intercept = $31.17 \times 10^{-2} \pm 7.36 \times 10^{-2}$
correlation coefficient = 0.99

Table A1 The observed rate constant (k_{obs}) at various concentrations of CO, for the reaction of CO with (η^6-ethylbenzene)$Cr(CO)_2$(cyclohexane) at 298K.

$[CO] \times 10^3$ mol dm^{-3}	k_{obs} (s^{-1}) x 10^{-3}
2.25	17.56
4.50	33.70
6.75	51.03
9.00	65.49

slope = $7.15 \times 10^6 \pm 1.74 \times 10^5$
intercept = $16.85 \times 10^{-2} \pm 8.74 \times 10^{-2}$
correlation coefficient = 0.99

Table A2 The observed rate constant (k_{obs}) at various concentrations of CO, for the reaction of CO with (η^6-*o*-xylene)$Cr(CO)_2$(cyclohexane)at 298K.

$[CO] \times 10^3$ mol dm^{-3}	k_{obs} $(s^{-1}) \times 10^{-3}$
2.25	14.30
4.50	31.94
6.75	46.81
9.00	68.12

slope = $7.83 \times 10^6 \pm 3.88 \times 10^5$
intercept = $37.88 \times 10^2 \pm 19.51 \times 10^2$
correlation coefficient = 0.99

Table A3 The observed rate constant (k_{obs}) at various concentrations of CO, for the reaction of CO with (η^6-*t*-butylbenzene)$Cr(CO)_2$(cyclohexane) at 298K.

$[CO] \times 10^3$ mol dm^{-3}	k_{obs} $(s^{-1}) \times 10^{-4}$
2.25	13.01
4.50	22.10
6.75	39.12
9.00	52.70

slope = $6.04 \times 10^7 \pm 4.76 \times 10^6$
intercept = $- 22.9 \times 10^{-3} \pm 23.9 \times 10^{-3}$
correlation coefficient = 0.99

Table A4 The observed rate constant (k_{obs}) at various concentrations of CO, for the reaction of CO with (η^6-hexamethylbenzene)$Cr(CO)_2$(cyclohexane) at 298K.

[CO] x 10^3 mol dm^{-3}	k_{obs} (s^{-1}) x 10^{-3}
2.25	12.64
4.50	22.41
6.75	34.99
9.00	44.61

slope = 4.84 x 10^6 ± 1.78 x 10^5
intercept = 13.93 x 10^2 ± 8.92 x 10^2
correlation coefficient = 0.99

Table A5 The observed rate constant (k_{obs}) at various concentrations of CO, for the reaction of CO with (η^6-chlorobenzene)Cr$(CO)_2$(cyclohexane) at 298K.

[CO] x 10^3 mol dm^{-3}	k_{obs} (s^{-1}) x 10^{-3}
2.25	8.53
4.50	18.14
6.75	28.31
9.00	34.65

slope = 3.93 x 10^6 ± 2.28 x 10^5
intercept = 27.7 x 10^2 ± 13.48 x 10^2
correlation coefficient = 0.99

Table A6 The observed rate constant (k_{obs}) at various concentrations of CO, for the reaction of CO with (η^6-1,2-dichlorobenzene)Cr$(CO)_2$(cyclohexane) at 298K.

[CO] x 10^3 mol dm^{-3}	k_{obs} (s^{-1}) x 10^{-3}
2.25	9.12
4.50	16.92
6.75	27.38
9.00	39.64

slope = 4.19 x 10^6 ± 1.73 x 10^5
intercept = -9.79 x 10^2 ± 8.7 x 10^2
correlation coefficient = 0.99

Table A7 The observed rate constant (k_{obs}) at various concentrations of CO, for the reaction of CO with (η^6-*p*-chlorotoluene)$Cr(CO)_2$(cyclohexane) at 298K.

[CO] x 10^3 mol dm^{-3}	k_{obs} (s^{-1}) x 10^{-3}
2.25	6.48
4.50	16.49
6.75	21.40
9.00	32.60

slope = 3.69 x 10^6 ± 3.67 x 10^5
intercept = -15.66 x 10^{-2} + 18.48 x 10^{-2}
correlation coefficient =0.99

Table A8 The observed rate constant (k_{obs}) at various concentrations of CO, for the reaction of CO with (η^6-*p*-fluorotoluene)$Cr(CO)_2$(cyclohexane) at 298K.

[CO] x 10^3 mol dm^{-3}	k_{obs} (s^{-1}) x 10^{-3}
4.50	4.47
5.85	6.41
7.65	8.93
9.00	11.58

slope = $1.55 \times 10^6 \pm 8.09 \times 10^4$
intercept = $-26.14 \times 10^2 \pm 2.77 \times 10^2$
correlation coefficient = 0.99

Table A9 The observed rate constant (k_{obs}) at various concentrations of CO, for the reaction of CO with (η^6-benzene)Mo$(CO)_2$(cyclohexane) at 298K.

[CO] x 10^3 mol dm^{-3}	k_{obs} (s^{-1}) x 10^{-3}
4.5	4.81
5.85	7.14
7.65	9.20
9.00	12.51

slope = $1.63 \times 10^6 \pm 1.71 \times 10^4$
intercept = $- 26.09 \times 10^2 \pm 5.87 \times 10^2$
correlation coefficient = 0.99

Table A10 The observed rate constant (k_{obs}) at various concentrations of CO, for the reaction of CO with (η^6-*p*-xylene)Mo$(CO)_2$(cyclohexane) at 298K.

[CO] x 10^3 mol dm^{-3}	k_{obs} (s^{-1}) x 10^{-3}
4.5	4.50
5.85	6.47
7.65	9.25
9.00	12.87

slope = $1.81 \times 10^6 \pm 1.86 \times 10^5$
intercept = $-39.90 \times 10^2 \pm 6.37 \times 10^2$
correlation coefficient = 0.99

Table A11 The observed rate constant (k_{obs}) at various concentrations of CO, for the reaction of CO with (η^6-1,3,5-mesitylene)Mo$(CO)_2$(cyclohexane) at 298K.

[CO] x 10^3 mol dm^{-3}	k_{obs} (s^{-1}) x 10^{-3}
4.50	6.87
5.85	10.36
7.65	13.20
9.00	16.91

slope = $2.13 \times 10^6 \pm 1.59 \times 10^5$
intercept = $-26.04 \times 10^{-2} + 3.48 \times 10^{-2}$
correlation coefficient =0.99

Table A12 The observed rate constant (k_{obs}) at various concentrations of CO, for the reaction of CO with (η^6-hexamethylbenzene)Mo$(CO)_2$(cyclohexane) at 298K.

[CO] x 10^2 mol dm^{-3}	k_{obs} (s^{-1}) x 10^{-4}
0.4	6.1
0.8	9.5
1.2	15.6
1.6	21.5

slope = 13.056 x 10^6 ± 11.2 x 10^5
intercept = 15.23 x 10^2 ± 10.04 x 10^2
correlation coefficient = 0.99

Table A13 The observed rate constant (k_{obs}) at various concentrations of CO, for the reaction of CO with (η^6-benzene)Cr$(CO)_2$(pentane) at 298K.

[CO] x 10^2 mol dm^{-3}	k_{obs} (s^{-1}) x 10^{-4}
0.3	6.3
0.6	13.8
0.9	20.8
1.2	26.2

slope = 22.23 x 10^6 ± 11.36 x 10^5
intercept = 1.0 x 10^2 ± 6.25 x 10^2
correlation coefficient =0.99

Table A14 The observed rate constant (k_{obs}) at various concentrations of CO, for the reaction of CO with (η^6-benzene)Cr$(CO)_2$(heptane) at 298K.

[CO] x 10^3 mol dm^{-3}	k_{obs} (s^{-1}) x 10^{-4}
2.15	5.94
4.25	11.10
6.37	17.62
8.5	23.51

slope = 27.98 x $10^6 \pm 8.14$ x 10^5
intercept = -33.63 x $10^2 \pm 38.52$ x 10^2
correlation coefficient = 0.99

Table A15 The observed rate constant (k_{obs}) at various concentrations of CO, for the reaction of CO with (η^6-benzene)Cr$(CO)_2$(decane) at 298K.

[CO] x 10^3 mol dm-3	k_{obs} (s^{-1}) x 10^{-4}
1.7	7.5
3.4	13.48
5.1	20.04
6.8	24.91

slope = 33.96 x $10^6 \pm 18.31$ x 10^5
intercept = 22.68 x $10^3 \pm 70.77$ x 10^2
correlation coefficient = 0.99

Table A16 The observed rate constant (k_{obs}) at various concentrations of CO, for the reaction of CO with (η^6-benzene)Cr$(CO)_2$(dodecane) at 298K.

[CO] x 10^3 mol dm^{-3}	k_{obs} (s^{-1}) x 10^{-4}
1.57	12.45
3.1	23.58
4.71	32.12
6.29	43.47

slope = 64.3 x 10^6 ± 27.0 x 10^5
intercept = 26.771 x 10^3 ± 96.665 x 10^2
correlation coefficient = 0.99

Table A17 The observed rate constant (k_{obs}) at various concentrations of CO, for the reaction of CO with (η^6-benzene)Cr$(CO)_2$(cyclooctane) at 298K.

[CO] x 10^2 mol dm-3	k_{obs} (s^{-1}) x 10^{-5}
3.0	3.70
6.0	7.90
9.0	11.9
1.2	13.4

slope = 110.3 x 10^6 ± 152.28 x 10^5
intercept = 95.0 x 10^3 ± 1.02 x 10^2
correlation coefficient = 0.98

Table A18 The observed rate constant (k_{obs}) at various concentrations of CO, for the reaction of CO with (η^6-hexaethylbenzene)Cr$(CO)_2$(heptane) at 298K.

[CO] x 10^2 mol dm-3	k_{obs} (s^{-1}) x 10^{-4}
0.6	9.15
0.78	11.76
1.02	16.26
1.20	21.05

slope = 1.97 x 10^6 ± 1.7 x 10^5
intercept = -31.68 x 10^2 ± 7.78 x 10^2
correlation coefficient = 0.99

Table A19 The observed rate constant (k_{obs}) at various concentrations of CO, for the reaction of CO with (η^6-1,3,5-mesitylene)$Mo(CO)_2$(heptane) at 298K.

[CO] x 10^3 mol dm-3	k_{obs} (s^{-1}) x 10^{-4}
4.5	11.20
5.52	15.76
7.22	19.06
8.5	22.21

slope = 2.5 x 10^6 ± 2.2 x 10^5
intercept = 11.14 x 10^2 ± 71.4 x 10^2
correlation coefficient = 0.99

Table A20 The observed rate constant (k_{obs}) at various concentrations of CO, for the reaction of CO with (η^6-1,3,5-mesitylene)$Mo(CO)_2$(decane) at 298K.

Appendix B

Data for the determination of activation parameters.

Temp. (K)	$1/T \times 10^3$ (K^{-1})	k_{obs} (s^{-1}) $\times 10^{-4}$	$Ln(k_{obs}/[CO])$	$Ln(k_{obs}/[CO] . T)$
283	3.53	3.75	15.24	9.6
288	3.47	4.85	15.50	9.83
293	3.41	5.98	15.71	10.01
298	3.35	7.20	15.89	10.20
303	3.30	8.49	16.06	10.35
308	3.25	9.97	16.20	10.47
313	3.19	12.01	16.41	10.06

Arrhenius Plot

Slope	= -3361 ± 79
Intercept	= 27.14 + 0.02
Correlation coefficient	= 0.99

Eyring Plot

Slope	= -3062. ± 72.
Intercept	= 20.44 ± 0.02
Correlation coefficient	= 0.99

$E_a^{\neq} = 28 \pm 2$ kjmol^{-1}
$\Delta H^{\neq} = 25 \pm 2$ kjmol^{-1}
$\Delta S^{\neq} = -28 \pm 5$ jmol^{-1}K^{-1}
$\Delta G^{\neq} = 33 \pm 2$ kjmol^{-1}

Table B1 Experimental data for the determination of the activation parameters for the formation of (η^6-ethylbenzene)$Cr(CO)_3$ following flash photolysis at 355nm in cyclohexane under 1 atm. of CO.

Temp. (K)	1/T x 10^3 (K^{-1})	k_{obs} (s^{-1}) x 10^{-4}	Ln(k_{obs}/[CO])	Ln(k_{obs}/[CO] . T)
289	3.46	5.04	15.54	9.87
294	3.40	6.12	15.73	10.04
299	3.34	7.10	15.88	10.18
303	3.30	8.54	16.06	10.35
308	3.25	10.76	16.29	10.56
313	3.19	12.23	16.42	10.69
318	3.14	14.38	16.58	10.82

Arrhenius Plot	
Slope	= -3329 ± 103
Intercept	= 27.04 ± 0.03
Correlation coefficient	= 0.99

Eyring Plot	
Slope	= -3043 ± 126
Intercept	= 20.39 ± 0.03
Correlation coefficient	= 0.99

$E_a^{\neq}$ = 28 ± 2 kjmol^{-1}
$\Delta H^{\neq}$ = 25 ± 2 kjmol^{-1}
$\Delta S^{\neq}$ = -28 ± 5 jmol^{-1}K^{-1}
$\Delta G^{\neq}$ = 33 ± 2 kjmol^{-1}

Table B2 Experimental data for the determination of the activation parameters for the formation of (η^6-*o*-xylene)Cr(CO)$_3$ following flash photolysis at 355nm in cyclohexane under 1 atm. of CO.

Temp. (K)	$1/T \times 10^3$ (K^{-1})	k_{obs} (s^{-1}) $\times 10^{-5}$	$Ln(k_{obs}/[CO])$	$Ln(k_{obs}/[CO] . T)$
288	3.47	4.20	17.66	12.03
294	3.40	5.37	17.90	12.22
299	3.34	6.04	18.02	12.32
303	3.30	6.60	18.11	12.39
308	3.25	8.04	18.31	12.58
313	3.19	9.7	18.49	12.75
318	3.14	11.10	18.63	12.86

Arrhenius Plot

Slope	= -2920 ± 100
Intercept	= 27.27 ± 0.02
Correlation coefficient	= 0.99

Eyring Plot

Slope	= -2600 ± 111
Intercept	= 21.05 + 0.03
Correlation coefficient	= 0.99

$E_a^{\neq} = 24 \pm 2$ kjmol^{-1}
$\Delta H^{\neq} = 22 \pm 2$ kjmol^{-1}
$\Delta S^{\neq} = -23 \pm 5$ jmol^{-1}K^{-1}
$\Delta G^{\neq} = 24 \pm 2$ kjmol^{-1}

Table B3 Experimental data for the determination of the activation parameters for the formation of (η^6-hexaethylbenzene)Cr(CO)$_3$ following flash photolysis at 355nm in cyclohexane under 1 atm. of CO.

Temp. (K)	1/T x 10^3 (K^{-1})	k_{obs} (s^{-1}) x 10^{-4}	Ln(k_{obs}/[CO])	Ln(k_{obs}/[CO] . T)
289	3.46	3.21	15.08	9.42
293	3.41	3.70	15.23	9.55
299	3.34	4.70	15.47	9.77
303	3.29	5.91	15.69	9.98
308	3.24	6.84	15.84	10.11
311	3.19	7.31	15.91	10.16

Arrhenius Plot
Slope = -3256 ± 188
Intercept = 26.35 ± 0.43
Correlation coefficient = 0.99

Eyring Plot
Slope = -2963 ± 188
Intercept = 19.67 ± 0.43
Correlation coefficient = 0.99

$E_a^{\neq}$ = 27 ± 2 kjmol^{-1}
$\Delta H^{\neq}$ = 25 ± 2 kjmol^{-1}
$\Delta S^{\neq}$ = -34 ± 5 jmol^{-1}K^{-1}
$\Delta G^{\neq}$ = 35 ± 2 kjmol^{-1}

Table B4 Experimental data for the determination of the activation parameters for the formation of (η^6-*p*-chlorotoluene)Cr(CO)$_3$ following flash photolysis at 355nm in cyclohexane under 1 atm. of CO.

Temp. (K)	1/T x 10^3 (K^{-1})	k_{obs} (s^{-1}) x 10^{-4}	Ln(k_{obs}/[CO])	Ln(k_{obs}/[CO] . T)
285	3.50	1.5	14.33	8.68
289	3.46	1.66	14.43	8.76
294	3.40	2.07	14.65	8.97
298	3.35	2.25	14.73	9.03
303	3.30	2.68	14.91	9.20
309	3.23	3.63	15.21	9.48
313	3.19	4.17	15.35	9.62

Arrhenius Plot
Slope = -3286 ± 151
Intercept = 25.8 ± 0.04
Correlation coefficient = 0.99

Eyring Plot
Slope = -3025 ± 164
Intercept = 19.23 ± 0.46
Correlation coefficient = 0.99

$E_a^{\neq}$ = 27 ± 2 kjmol^{-1}
$\Delta H^{\neq}$ = 25 ± 2 kjmol^{-1}
$\Delta S^{\neq}$ = -38 ± 5 jmol^{-1}K^{-1}
$\Delta G^{\neq}$ = 36 ± 2 kjmol^{-1}

Table B5 Experimental data for the determination of the activation parameters for the formation of (η^6-*p*-fluorotoluene)$Cr(CO)_3$ following flash photolysis at 355nm in cyclohexane under 1 atm. of CO.

Temp. (K)	1/T x 10^3 (K^{-1})	k_{obs} (s^{-1}) x 10^{-4}	Ln(k_{obs}/[CO])	Ln(k_{obs}/[CO] . T)
288	3.47	4.80	15.49	9.82
293	3.40	5.09	15.66	9.98
298	3.35	6.75	15.83	10.13
303	3.30	7.6	15.95	10.25
308	3.25	9.13	16.13	10.40
313	3.19	10.76	16.30	10.55

Arrhenius Plot

Slope	= -2931 ± 78
Intercept	= 25.64 ± 0.02
Correlation coefficient	= 0.99

Eyring Plot

Slope	= -2698 ± 34
Intercept	= 19.16 ± 0.08
Correlation coefficient	= 0.99

$E_a^{\neq} = 24 \pm 2$ kjmol^{-1}
$\Delta H^{\neq} = 22 \pm 2$ kjmol^{-1}
$\Delta S^{\neq} = -38 \pm 5$ jmol^{-1}K^{-1}
$\Delta G^{\neq} = 33 \pm 2$ kjmol^{-1}

Table B6 Experimental data for the determination of the activation parameters for the formation of (η^6-chlorobenzene)Cr(CO)$_3$ following flash photolysis at 355nm in cyclohexane under 1 atm. of CO.

Temp. (K)	1/T x 10^3 (K^{-1})	k_{obs} (s^{-1}) x 10^{-4}	Ln(k_{obs}/[CO])	Ln(k_{obs}/[CO] . T)
288	3.47	2.62	14.87	9.21
293	3.41	2.96	14.98	9.30
298	3.35	3.60	15.20	9.51
303	3.30	5.00	15.42	9.70
308	3.25	5.60	15.85	9.82
313	3.19	6.32	15.66	9.91

Arrhenius Plot

Slope	= -3000 ± 170
Intercept	= 25.27 ± 0.04
Correlation coefficient	= 0.99

Eyring Plot

Slope	= -2718 ± 199
Intercept	= 18.62 ± 0.05
Correlation coefficient	= 0.99

$E_a^{\neq}$ = 25 ± 2 kjmol^{-1}
$\Delta H^{\neq}$ = 22 ± 2 kjmol^{-1}
$\Delta S^{\neq}$ = -43 ± 5 jmol^{-1}K^{-1}
$\Delta G^{\neq}$ = 35 ± 2 kjmol^{-1}

Table B7 Experimental data for the determination of the activation parameters for the formation of (η^6-1,2 dichlorobenzene)$Cr(CO)_3$ following flash photolysis at 355nm in cyclohexane under 1 atm. of CO.

Temp. (K)	$1/T \times 10^3$ (K^{-1})	$Ln(k_2)$	$Ln(k_2/T)$
288	3.46	13.81	8.15
293	3.40	14.03	8.35
298	3.34	14.25	8.55
303	3.30	14.30	8.59
308	3.25	14.56	8.83
313	3.19	14.65	8.91

Arrhenius Plot

Slope	$= -3206 \pm 218$
Intercept	$= 24.92 \pm 0.04$
Correlation coefficient	$= 0.99$

Eyring Plot

Slope	$= -2885 \pm 188$
Intercept	$= 18 \pm 0.04$
Correlation coefficient	$= 0.99$

$E_a^{\neq} = 27 \pm 2$ kjmol^{-1}
$\Delta H^{\neq} = 24 \pm 2$ kjmol^{-1}
$\Delta S^{\neq} = -46 \pm 5$ jmol^{-1}K^{-1}
$\Delta G^{\neq} = 38 \pm 2$ kjmol^{-1}

Table B8 Experimental data for the determination of the activation parameters for the formation of (η^6-benzene)Mo(CO)$_3$ following flash photolysis at 266nm in cyclohexane under CO.

Temp. (K)	$1/T \times 10^3$ (K^{-1})	$Ln(k_2)$	$Ln(k_2/T)$
288	3.46	13.89	8.23
293	3.401	12.98	8.30
298	3.34	14.30	8.60
303	3.30	14.39	8.68
308	3.25	14.63	8.90
313	3.19	14.71	8.96

Arrhenius Plot
Slope = -3140 ± 230
Intercept = 24.77 ± 0.05
Correlation coefficient = 0.99

Eyring Plot
Slope = -2829 ± 232
Intercept = 18.03 ± 0.05
Correlation coefficient = 0.99

$E_a^{\neq} = 26 \pm 2$ kjmol^{-1}
$\Delta H^{\neq} = 23 \pm 2$ kjmol^{-1}
$\Delta S^{\neq} = -47 \pm 5$ jmol^{-1}K^{-1}
$\Delta G^{\neq} = 23 \pm 2$ kjmol^{-1}

Table B9 Experimental data for the determination of the activation parameters for the formation of (η^6-*p*-xylene)Mo(CO)$_3$ following flash photolysis at 266nm in cyclohexane under CO.

Temp. (K)	1/T x 10^3 (K^{-1})	Ln(k_2)	Ln(k_2/T)
288	3.47	14.10	8.44
293	3.41	14.35	8.67
298	3.35	14.41	8.71
303	3.30	14.65	8.93
308	3.25	14.82	9.09
313	3.19	14.91	9.19

Arrhenius Plot
Slope = -3076 ± 233
Intercept = 24.77 ± 0.05
Correlation coefficient = 0.99

Eyring Plot
Slope = -2819 ± 251
Intercept = 18.21 ± 0.05
Correlation coefficient = 0.98

$E_a^{\neq}$ = 25 ± 2 kjmol^{-1}
$\Delta H^{\neq}$ = 23 ± 2 kjmol^{-1}
$\Delta S^{\neq}$ = -46 ± 5 jmol^{-1}K^{-1}
$\Delta G^{\neq}$ = 23 ± 2 kjmol^{-1}

Table B10 Experimental data for the determination of the activation parameters for the formation of (η^6-1,3,5-mesitylene)Mo(CO)$_3$ following flash photolysis at 266nm in cyclohexane under CO.

Temp. (K)	1/T x 10^3 (K^{-1})	Ln(k_2)	Ln(k_2/T)
288	3.47	14.11	8.45
293	3.41	14.33	8.65
298	3.35	14.57	8.88
303	3.30	14.65	9.93
308	3.25	14.79	9.07
313	3.19	14.99	9.24

Arrhenius Plot

Slope	= -3047 $\pm$ 162
Intercept	= 24.72 $\pm$ 0.04
Correlation coefficient	= 0.99

Eyring Plot

Slope	= -2739 $\pm$ 172
Intercept	= 17.99 $\pm$ 0.04
Correlation coefficient	= 0.99

$E_a{\neq} = 25 \pm 2$ kjmol^{-1}
$\Delta H{\neq} = 23 \pm 2$ kjmol^{-1}
$\Delta S{\neq} = -48 \pm 5$ jmol^{-1}K^{-1}
$\Delta G{\neq} = 23 \pm 2$ kjmol^{-1}

Table B11 Experimental data for the determination of the activation parameters for the formation of (η^6-hexamethylbenzene)Mo(CO)$_3$ following flash photolysis at 266nm in cyclohexane under CO.

Temp. (K)	1/T x 10^3 (K^{-1})	k_{obs} (s^{-1}) x 10^{-4}	Ln(k_{obs}/[CO])	Ln(k_{obs}/[CO] . T)
273	3.66	9.72	15.62	10.01
278	3.58	12.48	15.87	10.25
283	3.53	15.25	16.07	10.43
288	3.47	17.19	16.19	10.53
293	3.41	21.86	16.43	10.75
298	3.35	28.32	16.69	11.00
303	3.3	35.67	16.92	11.21

Arrhenius Plot
Slope = -3545 ± 153
Intercept = 28.6 ± 0.04
Correlation coefficient = 0.99

Eyring Plot
Slope = -3086 ± 135
Intercept = 21.3 ± 0.03
Correlation coefficient = 0.99

$E_a^{\neq}$ = 28 ± 2 kjmol^{-1}
$\Delta H^{\neq}$ = 25 ± 2 kjmol^{-1}
$\Delta S^{\neq}$ = -20 ± 5 jmol^{-1}K^{-1}
$\Delta G^{\neq}$ = 31 ± 2 kjmol^{-1}

Table B12 Experimental data for the determination of the activation parameters for the formation of (η^6-benzene)Cr(CO)$_3$ following flash photolysis in pentane at 355nm under 1 atm. of CO.

Temp. (K)	1/T x 10^3 (K^{-1})	k_{obs} (s^{-1}) x 10^{-4}	Ln(k_{obs}/[CO])	Ln(k_{obs}/[CO] . T)
284	3.52	13.20	16.30	10.65
289	3.46	17.5	16.58	10.91
294	3.40	19.77	16.70	11.02
298	3.35	23.08	16.86	11.16
303	3.30	31.04	17.15	11.44
308	3.25	35.3	17.28	11.55
313	3.19	42.96	17.48	11.73

Arrhenius Plot

Slope	= -3495 ± 166
Intercept	= 28.55 ± 0.05
Correlation coefficient	= 0.99

Eyring Plot

Slope	= -3191 ± 168
Intercept	= 21.83 ± 0.05
Correlation coefficient	= 0.99

$E_a^{\neq}$ = 28 ± 2 kjmol^{-1}
$\Delta H^{\neq}$ = 26 ± 2 kjmol^{-1}
$\Delta S^{\neq}$ = -16 ± 5 jmol^{-1}K^{-1}
$\Delta G^{\neq}$ = 31 ± 2 kjmol^{-1}

Table B13 Experimental data for the determination of the activation parameters for the formation of (η^6-benzene)Cr(CO)$_3$ following flash photolysis in heptane at 355nm under 1 atm. of CO.

Temp. (K)	1/T x 10^3 (K^{-1})	k_{obs} (s^{-1}) x 10^{-4}	Ln(k_{obs}/[CO])	Ln(k_{obs}/[CO] . T)
288	3.47	14.95	16.68	11.02
293	3.42	19.70	16.96	11.28
298	3.35	23.01	17.11	11.41
303	3.30	28.20	17.31	11.60
308	3.24	35.20	17.53	11.80

Arrhenius Plot
Slope = -3515 ± 258
Intercept = 28.92 ± 0.05
Correlation coefficient = 0.99

Eyring Plot
Slope = -3222 ± 250
Intercept = 22.23 ± 0.05
Correlation coefficient = 0.99

$E_a^{\neq}$ = 29 ± 2 kjmol^{-1}
$\Delta H^{\neq}$ = 26 ± 2 kjmol^{-1}
$\Delta S^{\neq}$ = -12 ± 5 jmol^{-1}K^{-1}
$\Delta G^{\neq}$ = 29 ± 2 kjmol^{-1}

Table B14 Experimental data for the determination of the activation parameters for the formation of (η^6-benzene)Cr(CO)$_3$ following flash photolysis in decane at 355nm under 1 atm. of CO.

Temp. (K)	1/T x 10^3 (K^{-1})	k_{obs} (s^{-1}) x 10^{-4}	Ln(k_{obs}/[CO])	Ln(k_{obs}/[CO] . T)
287	3.48	14.1	16.84	11.19
293	3.41	17.90	17.08	11.41
296	3.35	23.41	17.30	11.66
303	3.30	27.82	17.53	11.81
308	3.25	32.00	17.67	11.93
318	3.14	39.01	17.86	12.12

Arrhenius Plot
Slope = -3567 ± 129
Intercept = 29.27 ± 0.03
Correlation coefficient = 0.99

Eyring Plot
Slope = -3234 ± 127
Intercept = 22.46 ± 0.03
Correlation coefficient = 0.99

$E_a^{\neq}$ = 29 ± 2 kjmol^{-1}
$\Delta H^{\neq}$ = 26 ± 2 kjmol^{-1}
$\Delta S^{\neq}$ = -10 ± 5 jmol^{-1}K^{-1}
$\Delta G^{\neq}$ = 29 ± 2 kjmol^{-1}

Table B15 Experimental data for the determination of the activation parameters for the formation of (η^6-benzene)Cr(CO)$_3$ following flash photolysis in dodecane at 355nm under 1 atm. of CO.

Temp. (K)	$1/T \times 10^3$ (K^{-1})	k_{obs} $(s^{-1}) \times 10^{-4}$	$Ln(k_{obs}/[CO])$	$Ln(k_{obs}/[CO] . T)$
290	3.44	31.00	17.71	12.04
298	3.35	40.99	17.99	12.29
303	3.30	51.01	18.20	12.49
307	3.25	54.92	18.28	12.56
313	3.19	70.89	18.53	12.79

Arrhenius Plot

Slope	= -3221 ± 181
Intercept	= 28.79 ± 0.03
Correlation coefficient	= 0.99

Eyring Plot

Slope	= -2952± 176
Intercept	= 22.194 ± 0.03
Correlation coefficient	= 0.99

$E_a^{\neq} = 27 \pm 2$ kjmol^{-1}
$\Delta H^{\neq} = 24 \pm 2$ kjmol^{-1}
$\Delta S^{\neq} = -13 \pm 5$ jmol^{-1}K^{-1}
$\Delta G^{\neq} = 28 \pm 2$ kjmol^{-1}

Table B16 Experimental data for the determination of the activation parameters for the formation of (η^6-benzene)Cr(CO)$_3$ following flash photolysis in cyclooctane at 355nm under 1 atm. of CO.

Temp. (K)	$1/T \times 10^3$ (K^{-1})	$Ln(k_2)$	$Ln(k_2/T)$
288	3.47	14.14	8.48
293	3.41	14.39	8.71
298	3.35	14.49	8.79
303	3.30	14.62	8.91
308	3.25	14.89	9.17
313	3.19	14.95	9.21

Arrhenius Plot

Slope	= -3066 ± 248
Intercept	= 24.78 ± 0.05
Correlation coefficient	= 0.99

Eyring Plot

Slope	= -2777 ± 254
Intercept	= 18.11 ± 0.06
Correlation coefficient	= 0.98

$E_a^{\neq} = 25 \pm 2$ kjmol^{-1}
$\Delta H^{\neq} = 23 \pm 2$ kjmol^{-1}
$\Delta S^{\neq} = -46 \pm 5$ jmol^{-1}K^{-1}
$\Delta G^{\neq} = 25 \pm 2$ kjmol^{-1}

Table B17 Experimental data for the determination of the activation parameters for the formation of (η^6-1,3,5-mesitylene)Mo(CO)$_3$ following flash photolysis in heptane at 266nm under CO.

Temp. (K)	1/T x 10^3 (K^{-1})	Ln(k_2)	Ln(k_2/T)
288	3.47	14.32	8.65
293	3.41	14.54	8.85
298	3.35	14.75	9.08
303	3.30	14.93	9.22
308	3.25	15.07	9.34
313	3.19	15.23	9.48

Arrhenius Plot
Slope = -3277 ± 110
Intercept = 25.71 ± 0.02
Correlation coefficient = 0.99

Eyring Plot
Slope = -2990 ± 154
Intercept = 19.06 ± 0.03
Correlation coefficient = 0.99

$E_a^{\neq} = 27 \pm 2$ kjmol^{-1}
$\Delta H^{\neq} = 25 \pm 2$ kjmol^{-1}
$\Delta S^{\neq} = -39 \pm 5$ jmol^{-1}K^{-1}
$\Delta G^{\neq} = 25 \pm 2$ kjmol^{-1}

Table B18 Experimental data for the determination of the activation parameters for the formation of (η^6-1,3,5-mesitylene)Mo(CO)$_3$ following flash photolysis in decane at 266nm under CO.

Temp. (K)	1/T x 10^3 (K^{-1})	k_{obs} (s^{-1}) x 10^{-3}	Ln(k_{obs}/ [sample])	Ln(k_{obs}/[sample]/ T)
286	3.49	4.92	16.04	10.38
289	3.46	5.07	16.07	10.40
304	3.29	6.68	16.34	10.63
309	3.24	7.65	16.48	10.73
313	3.19	7.91	16.52	10.77

Arrhenius Plot

Slope	= -1671 ± 95
Intercept	= 21.86 ± 0.02
Correlation coefficient	= 0.99

Eyring Plot

Slope	= -1386 ± 62
Intercept	= 15.2 ± 0.02
Correlation coefficient	= 0.99

$E_a^{\neq}$ = 14 ± 2 kjmol^{-1}
$\Delta H^{\neq}$ = 11 ± 2 kjmol^{-1}
$\Delta S^{\neq}$ = -71 ± 5 jmol^{-1}K^{-1}
$\Delta G^{\neq}$ = 14 ± 2 kjmol^{-1}

Table B19 Experimental data for the determination of the activation parameters for the formation of (η^6-benzene)$_2$Mo$_2$(CO)$_5$ following flash photolysis in cyclohexane at 266nm under 1 atm. of argon.

Temp. (K)	$1/T \times 10^3$ (K^{-1})	k_{obs} (s^{-1}) x 10^{-3}	Ln(k_{obs}/ [sample])	Ln(k_{obs}/[sample]/ T)
288	3.47	1.88	15.88	10.22
293	3.41	2.06	15.97	10.29
298	3.35	2.30	16.08	10.38
303	3.3	2.53	16.18	10.47
308	3.25	2.80	16.28	10.55
313	3.19	3.17	16.40	10.66

Arrhenius Plot

Slope	= -1878 ± 48
Intercept	= 22.383 ± 0.01
Correlation coefficient	= 0.99

Eyring Plot

Slope	= -1588 ± 57.6
Intercept	= 15.71 ± 0.02
Correlation coefficient	= 0.99

$E_a^{\neq} = 15 \pm 2$ kjmol^{-1}
$\Delta H^{\neq} = 13 \pm 2$ kjmol^{-1}
$\Delta S^{\neq} = -67 \pm 5$ jmol^{-1}K^{-1}
$\Delta G^{\neq} = 15 \pm 2$ kjmol^{-1}

Table B20 Experimental data for the determination of the activation parameters for the formation of (η^6-1,3,5-mesitylene)$_2$Mo$_2$(CO)$_5$ following flash photolysis in cyclohexane at 266nm under 1 atm. of argon.

Appendix C

Data for determination of extinction coefficients.

(C1) (η^6-ethylbenzene)$Cr(CO)_3$ in cyclohexane.

mol dm^{-3} x 10^{-4}	O.D at 355nm (AU)
0	0
0.56	0.19
1.12	0.37
1.68	0.56
2.25	0.73
2.80	0.92

(C2) (η^6-*o*-xylene)$Cr(CO)_3$ in cyclohexane.

mol dm^{-3} x 10^{-4}	O.D at 355nm (AU)
0	0
0.5	0.21
1.0	0.40
1.5	0.62
2.0	0.82
2.5	1.04

(C3) (η^6-hexaethylbenzene)$Cr(CO)_3$ in cyclohexane.

mol dm^{-3} x 10^{-4}	O.D at 355nm (AU)
0	0
1.05	0.33
2.11	0.71
3.17	1.06
4.23	1.41
5.29	1.77

(C4) (η^6-*t*-butylbenzene)$Cr(CO)_3$ in cyclohexane.

mol dm^{-3} x 10^{-4}	O.D at 355nm (AU)
0	0
0.5	0.17
1.0	0.33
1.5	0.49
2.0	0.65
2.5	0.81

(C5) (η^6-*p*-chlorotoluene)$Cr(CO)_3$ in cyclohexane.

mol dm^{-3} x 10^{-4}	O.D at 355nm (AU)
0	0
0.51	0.20
1.02	0.39
1.53	0.62
2.04	0.79
2.55	1.02

(C6) (η^6-*p*-fluorotoluene)$Cr(CO)_3$ in cyclohexane.

mol dm^{-3} x 10^{-4}	O.D at 355nm (AU)
0	0
0.58	0.28
1.16	0.45
1.73	0.65
2.31	0.85
2.89	1.014

(C7) (η^6-chlorobenzene)$Cr(CO)_3$ in cyclohexane.

mol dm^{-3} x 10^{-4}	O.D at 355nm (AU)
0	0
0.5	0.17
1.0	0.36
1.5	0.57
2.0	0.76
2.5	0.95

(C8) (η^6-1,2-dichlorobenzene)$Cr(CO)_3$ in cyclohexane.

mol dm^{-3} x 10^{-4}	O.D at 355nm (AU)
0	0
0.18	0.17
0.35	0.31
0.71	0.54
1.42	0.97
2.83	1.8

(C9) (η^6-benzene)$Cr(CO)_3$ in pentane.

mol dm^{-3} x 10^{-4}	O.D at 355nm (AU)
0	0
0.58	0.18
1.10	0.37
1.70	0.56
2.30	0.76
2.89	0.93

(C10) (η^6-benzene)Cr(CO)$_3$ in heptane.

mol dm^{-3} x 10^{-4}	O.D at 355nm (AU)
0	0
0.48	0.12
9.7	0.25
14.6	0.36
19.4	0.49
24.3	0.59

(C11) (η^6-benzene)Cr(CO)$_3$ in decane.

mol dm^{-3} x 10^{-4}	O.D at 355nm (AU)
0	0
0.56	0.19
1.12	0.44
1.68	0.65
2.68	1.01
3.36	1.39

(C12) (η^6-benzene)Cr(CO)$_3$ in dodecane.

mol dm^{-3} x 10^{-4}	O.D at 355nm (AU)
0	0
0.26	0.13
1.03	0.42
1.71	0.61
2.05	0.72
2.87	0.91

(C13) (η^6-benzene)Cr(CO)$_3$ in cyclooctane.

mol dm^{-3} x 10^{-4}	O.D at 355nm (AU)
0	0
0.42	0.23
0.84	0.46
1.26	0.68
1.68	0.88
2.10	1.09

(C14) (η^6-benzene)Cr(CO)$_3$ in 1,1,2-trichlorotrifluorobenzene.

mol dm^{-3} x 10^{-4}	O.D at 355nm (AU)
0	0
0.5	0.21
1.0	0.39
2.0	0.64
4.1	1.08
6.1	1.52

(C15) (η^6-benzene)Cr(CO)$_3$ in perfluoromethylcyclohexane.

mol dm^{-3} x 10^{-4}	O.D at 355nm (AU)
0	0
1.0	0.19
2.0	0.28
3.0	0.40

(C16) (η^6-hexaethylbenzene)$Cr(CO)_3$ in heptane.

mol dm^{-3} x 10^{-4}	O.D at 355nm (AU)
0	0
1.0	03.4
1.5	0.60
2.0	0.74
2.5	1.02

(C17) (η^6-benzene)$Mo(CO)_3$ in cyclohexane.

mol dm^{-3} x 10^{-4}	O.D at 266nm (AU)	O.D at 355nm (AU)
0	0	0
0.5	0.16	0.13
1.0	0.29	0.20
1.5	0.39	0.28
2.0	0.47	0.37
2.5	0.56	0.46

(C18) (η^6-*p*-xylene)$Mo(CO)_3$ in cyclohexane.

mol dm^{-3} x 10^{-4}	O.D at 266nm (AU)	O.D at 355nm (AU)
0	0	0
1.0	0.15	0.14
1.5	0.22	0.20
2.0	0.31	0.26
2.5	0.39	0.33

(C19) (η^6-mesitylene)Mo(CO)$_3$ in cyclohexane.

mol dm^{-3} x 10^{-4}	O.D at 266nm (AU)	O.D at 355nm (AU)
0	0	0
0.5	0.12	0.08
1.0	0.27	0.21
1.5	0.40	0.32
2.0	0.56	0.43
2.5	0.73	0.52

(C20) (η^6-hexamethylbenzene)Mo(CO)$_3$ in cyclohexane.

mol dm^{-3} x 10^{-4}	O.D at 266nm (AU)	O.D at 355nm (AU)
0	0	0
0.55	0.23	0.31
1.09	0.69	0.52
1.65	0.57	0.78
2.19	0.74	1.05
2.75	0.98	1.30

(C21) (η^6-mesitylene)Mo(CO)$_3$ in heptane.

mol dm^{-3} x 10^{-4}	O.D at 355nm (AU)	O.D at 266nm (AU)
0	0	0
0.15	0.11	0.15
0.30	0.22	0.30
0.45	0.32	0.45
0.65	0.49	0.65
0.76	0.55	0.76

(C22) (η^6-mesitylene)Mo(CO)$_3$ in decane.

mol dm^{-3} x 10^{-4}	O.D at 355nm (AU)	O.D at 355nm (AU)
0	0	0
0.5	0.25	0.34
1.333	0.62	0.89
2.66	1.24	1.67
3.33	1.65	2.16

(C23) (η^6-allylbenzene)Cr(CO)$_3$ in cyclohexane.

mol dm^{-3} x 10^{-4}	O.D at 355nm (AU)
0	0
0.5	0.14
1.1	0.28
1.65	0.42
2.2	0.55
2.75	0.72

(C24) (η^6-tetrahydronaphthalene)Cr(CO)$_3$ in cyclohexane.

mol dm^{-3} x 10^{-4}	O.D at 355nm (AU)
0	0
0.5	0.21
1.0	0.42
1.5	0.64
2.0	0.84
2.5	1.1

(C25) (η^6-naphthalene)$Cr(CO)_3$ in cyclohexane.

mol dm^{-3} x 10^{-4}	O.D at 266nm (AU)	O.D at 355nm (AU)
0	0	0
0.5	0.42	0.49
1.0	0.83	0.97
1.5	1.25	1.48
2.0	1.67	1.96
2.5	2.06	2.41

(C24) (η^6-phenanthrene)$Cr(CO)_3$ in cyclohexane.

mol dm^{-3} x 10^{-4}	O.D at 266nm (AU)	O.D at 355nm (AU)
0	0	0
0.5	0.61	0.38
1.0	1.21	0.76
1.5	1.81	1.15
2.0	2.38	1.56
2.5	2.83	1.92

(C26) (η^6-pyrene)$Cr(CO)_3$ in cyclohexane.

mol dm^{-3} x 10^{-4}	O.D at 266nm (AU)	O.D at 355nm (AU)
0	0	0
0.5	0.64	0.27
1.0	1.2	0.50
1.5	1.64	0.77
2.0	2.1	0.95
2.5	2.92	1.2

(C27) (η^6-*trans*-1,2 diphenylethene)$Cr(CO)_3$ in cyclohexane.

mol dm^{-3} x 10^{-4}	O.D at 355nm (AU)
0	0
0.52	0.37
1.04	0.73
1.56	1.08
2.08	1.42
2.60	1.75

(C28) (η^6-*cis*-1,2 diphenylethene)$Cr(CO)_3$ in cyclohexane.

mol dm^{-3} x 10^{-4}	O.D at 355nm (AU)
0	0
0.52	0.37
1.04	0.56
1.56	1.04
2.08	1.35
2.60	1.64

(C29) (η^6-*trans,trans*-1,4-diphenyl-1,3-butadiene)$Cr(CO)_3$ in cyclohexane.

mol dm^{-3} x 10^{-4}	O.D at 355nm (AU)
0	0
0.61	0.25
1.22	0.46
2.5	0.96
5.0	1.58

(C30) (η^1-C_5H_7)Mn$(CO)_5$ in cyclohexane.

mol dm^{-3} x 10^{-4}	O.D at 355nm (AU)
0	0
0.38	0.10
0.76	0.22
1.14	0.33
1.50	0.43

(C31) (η^3-C_5H_7)Mn$(CO)_4$ in cyclohexane.

mol dm^{-3} x 10^{-4}	O.D at 266nm (AU)
0	0
1.0	0.23
1.5	0.36
2.0	0.51

(C32) (η^5-C_5H_7)Mn$(CO)_3$ in cyclohexane.

mol dm^{-3} x 10^{-4}	O.D at 355nm (AU)
0	0
4.6	0.11
9.13	0.22
13.7	0.32
18.3	0.39

(C33) $Mn(CO)_4(\mu^3\text{-}C_3H_4\text{-}C_6H_5)Cr(CO)_3$ in cyclohexane.

mol dm^{-3} x 10^{-4}	O.D at 355nm (AU)
0	0
0.26	0.21
0.53	0.43
0.80	0.64
1.06	0.87
1.33	1.072